Development and Characterization of Soymilk Okara Gels Modified by Citric Acid

by

Minh Xuan Nguyen

A thesis

presented to the University of Waterloo

in fulfillment of the

thesis requirement for the degree of

Master of Applied Science

in

Chemical Engineering

Waterloo, Ontario, Canada, 2023

© Minh Xuan Nguyen 2023

Author's Declaration

This thesis consists of material all of which I authored or co-authored: see Statement of Contributions included in the thesis. This is a true copy of the thesis, including any required final revisions, as accepted by my examiners.

I understand that my thesis may be made electronically available to the public.

Statement of Contributions

Minh Xuan Nguyen was the sole author of all chapters (chapter 1 to 6) which were written under the supervision of Dr. Christine Moresoli. Chapter 3 and Chapter 4 are preliminary results and are not written for publication. Chapter 5 is a manuscript written for publication. Specifically:

Chapter 3

This research was conducted at the University of Waterloo by Minh Xuan Nguyen under the supervision of Dr. Christine Moresoli. Minh Xuan Nguyen was responsible for developing methodology for preparation of soymilk and soymilk okara gels, conducting experiments, analyzing and visualizing data, and writing of the chapter. Dr. Christine Moresoli provided guidance, reviewed and edited the chapter.

Chapter 4

This research was conducted at the University of Waterloo by Minh Xuan Nguyen under the supervision of Dr. Christine Moresoli. Minh Xuan Nguyen was responsible for developing methodology for preparation of soymilk okara gels for characterization, conducting experiments, analyzing and visualizing data, and writing of the chapter. Dr. Christine Moresoli provided guidance, reviewed and edited the chapter.

Chapter 5

This research was conducted at the University of Waterloo by Minh Xuan Nguyen under the supervision of Dr. Christine Moresoli. This chapter has been prepared for submission to a scientific journal. Minh Xuan Nguyen was responsible for forming research hypothesis, designing experimentation, developing methods for characterizations, conducting experiments, analyzing

and interpreting results. The initial drafts of the manuscripts were written by Minh Xuan Nguyen which were reviewed and edited by Dr. Christine Moresoli and Minh Xuan Nguyen.

Abstract

The present study aimed to explore the effects of citric acid (CA) modified okara materials on the characterization of soymilk okara gels as well as gain understanding of the underlying mechanisms of okara modification and soymilk gelation. After the modification with CA, the fiber in okara is hypothesized to be hydrolyzed, along with the release of soluble polysaccharides such as pectic substances, ultimately enhancing the compatibility of the CA modified okara with the soymilk protein matrix. To maintain uniform soymilk quality across experiments, the solid content of soymilk kept constant at 15 to 16 % (w:w).

The impacts of the physical state of CA (liquid or solid) and the drying time of okara on the textural characterization of the soymilk gels were first examined. The findings revealed that both liquid and solid forms of CA, at a concentration of 5% (w:w), had similar effects on okara, as evidenced by visual observations, rheological properties, and mechanical attributes of the resulting gels. However, the liquid form of CA improved the uniformity and consistency of the textural properties of the soymilk okara gels, which might be attributed to the more uniform distribution of the CA in the mixture during the treatment of okara. The increase in the drying duration of okara materials, from 20 to 50 h led to notable increase in colour intensity, along with the formation of products from Maillard and caramelization reactions detected by FTIR analysis. Consequently, a drying time of 20 h was selected as appropriate, as it allowed okara materials to reach a constant weight without significant alterations in color and composition.

Soymilk okara gels exhibited weak gel structure through visual observation, making it challenging to cut them into precise shapes and dimensions from bulk gels for subsequent measurements of rheological and mechanical properties without causing damage. To minimize the cutting effects, soymilk gels were prepared at the desired measurement thickness followed by cutting to the final

width and shape dimensions. The desired thickness was 2-3 mm for rheological properties measurements followed by careful cutting into thin square disk and 10-mm height for mechanical properties measurements followed by carefully cutting into cylindrical shapes.

In the final formulation, okara was modified with CA solutions at concentrations ranging from 2.5 to 10 % (w:w), and then dried at 60 °C for 20 h. Soymilk okara gels were subsequently prepared using heat treatment at 95 °C for 45 min. Higher CA concentrations induced more significant degradation of okara fibers and release of pectin, as evidenced by TGA and FTIR, leading to changes in the texture and protein-protein interactions of soymilk okara gels.

Soy gel containing modified okara at CA's concentration of 2.5 % displayed the highest level of rheological and mechanical properties. As the CA concentration increased, the soymilk okara gels exhibited increased homogeneity, as indicated by lower porosity in optical images. This was accompanied by reduced viscoelasticity and a decrease in hydrophobic protein-protein interactions. Notably, water holding capacity and mechanical properties remained constant and were unaffected by the CA level. Additionally, the unreacted CA on modified okara materials had an impact on gelation, resulting in a protein particulate structure, different from the fine-stranded protein structure of soymilk okara gels without CA observed in CLSM images. The fabrication of soymilk okara gels with improved homogeneity through the modifications of okara with CA was confirmed. The alterations in the textural profiles and protein – protein interactions when varying the concentration of CA solution examined in this study could be further applied in the development of desired textural profiles matching commercial products.

Acknowledgements

I would like to express my deep appreciation and gratitude to my supervisor, Professor Christine Moresoli for her continual guidance and support. Her mentorship has shaped me into a diligent and open-minded researcher. I have learnt a lot from her profound knowledge and her dedicated approach to research.

I would like to thank Professor Tizazu Mekonnen for providing valuable resources and granting access to the equipment in his lab. His feedback and suggestions as a reader of this thesis have been invaluable. I would like to thank Professor Alexander Penlidis for taking the time to review our work and offering insightful feedback.

I would like to express my gratitude to all those who have supported me throughout my academic journey. I would like to make mention of Dylan Jubinville for his assistance with the training of mechanical and rheological equipment. My colleague and friend, Jing Sy, has been with me since the beginning, offering valuable training and support. I would also like to thank my colleague, Bhoomi Mavani, who has been a constant source of care and encouragement like an older sister.

Finally, but the most importantly, I would like to express my deepest appreciation to my family, Mom, Dad, Sister and Grandparents for their unwavering mental and financial support, encouragement, and boundless love throughout my Master's journey. To Rohan Shorey for always being my pilar of strength. Your unconditional love and support continually inspire me to be the best version of myself.

Table of Contents

Author's Declaration ii

Statement of Contributions iii

Abstract v

Acknowledgements vii

Table of Contents viii

List of Figures xiii

List of Tables xix

List of Abbreviations xxii

List of Symbols xxiv

Chapter 1: Introduction 1

1.1. Research Aim 1

1.2. Objectives 2

1.3. Thesis Structure 5

Chapter 2: Literature Review 7

2.1. Cheese Derived from Animal Milk 7

2.1.1. Milk Proteins 8

2.1.2. Cheesemaking process 10

2.1.3. Dairy-based Cheese Analogues 14

2.2. Cheese Analogues 17

2.2.1. Partial Dairy-based Cheese Analogues 20

2.2.2. Plant-based Cheese Analogues 21

2.3. Soybeans 23

2.3.1. Soybean Morphology and Composition 23

2.3.2. Soymilk 27
2.3.3. Okara 29
2.4. Soymilk Gel (Tofu) 30
2.4.1. Heat-induced Soy Gel 32
2.4.2. Acid-induced Soy Gel 34
2.4.3. Salt-induced Soy Gel 36
2.4.4. Enzyme-induced Soy Gel 37
2.5. Okara-added Soy Products 38
2.5.1. Physical Modification Methods 39
2.5.2. Non-physical Modification Methods 43
2.5.3. Combined Modification Methods 47
2.6. Effect of Citric Acid Treatment on Soy Polysaccharides 47
2.6.1. Overview of Citric Acid 47
2.6.2. Hydrolysis Activity 47
2.6.3. Chelating Property 48
2.6.4. Extraction of Pectic Substances 49
2.6.5. Cross-linking Property 50
2.7. Protein – Polysaccharide Conjugated Gels 51
2.7.1. Maillard Reaction 51
2.7.2. Maillard Conjugation Methods 52
2.7.3. Detection of Maillard reactions by FTIR 53
2.7.4. Application of Maillard Reaction in Improving Soy Protein Functionality 55
2.7.5. Maillard Reaction Protein – Polysaccharide Conjugated Gels 60
Chapter 3: Standardization of Soymilk Okara Gels Preparation 62
3.1. Introduction 62

3.2. Materials and Methods 63

3.2.1. Materials 63

3.2.2. Preparation of Soymilk and Okara 63

3.2.3. Estimation of Soymilk Solid Content 64

3.2.4. Okara Modification with Citric Acid (CA) 65

3.2.5. Preparation of Soymilk Okara Gels 66

3.2.6. Characterization of Okara Materials by Fourier Transform Infrared Spectroscopy (FTIR) 67

3.2.7. Structural Characterization of Soymilk Okara Gels 68

3.2.8. Rheological Properties of Soymilk Okara Gels 69

3.2.9. Mechanical Properties of Soymilk Okara Gels 71

3.2.10. Statistical Analysis 72

3.3. Results and Discussion 72

3.3.1. Standardization of Soymilk Preparation and Measurement of Its Solid Content 72

3.3.2. Effect of States of Citric Acid in Okara Modification on the Structural and Textural Characteristics of Soymilk Okara Gels 75

3.3.3. The Effect of Drying Time on the CA Modified Okara 82

3.4. Conclusions 89

Chapter 4: Methodology of Sample Preparation for Texture Characterization and Protein – Protein Interactions Characterization of Soymilk Okara Gels 90

4.1. Introduction 90

4.2. Materials and Methods 91

4.2.1. Materials 91

4.2.2. Preparation of Soymilk Okara Gels 92

4.2.3. Rheological Properties 92

4.2.4. Mechanical Properties 94

4.2.5. Protein – Protein Interactions 95

4.3. Results and Discussion 99

4.3.1. Effect of Sample Preparation on the Reproducibility of Rheological Properties 99

4.3.2. Effect of Sample Preparations on the Reproducibility of Mechanical Properties ... 100

4.3.3. Standardization of Protein – Protein Interactions Methodology 102

4.4. Conclusions 107

Chapter 5: Unveiling the Effects of Citric Acid on Texture Profiles and Chemical Interactions in Soymilk Okara Gels 109

5.1. Abstract 109

5.2. Introduction 110

5.3. Materials and Methods 113

5.3.1. Materials 113

5.3.2. Preparation of Soymilk and Okara 113

5.3.3. Okara Modifications with Citric Acid 114

5.3.4. Characterization of Modified Okara 116

5.3.5. Preparation of Soymilk Okara Gels 116

5.3.6. Structural Characterization of Soymilk Okara Gels 118

5.3.7. Measurement of Syneresis and Water Holding Capacity (WHC) of Soymilk Okara Gels 120

5.3.8. Rheological Properties of Soymilk Okara Gels 121

5.3.9. Mechanical Properties of Soymilk Okara Gels 121

5.3.10. Protein – protein Interactions 122

5.3.11. Statistical Analysis 124

5.4. Results and Discussion 125

5.4.1. Characterization of Modified Okara 125

5.4.2. Structural Characterization of Soymilk Okara Gels 139

5.4.3. Syneresis and Water Holding Capacity (WHC) of Soymilk Okara Gels 143
5.4.4. Texture Properties of Soymilk Okara Gels 145
5.4.5. Protein – Protein Interactions 150
5.4.6. Proposed Mechanism of CA Okara Modification 152
5.5. Conclusion 157
Chapter 6: Conclusions and Recommendations 159
Letters of Copyright Permission 163
References 166
Appendices 187
Appendix A: Standardization of Soymilk Okara Gels Preparation 187
Appendix A.1: Standardization of Soymilk Preparation and Measurement of Its Solid Content 187
Appendix A.2: Effect of States of Citric Acid in Okara Modification on the Structural and Textural Characteristics of Soymilk Okara Gels 188
Appendix B: Methodology of Sample Preparation for Texture Characterization and Protein – Protein Interactions Characterization of Soymilk Okara Gels 190
Appendix B.1: Effect of Sample Preparation on the Reproducibility of Rheological Properties 190
Appendix B.2: Effect of Sample Preparation on the Reproducibility of Mechanical Properties 191
Appendix B.3: Methodology of Protein – Protein Interactions Characterization of Soymilk Okara Gels 192
Appendix C: Unveiling the Effects of Citric Acid on Textural Profiles and Chemical Interactions in Soymilk Okara Gels 196

List of Figures

Figure 1. 1: Flowchart of the objectives and associated approaches of the Master thesis..... 4

Figure 2. 1: Spectrum of cheese, classified by their softness [19]. Reprinted from N. Y. Farkye, "Cheese technology," International Journal of Dairy Technology, vol. 57, no. 2 - 3, pp. 91 - 98, 2004, with permission from Wiley. 8

Figure 2. 2: a) Dual bonding model of casein micelle structure proposed by Horne [23]. b) Model of casein micelle proposed by Walstra [25]. Reprinted from D. S. Horne, "Casein Interactions: Casting Light on the Black Boxes, the Structure in Dairy Products," International Dairy Journal, vol. 8, no. 3, pp. 171 - 177, 1998.; P. Walstra, "Casein sub-micelles: do they exist?," International Dairy Journal, vol. 9, no. 3 - 6, pp. 189 - 192, 1999. with permission from Elsevier. 10

Figure 2. 3: A schematic representation illustrating the stages of the cheese curd formation [20]. Reprinted from P. F. Fox, P. L. McSweeney, T. M. Cogan and T. P. Guinee, "Fundamentals of Cheese Science," 2 ed., Springer, 2017., with permission from Springer. 13

Figure 2. 4: The approach for the design of dairy-based analogues [29]. Reprinted from R. Kamath, S. Basak and J. Gokhale, "Recent trends in the development of healthy and functional cheese analogues-a review," *LWT - Food Science and Techonology*, vol. 155, p. 112991, 2022, with permission from Elsevier. 16

Figure 2. 5: Classification of cheese analogues [28]. Reprinted from M. Shaw, "Cheese substitues: threat or opportunity?," *Journal of the Society of Dairy Technology*, vol. 37, pp. 27 - 31, 1984, with permission from Wiley. 18

Figure 2. 6: Flow process chart comparing the different processing routes for plant-based cheese production: a) material fractionation route, b) tissue disruption route [26]. Reprinted from L. Grossmann and D. J. McClements, "The science of plant-based foods: Approaches to create nutritious and sustainable plant-based cheese analogs," *Trends in Food Science & Technology*, vol. 118, pp. 207 - 229, 2021, with permission from Elsevier..... 22

Figure 2. 7: Image of soybeans (about 5 mm in size) and scanning electron microscopy (SEM) image of a pre-soaked soybean [48]. Reprinted from K.E.Preece, N.Hooshyar and N.J.Zuidamc,

"Whole soybean protein extraction processes: A review," *Innovative Food Science & Emerging Technologies*, vol. 43, pp. 163-172, 2017, with permission from Elsevier. 23

Figure 2. 8: Schematic representation of the structure of a) soybean glycinin 11S and c) β-conglycinin 7S; b) A schematic illustration of the distribution of hydrophobic residues in soybean glycinin and β-conglycinin [54]. Reprinted from C. Salas, O. J. Rojas, L. A. Lucia, M. A. Hubbe and J. Genzer, "On the Surface Interactions of Proteins with Lignin," ACS Applies Materials and Interfaces, vol. 5, no. 1, pp. 199 - 206, 2013, with permission from ACS publications..... 25

Figure 2. 9: Schematic representation of the structure of okara fiber [72]. Reprinted from H. Yoshii, T. Furuta, H. Maeda and H. Mori, "Hydrolysis Kinetics of Okara and Characterization of Its Water-soluble Polysaccharides," Bioscience, Biotechnology, and Biochemistry, vol. 60, no. 9, p. 1406–1409, 1996, with permission from Oxford University Press. 30

Figure 2. 10: Schematic representation of the steps leading to the gelation of soy protein isolate in aqueous solutions during heating [77]. Reprinted from T. Nicolai and C. Chassenieux, "Heat-induced gelation of plant globulins," Current Opinion in Food Science, vol. 27, pp. 18 - 22, 2019, with the permission from Elsevier. 33

Figure 2. 11: Schematic depiction of β-conglycinin and glycinin thermal aggregation behavior at pH 7.0. N, native state; U, unfolded state; Agg., aggregates [78]. Reprinted from J. Guo, X.-Q. Yang, X.-T. He, N.-N. Wu, J.-M. Wang, W. Gu and Y.-Y. Zhang, "Limited aggregation behavior of β-conglycinin and its terminating effect on glycinin aggregation during heating at pH 7.0," *Journal of Agricultural and Food Chemistry*, vol. 60, no. 14, pp. 3782 - 3791, 2012, with permission from ACS Publications..... 34

Figure 2. 12: Gelation mechanism of soybean proteins in the presence of GDL or CaSO4; Circles are denoted as protein molecules and black area is denoted as hydrophobic regions [83]. Reprinted from K. Kohyama, Y. Sano and E. Doi, "Rheological characteristics and gelation mechanism of tofu (soybean curd)," *Journal of Agricultural and Food Chemistry*, vol. 43, pp. 1808 - 1812, 1995, with permission of ACS Publications. 35

Figure 2. 13: Three stages of the Maillard reaction and sub-products characteristics [105]. Reprinted from R. R. Naik, Y. Wang and C. Selomulya, "Improvements of plant protein functionalities by Maillard conjugation and Maillard reaction products," *Critical Reviews in Food*

Science and Nutrition, vol. 62, no. 25, pp. 7036 - 7061, 2022., with permission of Taylor & Francis. 52

Figure 3. 1: Objectives of the standardization of the methodology for the preparation of soymilk okara gels with steps of the gel preparation (solid lines and boxes) and standardization objectives on (dashed lines and boxes). 63

Figure 3. 2: Comparison of solid contents in 3 different batches of soymilk in 3 weeks, measured by drying and UV-vis method. Data expressed in mean ± standard deviation (n = 3). 74

Figure 3. 3: Optical images of okara materials (O, OCAS5, OCA5); optical images and microstructural images determined by CLSM of soymilk okara gels (M, MO, MOCAS5, MOCA5). In CLSM images (at the objective of 20 x), red region represents for protein part with the scale bar indicates 20 μm. 77

Figure 3. 4: Typical curves of a) storage modulus G' (filled symbols), loss modulus G'' (open symbols) and b) tangent delta (tanδ) over angular frequency ω (rad/s) of soymilk okara gels (M, MO, MOCAS5, MOCA5)..... 79

Figure 3. 5: Mechanical properties of soymilk okara gels (M, MO, MOCAS5, MOCA5), (a) Typical fracture stress – fracture strain curves, (b) True fracture stress, (c) True fracture strain, (d) Young's modulus. Data of (b – d) expressed as mean ± standard deviation (n = 5). Means that do not share a common letter are statistically different (ANOVA followed by Tukey's post-hoc: $p < 0.05$). 81

Figure 3. 6: Visual appearance and solids content of OCA10 at different drying durations (20 h, 26 h, 44 h and 50 h). 83

Figure 3. 7: a) FTIR spectra of control (unmodified O), CA modified okara (OCA10) at different drying times and citric acid (CA), b) zoomed-in view within the range from 2000 – 800 cm^{-1}. . 88

Figure 3. 8: Visual observation of soymilk okara gels (M, MO, MOCA5) in soaking solutions (SA, SB, SC, SD) at a) 10 min and b) 45 min after the addition of Bradford dye. 107

Figure 4. 1: Overall framework (solid lines and boxes) and specific questions addressed in this chapter (dashed lines and boxes) for the sample preparation and chemical interaction characterization of soymilk okara gels. 91

Figure 4. 2: a) Original sample preparation in 100-mL beaker and b) alternative sample preparation in petri dish for the rheological measurements. 93

Figure 4. 3: a) Original sample preparation, proposed new sample preparations in b) 100-mL beakers and c) 250-mL beaker for the mechanical properties test. 95

Figure 4. 4: Viscoelasticity properties of soymilk okara gels (M, MO) prepared in petri dish (P) and beaker (B): Typical curves of a) storage modulus G' (filled symbols) and loss modulus G'' (empty symbols), b) tan(δ) over angular frequency. (c) Storage (G_o') and (d) viscous (G_o'') moduli at 1 rad/s. Data of c – d expressed in mean ± standard deviation (n = 3). 100

Figure 4. 5: Mechanical properties of soymilk okara gels (M, MO) prepared in 100-mL beakers (SB) and 250-mL beakers (LB): (a) Typical fracture stress – fracture strain curves, (b) True fracture stress, (c) True fracture strain, (d) Young's modulus. Data of (b – d) expressed in mean ± standard deviation (n = 4). 102

Figure 4. 6: Visual observation of soymilk okara gels (M, MO, MOCA5) soaked in solution (SA, SB, SC, SD) before and after centrifugation at 10,000 rpm, 25 °C for 30 min. 103

Figure 4. 7: Comparison of BSA standard curves constructed in phosphate buffer pH 7.0 solution (dashed line) and soaking solution SD (0.6M NaCl + 8M urea) (dotted line). 105

Figure 5. 1: The flowchart of making soymilk and soymilk okara gels (M, MO, MOCA2.5, MOCA5, MOCA10). 115

Figure 5. 2: Characterization of soymilk (M) and soymilk okara gels (MO, MOCA2.5, MOCA5, MOCA10) with the total number of replicates for each experimental test. 118

Figure 5. 3: Visual observation of okara materials (O, OCA2.5, OCA5, OCA10) after drying in oven and after grinding. 126

Figure 5. 4: a) Thermogravimetry (TGA), b) derivative thermogravimetry (DTG) curves of control (M, O, CA) and CA modified okara materials (OCA2.5, OCA5, OCA10), c) zoomed-in view of DTG. 129

Figure 5. 5: a) Full FTIR spectra of M, O, citric acid (CA), and CA modified okara (OCA2.5, OCA5, OCA10) and b) FTIR spectra within the range from 2000 – 800 cm^{-1}. 138

Figure 5. 6: a) Visual observations of the cross-section surface of soymilk okara gels (M, MO, MOCA2.5, MOCA5, MOCA10); b) Binary images generated by ImageJ with the gel size of 30 x 30 mm; c) Porous regions (blue lines) detected by ImageJ. 140

Figure 5. 7: CLSM images at three different magnifications a) 20 x, b) 63 x and c) 100 x of soymilk okara gels (M, MO, MOCA2.5, MOCA5, MOCA10). The red region represents the Rhodamine B labelled protein, and the scale bars represent 20 μm (for 20 x), 10 μm (for 63 x), 5 μm (for 100 x). 143

Figure 5. 8: Syneresis and water holding capacity (WHC) of soymilk okara gels after 24-h storage at 4 ^{o}C. Data of syneresis expressed as mean standard deviation (n = 3). Data of WHC expressed as mean standard deviation (n = 6). Means within one column that do not share a common letter are statistically different (ANOVA followed by Tukey's post-hoc: $p < 0.05$). 145

Figure 5. 9: Viscoelasticity properties of soymilk okara gels (M, MO, MOCA2.5, MOCA5, MOCA10): Typical curves of a) storage modulus G' (filled symbols) and loss modulus G'' (open symbols), b) complex viscosity and c) tan(δ) over angular frequency. 148

Figure 5. 10: Mechanical properties of soymilk okara gels (M, MO, MOCA2.5, MOCA5, MOca10): (a) Typical fracture stress – fracture strain curves, (b) True fracture stress, (c) True fracture strain, (d) Young's modulus. Data of (b – d) expressed as mean ± standard deviation (n = 18). Means within one column that do not share a common letter are statistically different (ANOVA followed by Tukey's post-hoc: $p < 0.05$). 150

Figure 5. 11: Protein – protein interactions including ionic bonds, hydrogen bonds and hydrophobic interactions of soymilk okara gels (M, MO, MOCA2.5, MOCA5, MOCA10). Data expressed as mean ± standard deviation (n = 3). Means within one column that do not share a common letter are statistically different (ANOVA followed by Tukey's post-hoc: $p < 0.05$)... 152

Figure 5. 12: Proposed mechanism for the effect of citric acid modification on okara's structure (Stage 1) and on soymilk okara gels (Stage 2). 156

Figure S. 1: Standard curve of solid content in soymilk (g/100 mL solution A), measured at the wavelength of 400 nm. 187

Figure S. 2: a) Curves of storage modulus (G') and loss modulus (G'') over strain (γ) of different type of soymilk okara gels. Curves of G' and G'' over angular frequency (ω) of b) M, c) MO, d) MOCAS5, e) MOCA5. 188

Figure S. 3: Fracture stress – fracture stain curves of different type of soymilk okara gels: a) M, b) MO, c) MOCAS5, d) MOCA5)..... 189

Figure S. 4: a) Curves of storage modulus (G') and loss modulus (G'') over strain (□) of M and MO prepared in beakers (B) and petri dish (P). Curves of G' and G'' over angular frequency (□) of b) M – P, c) M – B, d) MO – P, e) MO – B..... 190

Figure S. 5: Fracture stress – fracture stain curves of soymilk gel (M) prepared in a) 250-mL beaker (LB), b) 100-mL beaker (SB); soymilk unmodified okara gel (MO) prepared in c) 250-mL beaker (LB), d) 100-mL beaker (SB)..... 191

Figure S. 6: Changes in pH of soymilk and modified okara mixture during the 15-min mixing. 196

Figure S. 7: a) Curves of storage modulus (G') and loss modulus (G'') over strain (γ) of soymilk okara gels (M, MO, MOCA2.5, MOCA5, MOCA10). Curves of G' and G'' over angular frequency (ω) of b) M, c) MO, d) MOCA2.5, e) MOCA5, f) MOCA10. 197

Figure S. 8: Fracture stress – fracture stain curves of soymilk gel of soymilk okara gels a) M, b) MO, c) MOCA2.5, d) MOCA5, e) MOCA10..... 198

List of Tables

Table 2. 1: Classification of cheese based on moisture content, according to the National Dairy code of Canadian dairy information center [18]. 7

Table 2. 2: Ingredients used in the manufacture of cheese analogues [37]. Adapted from R. S. Chavan and A. Jana, "Cheese substitutes: An alternative to natural cheese - A review," International Journal of Food Science, Technology & Nutrition, vol. 2, no. 2, pp. 25 - 39, 2007. 18

Table 2. 3: Typical coagulants and their mechanism in tofu production [76]. Adapted from Q. Zhang, C. Wang, B. Li, L. Li, D. Lin, H. Chen, Y. Liu, S. Li, W. Qin, J. Liu, W. Liu and W. Yang, "Research progress in tofu processing: From raw materials to processing conditions," Critical Reviews in Food Science and Nutrition, vol. 58, no. 9, pp. 1448 - 1467, 2017, with permission of Taylor & Francis. 31

Table 2. 4: Published studies on the improvement of okara-added soy gels through physical techniques. 40

Table 2. 5: Published studies on the improvement of okara-added soy gels through non-physical techniques 44

Table 2. 6: Summary of the FTIR frequencies (cm^{-1}) of Maillard reactions corresponding to functional groups of proteins, polysaccharides, and Maillard reaction products, adapted from existing literature [111, 112, 113, 114]. 54

Table 2. 7: Summary of existing studies on the conjugation of soy protein isolate (SPI) with glucose and, polysaccharides derived from okara and pectic substances, using dry heating method. 57

Table 2. 8: Summary of existing studies on the conjugation of soy protein isolate (SPI) with glucose and pectic substances, using wet heating method. 59

Table 3. 1: Changes in mass of soybeans after hydration, dehull and extraction in three different batches. The percentage of solid content was measured by the drying method and expressed in mean ± standard deviation (n = 3). 73

Table 3. 2: Properties of okara materials (O, OCAS5, OCA5)..... 76

Table 3. 3: Viscoelastic properties of soymilk okara gels (M, MO, MOCAS5, MOCA5) based on power law parameters of **Equation 3. 4** and **Equation 3. 5** from frequency sweep tests. Data expressed as mean ± standard deviation (n = 3). Means within one column that do not share a common letter are statistically different (ANOVA followed by Tukey's post-hoc: $p < 0.05$)..... 80

Table 3. 4: Frequencies (cm^{-1}) of functional groups in okara presented in literature and experimental data..... 84

Table 4. 1: Soaking solutions (SA, SB, SC, SD) prepared in 0.05M phosphate buffer pH 7.0 and their target intermolecular bonds [167]..... 96

Table 5. 1: Mass of soybeans after hydration, dehulling, corresponding soymilk and okara for three different batches. The percentage of solid content was calculated using **Equation 5. 1**. Data was expressed in mean ± standard deviation (n = 3). 114

Table 5. 3: Preparation of okara mixtures (O, OCA2.5, OCA5, OCA10), mass, pH values after CA modifications and mass of dried solid. Data was expressed as mean standard deviation (n = 3). 125

Table 5. 4: Reaction scheme of A – Acid hydrolysis, B – Esterification of pectin, C – Maillard reaction and the corresponding FTIR frequencies (cm^{-1}) of their functional groups in unmodified and modified okara reported in the literature and observed in this study..... 133

Table 5. 5: Porosity estimates of soymilk okara gels (M, MO, MOCA2.5, MOCA5, MOCA10) based on binary images with the aid of ImageJ. Data expressed as mean standard deviation (n = 3). Means within one column that do not share a common letter are statistically different (ANOVA followed by Tukey's post-hoc: $p < 0.05$)..... 140

Table 5. 6: Viscoelastic properties of soymilk okara gels (M, MO, MOCA2.5, MOCA5, MOCA10) based on power law parameters of **Equation 5. 4** and **Equation 5. 5** from frequency sweep tests. Data expressed as mean ± standard deviation (n = 9). Means within one column that do not share a common letter are statistically different (ANOVA followed by Tukey's post-hoc: $p < 0.05$)..... 147

Table S. 1: BSA standard solutions in 0.05M phosphate buffer pH 7.0 at different concentrations in range of 0.05 – 0.50 μg/μL. 192

Table S. 2: BSA standard solutions in soaking solution SD at different concentrations in range of 0.05 – 0.50 mg/mL. 193

Table S. 3: Calculations of protein concentration in different types of soy samples. 194

Table S. 4: Final pH values of soymilk okara gels (M, MO, MOCA2.5, MOCA5, MOCA10) at the end of 15-min mixing. Data expressed as mean standard deviation (n = 3). Means within one column that do not share a common letter are statistically different (ANOVA followed by Tukey's post-hoc: $p < 0.05$). 196

List of Abbreviations

Abbreviations	Full name
AGEs	Advanced glycation end products
AP	Apple pectin
CA	Citric acid
CLSM	Confocal laser scanning microscopy
CP	Citrus pectin
DF	Dietary fiber
DI	Deionized
DSC	Differential scanning calorimetry
DTG	Derivative thermogravimetry
FTIR	Fourier transform infrared spectroscopy
GDL	Glucono-d-lactone
HFT	High-fiber tofu
HSPI	Heated soy protein isolate
LAB	Lactic acid bacteria
LVR	Linear viscoelastic region
MDF	Micro-sized dietary fiber
MTGase or TGase	Microbial transglutaminase

NDF	Nano dietary fiber
NFE	Nitrogen-free extract
O-IDF	Okara insoluble dietary fibers
SDF	Soluble dietary fiber
SE	Steam explosion
SEM	Scanning electron microscopy
SOS	Soy oligosaccharide
SPI	Soy protein isolate
TGA	Thermogravimetric analysis
TPA	Texture profile analysis
UHPH	Ultra-high-pressure homogenization
W/O/W	Water-in-oil-in-water
WHC	Water holding capacity

List of Symbols

Symbols	Meaning
G'	Storage modulus
G''	Loss modulus
G'_o	Storage moduli at 1 rad/s
G''_o	Loss moduli at 1 rad/s
$tan\,\delta$	Tangent delta
ω	Angular frequency
n'	Influence degree of ω on G’
n''	Influence degree of ω on G’’
$\sigma(t)$	True stress
ϵ	True strain
$F(t)$	Force applied on sample, measured during compression at time t
$l(t)$	Height of sample measured during compression at time t
A_0	Initial cross-sectional area of gel
l_0	Initial height of gel
$W_{pre-dried\ SM}$	Mass of soymilk before the drying in the estimation of soymilk solid content
$W_{dried\ SM}$	Mass of soymilk after the drying in the estimation of soymilk solid content

$W_{pre-diluted\ SM}$	Mass of undiluted soymilk used in the estimation of soymilk solid content by UV-vis absorbance method
W_{gel}	Mass of gel used in the estimation of syneresis
$W_{liquid\ released}$	Mass of liquid released from gel after 24 hours storage in a fridge
W_t	Initial mass of gel used in the estimation of water holding capacity
W_r	Mass of liquid released from gel after centrifugation in the estimation of water holding capacity
A_{400}	UV-vis absorbance measured at the wavelength of 400 nm
A_{595}	UV-vis absorbance measured at the wavelength of 595 nm

Chapter 1: Introduction

1.1. Research Aim

Okara, a valuable resource rich in fiber (53 – 58 %), protein (25 – 28 %), and lipids (9 – 11 %), also contains significant isoflavones and essential minerals, offering nutritional and health benefits [1, 2]. Recent research aims to enhance its utilization in high-fiber tofu [3, 4, 5, 6, 7], but incorporating soymilk with okara for the gelation results in a heterogeneous, gritty network structure due to its high water absorbing capacity and large particle size [82].

To enhance the textural qualities and sensory attributes of soy gels incorporating okara, various okara modification approaches including physical and non-physical have been employed. Physical methods including wet media milling, ultrasound, and ultra-high-pressure homogenization which focus on reducing okara particle size, leading to the increase in surface hydrophobicity and free sulfhydryl groups, and formation of a more uniform gel network [3, 4, 5]. However, nano-sized okara may reduce gel strength due to its high surface charge and water absorption capacity [3, 8]. Non-physical methods offer alternative modifications, like layer-by-layer coatings with chitosan and pectin to improve the compatibility between okara [6] and protein matrix or the use of microbial transglutaminase to form a more organized protein structure wrapping around okara particles [7]. While physical methods require the control of the size of okara particles to form a strong gel, current non-physical approaches are complex and extensive. To the best of the authors' knowledge, the application of okara modified by non-physical approach using food grade chemical in high-fiber tofu remains limited.

Citric acid (CA), a tricarboxylic acid, has been used in tofu production as a coagulant, resulting in gels with high storage modulus, hardness, and water-holding capacity due to its rapid acidification

rate [9, 10]. CA also finds applications in polysaccharide treatments and modifications with its unique acidic and chelating properties. The acid hydrolysis ability of CA has been used to partially remove cellulose, hemicellulose, and lignin from agricultural biomass to facilitate further hydrolysis induced by enzymes [11, 12, 13]. Additionally, CA is used in the extraction of soluble polysaccharide, particularly pectic substances from biomass sources like soy hulls and fruit peels, yielding pectin with higher molecular weight and improved viscosity for thickening and emulsifying purposes [14, 15, 16, 17]. Therefore, the action of CA on okara is hypothesized to hydrolyze okara fibers and release soluble polysaccharides like pectic substances, improving compatibility with the soymilk protein matrix. The excess of CA on modified okara might also interact with soy protein to form a strong soymilk okara gel.

The present study aimed to explore the effects of CA on the structure of okara, and its subsequent effects on the texture profiles and protein-protein interactions within soymilk okara gels. The appropriate level of CA for okara modification was also investigated, considering its impact on fiber degradation and the soymilk gelation process. The structural alterations in okara following CA modifications were examined through visual observations, TGA and FTIR. The impact of CA-modified okara on the characterization of soymilk gel was further assessed through microscopic visualization by confocal laser scanning microscopy, measurements of syneresis, water holding capacity, rheological and mechanical properties, and evaluations of protein-protein interactions.

1.2. Objectives

The main objective of this research was to develop and characterize soymilk okara gel modified by citric acid (CA). To achieve this objective, a series of essential steps were undertaken, illustrated in **Figure 1. 1**.

The initial step involved the standardization of soymilk and soymilk okara gel preparation. The quality of soymilk, particularly its solid content, played a pivotal role in determining the characteristics of the resulting soy gels. Hence, standardizing the soymilk production process and establishing a rapid solid content measurement method were crucial. This phase also encompassed defining the experimental conditions for making soymilk okara gels. It considered factors including the physical state (liquid or solid) of CA and the duration of drying in the okara modification process, with a focus on their impact on okara's structure, as well as the rheological and mechanical properties of soymilk okara gels.

The second step was to revise the preparation of soymilk okara gels for the texture characterization and finalize the methodology of protein-protein interactions of soy gels. Sample prepared for the measurements required a precise shapes and dimensions that needed to be cut from bulk gel. Therefore, exploring alternative methods to prepare soymilk okara gels for rheological and mechanical properties testing to minimize cutting effects was necessary. Additionally, the methodology of evaluating protein – protein interactions in soy gels, adapted from literature, was also revised and modified.

With mentioned two preliminary steps, the final and main objective III could be approached: unveiling the effects of CA on texture profiles and chemical interactions of soymilk okara gels. The concentration of CA used in okara modification was varied from 2.5 to 5 and 10 % (w:w). The alternations of okara’s structure, as well as the homogeneity, micro-characterization, textural properties and protein-protein interactions of soymilk okara gels when varying the concentration of CA were studied. The mechanism of okara modification and gelation using CA was also investigated.

	OBJECTIVE	APPROACHES	CHAPTER
I	Standardization of Soymilk Okara Gels Preparation	• Standardize the soymilk preparation to ensure consistent soymilk quality, reflected from the solid content measured by drying or UV-vis method. • Standardize the soymilk okara gels preparation by studying the effects of states of citric acid (CA) and drying time in okara treatment on: - Structural characteristics (by FTIR) of CA modified okara during the treatment. - Morphological (visual observation, CLSM) and textural characteristics (rheological and mechanical properties) of soymilk okara gels.	3
II	Methodology of Sample Preparation for Texture Characterization and Protein – Protein Interactions Characterization of Soymilk Okara Gels	• Alternative method for soymilk okara gels preparation to minimize the effect of cutting and inconsistency in samples' thickness to the reproducibility and accuracy of textural characterization (rheological and mechanical properties). • Revise and modify the methodology for determination of protein – protein interactions in soymilk okara gels, based on method adapted from literature	4
III	Unveiling the Effects of Citric Acid on Texture Profiles and Chemical Interactions in Soymilk Okara Gels	• Prepare gels containing soymilk and okara modified with CA solution at various concentrations with standardized methodology from chapter 3 and 4. • Conduct visual observation and structural characterization of CA modified okara materials (by TGA, FTIR). • Conduct morphological characterization (visual observation, CLSM), textural profiles (water holding capacity, rheological and mechanical properties) and chemical (protein – protein) interactions of soymilk okara gels	5

Figure 1. 1: Flowchart of the objectives and associated approaches of the Master thesis.

1.3. Thesis Structure

The organization of the thesis consists of six main chapters as follows:

Chapter 1: Introduction

- Overview of the thesis, including research aim, objectives, and thesis structure.

Chapter 2: Literature Review

- Dairy cheese and cheese analogues (Sections 2.1 and 2.2).
- Explores topics related to soybeans, soymilk, okara, soymilk gels, and okara-added soy gels (Sections 2.3 to 2.5).
- Citric acid and its effects on polysaccharides (Section 2.6)
- Maillard reaction and its application in protein-polysaccharides conjugated gels (Section 2.7).

Chapter 3: Standardization of Soymilk Okara Gels Preparation

- Standardization of soymilk preparation to ensure consistent solid content.
- Effects of citric acid's physical state and drying time during okara modification on structural characteristics of okara, as well as the morphological, rheological, and mechanical properties of soymilk okara gels.

Chapter 4: Methodology of Sample Preparation for Texture Characterization and Protein – Protein Interactions Characterization of Soymilk Okara Gels

- Development of sample preparation methods for measuring rheological and mechanical properties to enhance reproducibility and accuracy.
- Revision and modification of methodology for evaluating the distribution of protein-protein interactions within soy gels adapted from literature.

Chapter 5: Unveiling the Effects of Citric Acid on Texture Profiles and Chemical Interactions in Soymilk Okara Gels

- Effects of citric acid on okara modification using TGA and FTIR.
- Discusses the effects of citric acid on the macro and micro characterizations, texture profiles, and protein-protein interactions of soymilk okara gels.
- This chapter has been prepared for submission to the journal “Food Hydrocolloids”.

Chapter 6: Conclusions and Recommendations

- Summarizes the overall findings and provides recommendations based on the research.

Chapter 2: Literature Review

2.1. Cheese Derived from Animal Milk

According to the National Dairy code of Canadian dairy information center [18], cheese is defined as the fresh or matured, solid or semi-solid dairy food produced by coagulating milk, milk products or any combination of these materials using bacterial culture, rennet and/or other suitable coagulating agents. This process also involves partially draining the resulting whey from such coagulation. Cheeses can be categorized into fresh soft, soft, semi-soft (semi-hard), firm, or hard types based on their moisture percent calculated on fat-free basis content as shown in **Table 2. 1** [18]. This classification system is useful for grouping cheeses with similar fundamental characteristics, such as moisture content, which plays a crucial role in determining the cheese's texture, consistency, and compactness [19]. **Figure 2. 1** displays a range of cheese varieties arranged in ascending order based on their moisture content and the production methods. In general, cheeses coagulated using acid tend to be soft, while those set with rennet exhibit a firmer texture [19].

Table 2. 1: Classification of cheese based on moisture content, according to the National Dairy code of Canadian dairy information center *[18].*

	Moisture (%) on fat-free basis content
Soft fresh cheese	≥ 80%
Soft cheese	67 % – 80 %
Semi-soft cheese	62 % – 67 %
Firm cheese	50 % – 62 %
Hard cheese	≤ 50 %

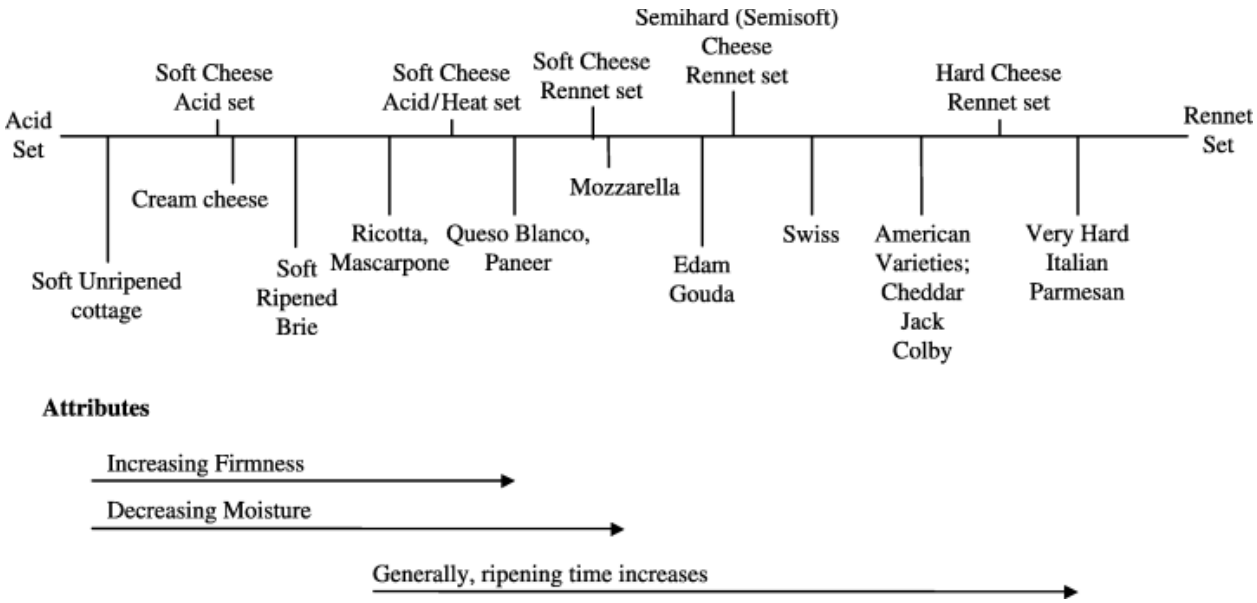


Figure 2. 1: Spectrum of cheese, classified by their softness *[19]*. Reprinted from N. Y. Farkye, "Cheese technology," *International Journal of Dairy Technology*, vol. 57, no. 2 - 3, pp. 91 - 98, 2004, with permission from Wiley.

2.1.1. Milk Proteins

The proteins of milk play the most crucial role in the cheese production. Milk proteins can be classified into two primary categories based on their solubility at a specific condition. Caseins are defined as phosphoproteins precipitating from raw skim milk by acidification to pH 4.6 at 20 °C, whereas serum or whey proteins remain soluble at similar conditions [20, 21].

2.1.1.1. Caseins

Based on the similarity in their primary amino acid sequences, bovine casein proteins are categorized into four families α_{s1}-, α_{s2}-, β- and κ-casein, comprising approximately 38%, 10%, 34%, and 15%, respectively, of the total casein content. Caseins have low levels of secondary and tertiary structures describes as rheomorphic characteristic, resulting in a high degree of flexibility. This unique structural characteristic makes caseins resistant to thermal denaturation, accompanied

with the ability of being susceptible to proteolysis, which is an important aspect of cheese ripening. Furthermore, the variation in the distribution of hydrophobic, polars domains and charged residues throughout the protein sequences result in amphipathic structures with highly surface-active ability [20, 21].

2.1.1.2. Casein Micelle

Within casein proteins, while α_{s1}-, α_{s2}-, and β-caseins undergo precipitation when calcium binds to their phosphoserine residues with a significant low calcium content, κ-casein remains soluble in the presence of calcium and plays a crucial role in interacting with and stabilizing calcium insoluble caseins to initiates the formation of a stable colloidal state called micelle [22]. The structure of casein micelle has been unveiled by numerous efforts of Horne [23], Kruif and Holt [24], Walstra [25] and more, presented in **Figure 2. 2**. It is widely accepted that the core of sub-micelles consists primarily of the calcium-sensitive α_{s1}-, α_{s2}- and β-caseins, with varying amounts of κ-casein mainly located on the sub-micelles' surface. These sub-micelles exhibit varying compositions, primarily falling into two main types: one composed mainly of α_s- and β-caseins, and the other consisting of α_s- and κ-caseins. Small calcium phosphate clusters function as the bridge between sub-micelles, promoting their aggregation into a micelle. In the resulting micelle, κ-casein is positioned on the exterior, and consequently, the molecular chains of the C-terminal end of κ-casein stick out from the micelle surface, forming a "hairy" layer. This layer prevents further aggregation of sub-micelles through steric and electrostatic repulsion and has the responsibility of stabilizing micelles against flocculation [20, 25].

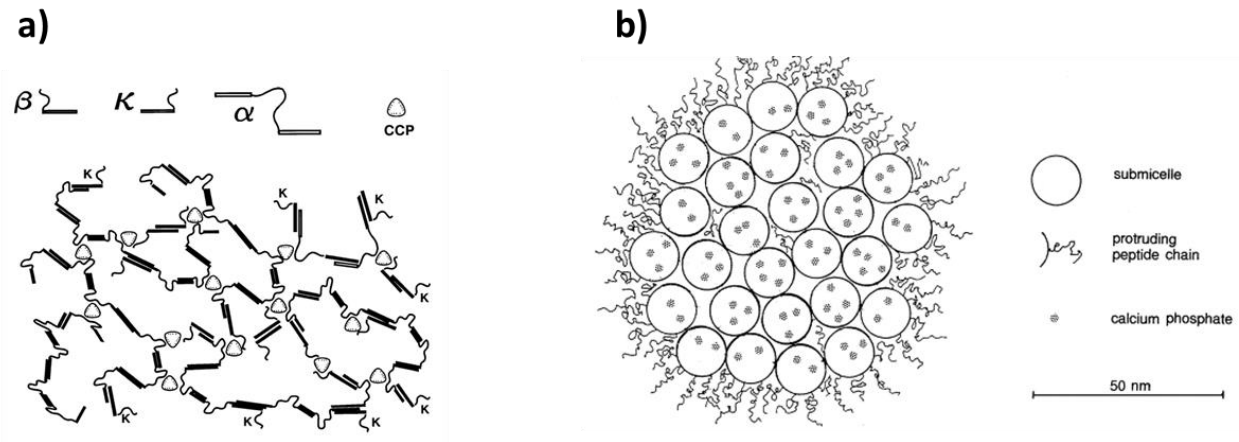


Figure 2. 2: a) Dual bonding model of casein micelle structure proposed by Horne *[23]*. b) Model of casein micelle proposed by Walstra *[25]*. Reprinted from D. S. Horne, "Casein Interactions: Casting Light on the Black Boxes, the Structure in Dairy Products," *International Dairy Journal*, vol. 8, no. 3, pp. 171 - 177, 1998.; P. Walstra, "Casein sub-micelles: do they exist?," *International Dairy Journal*, vol. 9, no. 3 - 6, pp. 189 - 192, 1999. with permission from Elsevier.

2.1.1.3. Whey Proteins

The whey fraction of bovine milk consists of four main proteins including β-lactoglobulin, α-lactalbumin, blood serum albumin, and immunoglobulins. Unlike caseins, whey are globular proteins exhibiting a considerable presence of secondary, tertiary, and quaternary structures. Whey proteins are denatured when subjected to heat, typically at temperatures as low as 90°C for 10 min. While whey proteins do not play a direct role in the cheesemaking process, the heat-induced interactions between whey proteins and κ-casein at temperatures exceeding 75°C can lead to undesirable effects on rennet coagulation. This, in turn, can result in alterations in the structure and rheology of the cheese [20, 21].

2.1.2. Cheesemaking process

The primary goal of the cheesemaking process is to transform liquid milk into a viscoelastic solid substance through the induction of a sol-gel transition, resulting in the collection of curd that typically contains approximately ten times more protein than the original milk [26]. The processing

method varies depending on the type of cheese, however, it generally involves a series of steps that commonly include: Standardization and pasteurization, acidification through the production of lactic acid by selected bacteria, coagulation that can be achieved either through acidification or limited proteolysis, curd processing and ripening (maturation) [19, 26, 20].

2.1.2.1. Standardization and Pasteurization

To ensure consistent cheese production that meets the regulatory standards for a particular cheese variety, the initial step is the standardization of milk by adjusting the ratio between casein and fat (C:F) to a set value. Modifying the C:F ratio can be accomplished by either increasing the casein content through the addition of skim milk powder, condensed skim milk, milk protein concentrate (in liquid or powder form), or caseinates, or by removing fat as cream, or by increasing the fat content through the addition of cream. Other ingredients may also be incorporated into the milk, including annatto for colouring purpose or $CaCl_2$ to assist the later coagulation [19, 20].

Subsequently, standardized cheese milk undergoes pasteurization at 72 °C for 15 s. This pasteurization step is crucial for ensuring public health safety and eliminating undesirable microorganisms that could adversely affect the texture and flavor of the final product. Alternatively, there are other methods available for achieving pasteurization without heat treatment including treatment with H_2O_2, activation of the lactoperoxidase-H_2O_2-thiocyanate system, bactofugation and microfiltration [19, 20].

2.1.2.2. Acidification

In the cheese-making process, acidification occurs through the generation of lactic acid by selected cultures of different species of lactic acid bacteria (LAB) introduced into cheese milk before the addition of rennet for coagulation. The production of lactic acid decreases the pH of both the curd

and whey, which serves several crucial purposes. It enhances the activity of rennet, facilitates the expulsion of whey from the curd, and acts as a deterrent to the growth of undesirable bacteria within the cheese. The presence of LAB not only initiates the production of lactic acid, but also has important role in shaping the flavor profile of the cheese [19, 20]. For instance, in the production of Cheddar, the essential buttery flavor diacetyl is generated by a specific bio variant known as *diactelylactis*, or *L. lactis* citrate^{+}. In addition to LAB, secondary cultures comprising bacteria and yeast can also be introduced. This practice leads to the creation of unique flavors and textures in the resulting cheese. In the case of cheese like Camembert and Brie, a white mold called *Penicillium caseicolum* is employed to impart a snow-white appearance and a subtle flavor profile to the final products [27].

2.1.2.3. Coagulation

The crucial step in the production of all cheese varieties is the coagulation of the casein component within the milk protein system, resulting in the formation of a gel entrapping the fat. This coagulation process can be achieved through several methods, including limited proteolysis (rennet), acidification to pH of 4.6, or acidification to a pH of 5.2 in combination with heating to 90 °C. Among these methods, rennet is the most common coagulant, used with chymosin the most prevalent variety [19, 20]. A schematic representation illustrating the stages involved in cheese curd formation is depicted in **Figure 2. 3**.

In the primary phase, rennet is responsible for the cleavage of Phenylalanine$_{105}$–Methionine$_{106}$ (Phe$_{105}$–Met$_{106}$) bond in κ-casein molecule, resulting in the retention of para-κ-casein within the curd, while the hydrophilic glycomacropeptide is released in the whey fraction. The hydrolysis of κ-casein removes glycomacropeptide, which is also known as the hairy layer of the casein micelle, leading to the destruction of micelle-stabilizing factors and their colloidal stability. In the

secondary phase, when around 80 – 85 % of Phe_{105}–Met_{106} bond is cleaved in the presence of Ca^{2+} at approximately 30°C, the stability of the micelles diminishes to a point when collision occurs, they remain in contact, ultimately form a three-dimensional network referred to as a coagulum or gel [19, 20, 27]. It's important to note that the activity of chymosin and other milk-clotting enzymes is influenced by the pH of the milk, with their activity increasing as the pH decreases [19, 27].

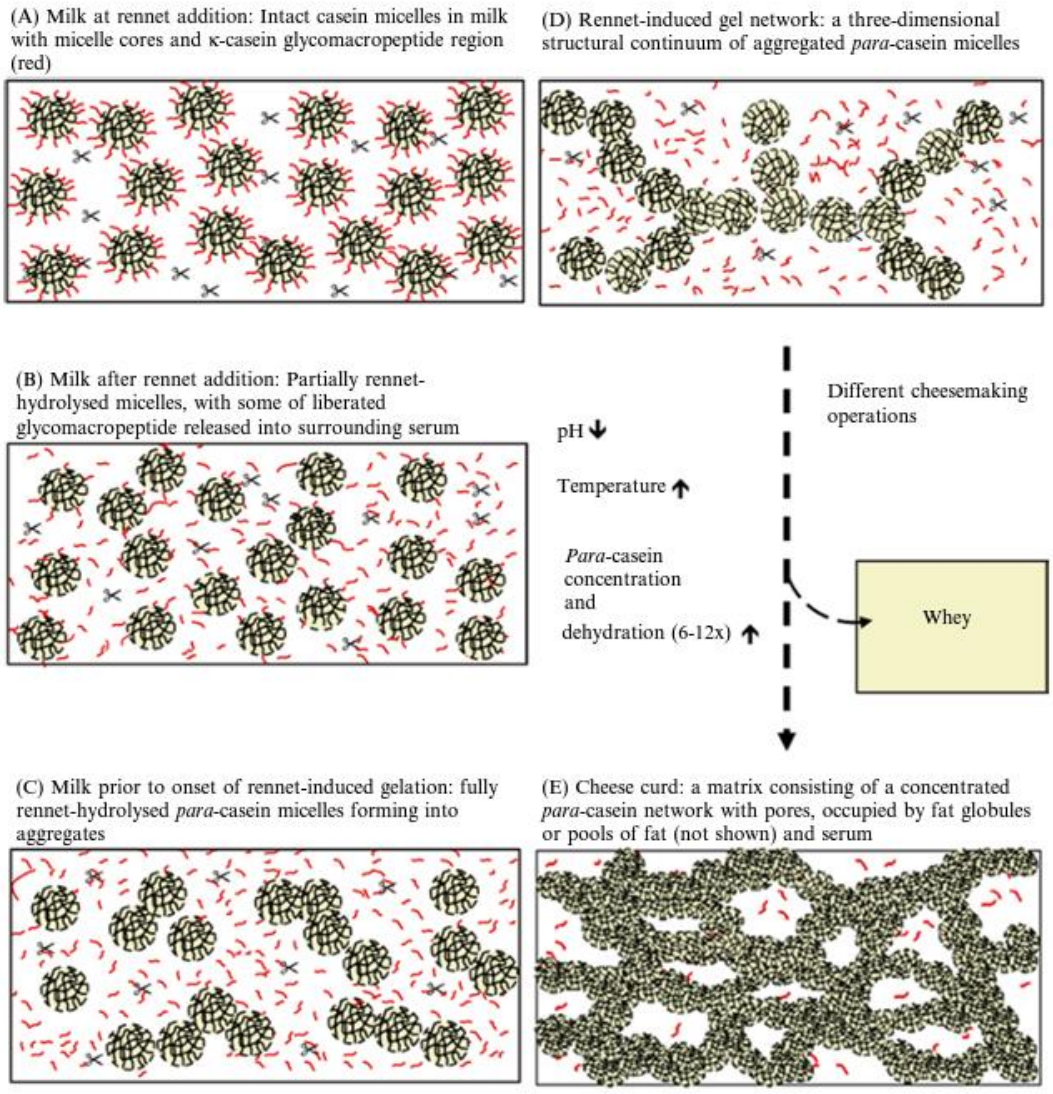


Figure 2. 3: A schematic representation illustrating the stages of the cheese curd formation *[20]*. Reprinted from P. F. Fox, P. L. McSweeney, T. M. Cogan and T. P. Guinee, "Fundamentals of Cheese Science," 2 ed., Springer, 2017., with permission from Springer.

2.1.2.4. Ripening

The maturation of cheese is the result of biochemical and metabolic processes commonly known as glycolysis, lipolysis, and proteolysis. The alterations that take place during the ripening phase ultimately shape the flavor, aroma, and texture of the fully developed cheese and are primarily influenced by the initial manufacturing process. This includes composition, particularly moisture content, NaCl levels, pH, residual coagulant activity and starter culture type [19, 20].

2.1.3. Dairy-based Cheese Analogues

While traditional cheese is primarily derived from animal milk, dairy-based cheese substitutes offer an innovative method by substituting animal milk with casein or whey sources. This substitution allows for the replication of the physical, chemical, and sensory characteristics of specific traditional cheeses at a reduced cost [26, 28]. Dairy-based cheese analogues are primarily categorized into casein and whey-based variants. **Figure 2. 4** provides a visual representation of the methodology for designing dairy-based cheese analogues [29].

Within the casein-based cheese analogue group, protein sources such as acid casein, rennet casein, a blend of acid casein and rennet casein, and Ca/Na-caseinate or their combinations are commonly employed [29]. In a study conducted in [30], mozzarella cheese analogue was prepared using acid casein, rennet casein, and their combination. It was shown that their functional properties including shredding ability, meltability, stretch value, and fat leakage were superior in long-term storage (< 28 days), compared to the traditional mozzarella version. Several cheese analogues have also been developed using Ca-caseinate as the primary protein source. Ca-caseinate's structure comprises water-soluble phosphate groups at one end of the protein, along with a non-polar, fat-soluble group

at the other end, which can function as an emulsifier, reducing the need for additional emulsifying salts [31].

Whey-based cheese analogues, contain whey proteins due to their more favorable effect compared to casein with a greater postprandial protein retention and essential amino acids in the bloodstream. Whey protein outperforms casein and casein hydrolysate in promoting postprandial muscle protein accretion in healthy older men. This enhanced muscle protein synthesis is likely due to its quicker digestion and absorption rates and higher leucine content, which further boosts plasma leucine concentrations post-meal [32]. However, whey protein is not as amphipathic as casein, leading to necessitating the use of additional emulsifying salts in cheese analogue formulations [29]. In addition to whey protein concentrates, whey protein polymers, obtained by heating whey protein isolate solutions, are commonly used in cheese analogues. Whey protein polymers can form a strong disulfide-bonded gel at the pH higher than the isoelectric point, leading to higher viscous characteristic than non-polymerized whey proteins gel [33]. A study in [34] examined the effect of native and polymerized whey protein isolate addition on the surface and microstructural properties of processed cheeses and their meltability. It was observed that at higher concentrations of polymerized whey protein isolates, the surface of cheese analogues became more hydrophobic, while the increase in whey protein isolate addition promoted hydrophilic cheese surfaces. When increasing protein content, the meltability decreased while the stability of cheeses increased.

Furthermore, both casein and whey proteins can be used in combination. A study in [35] investigated the texture, rheology, and meltability of processed cheese analogues prepared using rennet or acid casein with or without the addition of whey proteins. Rennet casein produced firmer cheeses suitable for shredding but with lower meltability, especially when combined with whey protein isolate. In contrast, the use of acid casein in conjunction with whey products yielded a

spreadable-type cheese analogue that was less adhesive, more cohesive, and had superior melting characteristics. The incorporation of whey protein concentrates in mozzarella cheese analogues based on rennet casein was examined in [36]. This incorporation enhanced the nutritional profile of the cheese product, improved its flavor, and reduced its chewiness, ultimately making it a more palatable option as a pizza topping.

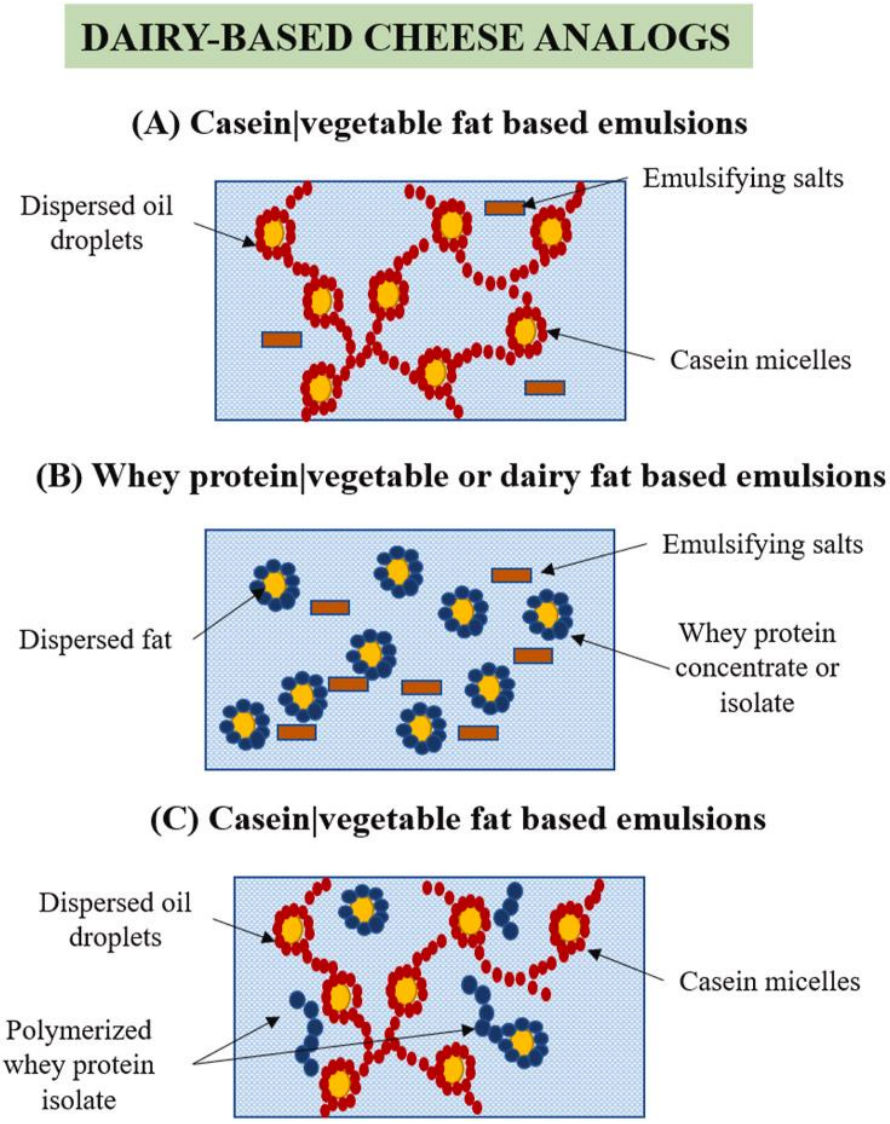


Figure 2. 4: The approach for the design of dairy-based analogues [29]. Reprinted from R. Kamath, S. Basak and J. Gokhale, "Recent trends in the development of healthy and functional cheese analogues-a review," *LWT - Food Science and Techonology*, vol. 155, p. 112991, 2022, with permission from Elsevier.

2.2. Cheese Analogues

While conventional cheese relies primarily on animal milk, cheese analogues represent a novel approach by incorporating plant-based lipid or/and protein sources to replicate the physicochemical and sensory attributes of specific traditional cheeses [26, 28]. Cheese analogues can be viewed as engineered products to replicate a wide range of functional cheese properties including texture profiles, melting and shredding ability [31]. An overview of the ingredients used in creating cheese analogues and their respective function obtained from [37] is found in the

Table 2. ***2***. Manufacturing methods for cheese analogues exhibit some variations, but typically involve common key steps. Initially, the fat is melted and heated to a temperature of 70°C, after which a stabilizer and water are introduced. This mixture is thoroughly blended to create an oil-in-water emulsion. Gradually, proteins are added to the mix, followed by salt and acid addition to initiate the development of the desired texture [31]. Based on the raw materials, cheese analogues are classified into three types, as shown in **Figure 2. 5**: dairy, partial dairy and synthetic or plant-based cheese analogues [28, 29].

The replacement of animal milk fat with vegetable oils, or animal milk with casein lowers the cost compared to conventional animal cheese [28]. Furthermore, cheese analogues that substitute buttermilk with polyunsaturated vegetable fats and oils offer health and dietary benefits, being cholesterol-free [38]. This substitution also extends the shelf life of cheese analogues, addressing the susceptibility to oxidation associated with saturated fatty acids [31]. As for non-dairy or plant-based cheese, the growing demand for these alternatives is driven factors related to lactose intolerance, environmental sustainability, health, animal welfare, and evolving social trends [26].

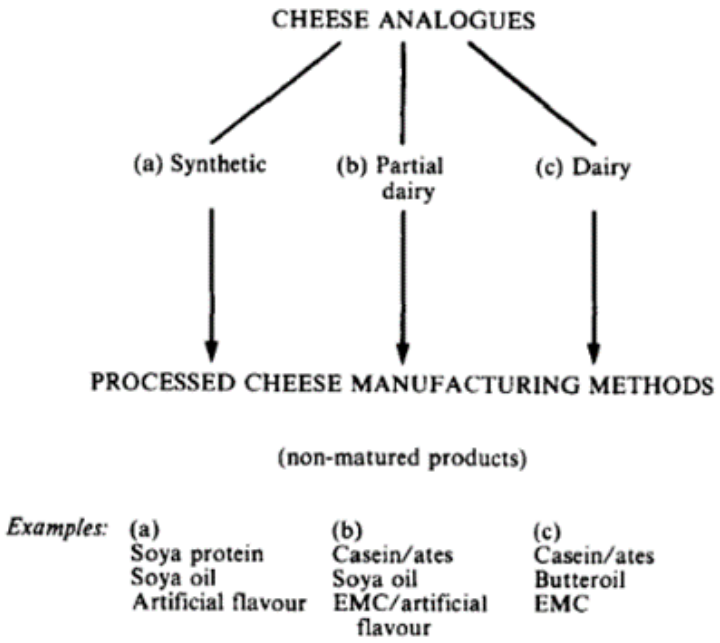


Figure 2. 5: Classification of cheese analogues [28]. Reprinted from M. Shaw, "Cheese substitues: threat or opportunity?," *Journal of the Society of Dairy Technology*, vol. 37, pp. 27 - 31, 1984, with permission from Wiley.

Table 2. 2: Ingredients used in the manufacture of cheese analogues *[37]*. Adapted from R. S. Chavan and A. Jana, "Cheese substitutes: An alternative to natural cheese - A review," *International Journal of Food Science, Technology & Nutrition*, vol. 2, no. 2, pp. 25 - 39, 2007.

Ingredient	Main function	Examples
Fat	Nutritional, desired composition, texture and meltability characteristics, butter oil imparts dairy flavour	Butter, anhydrous milk fat, native or partly hydrogenated soybean oil, corn oil, palm kernel oil.
Milk proteins	Nutritional and functional, desired composition, semihard texture with good shredding ability, flow and stretching characteristics	Casein, caseinates, whey proteins

Vegetable proteins	Nutritional and economic, desired composition and cost reduction.	Soyabean protein, peanut protein, wheat gluten
Starches	Functional, economic, substitution for casein and cost reduction	Native and modified forms of maize, rice potato starches.
Emulsifying salts	Functional, formation of physicochemical stable product; modifies texture properties	Sodium phosphate and sodium citrate.
Hydrocolloids carrageenan	Functional, product stability; modifies texture properties	Guar gum, xanthan gum, carrageenan.
Acidifying agents	Control of pH in final product.	Organic acids e.g. lactic, acetic, citric, phosphoric.
Flavors and flavors enhancers	Imparting flavour; accentuates flavour.	Enzyme modified cheese, starter distillates, wood smoke extracts, spices, sodium chloride, yeast extract.
Colors	Imparting desired colour	Annatto, paprika, artificial colours
Preservatives	Stability, slowing down mould growth; prolongs shelf-life	Nisin, K-sorbate, Ca- or Na-propionate.
Mineralized vitamin preparations	Nutritional, micronutrient content	Magnesium oxide, zinc oxide, iron, vitamin A palmitate, riboflavin, thiamine, folic acid.

2.2.1. Partial Dairy-based Cheese Analogues

The formulation of partial dairy-based cheese analogues is based on the concept of the replacement of dairy fat such as butter, cream by vegetable oil or polysaccharides [29]. Dairy fat sources can be replaced with more cost-effective vegetable oils, which serve as fat mimetics. Common options include soy oil, rapeseed oil, palm oil, or their hydrogenated counterparts [29]. The substitution of animal fat with vegetable polyunsaturated fatty acids can result in the alternation in the ripening process, microstructure, and sensory characteristics of the cheese. An illustrative study cited in [39] investigated the impact of butter oil, partially hydrogenated soybean fat, and soybean oil on the functionality, rheology, and sensory acceptance of spreadable cheese analogues and reported that analogues made with partially hydrogenated soybean fat or soybean oil exhibited smaller fat globule sizes, resulting in reduced melting, diminished spreadability, increased hardness, and higher elastic and viscous moduli. The increased hardness and shear resistance may be attributed to the limited number of dispersed fat droplets due to their larger mean size, consequently forming a high protein mass per unit fat area. High protein densities in cheese analogues have been correlated with increased hardness and firmness, as the protein matrix is the primary structural component in cheese analogues that offers the highest resistance to deformation [40].

The use of polysaccharides such as inulin and modified starches and gum can also function as dairy fat replacer to reduce the fat content of cheeses [29]. Inulin, with the added benefit of not being hydrolyzed by gastric secretions, serves as a valuable prebiotic. It is a versatile additive, functioning as a dietary fiber, sweetener, and enhances organoleptic properties. In cheese, inulin is predominantly employed both as a fat replacer, due to the similarity in its rheological properties to solid fats, and as a texture modifier [41]. Inulin promotes proteolysis by the cultures, leading to improved springiness and reduced gumminess [29]. In a study conducted in [42], native and

retrograded resistant starch were used to as source of fibre to partially replace fat in imitation cheese. The resulting imitation cheeses exhibited increased hardness and enhanced rheological properties as the content of fiber increased. An increase in cohesiveness was observed in imitation cheese with the addition of native resistant starch, but this effect was not observed in the case of cheeses containing retrograded resistant starch. The substitution of up to 50 % of fat with resistant starch reinforced the internal structure without impacting the meltability.

2.2.2. Plant-based Cheese Analogues

Plant-based cheese analogues are prepared purely from plant-based ingredient, characterized by high content of fiber and complex carbohydrates. Based on the processing route, plant-based cheese analogues can be categorized into two types: material fractional route and tissue disruption route, as depicted in **Figure 2. 6**. In the fractional route, isolated and refined functional ingredients such as polysaccharides, proteins and fats are input materials. The fractionated protein and/or polysaccharide components are typically dissolved in water and homogenized with oil to form an oil in water emulsion. In the tissue disruption route, the foundation is an intact, plant-based raw material. In both processing routes, the final mixture can be solidified using a range of methods, including heating, cooling, pH adjustment, enzyme incorporation, or salt addition [26].

The cheese analogues obtained by the fractional route cheese, starch and proteins are the most common ingredients to establish a gel network. Starch is favored due to their remarkable capacity to generate a thick paste or gel through gelatinization obtained by heating and retrogradation and a subsequent cooling stage. After these stages, fluid and other ingredients are successfully entrapped within the 3D-polysaccharide network [43]. To achieve the desired functional properties, an assortment of starch types is needed blending or subjecting to modifications [44]. Globular plant proteins can also be used to generate a gel network, forming colloidal particles with

dimensions around 200 nm, similar to casein micelles, through controlled aggregation. This aggregation can be induced by thermal treatment at pH values below the protein's isoelectric point, acid treatment or the use of enzymatic cross-linkers. However, the distinct aggregation behavior of plant proteins in contrast to casein micelles, leads to variations in the texture properties of the resulting gels [45]. Furthermore, similar plant proteins can yield diverse texture characteristics by manipulating the gelation conditions as demonstrated in [46]. In the case of pea protein, the sequential application of thermal, acidification, and enzymatic treatments induces gelation, resulting in an array of final gel structures, ranging from soft to firm plant-based cheeses [46].

In the tissue disruption approach, whole plant materials are broken down into a colloidal dispersion comprising small particles and dissolved substances, often referred to as plant-based milk or a plant-based paste. Subsequently, the blend is converted into a cheese analogue by induction of a sol-gel transition, using heat treatment, acidification, enzymatic crosslinking, and salting-out, either alone or in combination. The gelation of plant-based milk or paste closely resembled the production of conventional cheese from regular animal milk [26].

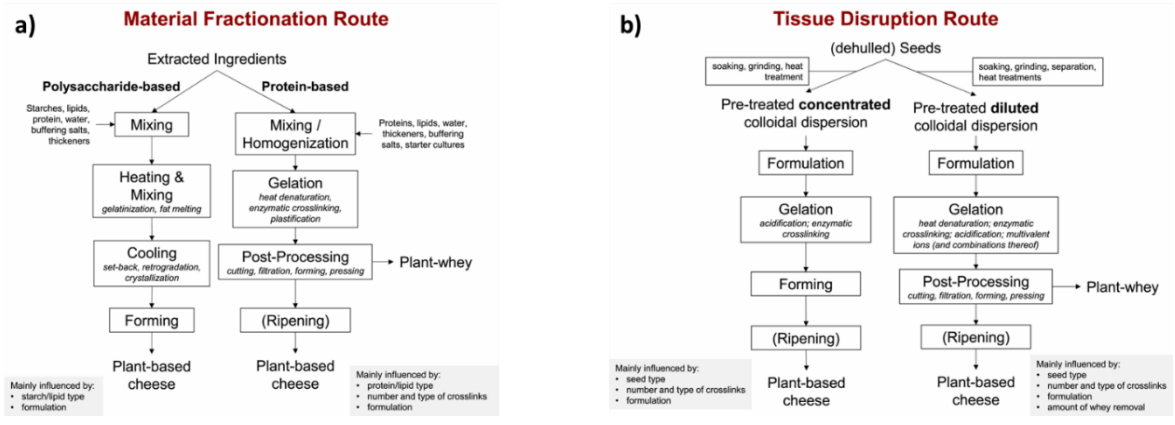


Figure 2. 6: Flow process chart comparing the different processing routes for plant-based cheese production: a) material fractionation route, b) tissue disruption route [26]. Reprinted from L. Grossmann and D. J. McClements, "The science of plant-based foods: Approaches to create nutritious and sustainable plant-based cheese analogs," *Trends in Food Science & Technology*, vol. 118, pp. 207 - 229, 2021, with permission from Elsevier.

2.3. Soybeans

2.3.1. Soybean Morphology and Composition

The soybean seed consists of two main components: the seed coat (also known as the hull) and the embryo. The embryo constitutes 90% of the seed's overall weight and includes two cotyledons along with the embryonic axis [47]. The main constituent of the soybean, cotyledon cells, are organized within the bulk in a space-filling arrangement, as depicted in **Figure 2. 7** [48]. Within the cotyledon cell, the primary wall is comprised of pectin, hemicellulose and cellulose microfibrils cross-linked with proteins, whereas the secondary wall contains cellulose and hemicellulose connected to protein molecules [48, 49]. Soy protein and oil are encapsulated within distinct subcellular structures, denoted as protein bodies and oil bodies, respectively [47]. Soybean seeds contain approximate 40 % protein, 35 % carbohydrates and 20 % lipid on a dry weight basis and minor constituents, trypsin inhibitors, phytates, and oligosaccharides [47, 50]**.**

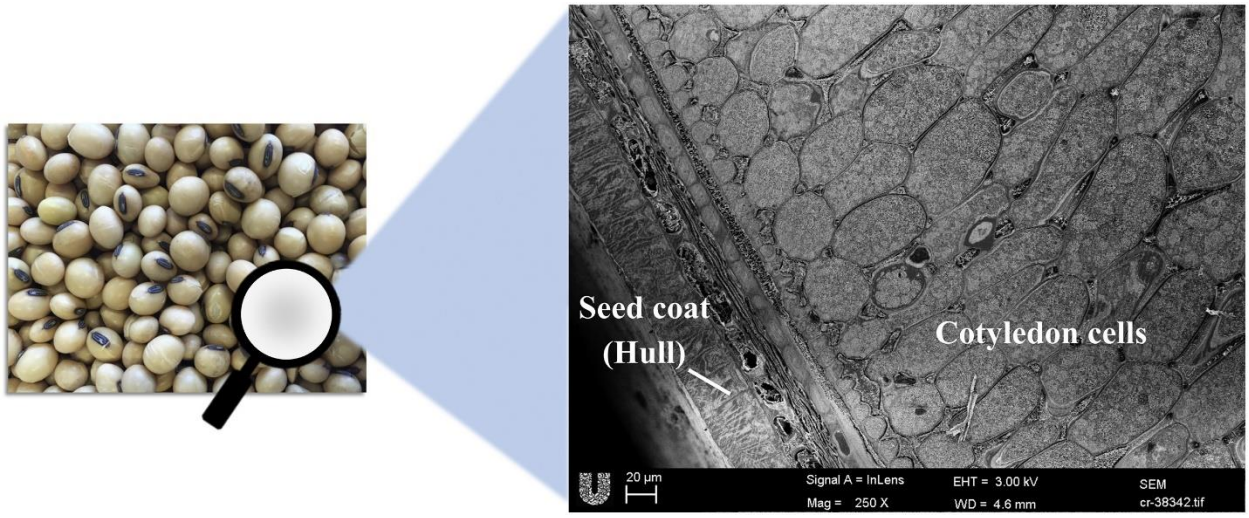


Figure 2. 7: Image of soybeans (about 5 mm in size) and scanning electron microscopy (SEM) image of a pre-soaked soybean [48]. Reprinted from K.E.Preece, N.Hooshyar and N.J.Zuidamc, "Whole soybean protein extraction processes: A review," *Innovative Food Science & Emerging Technologies*, vol. 43, pp. 163-172, 2017, with permission from Elsevier.

2.3.1.1. Soy Proteins

The protein content of soybeans is approximately 40 % on a dry matter basis. When water is used for extraction, about 90 % of these proteins are obtained. Subsequently, approximately 90 % of the extracted proteins can be precipitated within the pH range of 4.5 to 4.8. The precipitated proteins are known as acid-precipitable proteins or soybean globulins, also referred to as storage proteins [51]. Soybean globulins are composed of 4 major components, labeled as 2S, 7S (β-conglycinin), 11S (glycinin) and 15S according to their sedimentation coefficients, which reflect their settling characteristics during centrifugation [52]. The 2S fraction contains the trypsin inhibitors and other small molecular weight enzymes, while the 15S fraction is reported to be a dimer of glycinin [53].

The 7S (β-conglycinin) and 11S (glycinin) fractions make up more than 80 % of the total protein content, with the ratio of 7S to 11S varying between 0.5 to 1.3 depending on the soybean varieties [52]. The structure the of 7S (β-conglycinin) and 11S (the glycinin) are made up of specific subunits as presented in **Figure 2.** ***8*** [54]. The β–conglycinin has the molecular weight ranging from 180 – 210 kDa and has a hetero-trimer structure of three subunits α, α' and β that are non-covalent associated. The glycinin with molecular weight of 320 kDa forms a hexamer structure of acidic subunits A and basic subunits B that are linked by a disulfide bond [52].

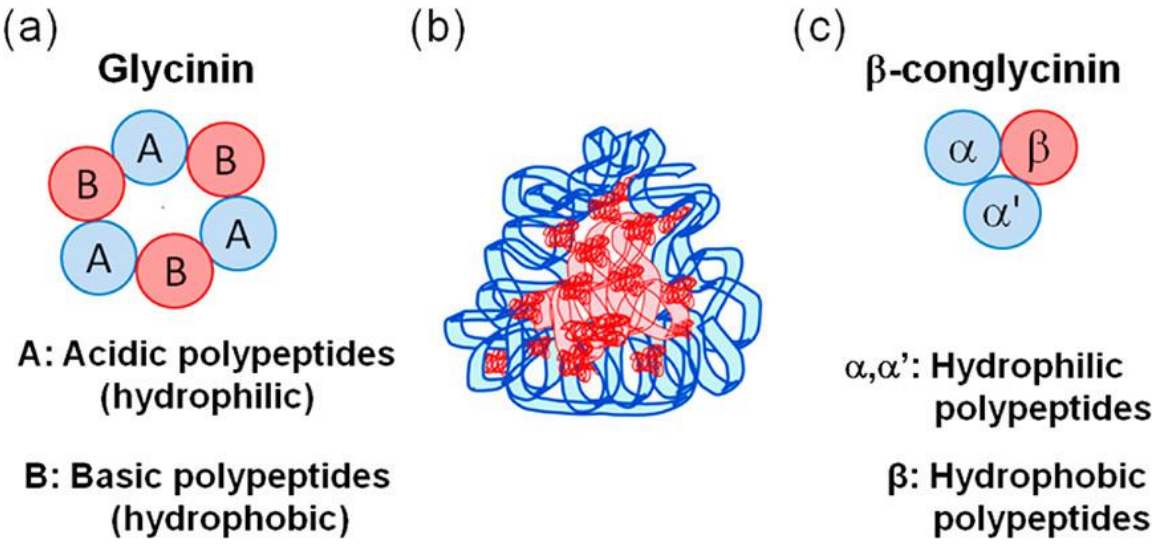


Figure 2. 8: Schematic representation of the structure of a) soybean glycinin 11S and c) β-conglycinin 7S; b) A schematic illustration of the distribution of hydrophobic residues in soybean glycinin and β-conglycinin *[54]*. Reprinted from C. Salas, O. J. Rojas, L. A. Lucia, M. A. Hubbe and J. Genzer, "On the Surface Interactions of Proteins with Lignin," *ACS Applies Materials and Interfaces*, vol. 5, no. 1, pp. 199 - 206, 2013, with permission from ACS publications.

2.3.1.2. Soy Carbohydrates

Soybeans contain roughly 6 % crude fiber and 27 % nitrogen-free extract (NFE) on a dry basis. NFE is made up of non-structural carbohydrates, while the crude fiber and the remaining constituents are structural polysaccharides [55].

Approximately 50 % of the carbohydrate content of soybeans are non-structural carbohydrates which encompasses low molecular weight sugars, oligosaccharides, and storage polysaccharides which represents 14 %, 5 % and 1 % on a dry basis, respectively. Among these, the low molecular weight sugars, such as sucrose, glucose, and fructose, are primarily located in the cotyledon of soybeans, with sucrose being the predominant component [56]. The major oligosaccharides in soybeans are galacto-oligosaccharides, including stachyose, raffinose, and verbascose in descending order. These galacto-oligosaccharides are composed of 1, 2, or 3 α-1-6 linked units of

galactose, linked through α-1-3 bonds to a terminal sucrose [57]. Storage polysaccharides are present in soybeans in relatively low concentrations, with starch being the main representative [55].

The remaining 50 % of the carbohydrates comprises structural polysaccharides, commonly referred to as dietary fiber, which includes cellulose, pectin, and hemicelluloses [55]. Cellulosic and hemicellulosic polysaccharides are insoluble, unbranched polymers. Cellulose is made up of linear β-1,4 linked d-glucose residues held together through hydrogen bonding and van der Waals forces. Hemicelluloses are lower molecular weight polysaccharides with xylan as their primary structural component that is formed by β-1,4 linkages between xylose residues with a small proportion of glucuronic acids attached as monomeric branches via 1–2 linkages [58]. Soybean pectin is soluble polysaccharide, with diverse and complex composition, consisting of both acidic and neutral components. In comparison to citrus pectin, the acidic pectic elements in soybeans are branched and possess a heterogenous monosaccharide composition, primarily including galacturonic acid, galactose, arabinose, xylose, fucose, and rhamnose. These monosaccharides are organized into three main types, homogalacturonan as the backbone, rhamnogalacturonan I and rhamnogalacturonan II as hairy regions [59].

2.3.1.3. Soy Lipids

Soy lipids are primarily stored in the soybean cotyledon and constitute about 20 % of its total weight on dry basis [47]. From a physiological standpoint, soybean lipids have a variety of functions, including being an integral component of membranes, an energy reservoir, signaling molecules, defense against pathogens, and solvent medium for various lipid-soluble substances [60].

Storage lipids are located primarily within oil bodies as triacylglycerols, whose structure is composed of three fatty acids esterified to a glycerol backbone. The most prevalent fatty acids making up the soybean triacylglycerols are linoleic acid (18:2), followed by oleic (18:1), palmitic (16:0), linolenic (18:3), and stearic (18:0) acids, in decreasing level. The composition and distribution of the fatty acids play a crucial role in determining the quality of the oil, its nutritional value, flavor, oxidative stability, melting point, and crystallization characteristics. Soybean oil is a rich source of unsaturated fatty acids, which contain double bonds in structure, leading to various positive effects to human health. However, the number of double bonds is also directly related to oil stability, which is relatively unstable and susceptible to oxidation and results in the development of off flavors [47].

Soybean seeds also contain other classes of lipids, including phospholipids, sphingolipids, and tocopherols. Phospholipids and sphingolipids are primarily found in the membranes of soybean seeds. The structure of phospholipids closely resembles that of triacylglycerols, with the difference being the replacement of the fatty acid on the sn-3 position of the glycerol molecule with a phosphate group. Sphingolipids are non-glyceride lipid components that have a ceramide backbone to which a sugar or phosphorylcholine group is attached. Ceramides consist of a fatty acid linked to a long-chain amino alcohol, sphingosine, through an amide bond. Tocopherols have a vital role in the defense mechanisms of plants, as they protect biological membranes from the oxidative degradation of polyunsaturated fatty acids. They act as natural safeguards to preserve the integrity of these membranes [47].

2.3.2. Soymilk

Soymilk is the aqueous extract of whole soybeans rich in protein, iron, unsaturated fatty acids, and niacin with lower amounts of fat, carbohydrates, and calcium when compared to cow's milk and

human milk. The composition of soymilk may vary depending on the extraction methods, with the average content of 3 % proteins, 2 % fat and 2 % non-lactose carbohydrates, on wet basis [61].

Traditionally, soymilk is prepared from whole soybean through a multi-step process. This process typically involves soaking soybeans in water overnight, wet grinding, heating and finally filtering the mixture through cheese cloth to separate the water-soluble portion from water-insoluble one [61, 62]. The traditional method is referred to cold-grind method, whereas the hot-grind method involves the grinding of soybeans in hot water [61]. The heating step is considered essential in soymilk production to ensure food safety, extend shelf life, and deactivate undesirable biologically active compounds such as trypsin inhibitors and lipoxygenase [63].

In addition to the traditional cold-grind and hot-grind methods, numerous studies have been dedicated to enhancing the soybean processing process and eliminate the unpleasant beany flavor, a significant challenge affecting the sensory appeal of soy-based products. For instance, a study conducted by Schroder and Jackson introduced the blanching technique, involving presoaking the beans in aqueous ethanol and subjecting them to thermal treatment with hot water. This method effectively deactivated lipoxygenase activity, resulting in a reduction of the beany flavor [64]. During the wet grinding phase, lipids in soybeans can undergo oxidation in the presence of water and air. This oxidation process is catalyzed by lipoxygenase and leads to the development of unwanted flavors in soymilk. Grinding soybeans at either high or low temperatures or at a low pH has proven effective in reducing the generation of off flavors [65]. Several other techniques have been applied to improve flavor and protein recovery by regulating factors such as soaking time and temperature, the bean-to-water ratio, the grinding method, filtration of the slurry before or after heat treatment, as well as heat treatment temperature and duration [66].

2.3.3. Okara

Okara, also known as soy pulp, is the residue left behind after the extraction of soymilk from the ground soybeans. Typically, for every kilogram of soybeans processed to make soy milk, approximately 1.1 kilograms of fresh okara is generated [67]. The nutritional composition of okara, has been extensively examined and is influenced by processing conditions, post-processing treatments, and the specific soybean cultivar. The average composition consists of approximately 25 – 38 % protein, 15 – 58 % dietary fiber, 4 – 5 % carbohydrates, and 9 – 22 % lipids on a dry basis. The fiber component of okara has been reported to include approximately 12 % hemicellulose, 6 % cellulose, 12 % lignin, and 0.17% phytic acid [68].

The structure of okara consists of intact cotyledon cells, cell walls of disrupted cells and agglomerated material in okara [69]. Plant cell wall is a complex matrix of polysaccharides, with around 30 % cellulose, 30 % hemicellulose and 35 % pectic substances, along with a minor 1 – 5 % content of structural protein. Within the plant cell wall, cellulose and hemicellulose polymers contribute to the wall's rigidity, while pectin imparts fluidity to the gel-like polysaccharide matrix. Cellulose, an insoluble unbranched polymer of β-(1,4)-D-glucose, forms a crystalline microfibril with a diameter of roughly 3 nm by associating with other cellulose chains through hydrogen bonding and Van der Waals forces. Hemicelluloses, are a heterogeneous group of polysaccharides with β-(1,4)-linked backbones featuring an equatorial configuration at C1 and C4, share a structural similarity among their backbones and are recognized for their tight binding to cellulose microfibrils via hydrogen bonds [70, 71]. Pectin contains “egg-box” regions where pectin molecules crosslink with others through calcium ion bridges, [71, 72]. The structural model of okara fiber including egg-box region and non-egg-box region, containing protein is depicted in **Figure 2. 9** [72].

With a significant volume of okara being generated as a byproduct of the soy milk and tofu manufacturing processes, various disposal methods such as animal feed, incineration, and landfill disposal have been employed [67]. However, in recent years, there has been a growing body of research focused on alternative methods for the utilization of okara including food ingredients, and biological applications [68]. For example, a study in [73] investigated the hypoglycaemic effects of bread and noodles that incorporated okara at concentrations ranging from 10 to 25 %. The findings indicate that bead and noodles formulated with okara exhibited lower glycemic index *in vivo*, compared to formulations without okara. Moreover, okara is also utilized for chemical production, such as citric acid obtained by fermentation with *Aspergillus niger* and *Aspergillus terreus* [74].

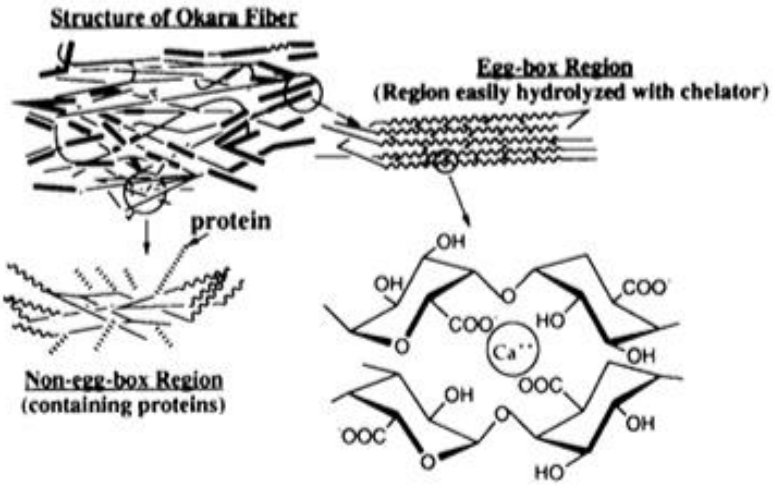


Figure 2. 9: Schematic representation of the structure of okara fiber *[72]*. Reprinted from H. Yoshii, T. Furuta, H. Maeda and H. Mori, "Hydrolysis Kinetics of Okara and Characterization of Its Water-soluble Polysaccharides," *Bioscience, Biotechnology, and Biochemistry*, vol. 60, no. 9, p. 1406–1409, 1996, with permission from Oxford University Press.

2.4. Soymilk Gel (Tofu)

Tofu is a highly hydrated gel-type food, which is formed by the gelation of soybean proteins. Based on the texture characteristics or is preparation, tofu can be categorized into soft or firm, packed or

pressed, and non-fermented or fermented tofu [75]. Typically, traditional tofu production involves a series of key operations, pre-treatment of raw soybeans, soaking, grinding, slurry heating, filtration, coagulation and pressing. These operations significantly impact the yield, texture attributes, and flavor of the resulting tofu, with critical parameters of thermal treatment of soymilk, types of coagulant, and pressing methods [76].

This section is dedicated to the methods of solidification in the tofu-making process, which include thermal treatment, the use of salt, acid and enzymatic coagulants (as shown in **Table 2. 3**) all contributing to the development of the desired tofu texture.

Table 2. 3: Typical coagulants and their mechanism in tofu production *[76]*. Adapted from Q. Zhang, C. Wang, B. Li, L. Li, D. Lin, H. Chen, Y. Liu, S. Li, W. Qin, J. Liu, W. Liu and W. Yang, "Research progress in tofu processing: From raw materials to processing conditions," *Critical Reviews in Food Science and Nutrition*, vol. 58, no. 9, pp. 1448 - 1467, 2017, with permission of Taylor & Francis.

Type	Typical coagulant	Possible mechanism
Acid	Glucono-d-lactone (GDL)	Reduction of pH to the isoelectric point of soybean proteins, and isoelectric precipitation via hydrophobic and electrostatic interaction
Salt	$CaCl_2$, $CaSO_4$, $MgCl_2$, $MgSO_4$	Cation Bridge theory
Enzyme	Microbial transglutaminase (MTGase)	Formation of cross-links or e-(g-glutamyl)lysine isopeptide bonds in protein polymers with high molecular weights

2.4.1. Heat-induced Soy Gel

The gelation process of soy protein isolate (SPI) under heat treatment can be described in four main steps, as depicted in **Figure 2. 10**. To begin, native globulins initially dissociate into smaller aggregates upon exposure to heat. Subsequently, these small aggregates reassociate into compact, spherical particles, typically with a radius ranging from 30 to 50 nm, followed by the formation of self-similar aggregates. The bonds between the proteins within these aggregates are sufficiently strong to resist cooling and dilution. Finally, self-similar aggregates percolate and form a system spanning network [77].

The thermal aggregation behaviors of soy β-conglycinin (7S) and glycinin (11S) at neutral pH was studied in several studies [78, 79, 80]. β-conglycinin is composed of three subunits, namely α, α′ and β, which are linked by hydrophobic interactions, whereas glycinin is comprised of six subunits, each linked through disulfide bonds at acidic A and basic B dimers [80]. Thermal studies using differential scanning calorimetry (DSC) showed that the denaturation temperature of β-conglycinin and glycinin is 77 °C and 92 °C, respectively [79]. As presented in **Figure 2. 11**, during heating, β-conglycinin forms limited-size, soluble aggregates, while glycinin creates insoluble aggregates with a densely packed core and a less dense outer shell. When a mixture of glycinin and β-conglycinin is thermally treated, both globulins dissociate into subunits. The dissociated β subunits of β-conglycinin have a preference for interacting with the basic polypeptides of glycinin, potentially contributing to the formation of a three-dimensional network in gels [80]. However, heating glycinin with β-conglycinin results in the decrease in size and compactness of the formed protein aggregates. This finding can likely be attributed to the presence of hydrophilic groups in the structure of β-conglycinin, which occupies the surface of the complex aggregates and terminates the aggregation of glycinin [78].

In order to enhance the texture qualities of tofu, a two-step heating process was explored based on the varying denaturation temperatures of soy proteins, specifically β-conglycinin and glycinin [81]. Soymilk with solid content ranging from 10 – 12 % was initially heated at 75 °C for 5 min and then subsequently heated at 95 °C for another 5 min. In comparison to the conventional one-step heating process (95 °C, 5 min), the two-step heating method increased the soymilk viscosity by 150 % and the tofu's apparent Young's modulus by 20 %, along with reduction in syneresis by 10 %. It is explained that while one-step heating causes dissociation of both β-conglycinin and glycinin simultaneously, two-step heating first leads to the dissociation of β-conglycinin at 75 °C, followed by dissociation of glycinin at 95 °C. During the initial step at 75 °C, the dissociated subunits of β-conglycinin tend to unfold, aggregate, and create a network that is evenly distributed throughout the soymilk system until the dissociation of glycinin. Consequently, after the second heating step, the dissociated subunits of glycinin interact with the networks formed by β-conglycinin to create larger yet finer and more organized macrocomplex structures [81].

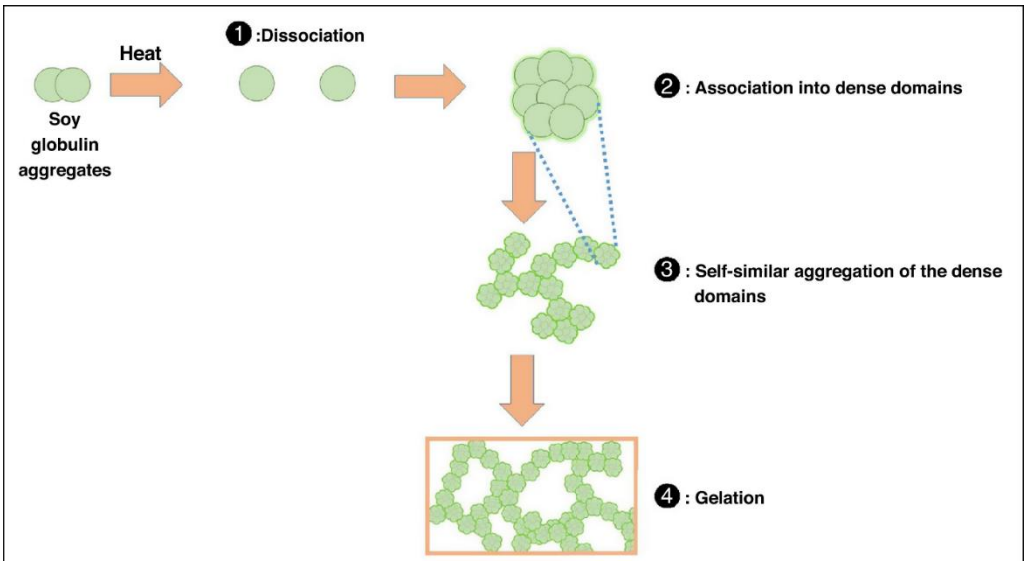


Figure 2. 10: Schematic representation of the steps leading to the gelation of soy protein isolate in aqueous solutions during heating *[77]*. Reprinted from T. Nicolai and C. Chassenieux, "Heat-induced gelation of plant globulins," *Current Opinion in Food Science*, vol. 27, pp. 18 - 22, 2019, with the permission from Elsevier.

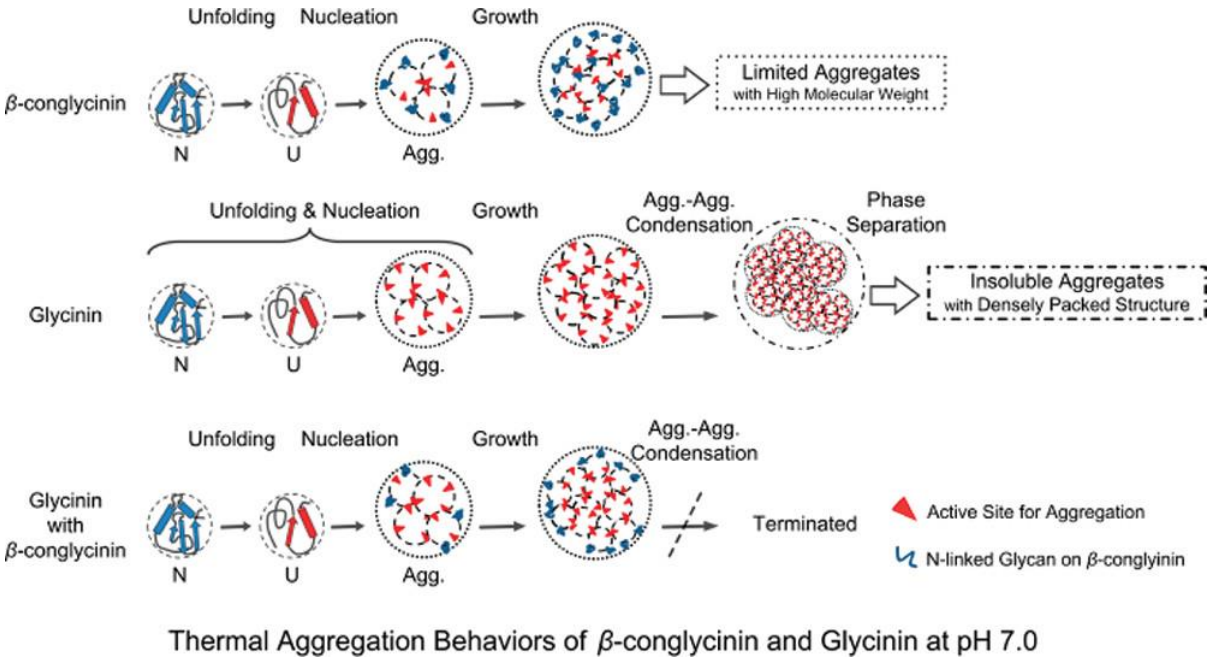


Figure 2. 11: Schematic depiction of β-conglycinin and glycinin thermal aggregation behavior at pH 7.0. N, native state; U, unfolded state; Agg., aggregates [78]. Reprinted from J. Guo, X.-Q. Yang, X.-T. He, N.-N. Wu, J.-M. Wang, W. Gu and Y.-Y. Zhang, "Limited aggregation behavior of β-conglycinin and its terminating effect on glycinin aggregation during heating at pH 7.0," *Journal of Agricultural and Food Chemistry*, vol. 60, no. 14, pp. 3782 - 3791, 2012, with permission from ACS Publications.

2.4.2. Acid-induced Soy Gel

Common acid coagulants employed in tofu production include glucono-d-lactone (GDL), lactic acid bacteria (LAB) and organic acids such as citric acid. The application of acid coagulants in tofu process involves the lowering of the pH level to the isoelectric point of soybean proteins facilitating the isoelectric precipitation of denatured soy proteins [82].

The detailed acid-induced gelation process is visually depicted in **Figure 2. 12**. Initially, as the thermal treatment progresses, protein molecules undergo denaturation, exposing more hydrophobic regions. The introduction of protons, induced by the acid coagulants, neutralizes the negatively charged denatured proteins, leading to the formation of protein aggregates through

hydrophobic interactions. The formation of these gels occurs via random aggregation and often results in turbidity, typically occurring in the vicinity of the isoelectric point [83].

In a study outlined in [84], an investigation was conducted into the variations in physicochemical and microstructural attributes of soy protein gels induced by LAB, GDL, and citric acid (CA). The findings revealed that the rate of acidification plays a pivotal role, directly influencing the distinctions in the texture, rheological properties, and microstructure of these acid-induced gels. CA-induced soy gel has the highest acidification rate, while soy gel acidified by LAB has the lowest rate. The LAB-induced soy gel has a strong hardness, a good texture and high water holding capacity, but significant lower viscoelastic properties, compared to GDL and CA gels. The microstructure of the GDL gel is the most densely packed gel. These results indicate that acidification conditions impact the degree of rearrangement that aggregating particles may undergo at an early stage of the gelation process. The higher level of acidification leads to the increase in the compactness of resulting gel [84].

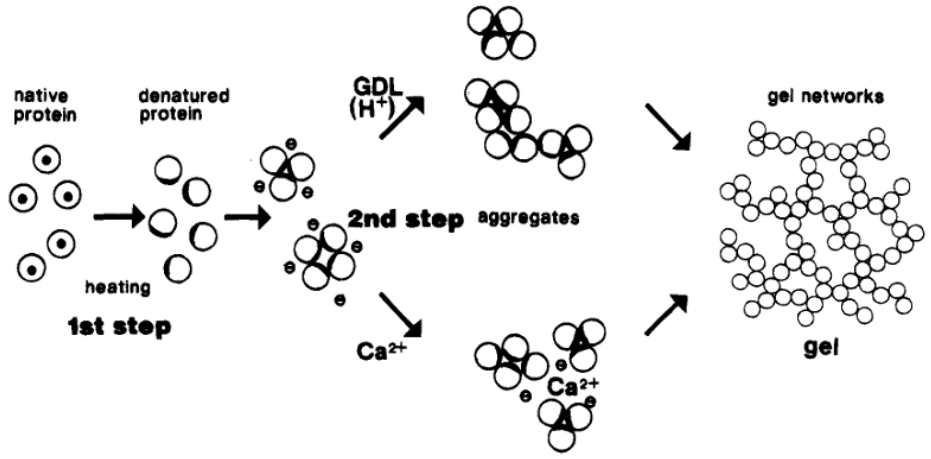


Figure 2. 12: Gelation mechanism of soybean proteins in the presence of GDL or CaSO4; Circles are denoted as protein molecules and black area is denoted as hydrophobic regions [83]. Reprinted from K. Kohyama, Y. Sano and E. Doi, "Rheological characteristics and gelation mechanism of tofu (soybean curd)," *Journal of Agricultural and Food Chemistry*, vol. 43, pp. 1808 - 1812, 1995, with permission of ACS Publications.

2.4.3. Salt-induced Soy Gel

Commonly used salt coagulants in tofu production include gypsum that is also referred as $CaSO_4.2H_2O$, and nigari, which is a combination of magnesium, calcium, and potassium ions as well as chloride, sulfate, iodide, and other ions [82]. The mechanism behind soy protein gelation induced by salt coagulants is not consistently well-defined [85, 86].

In [85], F.J Kao et.al represented the mechanism of calcium ion - induced soy gel with the Cation Bridge theory. The introduction of Ca^{2+} ions serves to mitigate the electrostatic repulsion between negatively charged denatured soy proteins. This reduction in electrostatic repulsion prompts protein aggregation, with Ca^{2+} ions acting as bridges to connect adjacent charged carboxylic groups with neighboring protein molecules [85]. Another gelation mechanism attributed to salt coagulants proposed in [86], involves an initial reaction of Ca^{2+} ions with phytic acid to produce non-ionizing products. These non-ionizing products are capable of attenuating the electrostatic screening effects of ions on protein molecules. This, in turn, fosters interactions between calcium ions and non-particulate soybean proteins, leading to the formation of new protein particles [86].

The effectiveness of gelation, as well as the resulting yield, texture, and taste of tofu, is influenced by the type of salt, its concentration, stirring speed, duration, and temperature [82]. Additionally, the rate of gelation, often overlooked, can also impact the properties of soy gels and tofu. Traditional salt coagulants like bittern are known for their rapid action, which can lead to undesirably high hardness and non-uniformity in tofu. Moreover, this quick gelation may result in reduced water-holding capacity, potentially leading to the loss of nutritional constituents and moisture [87]. To address this challenge, water-in-oil-in-water (W/O/W) emulsion coagulants containing a bittern solution as the internal aqueous phase have been developed. Replacing

traditional salt coagulants with (W/O/W) emulsion coagulants has been shown to slow down the gelation rate, subsequently increasing or modifying the yield and textural properties of tofu [87].

2.4.4. Enzyme-induced Soy Gel

In addition to acid and salt, enzymes can also be coagulants in the tofu-making process. Enzymatic coagulants have the capability to gradually break down soybean proteins in tofu, resulting in flavor enhancement compared to acid-induced tofu [82]. Notably, transglutaminase (MTGase) has become the most employed enzymatic coagulant due to its broad protein selection, high degree of cross-linking, and calcium-independent activity [88]. The gelation mechanism of MTGase is based on its catalyst function in facilitating transfer reactions among multiple proteins and cross-linking amino acid residues, particularly glutamine and lysine [88].

When compared to salt ($CaCl_2$) and acid (GDL)-induced SPI gels, SPI gel coagulated by MTGase has the highest gel strength and lowest water holding properties, characterized by a more homogeneous and thinner filamentous gel network [89]. The mechanical properties and microstructure of MTGase-induced soymilk gel can also be further modified with thermal pretreatment. The findings in [90] reveal that heat pretreatment, such as heating at 75 °C for 10 to 30 min, significantly enhances the gel strength of MTGase-induced tofu and reinforces the gel structure. At any enzyme concentration of MTGase, tofu produced from soymilk heated at 75 °C for 10 or 30 min exhibited the higher gel hardness, along with a distinct coral-like structure that was notably denser and more homogeneous than tofu made from soymilk heated at 95 °C for 5 min. The different microstructure of MTGase-induced tofu, resulting from thermal pretreatment methods, can be attributed to the covalent cross-links and noncovalent interactions, primarily hydrophobic interactions, among partially or completely denatured proteins. At 75 °C, covalent cross-links among partially denatured proteins induced by MTGase act as the most dominant

interaction driving gel formation. Conversely, at 95 °C, relatively stable macro-aggregates are formed, featuring hydrophobic groups within the interior and hydrophilic groups on the exterior, which restrict the cross-linking reactions among protein constituents with MTGase [90].

2.5. Okara-added Soy Products

Okara, which is the by product of soymilk and tofu production, has a high content of insoluble dietary fiber and protein and bioactive properties including antioxidant, hypolipidemic, and hypoglycemic properties [91]. Hence, the utilization of okara as a dietary fiber supplement and structure enhancement has been reported in food products such as vegetable paste, rice noodles to protein gels [92, 93, 94, 3].

The impact of soybean okara addition, whether in powder or paste form, on the gelation properties of tofu has been extensively studied in recent years [3, 4, 5, 6, 7]. The finding in [7] shows that high-fiber tofu prepared from whole soybean milk without separating okara has a heterogenous and disrupt network structure, possibly due to high water-absorbing capacity and the large particle size of okara. The large particle size of the coarse okara may be a primary factor contributing to its adverse effects on both the gelation process and the sensory attributes, particularly the mouthfeel characterized by grittiness, thereby limiting its application in high dietary fiber tofu products [3].

To enhance the texture qualities and sensory attributes of soy gels incorporating okara, there are modification approaches that can be categorized into two groups: physical and non-physical methods. The overview of relevant studies involving the improvement of okara-added soy gels through both physical and non-physical techniques is outlined **Table 2. *4*:** Published studies on

the improvement of okara-added soy gels through physical techniques.**Table 2. *4*** and **Table 2. *5*,** respectively, and will be discussed in the next sections.

2.5.1. Physical Modification Methods

Physical methods used in the manufacture of soy gels with okara include wet media milling, ultrasound, and ultra-high-pressure homogenization (UHPH). These methods primarily aim to diminish the particle size of okara. Wet media milling, for instance, can reduce the particle size of okara to a nanoscale level, whereas ultrasound and ultra-high-pressure homogenization not only reduces particle size but also induces protein denaturation, promoting enhanced protein cross-linking [3, 4, 5]. **Table 2. 4** presents published studies on the improvement of okara-added soy gels through physical techniques.

In the study by Ullah et.al [3], okara dietary fiber was reduced to an average particle size of 370 μm to obtain nano dietary fiber (NDF) using a pulverizer and high-energy wet media milling. In compared to tofu without okara dietary fiber, tofu incorporating NDF exhibited a soft texture, white color, and increased fiber content without a gritty mouthfeel. The high surface charge and water absorption capacity of NDF might lead to the formation of negatively charged, and aggregated NDF particles that can prevent protein aggregates from getting close to each other for aggregation, which weaken the protein interactions [3, 8].

Utilizing ultrasound or ultra-high-pressure homogenization (UHPH) with SPI-okara or soy flour suspensions enhances gel strength when compared to untreated SPI gels [4, 5]. Ultrasound treatment applied to the SPI-okara suspension was observed to reduce the mean particle size of the suspension while increasing the surface hydrophobicity and free sulfhydryl group content of protein component. This led to the development of a more uniform, compact and filamentous gel

network. Ultrasound treatment also promoted greater intermolecular crosslinking and increased water holding capacity (WHC), resulting in improved texture properties [4]. UHPH treatment of soy flour suspension also exhibited similar positive effects to ultrasound, which enhanced homogeneity, gel strength, and WHC in high-fiber tofu [5].

In addition to the methods mentioned above, steam explosion (SE) offers another avenue to enhance the incorporation of okara into soy gels by altering the physicochemical characteristics of okara. A study detailed in [95] revealed that steam explosion dramatically increased the soluble dietary fiber (SDF) content of okara by as much as 26-fold when operated at 1.5 MPa for 30 seconds. Following the SE treatment, the originally loose sheet structure of okara's surface underwent degradation into smaller fragments, resulting in increased water solubility along with reduced swelling capacity, as well as oil and water holding capacities of okara. Furthermore, SE treatment can dissociate macromolecular protein aggregates, leading to increased concentration of low molecular weight proteins [95].

Table 2. 4: Published studies on the improvement of okara-added soy gels through physical techniques.

Objective	Okara Treatment	Soy Gel Preparation	Results
Physical Modification Methods			
To produce nano-sized okara dietary fiber (NDF) by **wet media milling [3]**.	- Extracted dietary fiber (DF) from okara. - Coarse milled DF by a pulverizer to obtain micro-sized DF (MDF)	- Homogenized the suspension of MDF or NDF with soymilk at ratio from 0-50 % (v:v). - Heated the dispersion to 95 ± 3 °C for 10 min	- The increase of NDF content led to the gradual increase in yield, moisture, fiber content, syneresis and whiteness of tofu, along with the decrease in

	with average particle size of 110 μm. - Added water to DF and subjected to energy wet media mill for 8 h to obtain NDF with particle size of 370 nm.	then cooled rapidly to 85 °C. - Added $MgCl_2.6H_2O$ 0.02M as coagulant and incubated for 80 °C. - Transferred to wooden mold and pressed using a 1.5 kg weight. - Control sample: tofu prepared by same method, without MDF or NDF.	parameters of texture profile analysis (TPA). - At the similar ratio with NDF, MDF tofu showed significantly lower yield, fiber content, syneresis and whiteness, while higher TPA parameters. - NDF tofu formed porous and disconnected gel matrix, with the even distribution of NDF particles, while MDF were randomly imbedded in the continuous gel matrix of tofu.
Examine the cavitation effect of **ultrasound treatment** to	- Prepared a suspension of SPI, okara flour and water (4:11:100, w:w:v).	- Added GDL (1%, w:v) as coagulant to the treated suspension. - Heated at 80 °C for 30 min.	- Ultrasound treatment decreased the particle size of okara and unfolded proteins, leading to the increase of

SPI and okara suspension **[4]**.	- Treated the suspension with ultrasonic processor at 500, 600, 700, and 800 W for 20 min.	- Control sample: Tofu gel prepared from untreated SPI okara suspension.	surface hydrophobicity and free sulfhydryl group. - Okara tofu treated with ultrasound exhibited more uniform and denser gel network, with an increase in gel strength and water holding capacity (WHC).
To reduce particle size and non-thermally denatured proteins of soy flour by **ultra high-pressure homogenization** (UHPH) **[5]**.	None	- Non-thermally treated soy flour suspensions (15% and 20%, w:w) with UHPH in a valve-mode homogenizer for two or three cycles at two different pressures (100 and 150 MPa) - Control samples: tofu prepared from soy flour suspensions (15% and 20%) by heat treatment at 95 °C for 10 min.	- Compared to control, UHPH treated soy flour suspension obtained a smaller and more uniform particle size, leading to a regular, continuous honeycomb-like structure of tofu. - Under appropriate pressure and cycles the hardness, gumminess and chewiness of UHPH-treated tofu was

	similar to the control one.

2.5.2. Non-physical Modification Methods

Apart from physically reducing the size of okara particles, non-physical methods offer alternatives to modify okara or the protein network in different ways [6, 7, 96]. For example, a study in [6] focused on enhancing the hydrophilicity and smoothness of okara by applying a layer-by-layer coating with chitosan and pectin. Another approach employed microbial transglutaminase (TGase), which enhanced the formation of protein aggregates, providing a more organized protein structure wrapping okara particles [7]. **Table 2. *5*** presents published studies on the improvement of okara-added soy gels through non-physical techniques.

In the study detailed in [6], okara insoluble dietary fibers (O-IDF) was coated with chitosan and pectin to improve their surface properties, making them more compatible with the food matrix before reintroducing them into soymilk for tofu production. The changes in the surface properties of okara improved the texture characteristics, increased resistance to mechanical damage, and gave higher sensory ratings compared to tofu incorporating untreated O-IDF. A different alternative reported in [7] employed TGase alongside with the coagulant GDL where TGase promoted the formation of protein aggregates with greater organization, facilitated by covalent disulfide bonds, effectively wrapping the coarse okara particles. As a result, TGase-treated high-fiber tofu exhibited enhanced gel strength and water-holding capacity in comparison to the control gel,

Cellulase treatment of okara was explored as a mean to enhance the texture of whole soybean curd in a study detailed in [96]. This enzymatic treatment effectively broke down okara, increasing its

soluble dietary fiber content. At a cellulase concentration of 9 U per gram of soybean powder, notable improvements were observed in the hardness, cohesiveness, chewiness, and gel strength of the treated whole soybean curd when compared to the untreated one. However, the enzymatic treatment did not yield whole soybean curd with sensory ratings as high as those obtained with alternative physical methods, including superfine grinding and ultrasonic disruption in the same study [96].

Other non-physical methods for okara modification have been explored and include alkaline and microbial fermentation treatments [97, 98]. Optimal alkaline hydrogen peroxide treatment conditions (2% H_2O_2 and 42 °C for 5 h) led to remarkable results, including a 601 % increase in soluble fiber content, a 26 % boost in water absorption and holding capacity, swelling capacity, and a substantial 609 % increase in soluble protein content. Scanning electron micrographs unveiled a rougher surface and a more fragmented structure in the alkaline-treated okara [97]. Mixed fermentation and microwave treatment was found to significantly increase the soluble dietary fiber content and alter the composition of okara samples [98]. This method enhanced the bioactivity of modified okara, the glucose dialysis retardation index, α-amylase activity inhibition, and cholesterol absorption capacity, when compared to the unmodified one.

Table 2. 5: Published studies on the improvement of okara-added soy gels through non-physical techniques.

Objective	Okara Treatment	Soy Gel Preparation	Results
Non-physical Modification Methods			
To modify the surface properties of	Micronized O-IDF powder with an ultrafine grinder for the	Homogenized the suspension of O-IDF or O-IDF/C/P with	O-IDF/C/P showed enhancement in hydrophilicity and a

okara insoluble dietary fibre (O-IDF) via **layer-by-layer (LBL) coating** of chitosan/pectin **[6]**.	particle size < 400 mesh. - Prepared chitosan coated IDF particles (O-IDF/C). - Prepared pectin-coated O-IDF/C (O-IDF/C/P).	soymilk at concentration of 10 g/L. - Added GDL 5 % (w:v) as coagulant. - Heated at 85 °C for 30 min to form tofu curd.	smoother surface, compared to intact O-IDF. - The tofu incorporated with O-IDF/C/P exhibited better textural properties, stronger resistance to mechanical damage and higher sensory scores than the one with intact O-IDF
To modify protein network of high-fiber tofu with **MTGase [7]**.	None	- Mixture of okara and soymilk was milled with a colloid mill and homogenized with a high-pressure homogenizer at 40 MPa. - Added GDL 0.3 % (w:w) as coagulant. - Incubated at 85 °C for 30 min to form high-fiber tofu curd (HFT). - Or added extra TGase 0.15 % (w:w) to heated	- TGase promoted the formation of protein aggregates more orderly by covalent disulfide bonds and allowed to wrap the coarse okara particles. - TGase-HFT exhibited improvement in gel strength and WHC, compared to controls.

		soymilk and incubated at for 240 min before the 85°C-incubation to obtain TGase induced high-fiber tofu (TG-HFT) - Control samples: tofu prepared without okara (CT), high-fiber tofu (HFT).	
To decrease the particle size of soybean fiber using **cellulase enzymatic hydrolysis [96]**.	- Added a series of amount of cellulase to the suspension of soybean powder and water. - Thermally treated the mixture at different temperature and time.	- Cellulase-treated soy suspension was coagulated by the mixture of 0.5 % GDL, 0.07 % $MgCl_2$, and 0.02% MTGase. - Incubated at 50 °C for 1 h and at 85 °C for 20 min.	- Enzymatic treatment increased the soluble dietary fiber content in soybean powder. - Whole soybean curd made by cellulase treatment obtained higher textural properties (hardness, cohesiveness, chewiness, gel strength) and WHC, but a lower sensory score than traditional tofu.

2.5.3. Combined Modification Methods

In an effort to enhance the soluble dietary fiber content in okara, a combination of steam explosion and enzymatic hydrolysis treatment was employed, as described in [99]. The process was initiated with the treatment of okara using cellulase (40 U/g) at 55 °C for 3 h. Following this, the pH was adjusted to 4.8 with citric acid, and the mixture was dried at 60 °C. The cellulase-treated okara was then pulverized and sifted through a 100-mesh sieve before utilized in the preparation of egg tofu gel. The egg tofu was produced by heating a mixture of soymilk, modified okara, and liquid egg at 95 °C for 12 min. The outcome of these modifications demonstrated a substantial increase in the content of soluble dietary fiber in okara, rising from 2.14 % to 32.13 %. The egg tofu made with the modified okara exhibited improvements in terms of hardness, viscoelasticity, and water holding capacity when compared to tofu containing only the soluble dietary fiber fraction.

2.6. Effect of Citric Acid Treatment on Soy Polysaccharides

2.6.1. Overview of Citric Acid

Citric acid (CA) is a tricarboxylic acid with pKa values of 3.1, 4.7, and 6.4. It appears as a colorless, crystalline powder and can exist in either anhydrous or monohydrate form. Both anhydrous and monohydrate CA is highly soluble in water. It decomposes with loss of carbon dioxide (CO_2) above about 175 °C. Due to its pleasant taste, high water solubility, chelating and buffering properties, CA is widely used as a safe acidulant in the food industry [9]. The following sections will focus on various applications of CA in the treatments and modifications of polysaccharides.

2.6.2. Hydrolysis Activity

Citric acid has been used as a pre-treatment method to initiate and facilitate the hydrolysis of polysaccharides contained in agricultural biomass. One application is the biogas production by

enzymatic hydrolysis from various material including soy hull, sugarcane bagasse and rice straw, where citric acid addition has favored hydrolysis, the generation of fewer degradation products, and its environmentally friendly attributes [11, 12, 13].

Another application is reported in [12], the utilization of citric acid pretreatment was used for the valorization of raw sugarcane bagasse to recover fermentable sugars. Citric acid concentration was varied from 0.35 – 11.65 %, alongside with the duration spanning from 17.6 – 102.4 min, at a constant temperature of 100 °C. The results indicated that cellulose and hemicellulose components of the polysaccharide fraction underwent acid hydrolysis reactions. The extent of degradation increased with higher acid concentrations and longer reaction times, aligning with findings from previous [11, 13]. Scanning electron microscopy observations suggested that citric acid played a role in peeling and disintegrating the fibers. As a result of the citric acid hydrolysis, a partial removal of cellulose, hemicellulose, and lignin occurred, leading to the formation of surface grooves in the pretreated material and a partial structural rupture.

2.6.3. Chelating Property

In plant cell wall, Ca^{2+} has an important role in interacting with pectic acid polymers to form Ca^{2+} cross-linkages that increase the resistance of fibers to hydrolysis [71, 72]. In [72], the effect of chelators, including ethylenediaminetetraacetic acid and hexametaphosphate on citric acid hydrolysis of okara fibers was investigated. The findings revealed that chelators functioned by removing Ca^{2+} ions from the egg-box regions, which in turn loosen up the structural integrity and accelerated the hydrolysis process. It was proposed that, in the presence of a chelator, the reaction proceeded in two phases: an initial stage where hydrolysis primarily occurred within the egg-box regions, followed by a subsequent shift toward non-egg-box regions.

Citric acid is widely recognized for its exceptional metal-chelating properties and finds extensive applications in the food, cosmetic, nutraceutical, pharmaceutical industries, and even in soil washing processes [100]. Therefore, when reacting with soy polysaccharides, citric acid's chelating abilities could potentially play a similar role in facilitating acid hydrolysis.

2.6.4. Extraction of Pectic Substances

Citric acid, owing to its unique combination of acidic and chelating properties, finds wide application in the extraction of pectic substances from various sources, such as soy hulls and various fruit peels like citrus and apple [14, 15, 16, 17]. A comparison of the properties of pectin extracted using citric acid to those obtained from other organic and inorganic acids, indicate that citric-acid-extracted pectin has a higher molecular weight and improved viscosity, making it an excellent candidate for natural thickening and emulsifying purposes [14, 15, 16, 17]

The research in [15] examined the effect of common organic acid (i.e., citric acid) and inorganic acids (i.e., hydrochloric acid and nitric acid) on the pectin extraction from thinned-young apples. The extraction process involved subjecting freeze-dried sample-to-acidic solution (pH 1.5) with the ratio of 1:15 (w:v) at a temperature of 85 °C for a duration of 90 min. The findings revealed that all three acids yielded high methoxy pectin, rich in Rhamnogalacturonan I. Notably, the pectin extracted with citric acid exhibited the highest molecular weight, protein content, thermal stability, and shear-thinning properties.

Furthermore, in another study [16] that examined the effect of food-grade organic acids, tartaric, malic, and citric acids, in apple peel pectin production, citric acid emerged as the top performer. Pectin extracted with citric acid demonstrated the highest molecular weight and apparent viscosity

when compared to pectin extracted with other organic acids. Thess results highlight the ability of citric acid extraction processor generating high-viscosity apple peel pectin.

2.6.5. Cross-linking Property

Citric acid (CA) is capable of cross-linking with various polymer molecules due to its structure, which includes three carboxyl groups and one hydroxyl group. This cross-linking process between citric acid and biopolymer molecules primarily involves non-covalent bonds, such as hydrogen bonding and ionic interactions [101].

Under high-temperature conditions, generally above 100 °C, CA can undergo a chemical cross-linking process with cellulose through esterification reactions between the carboxyl groups of CA and the hydroxyl groups of cellulose. This process is initiated with the conversion of CA into an anhydride intermediate, which subsequently reacts with the hydroxyl groups of cellulose, forming ester bonds. This sequence continues with the anhydride intermediate combining with the carboxyl group of cellulose, resulting in an ongoing chemical cross-linking reaction [102].

On the other hand, cross-linking reaction between CA and proteins occurs mainly at low-temperature aqueous conditions (50 to 75 °C) [103, 104]. As the pH in the aqueous environment increases, the carboxyl group of CA and the amino group are deprotonated into -COO^- and - NH_2, respectively. The nucleophilic substitution results in the formation of amide groups. When multiple -COOH groups within a CA molecule are involved in the reaction, a single CA molecule can cross-link with more than one protein molecules. However, the addition of CA leads to a decrease in the pH of the aqueous environment, which falls below protein isoelectric point (at around 6 for most proteins). This pH shift results in the formation of positive-charged amine group (-NH_4^+) in protein that can hinder the interaction between carboxyl and amino groups. Therefore,

it is crucial to take into account both the pH of the solution and the protein's isoelectric point when aiming to facilitate cross-linking between the protein and CA [104].

2.7. Protein – Polysaccharide Conjugated Gels

2.7.1. Maillard Reaction

The Maillard reaction is a non-enzymatic reaction that occurs between amino groups of proteins and carbonyl groups in reducing sugars. This reaction takes place at temperatures lower than the denaturation temperature of proteins and is affected by the water activity conditions. As a result, it leads to the formation of various protein-polysaccharide conjugates linked by covalent bonds, along with Maillard reaction products [105].

A visual representation of the three stages of Maillard reaction, its sub-products, and their characteristics is depicted in **Figure 2.** ***13***. The early stage of the Maillard reaction yields Amadori products, which find applications in food products due to their emulsifying, foaming, solubility, gelling, and thermal stability properties. In the second stage, Advanced glycation end products (AGEs) with bioactive properties, such as antimicrobial and antioxidant effects, are formed. The final stage of the reaction leads to the creation of products which are generally considered unfavorable both in terms of flavor and health aspects [105, 106].

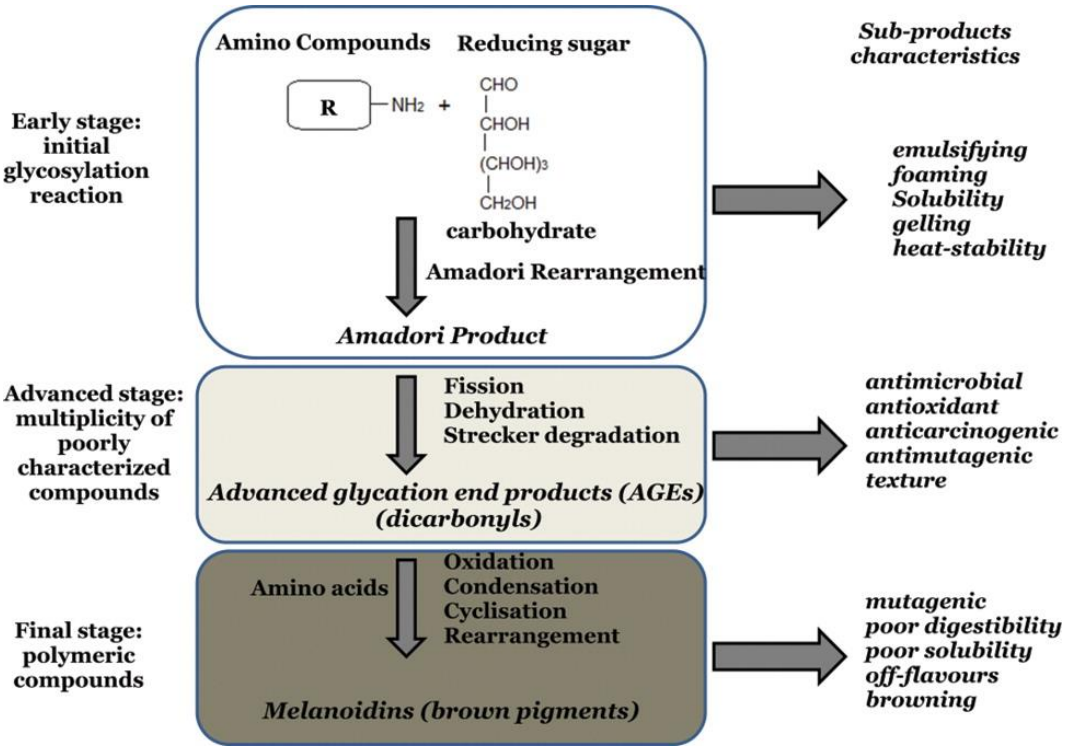


Figure 2. 13: Three stages of the Maillard reaction and sub-products characteristics *[105]*. Reprinted from R. R. Naik, Y. Wang and C. Selomulya, "Improvements of plant protein functionalities by Maillard conjugation and Maillard reaction products," *Critical Reviews in Food Science and Nutrition*, vol. 62, no. 25, pp. 7036 - 7061, 2022., with permission of Taylor & Francis.

2.7.2. Maillard Conjugation Methods

The Maillard conjugation methods can be divided into two categories, including dry state heating and wet state heating. In the dry state heating method, initially, the suspension of protein and carbohydrate is freeze-dried, followed by heating at controlled temperature, time and humidity [106]. Temperature ranges 40 to 80 °C and relative humidity between 60 % and 85 % are commonly employed in this method [107]. However, there are notable drawbacks associated with dry state heating, including the prolonged reaction times, which can extend to several days. Additionally, it necessitates the use of freeze-drying that is not feasible for large scale application. Moreover, controlling the formation of advanced glycation end products (AGEs) can be challenging [106].

To address these limitations, the wet state heating method has been introduced. This method relies on the principles of macromolecular crowding conditions [107, 108]. When the Maillard reaction occurs in an environment with a high concentration of macromolecules, it shifts towards the production of species with smaller excluded volumes. This, in turn, contributes to the stabilization of the protein structure [108]. In the wet state heating approach, the initial step is the solubilization of the proteins and carbohydrates in a buffer at specific ratios. The process continues with pH adjustment and controlled heat treatment. The resulting Maillard conjugates are then recovered by removing the excess solvent. The advantages of the wet state heating method are the elimination of the lyophilization step and the requirement for humidity control [106]. Moreover, the thermal stability and emulsifying properties of the resulting conjugates is obtained by preventing excessive protein denaturation and aggregation. However, the separation and recovery of the Maillard conjugates add to the complexity of the method [106].

2.7.3. Detection of Maillard reactions by FTIR

During the Maillard reaction, functional groups including amine groups from lysine may disappear, while the formation of products such as the Amadori compound (C=O), Schiff base (C=N), and pyrazines (C–N) will appear [109]. Fourier transform infrared spectroscopy (FTIR) is one method that can be used to monitor changes in protein and polysaccharide structures and the appearance of new structures [110].

Table 2. 6 presents a summary of the frequencies (cm^{-1}) corresponding to the functional groups of proteins, polysaccharides, and Maillard reaction products, as documented in the literature. The FTIR spectra of Maillard reactions will be reflected in the peaks associated with the amide I, II and III in protein-polysaccharide conjugate with decrease in intensity and an increase in the intensity of C-O and C-C stretching of polysaccharide. These changes are indicative of covalent

bond formation between amine and carboxyl groups. Additionally, peaks corresponding to Maillard reaction products typically will appear in the wavelength ranging from 1660 – 1550 cm^{-1} and 1160 – 1130 cm^{-1} [111, 112, 113, 114].

Table 2. 6: Summary of the FTIR frequencies (cm^{-1}) of Maillard reactions corresponding to functional groups of proteins, polysaccharides, and Maillard reaction products, adapted from existing literature *[111, 112, 113, 114]*.

Wavelength (cm^{-1})	**Corresponding functional groups**	**Changes indicating Maillard reaction**
Protein peaks		
1690 – 1600 **[111, 112, 113]**	C=O stretching (80%) and C-N (20%) of amide I bond	Decrease, compared to native protein.
1575 – 1500 **[111, 112, 113]**	N-H bending (60%) and C-N (40%) of amide II bond	Decrease, compared to native protein.
1300 – 1200 **[111, 112, 113]**	C-N stretching and N-H deformation of amide III bond	Decrease, compared to native protein.
Wavelength (cm^{-1})	**Corresponding functional groups**	**Changes indicating Maillard reaction**
Polysaccharide		
1630 – 1600 **[113]**	Carboxylate ion stretching	Increase, compared to native protein.
1450, 1150 – 1050 **[111, 112, 114]**	C-O and C-C stretching of polysaccharide	Increase, compared to native protein.
Wavelength (cm^{-1})	**Corresponding**	**Changes indicating**

	functional groups	Maillard reaction
Formation of new peaks		
1660 – 1648 **[111, 113]**		Schiff's base (C=N stretching vibration)
1640 – 1580 **[111, 113]**		β-diketones (C=O stretch, enol/keto form)
1610 – 1560 **[111, 113]**		C=C of carboxylate ion stretching (COOH)
1615 – 1565 **[111, 113]**		Pyridine derivatives (ring stretch, doublet)
1160 – 1120 **[113]**		Amadori product (C–N stretching)

2.7.4. Application of Maillard Reaction in Improving Soy Protein Functionality

Soy proteins are widely employed as a techno-functional ingredient in formulated foods, offering water and fat binding, emulsification, foaming, and gelation capabilities. However, the functionality of soy proteins, especially their water solubility, can vary depending on the extraction method employed. Moreover, major drawbacks of soy proteins are its unfavorable beany taste and concerns related to high allergenicity [107]. To address these challenges and enhance soy proteins' functional attributes, extensive studies have been conducted on the glycation of soy proteins with reducing carbohydrates, ranging from simple sugars like glucose and maltodextrin to more complex components such as okara dietary fiber and pectin [113, 115, 116, 117, 118, 119, 120, 121]. A summary of existing studies on the conjugation of soy protein isolate (SPI) with glucose,

polysaccharides derived from okara and pectic substances is presented in **Table 2. 7** and **Table 2. 8**.

In addition to convectional dry and wet state glycation methods, recent studies have focused on novel techniques with the addition of ultrasonication, pressure as pre-treatment or the utilization of ultrasound in conjugation of protein and polysaccharide [122, 119, 121].

For instance, the study in [121] investigated the effect of ultrasound on the functionality of SPI-pectin conjugates, in comparison to the wet state method where SPI and pectin, at the ratio of 1:1 (w:w), were initially dissolved in water, followed by the pH adjustment using NaOH to 6.0 – 12.0. Maillard reaction occurred at different temperatures ranging from 50 to 90 °C and over various durations from 4 to 24 h. The ultrasound treatment involved subjecting the SPI and pectin dispersion at pH 10.0 to ultrasound at different power levels ranging from 270 to 630 W, varying durations from 15 to 120 min), and temperatures ranging from 50 to 90 °C. The ultrasound treatment exhibited a significant role in unfolding the SPI, which resulted in more favorable structures for the Maillard reaction, including a substantial increase in surface hydrophobicity and emulsifying properties of SPI-pectin conjugates compared to those produced with the wet state method. In another study combining ultrasound with the wet state method [119], marked improvement in the flexibility, emulsification activity, and emulsion stability of SPI-glucose conjugates were observed when compared to conjugates generated by the wet state method alone. This improvement may be attributed to the effect of ultrasound in reducing protein particle size and loosening the protein structure.

Table 2. 7: Summary of existing studies on the conjugation of soy protein isolate (SPI) with glucose and, polysaccharides derived from okara and pectic substances, using dry heating method.

Protein (P)	**Carbohydrate** (C)	**Modification Technique**	**Functionalities**
Soy protein isolate (SPI) **[113]**	Soy soluble polysaccharide	- P:C ratio: 3:8, 1:2, 3:5, 4:5 (w:w) - Temperature: 55, 60 and 65 °C - Time: 36 – 96 h - Humidity: kept in desiccator with saturated NaCl.	- Increased emulsifying properties for citral-loaded emulsions. - Good potential as a carrier system for intestinal delivery of hydrophobic compounds.
SPI **[115]**	Soy-hull hemicellulose	- P:C ratio: 1:9, 2:8, 3:7, 4:6, 5:5, 6:4 (w:w) - Temperature: 60 °C - Time: 7 days - Humidity: kept in desiccator with saturated NaCl.	- Improved physical stability of oil in water emulsions for an extended storage period.
SPI **[116]**	Glucose	- P:C ratio: 4:1, 2:1, 1:1, 1:2 (w:w) - Temperature: 50 °C - Time: 6 h, 1 - 14 days	- Improved the solubility and resistance to heat and high ionic strength.

		- Humidity: kept in desiccator with saturated KI.	- Improved emulsifying activity and emulsion stability.
SPI **[117]**	Okara dietary fiber (ODF)	- P:C ratio: 1:1 (w:w) - Temperature: 60 °C - Time: 3 days (36 h) - Humidity: kept in desiccator with saturated NaCl.	- ODF-SPI conjugates were thermally stable, hydrophilic, and exhibited excellent Pickering emulsion stabilization potentials.
SPI **[118]**	Citrus or apple pectin (CP or AP)	- P:C ratio: 1:1 (w:w) - Temperature: 60 °C - Time: 1 – 7 days - Humidity: kept in desiccator with saturated KBr.	- Decreased the surface hydrophobicity due to the strong steric-hindrance effect of pectin - Improved the solubility and emulsifying properties of both SPI-CP and SPI-AP conjugates.

Table 2. 8: Summary of existing studies on the conjugation of soy protein isolate (SPI) with glucose and pectic substances, using wet heating method.

Protein (P)	**Carbohydrate** (C)	**Modification Technique**	**Functionalities**
SPI **[119]**	Glucose	- P:C ratio: 3:2 (w:w) - Solvent: phosphate buffered saline (0.2 M, pH 7.0) - Temperature: 90 °C - Time: 5 h	- Ultrasonic pretreatment resulted in the reduction of protein size and loosen the structure. - Improved protein emulsification activity and stability
SPI **[120]**	Glucose	- P:C ratio: 2:3 (w:w) - Solvent: phosphate buffered saline (0.02 M, pH 7.0) - Temperature: 60 °C - Time: 2 – 6 h	- The flexibility, surface hydrophobicity, free sulfhydryl group and turbidity increased when increasing the reaction time from 0 to 5 h. - Emulsifying activity and emulsion stability were positively correlated with flexibility.
SPI **[121]**	Citrus or apple pectin (CP or AP)	- P:C ratio: 1:1 (w:w)	- More time-consuming to form SPI-CP conjugates

	- Solvent: water, pH adjustment with NaOH to 6.0 – 12.0 - Temperature: 50 – 90 °C - Time: 4 – 24 h	with similar degree of grafting than SPI-AP, due to larger molecular weight and the more flexible structure of AP.

2.7.5. Maillard Reaction Protein – Polysaccharide Conjugated Gels

Besides well-known emulsifying and foaming properties, protein-polysaccharide conjugates can be utilized protein gel formation with desired texture [106]. For instance, study in [114] investigated the textural properties and microstructure of acid-induced gel prepared from heated soy protein isolate (HSPI)–soy oligosaccharide (SOS) glycation conjugates where HSPI was obtained by subjecting SPI dispersion to heat treatment at 95 °C for 15 min. The Maillard reaction was carried out by heating the mixture of HSPI dispersion and SOS at 90 °C for 30, 60, 90 and 120 min. For the preparation of acid-induce gel, HSPI–SOS conjugate dispersions were mixed with soy oil at a volume ratio of 4:1, and high-speed shearing at 18,000 rpm for 3 min, followed by gelation with GDL as coagulant. The Maillard reaction of HSPI with SOS induced the shift from α-type to β-type in the secondary protein structure, accompanied with lower free sulfhydryl groups, and improvement of the surface hydrophobicity that influenced directly to the properties of acid-induced gel. Consequently, the resulting gel obtained a higher gel hardness, water capacity holding, a more compact microstructure, and more heighten uniformity of emulsified oil droplets, compared to acid-induced soy protein gel.

The effect of Maillard reaction on the properties of protein-polysaccharide conjugated gel could be primarily attributed to the alterations in free sulfhydryl groups content, surface hydrophobicity and isoelectric point of the conjugate systems [123, 124]. The extent of the Maillard reaction can be controlled by adjusting reaction conditions including heating state, temperature, durations and molecular weight of the saccharide involved to different types of gels with various texture profiles can be created [123].

Chapter 3: Standardization of Soymilk Okara Gels Preparation

3.1. Introduction

The overall framework of this study and initial inquiries on the standardization of the methodology for the preparation of soymilk okara gels is presented briefly in **Figure 3. 1**. The preparation of soymilk okara gels with citric acid (CA) modified okara was adapted from the thesis of Jing Sy [125]. Initially, soymilk and its by product, okara, are extracted from soybeans. Okara then undergoes modifications with CA solid at varying concentrations (5%, 10%, w:w). Subsequently, the CA modified okara materials are reintroduced into soymilk and gelled by thermal treatments at 95 °C. However, certain challenges need to be addressed in the production of soymilk okara gels to ensure the consistency in characteristics of modified okara materials and textural properties of final gels, including:

1) Standardization of soymilk preparation with a consistent solid content.
2) Assessment of the physical state of CA at the concentration of 5 % (w:w) during modification of okara on the structural characteristics and textural profiles of soymilk okara gels.
3) Assessment of the okara drying time on the structural characteristics of CA modified okara with CA solution 10 % (w:w) .

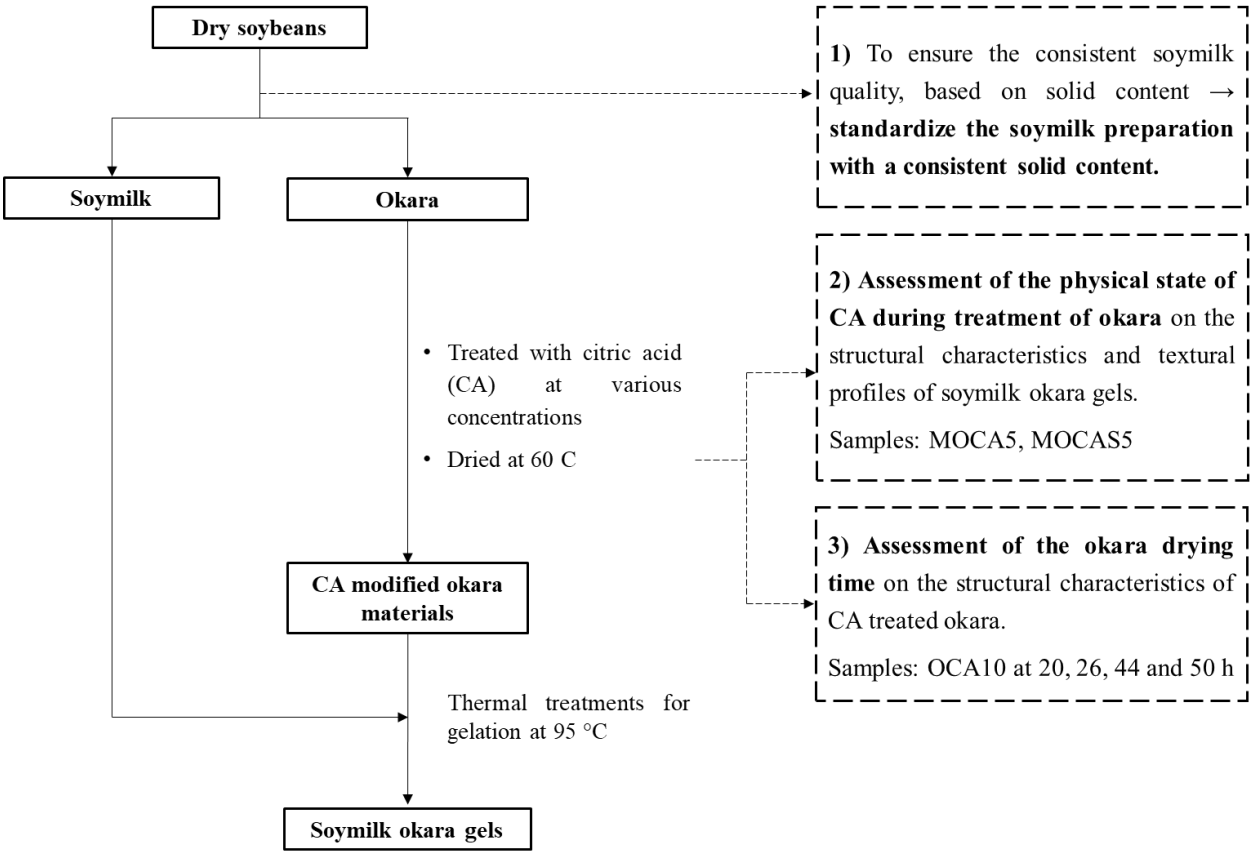


Figure 3. 1: Objectives of the standardization of the methodology for the preparation of soymilk okara gels with steps of the gel preparation (solid lines and boxes) and standardization objectives on (dashed lines and boxes).

3.2. Materials and Methods

3.2.1. Materials

Bags of dry soybeans, 4.5 kg, (Nupak, lot 11741D and 20181D) were purchased from a local supermarket (Waterloo, ON, Canada) and kept in Ziploc bags. Citric acid anhydrous (CA, lot 221510) was obtained from Fisher Scientific (Fair Lawn, NJ). Rhodamine B (lot SLBF0620V) was purchased from Sigma Aldrich (India).

3.2.2. Preparation of Soymilk and Okara

The preparation of soymilk and okara, modified okara materials and soymilk okara gels was adapted from [125] with modifications. Initially, a mass of dry soybeans was soaked in 3 parts of

deionized (DI) water for a duration of 22 – 24 h. The hydrated soybeans were then washed with DI water, and dehulled before blending with DI water at the ratio of 3:8 (mass of dry soybeans to volume of water) for 2 min at high speed in a commercial blender (Waring E11524). The resulting mixture was filtered, and the soymilk was extracted by squeezing the soy slurry through a cheesecloth bag (Scengclos, Woodridge, IL). The ratio of the mass of the extracted soymilk (M) to the remaining solid portion known as wet okara (O_w) was recorded as O_w:M for the preparation of soy gels at later stage.

3.2.3. Estimation of Soymilk Solid Content

The solid content of soymilk was determined using two methods, drying and UV-vis spectrophotometry, in order to assess and compare their efficiency in terms of rapidity and accuracy.

3.2.3.1. Drying Method

The solid content of soymilk measured by drying triplicates of 1 g ($W_{\text{pre-dried SM}}$) of freshly made soymilk in forced air oven (Fischer Isotemp 737F) at 60 °C for 3 h for the constant weight and calculated by **Equation 3. 1**. In the equation, $W_{\text{pre-dried SM}}$ and $W_{\text{dried SM}}$ are defined as the mass of soymilk before and after the drying.

$$Solid\ content\ (\%) = \frac{W_{dried\ SM}}{W_{pre-dried\ SM}} \times 100 \qquad \textbf{Equation 3. 1}$$

3.2.3.2. UV-vis Absorbance Method

The UV-vis absorbance method was adapted as described in [126] and [127] with some modifications.

To construct the standard curve of solid content in soymilk, a mass of 1 g of freshly made soymilk was weighed into a 30-mL beaker and dried for 3 h at 60 °C in forced air oven (Fischer Isotemp 737F) to constant weight ($W_{dried\ solid}$). The dried solid was dissolved in 20 mL of DI water and stored in the fridge overnight for a full dissolution. The solution was then transferred to a 100-mL volumetric flask and diluted to the volume to obtain solution A with concentration of $W_{dried\ solid}$/100 mL. A series of solutions with different solid content were prepared by diluting solution A with DI water by 1.5, 2, 3, and 6 times. The absorbance of the solutions was measured at 400 nm, using a spectrophotometer (Genesys 10S) and related to the corresponding solid content of the solutions. The correlation between solid content in solution A (100-fold diluted soymilk) and absorbance measured at 400 nm is shown in **Equation 3. 2** and **Figure S. 1** in **Appendix A.1.**

$$g\ solid/100\ mL\ solution\ A = \frac{A_{400}}{14.915} \times 2.5 \qquad \textbf{Equation 3. 2}$$

To prepare sample for solid content determination, one gram ($W_{pre\text{-}diluted\ SM}$) of freshly made soymilk was weighed into a 250-mL volumetric flask and diluted to volume to make solution B. Absorbance of diluted soymilk was determined at 400 nm by using a spectrophotometer (Genesys 10S). Three determinations were made per sample. The solid content of undiluted soymilk was determined using **Equation 3. 3**.

$$\%\ solid\ in\ soymilk = \frac{A_{400}}{14.915} \times \frac{2.5 \times 100}{W_{pre-diluted\ SM}} \qquad \textbf{Equation 3. 3}$$

3.2.4. Okara Modification with Citric Acid (CA)

Three types of modified okara were prepared, okara modified with 5 % CA liquid (OCA5) and 5 % CA solid (OCAS5) for the assessment of the physical state of CA and okara modified with 10 % CA solution (OCA10) for the assessment of okara drying time. For control sample, dried

unmodified okara (O) was obtained by drying a mixture containing 10 g of wet okara and 50 g of DI water at 60 °C for 20 h in a forced air oven (Fischer Isotemp 737F).

3.2.4.1. Okara Modification with Different Physical States of Citric Acid (CA)

The modified okara with solid CA (OCAS5) was prepared by initially dispersing 10 g of wet okara in 47 g of DI water, followed by the addition of 3 g of citric acid in solid form. The mixture was mixed for 1 h, at high speed with magnetic stirrer, then dried at 60 °C for 20 h in a forced air oven (Fischer Isotemp 737F). The modified okara with liquid CA (OCA5) was obtained by mixing 10 g of wet okara in 50 g of CA solution 6 % (w:w) for 1 h using a high-speed magnetic stirrer. The remaining process of preparing OCA5 was similar to that of O and OCAS5. The final concentration of CA in the mixture of wet okara, CA and water before drying of both OCA5 and OCAS5 was 5 % (w:w)

3.2.4.2. Okara Modification with CA Solution at Different Drying Times

The modified okara OCA10 was obtained by mixing 10 g of wet okara in 50 g of CA solution 12 % (w:w) for 1 h, at high speed with magnetic stirrer. The final concentration of CA in the mixture of wet okara, CA and water before drying of OCA10 was 10 % (w:w). Subsequently, the mixture was dried at 60 °C in a forced air oven (Fischer Isotemp 737F) for up to 50 h. The change in mass and visual appearance of OCA10 was recorded at the drying time intervals of 20 h, 26 h, 44 h and 50 h.

3.2.5. Preparation of Soymilk Okara Gels

Dried unmodified okara (O) and 5% CA modified okara (OCAS5, OCA5) were ground for 1 to 2 min to reduce particle size in a grinder (Blenderpro) and stored at room temperature in capped containers for soymilk okara gels preparation.

Dried and ground okara materials were introduced back to extracted soymilk (M) with the O_w:M ratio for the preparation of soymilk okara gels (MO, MOCAS5, MOCA5). The okara solids were evenly distributed into the soymilk with the aid of magnetic stirrer at 500 – 600 rpm for 15 min in 200-mL beakers. Care was taken to avoid excessive mixing, which could lead to the formation of air bubbles in the mixture and heterogeneity in the gels after. Subsequently, mixture of unmodified or CA modified okara and soymilk was then transferred to a 100-mL beaker coated with a thin layer of Pam oil cooking spray for the gelation. The beakers were then placed in the water bath (NesLab RTE-111) and heated at 95 °C for 45 min, following by cooling to room temperature for 3 h before overnight storage in the fridge for later use. As a comparison, the control soymilk gel (M), was obtained by heating around 50 mL of soymilk only in the water bath at 95 °C for 45 min. Soymilk gels (M, MO, MOCAS5, MOCA5) were used for visual appearance and textural profiles observations right after the 24-h storage in the fridge to prevent any changes in properties caused by syneresis.

3.2.6. Characterization of Okara Materials by Fourier Transform Infrared Spectroscopy (FTIR)

FTIR spectra of dried, control (O) and 10 % CA modified okara OCA10 at different drying time were collected with the use of Nicolet 6700 FTIR spectrometer (Thermo Scientific Nicolet 6700, Waltham, MA, USA), with 32 scans between the wavenumber range of 500 to 4000 cm^{-1} and a resolution of 4 cm^{-1}. Transmittance was baseline corrected and normalized using Omnic Software (Thermo Scientific) for the ease of comparison.

3.2.7. Structural Characterization of Soymilk Okara Gels

3.2.7.1. Macrostructural Characterization with Cross-sectional Images

The visualization of soymilk okara gels (M, MO, MOCAS5) at the macroscale was obtained by optical imaging of the cross-sectional area of gels cut into halves and captured by a dual-lens camera (Iphone 12).

3.2.7.2. Microstructural Characterization with Confocal Laser Scanning Microscopy (CLSM) Images

Gel sample preparation for CLSM analysis was performed, following method described previously [128] with some modifications. A mass of 4 g of the mixture of soymilk and either unmodified (MO) or modified okara (MOCAS5, MOCA5) prepared in **section 3.2.5** was combined with 20 µL of a 0.2 % (w:v) solution of rhodamine B, then stirred using a magnetic stirrer at 400 rpm for 1 h at room temperature while being covered with aluminum foil to prevent the degradation caused by light. The rhodamine B dye binds non-covalently to the protein network [129]. The rhodamine B labelled soy solutions were stored in vials covered with aluminum foil and placed overnight in the fridge, allowing the reaction to proceed completely.

Subsequently, two drops of rhodamine labelled mixture are placed into concave microscope slides (Eisco, 1'' x 3'' – 1.0-1.2 mm) and gently pressed down to prevent bubble formation with cover slide (Fisherbrand, 22x22 – 1.5 mm) and wrapped in aluminum foil. The slides containing the soy mixture were heated in a forced air oven (Fischer Isotemp 737F) at 95 °C for 45 minutes to replicate the gelling conditions. After cooling to room temperature, the slides with dyed soymilk gel, with or without okara, were ready for analysis using CLSM.

The microstructure of the gel was captured using a confocal laser scanning microscope (CLSM, Zeiss LSM 700, AxioObserver) equipped with a Plan-Apochromat 20x/0.8 objective lens. The gels were excited at wavelength of 555 nm and the emission wavelength was recorded between the range of 560 – 800 nm. The settings used for all samples included a pinhole size of 1 airy unit, laser power of 2.0%, and a detector gain of 500. Images were captured with a size of 1024 x 1024 pixel resolution, bit depth of 12 bit, at the averaging of 4 and scanning speed of 7. Image contrast was improved through post-processing using a gamma value of 0.45. For each type of gel sample, a representative image was chosen in a minimum of five images collected at different locations to illustrate each gel type.

3.2.8. Rheological Properties of Soymilk Okara Gels

3.2.8.1. Rheological Properties Measurement

The small amplitude oscillatory shear characteristics were obtained with a rheometer (Thermo Scientific, HAAKE MARS III, USA) equipped with a P35 Ti parallel plate geometry with the diameter of 35 mm and the gap setting between the upper and lower plate of 1 mm. For rheological characterization, soy gel samples (M, MO, MOCAS5, MOCA5) were cut into circular slices with a diameter of 40 mm, and around 2 – 3 mm in thickness using a sharp blade, then equilibrated at room temperature for 1 h prior to analysis. After loading to the rheometer, excess sample was trimmed off the edges for the optimal sample filling and allowed to rest to mechanical equilibrium for 2 min.

The strain sweep test was conducted once for each gel type within a strain range of 0.01 – 100%, at frequency of 1 Hz, and testing temperature of 25 °C to determine the linear viscoelastic region (LVR) for further analysis. LVR data of all gel samples is presented in **Figure S. 2** in **Appendix A.2.** The frequency sweep test was performed in triplicate for each gel type. During measurements,

the changes in the storage (G') and loss (G'') modulus were recorded at constant strain of 0.1 %, which was within the LVR of all sample types while varying angular frequency from 1 to 100 rad/s.

3.2.8.2. *Analysis of Rheological Properties Data*

Analysis of the rheological data was performed according to the method described in [130, 131]. A power law model was employed to describe the relationship between the angular frequency (ω) and the dynamic moduli (G', G") using **Equation 3. 4** and **Equation 3. 5**. Loss tangent (tan (δ)) is defined as the ratio between the loss modulus (G'', in kPa) and storage modulus (G', in kPa), as illustrated in **Equation 3. 6**, indicated the viscoelasticity of material indicated the viscoelasticity of material (e.g., more solid-like with G' value higher than G'' or liquid-like with G'' value higher than G')

While the storage moduli at 1 rad/s (G_o', in kPa) reflects the rigidity of the sample associated with the formation of an elastic gel structure, the loss moduli at 1 rad/s (G_o'', in kPa) represents the extension of the viscous element in the sample. The exponents n' and n" (both dimensionless) signify the influence angular frequency (ω, in rad/s) on each modulus, and is often used to indicate weak- or strong-gel behaviour [132, 133].

$$Storage\ modulus: G' = G'_0\omega^{n'} \qquad \textbf{Equation 3. 4}$$

$$Loss\ modulus: G'' = G''_0\omega^{n''} \qquad \textbf{Equation 3. 5}$$

$$Tangent\ delta:\ tan\,\delta = G''/G' \qquad \textbf{Equation 3. 6}$$

3.2.9. Mechanical Properties of Soymilk Okara Gels

3.2.9.1. Mechanical Properties Measurement

Mechanical properties of the various soymilk gels (M, MO, MOCAS5) were obtained for cylindrical shape samples with a diameter of 20 mm and a height of 10 mm w. The equipment was a mechanical tester (Shimadzu Autograph AGS-X) equipped with a 50-N load cell. Samples were allowed to equilibrate at room temperature for 1 h prior to testing. Samples were compressed uniaxially at a rate of 40 mm/min, at room temperature until visual fracture occurred. Five replicates were used for each type of gel.

3.2.9.2. Analysis of Mechanical Properties Data

The true stress (σ(t)), i.e. the overall stress acting on the sample during deformation and true strain (ε), i.e. the absolute deformation of sample were calculated using **Equation 3. 7** and **Equation 3. 8**, respectively [134, 135].

In the equations, l_0 and A_0 represent the initial height [m] and area [m^2] of the gel, while l(t) and F(t) denote the height [m] of the gel and force [N] measured during compression at time t. True fracture stress – true fracture strain point is measured as the maximum point of the true stress – true strain curve [136, 137] before clear decline in stress was observed. Young's modulus is determined as the initial slope of the true stress-strain curve within the linear region that located between one and two-thirds of the way to the point of maximum true stress.

$$True\ stress: \sigma(t) = \frac{F(t)}{A_0} \times \frac{l(t)}{l_0} \qquad \textbf{Equation 3. 7}$$

$$True\ strain: \epsilon = ln\left(\frac{l(t)}{l_0}\right) \qquad \textbf{Equation 3. 8}$$

3.2.10. Statistical Analysis

Statistical analysis was performed using Statistica (version 14.0.0.15, TIBCO software Inc.). Analysis of variance (ANOVA) was used to determine significant differences between the results, followed by a Tukey test to identify statistical differences between paired means at the level of 0.05.

3.3. Results and Discussion

3.3.1. Standardization of Soymilk Preparation and Measurement of Its Solid Content

Previous studies of tofu products [138, 139, 140] indicate the presence of a relationship between the total solid content of soymilk and the textural characteristics of the tofu product. Lower soymilk solid content leads to higher moisture content and softer tofu. Conversely, higher total solid of soymilk is linked to increased levels of hardness, cohesiveness, springiness, and chewiness in the resulting tofu. Therefore, maintaining a consistent level of soymilk solid content between batches becomes imperative to ensure and monitor the uniformity of the soymilk gel quality. However, the manual process of making soymilk described in **section 3.2.2**. required modifications to obtain similar soymilk solid content between batches. Hence, experiments in this section aimed at:

a) Standardization of the methodology of the preparation of soymilk and okara.

b) Defining a methodology for the measurement of the solid content of soymilk, based on oven-drying and (or) UV-vis absorbance.

3.3.1.1. Standardization of Soymilk Preparation

The mass of soybeans recorded after hydration, dehulling and extraction is presented in **Table 3. 1**. While the mass of soybeans after hydration and dehull is similar, the mass of extracted soymilk and wet okara was quite different within three experimental sets. The solid content of soymilk measured by drying method also showed the disparity between batches. This indicates that the variation in the soymilk's quality was mainly caused by the separation of soymilk and okara by hand. Therefore, to minimize the difference, it was decided to squeeze the soymilk until at set mass was reached (330 – 340 g / 100 g dry soybean (SB)), corresponding to the average of soymilk extracted from 100 g of dry soybeans in three batches.

Table 3. 1: Mass of soybeans (g/100 g dry SB) after each processing stage (hydration, dehull and extraction) in three different batches. The percentage of solid content of soymilk was measured by the drying method and expressed in mean ± standard deviation (n = 3).

Batch no.	Hydrated soybeans	Dehulled soybeans	Soymilk with its solid content	Wet okara
1	218	185	353 (14.5 ± 0.2)	63
2	217	184	328 (16.6 ± 0.1)	70
3	216	186	336 (15.9 ± 0.2)	75

3.3.1.2. Estimation of the Soymilk Solid Content

The estimation of the solid content for soymilk was obtained by drying and UV-vis methods for 3 batches of soymilk prepared in 3 consecutive weeks, as depicted in **Figure 3. 2**. The estimation of the solid content obtained by the UV-vis method was lower level (≈ 15 – 19%), in comparison to the oven-drying method. This might be due to the increase in color of dried soymilk used for the construction of standard curve. The soymilk batches prepared in week 2 and 3, while there was a

slight disparity in solid content (16.6 ± 0.1, 15.9 ± 0.2, %) determined by drying, measurements by UV-vis spectrophotometer displayed similar solid content between batches (13.5 ± 0.5, 13.6 ± 0.5, %). This also raised concerns about the validity of the solid content standard curve when used over a two-week period for determining solid contents in multiple batches. As multiple batches of soymilk will have to be prepared for the experiments, this will require more time and steps to construct the solid content standard curve than with the drying method, a short duration of the usability of the standard curve will not be suitable for this research.

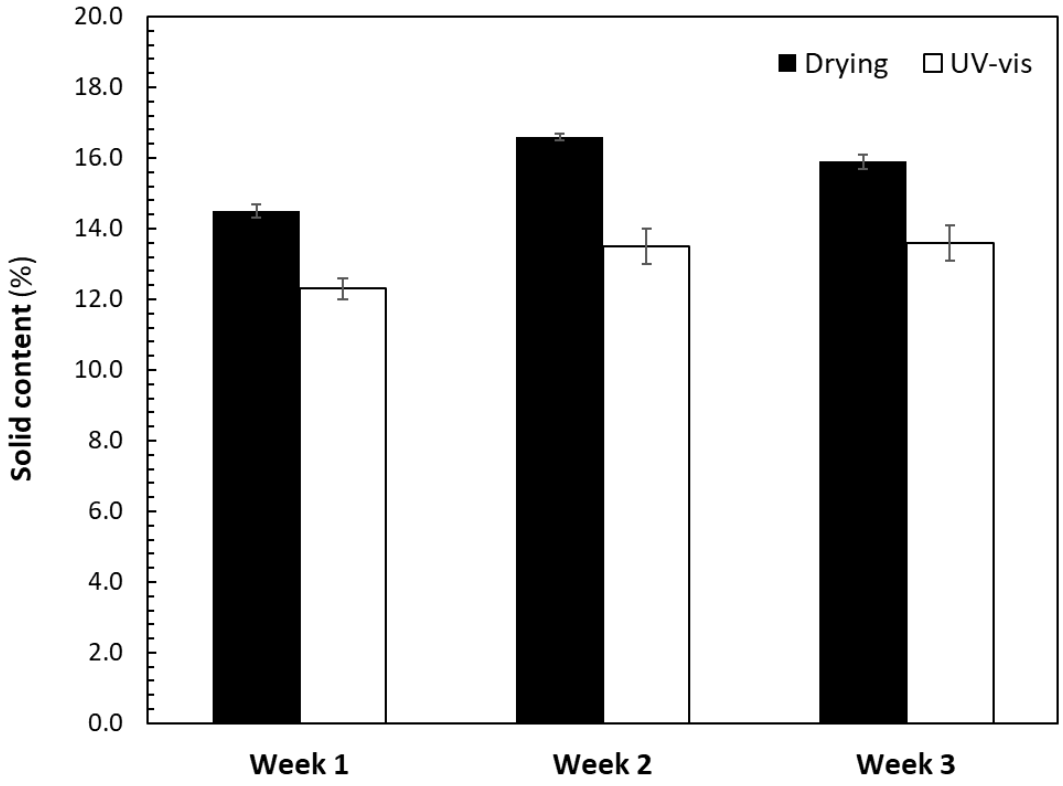


Figure 3. 2: Comparison of solid contents in 3 different batches of soymilk in 3 weeks, measured by drying and UV-vis method. Data expressed in mean ± standard deviation (n = 3).

3.3.2. Effect of States of Citric Acid in Okara Modification on the Structural and Textural Characteristics of Soymilk Okara Gels

The original method of modifying okara with CA (**section 3.2.4**), consisted in incorporating CA in solid state to the mixture of okara and water. This raised a question regarding the potential disparities in the structural and textural characteristics of CA modified okara and the resulting soymilk gels prepared from these materials. These disparities may be reduced by utilizing CA solution, considering that a solution would guarantee complete dissolution of CA in the mixture. Hence, the objective of this set of experiments was to examine the effect of the CA physical state (solution and solid) at the final concentration of 5 % (w:w) for okara modifications on the following properties:

a) Visual observation of okara (O, OCAS5, OCA5) and soymilk okara gels (M, MO, MOCAS5, MOCA5).

b) Microstructure of soymilk okara gels (M, MO, MOCAS5, MOCA5) obtained by CLSM imaging.

c) Mechanical and viscoelastic properties of soymilk okara gels (M, MO, MOCAS5, MOCA5) obtained by uniaxial compression and frequency sweep characterization.

3.3.2.1. Visual Observation of CA Modified Okara

Figure 3. 3 presents the optical images of the okara materials illustrating the effect of incorporating CA in both solid and solution form. At the final 5 % (w:w) CA concentration, okara modified with the solid form of CA resulted in a darker color and a more gummy texture material (OCAS5) compared to the crumbly, bright yellow unmodified okara O. Notably, okara modified with CA in solution (OCA5) and in solid form (OCAS5) had similar pH values, mass of dried solid (as Table

3. 2), yellow-brown color, and gummy texture. These observations suggest that both states of CA modified okara are indistinguishable.

Table 3. 2: Properties of okara materials (O, OCAS5, OCA5).

Samples	**Components**			**pH***	**Dried solid**** (g)
	Wet okara (g)	CA (g)	Water (g)		
O (control)	10	0	50	6.70	2.16
OCAS5	10	3	47	2.28	5.98
OCA5	10	3	47	2.28	5.92

* Final pH values of okara and citric acid solution mixture after 15-min mixing period.

** Dried solid of okara materials after 20-h drying at 60 °C in forced air oven.

3.3.2.2. Structural Characterization of Soymilk Okara Gels

Figure 3. 3 presents the effects of solid and liquid CA on the macro and microstructure of soymilk okara gels. In CLSM images, the red region represented the non-covalent labelling of the protein matrix with rhodamine B [128], while arrows indicated fiber strands from okara [69].

When analyzing the optical and CLSM images, soymilk gel (M) obtained by thermal aggregation displayed a smooth and uniform surface with a jelly-like texture. However, upon the addition of okara, the protein matrix in MO was disrupted by insoluble constituents of okara that can be seen as thin strands in CLSM images, and resulted in a heterogenous and crumbly structure, which agrees with previous studies [6, 4]. The gel MOCAS5 obtained from soymilk and CA modified okara was more homogeneous, as observed through both optical and microstructural images, compared to the unmodified okara soymilk gel (MO). There was no notable difference of the effect of CA state on the homogeneity of soymilk okara gels at micro and macro scales (MOCAS5 and MOCA5).

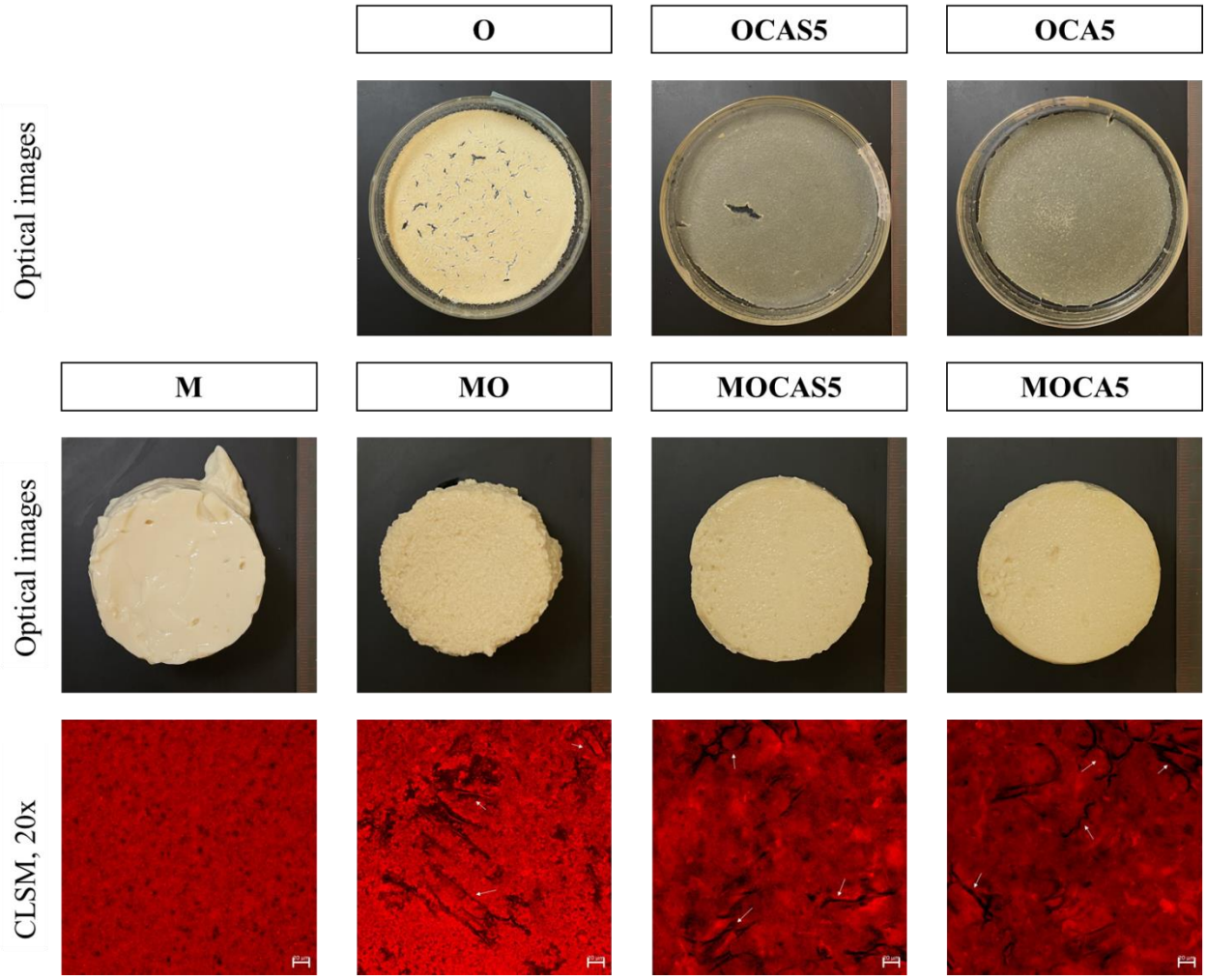


Figure 3. 3: Optical images of okara materials (O, OCAS5, OCA5); optical images and microstructural images determined by CLSM of soymilk okara gels (M, MO, MOCAS5, MOCA5). In CLSM images (at the objective of 20 x), red region represents for protein part with the scale bar indicates 20 μm.

3.3.2.3. Rheological Properties

Viscoelasticity of the soymilk okara gels is summarized in **Figure 3. 4** and **Table 3. 3**. The parameters G' and G'' represent the degree of elasticity and viscosity of gel, correspondingly [141]. Power law parameters n', n'' calculated from **Equation 3. 4** and **Equation 3. 5** are associated with weak- or strong-gel behaviour, and type of interactive forces within sample. Strong gels (n', n'' < 0.05), which are formed by breakable or deformable non-covalent cross-links,

display typical viscoelastic solids characteristic when subjected to small deformations. When increasing beyond the critical deformation threshold, materials experience rupture than flow. On the other hand, more frequency independent gels with n', n'' values larger than 0.05 are indicated as weak gel, which exhibit rheological characteristics between those of solutions and strong gels. Although under small deformation, weak gels resemble strong gels in mechanical behavior, their networks break into smaller cluster with the increase in deformation level. The network structure within weak gels is formed by strong permanent covalent crosslinks, but more vulnerable to disruption than strong gel system [132, 133].

All soymilk okara gels M, MO, MOCAS5, MOCA5 exhibited weak gel characteristic with G' remaining higher than G'' at all angular frequencies in range from 1 – 100 rad/s and n', n'' values fell in range of 0.12 – 0.16. Soymilk gel (M) had the lowest level of rigidity and viscosity reflected through G_o', G_o'' and tan (δ) values, in comparison to gels containing unmodified MO or modified okara MOCAS5, MOCA5. The gel strength and viscous property of soymilk gel improved significantly (G_o' = 38.48 ± 8.12 (kPa), G_o'' = 7.97 ± 1.77 (kPa)) when adding unmodified okara into the formulation.

Comparing soymilk gels containing okara with and without modification of CA of okara, MOCAS5 experienced an approximate 2-fold decrease in gel strength under shear stress in comparison to MO, represented by storage (G') and loss (G'') modulus, accompanied with an increase in tangent of phase angle (δ) over the investigated angular frequency range. The MOCAS5 and MOCA5 gels had similar G', G'' profiles. Additionally, their viscoelastic G_o' and G_o'' calculated from power law equations were not statistically significant different ($p < 0.05$). These results indicated that CA at 5% in both solid and solution state had similar effects on the rheological properties of soymilk okara gels. However, the viscoelastic properties of MOCAS5

had a wider standard deviation, in comparison to MOCA5. This observation suggests that CA in solution improves the consistency of the rheological properties of soymilk okara gels.

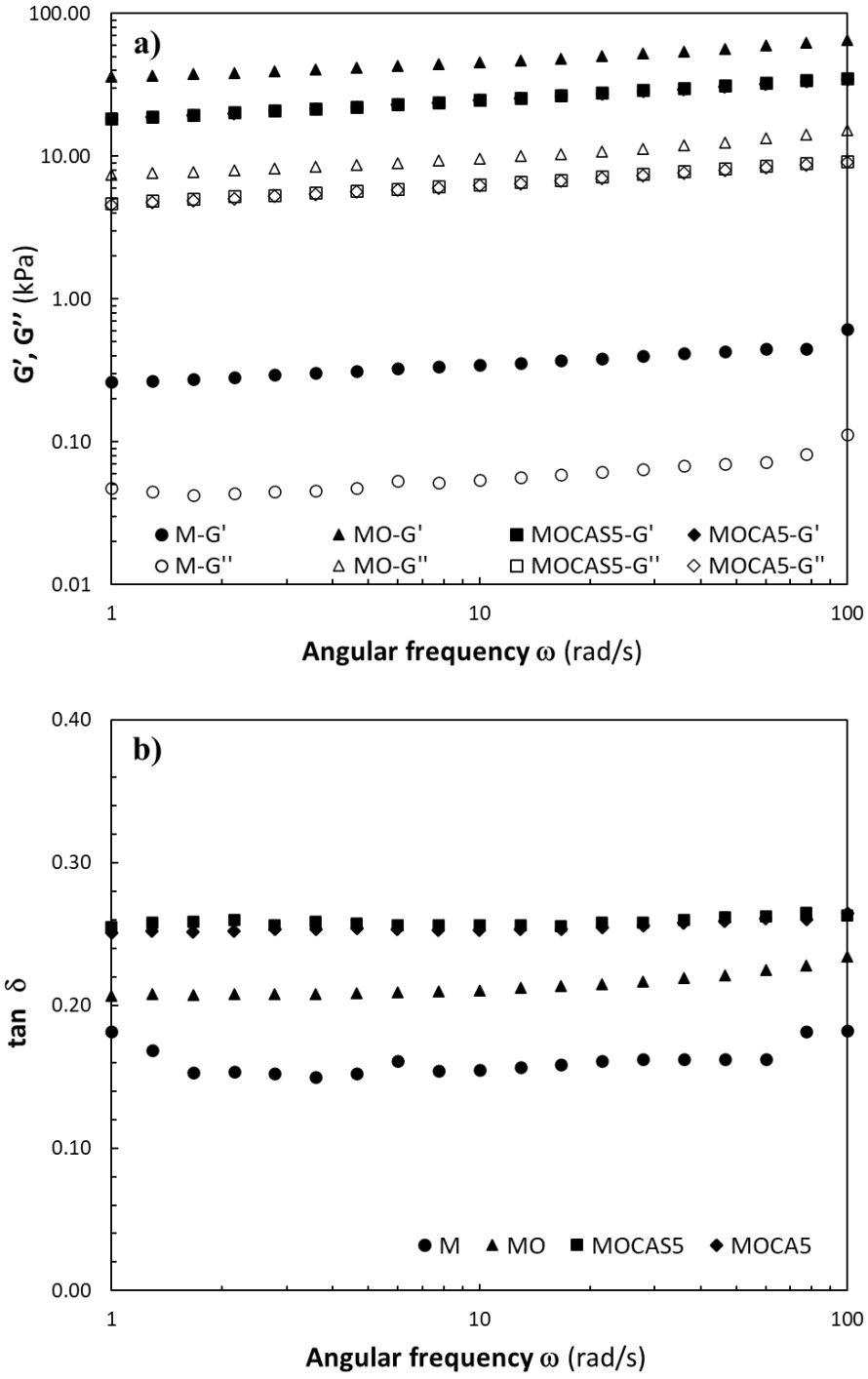


Figure 3. 4: Typical curves of a) storage modulus G' (filled symbols), loss modulus G'' (open symbols) and b) tangent delta (tanδ) over angular frequency ω (rad/s) of soymilk okara gels (M, MO, MOCAS5, MOCA5).

Table 3. 3: Viscoelastic properties of soymilk okara gels (M, MO, MOCAS5, MOCA5) based on power law parameters of **Equation 3. 4** and **Equation 3. 5** from frequency sweep tests. Data expressed as mean ± standard deviation (n = 3). Means within one column that do not share a common letter are statistically different (ANOVA followed by Tukey's post-hoc: $p < 0.05$).

Sample	G_0' (kPa)	n'	R^2	G_0'' (kPa)	n''	R^2
M	0.28 ± 0.04^a	0.12 ± 0.02^a	0.92 ± 0.04	0.04 ± 0.01^a	0.14 ± 0.02^a	0.78 ± 0.12
MO	38.48 ± 8.12^b	0.12 ± 0.01^a	0.99 ± 0.01	7.97 ± 1.77^b	0.14 ± 0.02^a	0.98 ± 0.01
MOCAS5	18.51 ± 2.20^c	0.14 ± 0.01^a	1.00 ± 0.00	4.65 ± 0.50^c	0.14 ± 0.00^a	0.99 ± 0.00
MOCA5	17.47 ± 1.13^c	0.15 ± 0.01^a	1.00 ± 0.00	4.37 ± 0.23^c	0.16 ± 0.01^a	0.99 ± 0.00

3.3.2.4. Mechanical properties

Mechanical properties obtained under uniaxial compression of soymilk okara gels (M, MO, MOCAS5, MOCA5), are summarized in **Figure 3. 5**. In the context of textural analysis, Young's modulus (or elastic modulus) is associated with qualities such as firmness or hardness, while the true fracture stress related to characteristics like toughness or chewiness, which also accounted for springiness and cohesiveness in addition to firmness properties of material [136]. The degree of deformation prior to gel fracture was represented by true fracture strain value [142].

Gel prepared from soymilk only (M) had a lower true fracture stress and Young's modulus, along with higher true fracture strain, when compared to soymilk gel with the addition of unmodified okara (MO). These findings suggest that M possessed characteristics of a weak but deformable gel, while MO expressed as strong and brittle gel [143].

When comparing the MO gel to the MOCAS5 gel, a notable increase, around 2-fold in the firmness and chewiness properties was observed. The MOCAS5 and MOCA5 gels had true fracture stress,

true fracture strain and Young's modulus values not statistically significant different ($p < 0.05$). However, the (MOCA5 gel showed a higher level of repeatability in mechanical properties compared to MOCAS5 gel. These results are aligned with the rheological data, indicating that CA at 5% used for okara modification in both solid and solution state had similar positive effects in mechanical properties, but increased uniformity in gel's texture when using CA in solution form.

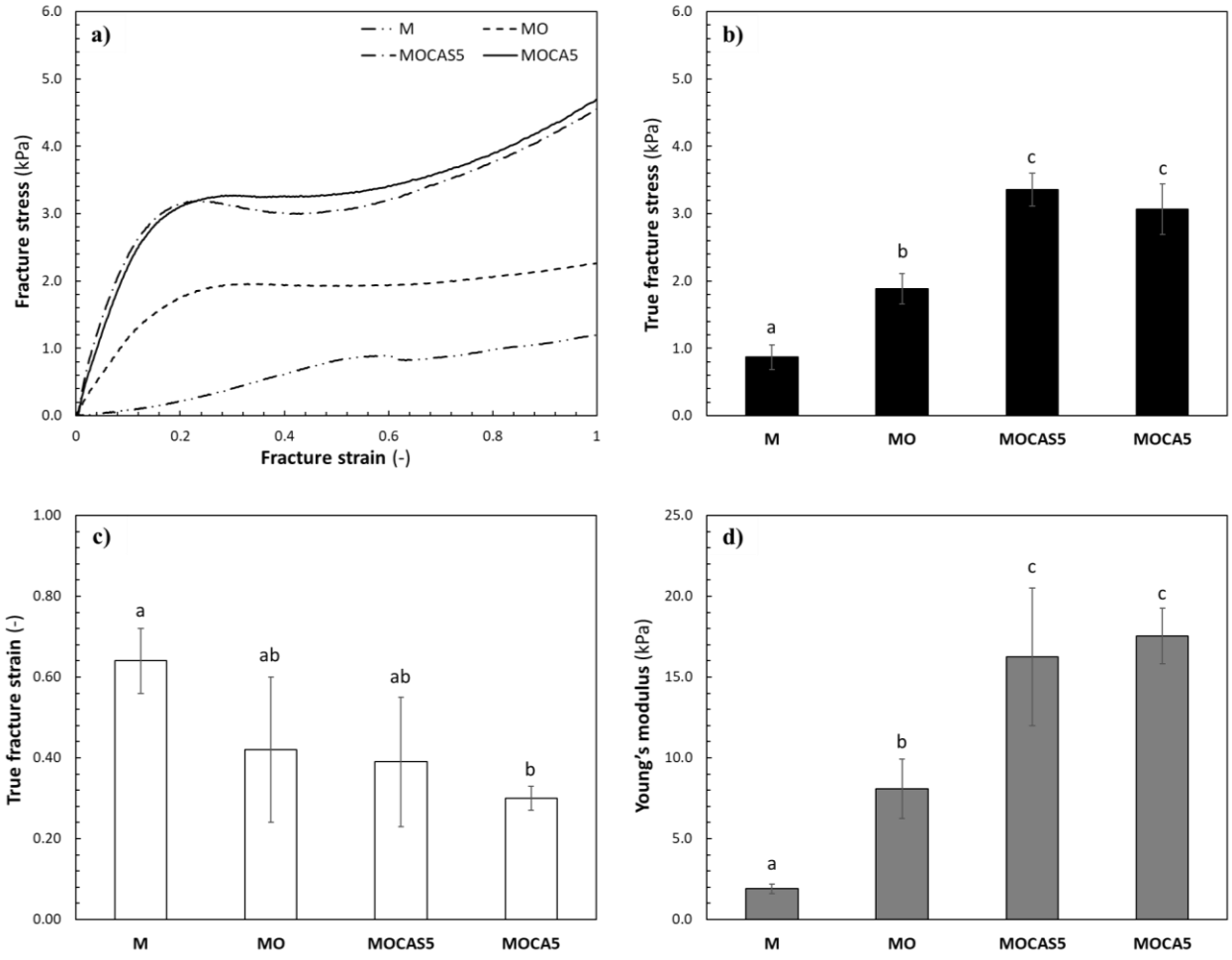


Figure 3. 5: Mechanical properties of soymilk okara gels (M, MO, MOCAS5, MOCA5), (a) Typical fracture stress – fracture strain curves, (b) True fracture stress, (c) True fracture strain, (d) Young's modulus. Data of (b – d) expressed as mean ± standard deviation (n = 5). Means that do not share a common letter are statistically different (ANOVA followed by Tukey's post-hoc: $p < 0.05$).

3.3.3. The Effect of Drying Time on the CA Modified Okara

Okara was modified with CA solutions, then dried at 60 °C for 20 h before being introduced back to soymilk to prepare soymilk okara gels. Intially, the drying time was selected as when okara materials dried visually. Therefore, this preliminary experiment was conducted to examine the effect of the drying time on the solid content, visual appearance and structural properties of CA modified okara materials with 10 % CA (OCA10). OCA10 was selected for the assessment due to most significant changes in the color and gumminess in texture, compared to unmodified okara (O).

3.3.3.1. Solid Content and Visual Observation of OCA10 According to Drying Time

The total solids content and visual appearance of okara modified with 10 % CA was investigated according to time over a 50 h drying period. After 20 h of drying, OCA10 had a solids content of 9.711 g and a brown color and gummy texture. Over the following 6 h of drying, the solids content decreased slightly by 0.27 g (≈ 3 %) with no noticeable alternations in color and texture. From 20 to 44 h of drying, the rate of change in solid content decreased compared to the previous period (20 to 26 h), as depicted in **Figure 3. 6**. However, during this period, there was a significant change in the color of OCA10, appearing darker. By the end of the drying period at 50 h, the solids content of OCA10 decreased by approximately 9%, accompanied by darker color, drier and crumbier texture in comparison to the state at 20 h.

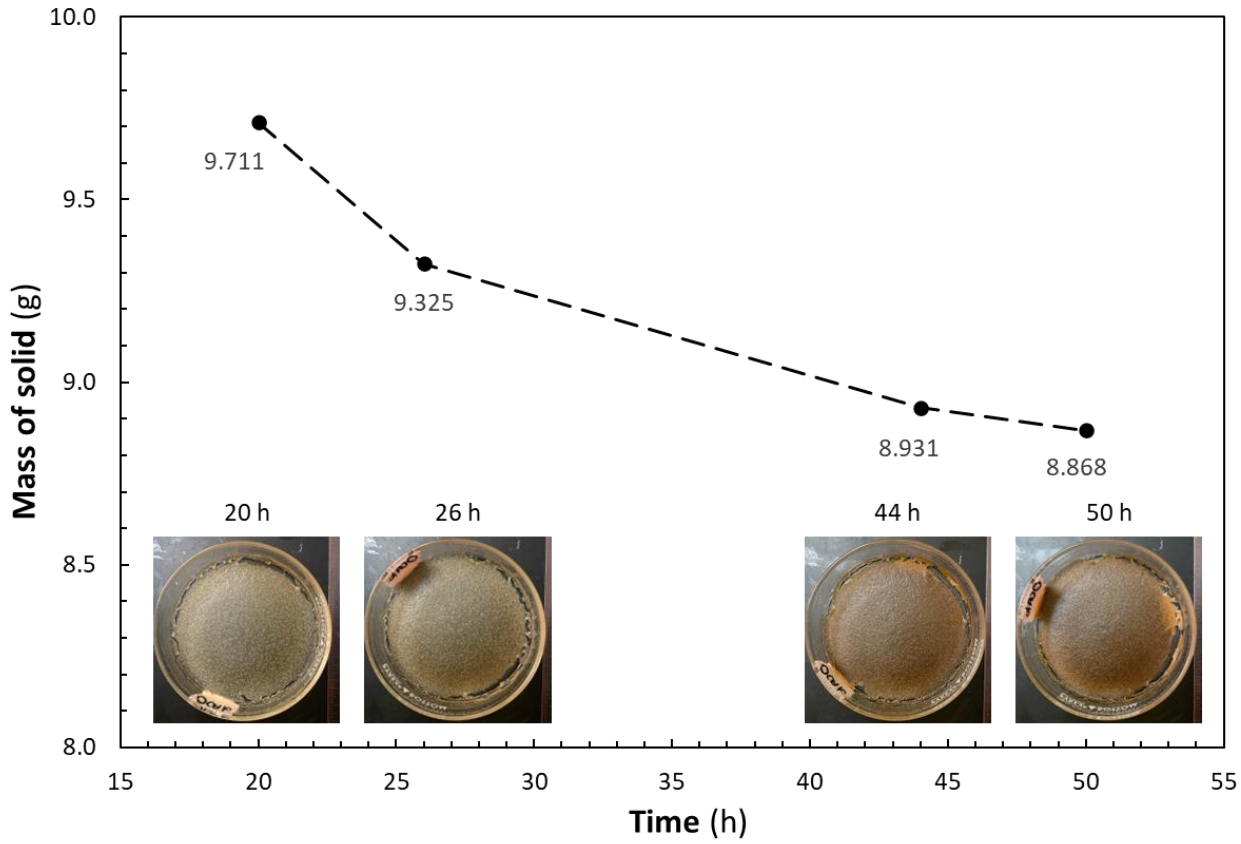


Figure 3. 6: Visual appearance and solids content of OCA10 at different drying durations (20 h, 26 h, 44 h and 50 h).

3.3.3.2. Structural Characterization of Okara by FTIR

FTIR analysis was employed to investigate the effect of drying time on the chemical structure of CA modified okara (OCA10) by analyzing changes in the transmittance intensity and frequency of major functional groups (**Figure 3. 7**). The FTIR spectra of unmodified okara (O), CA and CA modified okara (OCA10) at 20, 26, 44, 50 h of drying were divided in 4 different regions, region 1 (3650 – 3100 cm^{-1}); region 2 (3020 – 2750 cm^{-1}); region 3 (1800 – 1500 cm^{-1}) and region 4 (1300 – 800 cm^{-1}). The detected peaks, wavenumbers and assignments are presented in **Table 3. 4**.

Region 1 (3650 – 3000 cm^{-1}) contains the strong, broad absorption peak related to O-H stretching vibrations of intra- and intermolecular hydrogen bonds in polymer and moisture [144] or amine

(N-H) stretching vibrations in protein [145, 146], while narrow absorption peaks can be attributed to free hydroxyl groups or O-H bonds of carboxylic acids [147]. Region 2 (3020 – 2750 cm^{-1}) contains peaks at ~ 2960 – 2850 that can represent CH_n stretching [148, 149]. Region 3 (1800 – 1500 cm^{-1}) can provide information on the degree of esterification of polysaccharides and on the structure of protein molecules. Specifically, two peaks in the 1760 – 1730 cm^{-1} and 1640 – 1620 cm^{-1} range are associated to the stretching vibrations of C=O in ester carbonyl groups (-COOR) and C=C in carboxylate ion (-COOH), respectively [147, 150]. The amide I and II bonds in protein display peaks at wavelength of 1690 – 1600 cm^{-1} and 1560 – 1530 cm^{-1} [151, 152]. Region 4 (1300 – 800 cm^{-1}) is called the fingerprint region, in which bands' location and intensity are associated with different types of polysaccharides [153]. The major peaks in the 1200 – 1000 cm^{-1} range represent C-O-H stretching vibrations overlapping C-O-C glycosidic bond vibrations, distinctive characteristics of hemicellulose, cellulose, and lignin [154].

Table 3. 4: FTIR frequencies (cm^{-1}) of functional groups in okara presented in literature and experimental data.

Literature frequency range (cm^{-1})	**Observed frequency** (cm^{-1})	**Corresponding functional groups**
3650 – 3000 [144, 145, 146]	3650 – 3100	O-H stretching vibrations. N-H stretching vibrations.
2960 – 2850 [148, 149]	2955, 2921, 2855	CH_n stretching vibrations.
1760 – 1730 [147, 150]	1743 – 1710	C=O stretching of ester carbonyl group (COOR).

1690 – 1600 [151, 152]	1633 – 1627	C=O stretching (80%) and C-N (20%) of amide I bond.
1640 – 1620 [147, 150]	1633 – 1627	C=C of carboxylate ion stretching (COOH).
1560 – 1530 [151, 152]	1540	N-H bending (60%) and C-N (40%) of amide II bond.
1480 – 1200 [151, 152]	1234	C-N stretching and N-H deformation of amide III bond.
1200 – 1000 [144, 154]	1163, 1035	C-O tensile vibration in C-O-H and C-O-C of sugar rings.

The FTIR spectra of dried okara O reflects its major constituents, approximately 50% dietary fiber, 25% protein and 10% lipid [155]. FTIR spectra of O showed a broad band at 3283 cm^{-1} in region 1 along with peaks at 2955, 2921 and 2855 cm^{-1} in region 2 originating from the stretching vibration of CH_n, which is associated with the typical structure of protein, lipid and polysaccharide in okara [149]. Unmodified okara O exhibited a high level of cellulose, hemicellulose, and lignin with prominent peaks in region 3 and 4. Characteristic peaks were observed at ~ 1743 and 1633 cm^{-1}, which can be associated to stretching vibrations of esterified and unesterified carboxyl groups. Peak at 1163 cm^{-1} was caused by tensile vibration of C–O in C–O–H, while broad, strong band from 1130 – 930 cm^{-1} with the most intense peak at 1035 cm^{-1} represent tensile vibration peak of C–O in C–O–C of sugar rings in cellulose and hemicellulose [144]. The soy soluble polysaccharide (SSPS) has a pectin-like structure with the backbone composed from rhamnogalacturonan linked by the intervention of galacturonan chains, which obtained feature

FTIR peaks at 1011 cm^{-1}, 1035 cm^{-1} and 1065 cm^{-1} [152, 156]. The absorption peak at 891 cm^{-1} corresponds to the β-glycosidic linkage [157]. The protein content in okara is demonstrated by peaks at 1633 (amide I) and 1540 (amide II).

After the okara modification with CA solution 10 % (w:w) and 20-h drying, FTIR spectra of OCA10 observed a shift of O-H band from 3283 cm^{-1} to higher wavelength at 3496 cm^{-1}, which indicates a weaker hydrogen bonding of water molecules in OCA10 compared to unmodified O [158]. The significant reduction in intensity of CH_n peaks (2955, 2921 and 2855 cm^{-1}), and in the tensile vibration peaks of C–O in C–O–C (1163 cm^{-1}) and C–O–H (1035 cm^{-1}) of sugar rings, along with the disappearance of β-glycosidic linkage (891 cm^{-1}) in region 4 suggest the degradation of polysaccharide. The significant increase in area and intensity of peak at 1710 cm^{-1} (-COOR), accompanied with the decrease in intensity of peak at 1627 cm^{-1} (-COOH) are indications of the release of pectic substances [147, 159, 160, 161]. Furthermore, the presence of peaks within range of 1000 – 1150 cm^{-1} attributed to the abundance of homogalacturonans, which was the principal constituent of pectin, were also stable regardless of their state [147, 162]. Peaks situated at 1045 and 1076 cm^{-1} were associated with monosaccharides in pectic substances such as arabinose, xylose, and galactose [147]. This finding potentially accounted for the gummy texture observed in OCA10.

Throughout the drying process, significant alterations in the color of OCA10 were noted, with a more pronounced darkening observed after 44 h. This observation hinted at the occurrence of caramelization and Maillard reactions within the sample. Caramelization is series of complex reactions from dehydration, sugar molecule degradation, to the polymerization of intermediates [158]. Maillard reaction is chemical reaction between amino acids and reducing sugars leading the formation of Amadori compound (C=O), Schiff base (C=N), and pyrazines (C-N) at the early stage

of process [163, 164]. These two phenomena, caramelization and Maillard reaction can occur simultaneously with the appearance of both reducing sugars and amino acids in the system. Prominent regions in the FTIR spectrum of the protein – polysaccharide system, based on the covalent linkage between the carbonyl groups of reducing sugars and amino groups of proteins can serve as significant markers for reaction occurrences [165]. The FTIR spectra of OCA10, following drying times ranging from 20 to 50 h, the alternations were compared to unmodified okara O, with no significant disparity detected by FTIR analysis until the period of 50 h. Regarding to the characteristic peaks related to polysaccharides, a significant reduction in intensity along with a slight shift in the wavelength of the carboxylate ion C=O stretching to 1627 cm^{-1} were observed. This change was accompanied by a decrease in the C-O stretching vibrations (1163 and 1035 cm^{-1}) corresponding to sugar rings. Furthermore, reductions in the intensity of protein peaks were also evident including amide I (80% C=O stretching at 1627 cm^{-1}), amide II (N-H bending at 1540 cm^{-1}), and amide III (C-N stretching and N-H deformation at 1234 cm^{-1}). New peak formed at 1120 cm^{-1} was attributed to the C-N stretching characteristic of secondary amine in the Amadori product formed during the Maillard reaction [152], while new peaks produced within the range of 1050 – 950 cm^{-1} corresponding to side-chain vibrations originating from proteins, indicated structural modifications in the protein component [163].

Upon reaching a drying time of 50 hours, an increased number of peaks appeared in the regions of amide III (1300 – 1200 cm^{-1}) and the protein's side-chain vibrations (1050 – 950 cm^{-1}). An additional peak at 1743 cm^{-1} was observed, linked to the C=O stretching vibration of Amadori compounds formed during the initial stages of the Maillard reaction [166]. These findings indicate a more pronounced alteration in the protein component after the 50-hour drying. Notably, although significant color changes were noted in modified OCA10 after 44 hours, the observation in spectra

of OCA10 at the drying time of 20 to 50 h emphasized varying degrees of reaction can be detected through FTIR analysis.

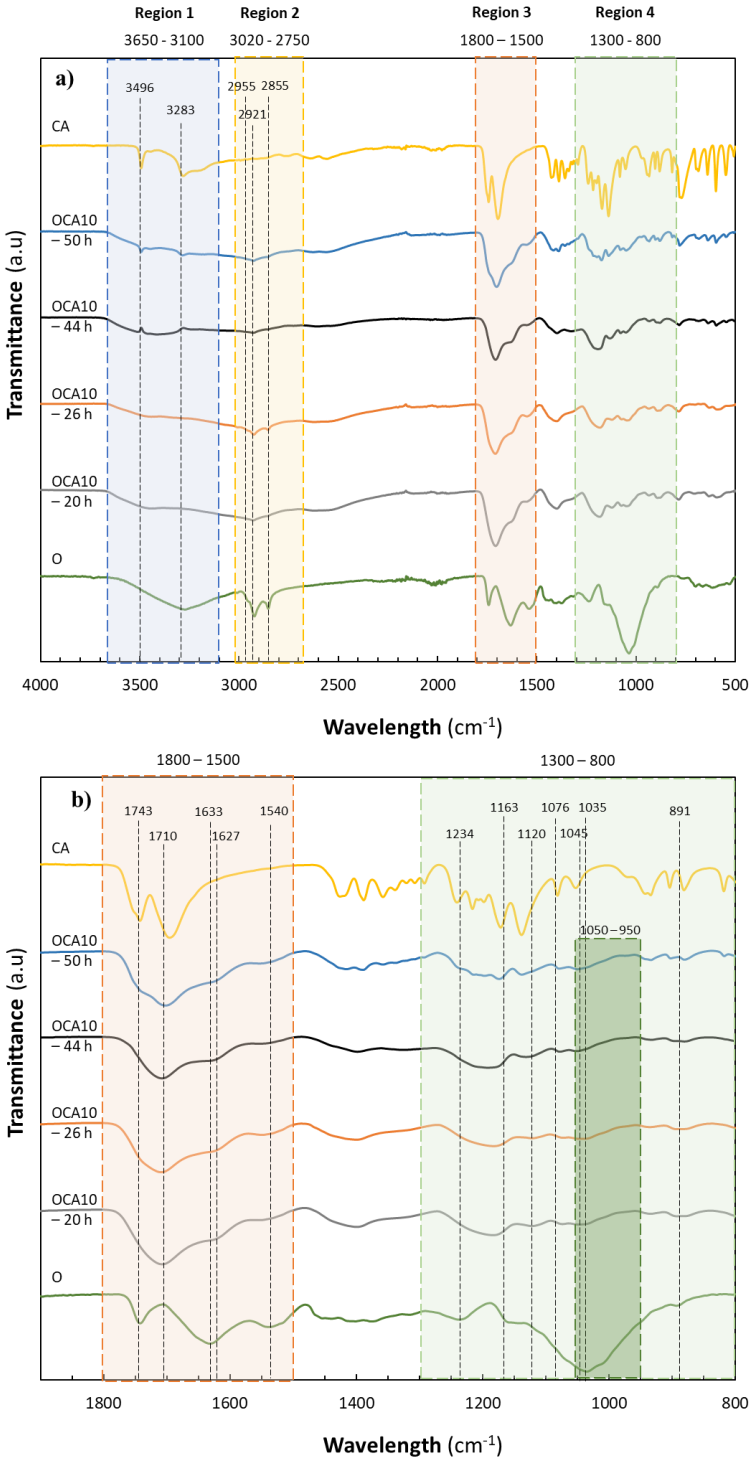


Figure 3. 7: a) FTIR spectra of control (unmodified O), CA modified okara (OCA10) at different drying times and citric acid (CA), b) zoomed-in view within the range from 2000 – 800 cm^{-1}.

3.4. Conclusions

The consistency of the preparation of soymilk and the citric acid modification of okara was improved by adjusting the methodology as follows:

1) For the standardization, the soymilk is prepared following steps described in **section 3.2.2** with an addition that soymilk will be squeezed out until reach the mass of 330 – 340 g / 100 g dry soybean. The solid content of soymilk will be in range from 15 – 16 %, which can be estimated with the drying method at 60 °C for the period of 3 h.

2) The solid and liquid state of CA at the final concentration of 5 % (w:w) had similar effects on the modification of okara, in comparison to unmodified okara (O): 1) change in color and texture of okara (OCAS5, OCA5) by visual observation, 2) improvement in the homogeneity of soymilk okara gels (MOCAS5, MOCA5) observed by optical and CLSM imaging and 3) increase in mechanical properties and decrease in the viscoelasticity of soymilk okara gels (MOCAS5, MOCA5). However, CA in solution form displayed a better ability in producing soymilk okara gels with high level of consistency in textural properties. The use of CA solution ensured that CA is fully dissolved and distributed well in the mixture, leading to a better reproducibility in texture properties. Therefore, CA solution was employed in this project.

3) The effect of the drying duration of okara materials between 20 and 50 h had been negligible on the level of water removal. However, notable changes were noticed in colour intensity, along with the formation of products from Maillard and caramelization reactions detected by FTIR analysis. Therefore, 20 h was selected as the appropriate time for drying okara materials to constant weight without major alternations in colour and composition.

Chapter 4: Methodology of Sample Preparation for Texture Characterization and Protein – Protein Interactions Characterization of Soymilk Okara Gels

4.1. Introduction

The overall framework of this study and the specific questions addressed in this chapter are presented briefly in **Figure 4. 1** and consists of the methodology for sample preparation and protein – protein interaction characterization of soymilk okara gels.

During the preparation of soymilk okara gel samples for rheological and mechanical properties measurements, inconsistencies were observed. The weak gel behavior of soymilk okara samples damaged the sample and resulted in inconsistent thickness while cutting. To address this issue, alternative sample preparation methods were explored with the objective of reducing the cutting effect and inconsistent thickness to improve reproducibility and accuracy of rheological and mechanical measurements.

The second part of this chapter presents initial results of the estimation of protein – protein interactions obtained by adapting the two-step methodology from reference [10], 1) gel dissolution in specific soaking solution; 2) measurement of soluble protein in samples by Bradford assay. Preliminary experiments were conducted to finalize the method by examining protein – protein dissolution conditions and investigating potential interferences of the soaking solutions for the construction of standard curve for the Bradford assay.

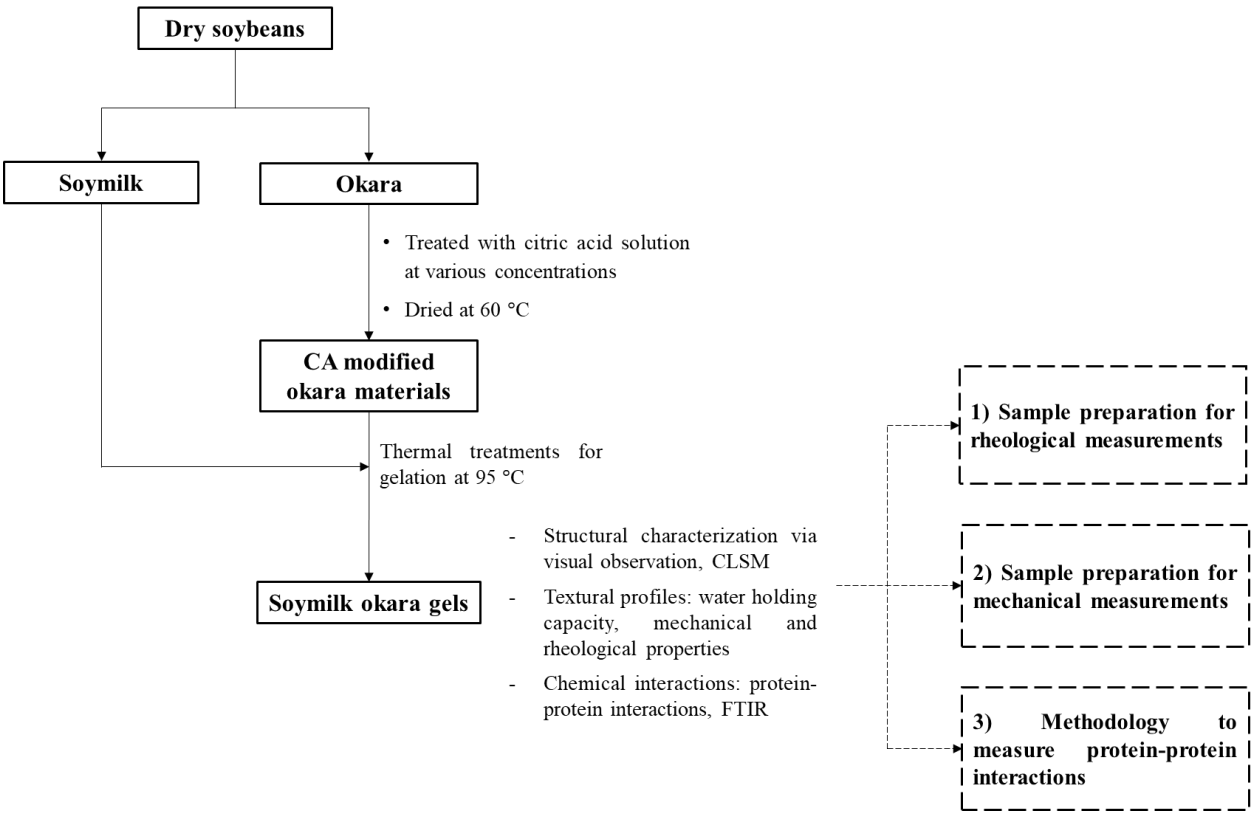


Figure 4. 1: Overall framework (solid lines and boxes) and specific questions addressed in this chapter (dashed lines and boxes) for the sample preparation and chemical interaction characterization of soymilk okara gels.

4.2. Materials and Methods

4.2.1. Materials

Soybeans (lot 11741D and 20181D, Nupak) were purchased from a local supermarket (Waterloo, ON, Canada) and kept in Ziploc bags for experiments. Citric acid anhydrous (CA, lot 221510) was obtained from Fisher Scientific (Fair Lawn, NJ).

The phosphate buffer 0.05M was prepared from sodium phosphate dibasic heptahydrate (lot A0386400), sodium dihydrogen phosphate dihydrate (lot A0399326) obtained from Acros Organics (India) and adjusted with either sodium hydroxide (lot MKCH5997) or hydrochloric acid (lot 209268) obtained from Sigma Aldrich (India) and Fisher Scientific (Fair Lawn, NJ). Urea (lot

BDH4602) and sodium chloride (lot 132465) were purchased from VWR (Canada) and Fisher Scientific (Fair Lawn, NJ). Bovine serum albumin (BSA) (lot 64499500) and concentrated Bradford dye reagent (lot 64509872) were purchased from Bio-rad (USA).

4.2.2. Preparation of Soymilk Okara Gels

Soymilk and okara were prepared following the procedure described in **section 3.2.2**. Okara modified by citric acid (CA) solution OCA5 and soymilk okara gels (M, MO, MOCA5) were prepared following the procedure described in **section 3.2.4.1** and **3.2.5**, respectively.

4.2.3. Rheological Properties

4.2.3.1. Sample Preparation for Rheological Properties Measurements

The sample preparation was reviewed to improve the consistency and accuracy of rheological measurements for soymilk okara gels. The desired target dimensions of the soy gel samples are 2 – 3 mm in thickness and ≥ 35 mm in diameter as presented in **Figure 4. 2**. In the original method, soymilk okara mixture in **section 4.2.2** was gelled in 100-mL beakers with a diameter of 40 mm and stored overnight in the fridge before being cut into thin slices (2 – 3 mm) using a sharp blade prior to the rheological measurements.

However, the weak gel behavior of soymilk okara samples posed challenges in this process, resulting in potential sample damage and inconsistent slice thickness. To address this issue, an alternative sample preparation method was examined with the objective of reducing the cutting effect and inconsistency in samples' thickness to ultimately improve the reproducibility and accuracy of rheological measurements. Control samples including pure soymilk gel (M) and soymilk with unmodified okara gel (MO) were selected for examination due to the differences in their rheological properties. The preliminary viscoelastic experiments conducted in **section 3.3.2.3**

indicated that soymilk gel M exhibited the lowest gel strength under shear stress, while MO displayed brittleness due to the disruption of insoluble polysaccharides within the protein gel.

In the alternative method, samples were gelled such that the gels had the desired thickness eliminating the need to cut a very thin sample. This was obtained with a glass petri dish covered with parchment paper and oiled with Pam spray to create a non-stick surface. A gel with the final thickness of 2 – 3 mm, required approximately 25 g of soymilk or 20 g of soymilk and unmodified okara mixture prepared in **section 4.2.2** to be added into petri dish for gelation of M and MO, respectively. The gelation occurred at the same conditions as in the original gel preparation (at 95 °C, for 45 min in water bath). Subsequently, gelled samples were stored in the fridge overnight before cutting into thin square disk with the dimension of 40x40 mm using a sharp blade.

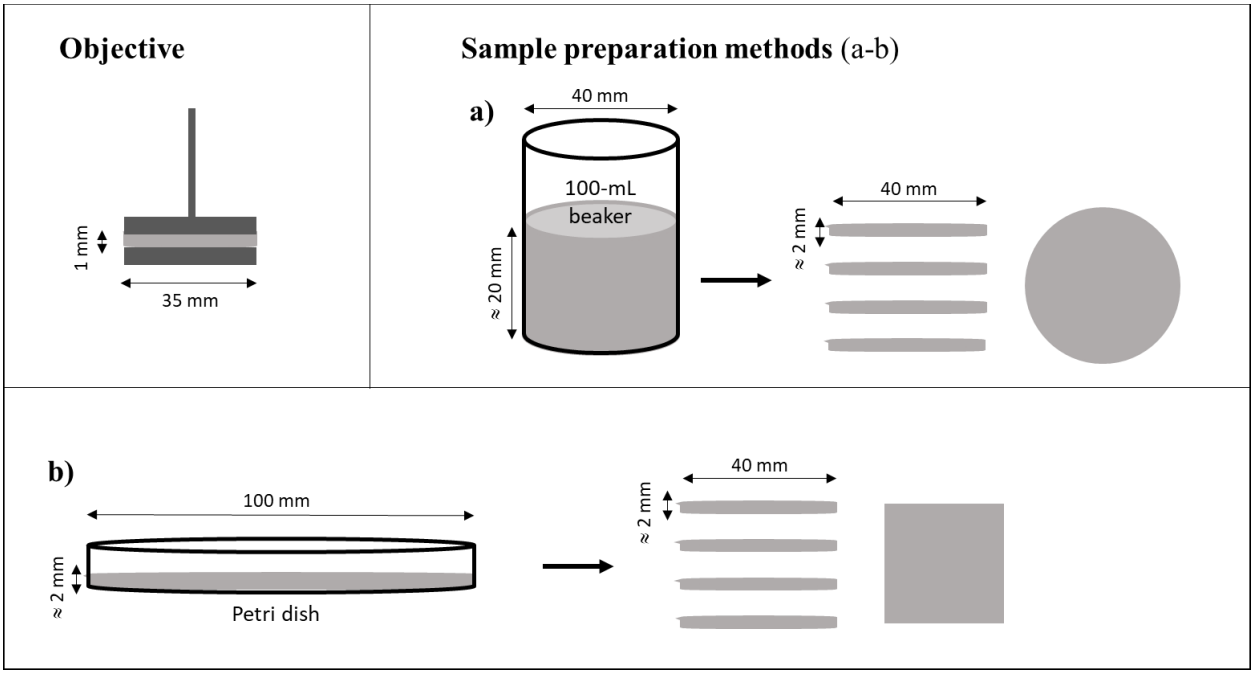


Figure 4. 2: a) Original sample preparation in 100-mL beaker and b) alternative sample preparation in petri dish for the rheological measurements.

4.2.3.2. Rheological Properties Measurement and Analysis

The rheological properties of soymilk okara gels were measured and analyzed following the procedure described in **section 3.2.8**. The linear viscoelastic region of samples determined from the strain sweep test is presented in **Figure S. 4** in **Appendix B.1**.

4.2.4. Mechanical Properties

4.2.4.1. Sample Preparation for Mechanical Properties Measurements

The preparation of gel samples for mechanical testing was reviewed to reduce the number of steps associated with the original method to obtain soy gel samples with a desired cylindrical shape with 10 mm in height and 20 mm in diameter as presented in **Figure 4. 3**. In the original method, soymilk okara mixture prepared in **section 4.2.2** was gelled in 100-mL beakers with a diameter of 40 mm and stored overnight in the fridge before being cut into cylindrical shapes using a sharp blade and metal corer.

However, multiple cutting steps led to potential sample damage and inconsistent sample dimensions, similar to the issues encountered during the preparation of samples for rheological tests. To address these concerns, an alternative sample preparation method was developed. Control samples including pure soymilk M gel and soymilk with unmodified okara gel MO, which exhibited different mechanical properties with sample M having characteristics of a weak but deformable gel, while MO having strong and brittle gel.

In the alternative method, M and MO were gelled in 100-mL beakers with diameter of 40 mm or in 250-mL beakers with diameter of 60 mm oiled with Pam spray to ensure non-stick surface. The mass of liquid was adjusted to obtain a gel with a final thickness of 10 mm, corresponding to approximately 25 g of soymilk or 20 g of soymilk and unmodified okara mixture prepared in

section 4.2.2 were added for gelation of M and MO, respectively for 100-mL beakers and around 35 g of soymilk or 30 g of soymilk and unmodified okara for 250-mL beakers. The gelation occurred at the same conditions with original gel preparation (at 95 °C, for 45 min in water bath). Subsequently, gelled samples were stored in the fridge overnight before cutting into thin cylindrical shape with the dimension of 10x20 mm by a metal corer.

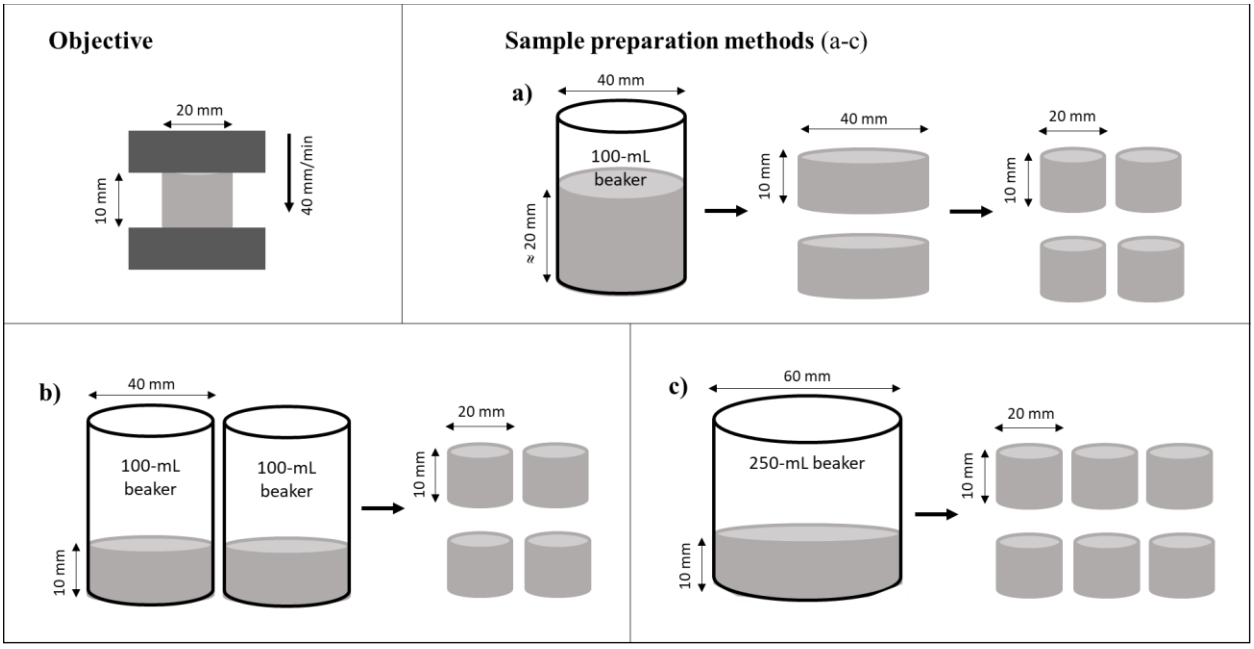


Figure 4. 3: a) Original sample preparation, proposed new sample preparations in b) 100-mL beakers and c) 250-mL beaker for the mechanical properties test.

4.2.4.2. Mechanical Properties Measurement and Analysis

The mechanical properties of soymilk okara gels were measured and analyzed following the procedure described in **section 3.2.9**.

4.2.5. Protein – Protein Interactions

This methodology is based on the differences of protein solubility in selective solutions that disrupt specific interactions presented in **Table 4. *1*** thus reflecting the contributions of ionic bond, hydrogen bonds and hydrophobic interactions in the protein gel matrix. The methodology was

adapted from [10], which consists of 2 main steps 1) gel dissolution in specific soaking solutions; 2) measurement of soluble protein by Bradford assay.

4.2.5.1. Chemicals and Solutions

Four different soaking solutions were prepared in 0.05M phosphate buffer pH 7.0: SA (0.05M NaCl), SB (0.6M NaCl), SC (0.6M NaCl + 1.5M urea), SD (0.6M NaCl + 8M urea). A volume of 500 mL of 0.05M phosphate buffer pH 7.0 was prepared by dissolving 3.872 g of sodium phosphate dibasic heptahydrate ($Na_2HPO_4.7H_2O$) and 1.646 g of sodium dihydrogen phosphate dihydrate ($NaH_2PO_4.2H_2O$) into 400 mL of DI water contained in a 1000mL beaker. The pH of the solution was adjusted to 7.0 with the addition of HCl 1M or NaOH 1M solution with a pH meter (Mettler Toledo, S47 SevenMulti Dual) while constant stirring. Subsequently, the solution was transferred to a 500 mL volumetric flask and filled with DI water to the mark.

Table 4. 1: Soaking solutions (SA, SB, SC, SD) prepared in 0.05M phosphate buffer pH 7.0 and their target intermolecular bonds *[167]*.

Soaking solution	**Reagents** (in 0.05M phosphate buffer pH 7.0)	**Target intermolecular bonds**	**Protein solubility difference**	**Interactions**
SA	0.05M NaCl	Non-specific associations		
SB	0.6M NaCl	Electrostatic, hydrogen	SB – SA	Ionic bonds
SC	0.6M NaCl + 1.5M Urea	Hydrogen	SC – SB	Hydrogen bonds
			SD - SC	

SD	0.6M NaCl + 8M Urea	Hydrogen, hydrophobic	Hydrophobic interactions

Bovine serum albumin (BSA) was used as the protein standard for the Bradford assay. The stock solution containing 1.51 mg/mL of BSA protein (Bio-rad, USA) was prepared in ultra-pure water as manufacturer's instruction and stored in the fridge at 4 ℃ for further use within 60 days or frozen at -20 ℃ for longer storage. The Bradford dye reagent was prepared by diluting 1 part of volume of concentrated Bio-rad dye reagent (Bio-rad, USA) with 4 parts volume of DI water. The solution was then filtered through Whatman no.1 filter paper to remove particles and stored in amber bottle at room temperature for 2 weeks. The dye solution should be re-filtered before use as it is easily precipitated [168].

4.2.5.2. Dissolution of Protein – Protein Interactions in Soymilk Okara Gels

A mass of 0.6 g soymilk okara gel (M, MO and MOCA5) was solubilized into 10 mL of a given soaking solution (SA, SB, SC and SD). The gel and soaking solution were then homogenized using vortex 1 min at room temperature incubated at room temperature for 24 h and finally centrifuged using ultracentrifuge (Optima XPN, Beckman Coulter) with swing bucket rotor (SW 41 Ti, Beckman Coulter) at 12,000g, which is relevant to the rotor speed of 10,000 rpm, at 25 °C for 30 min *[169]*. The conversion of rotor speed from g-force was performed and presented in **Appendix B.3**. supernatant phase was carefully pipetted out using a micropipette (Eppendorf) for analysis. The protein content of the supernatant phase represented the amount of protein solubilized from the gel upon incubation in the soaking solution and was determined using Bradford assay.

4.2.5.3. Measurement of Soluble Protein Content by Bradford Assay

The Bradford method is highly favored for protein quantification as its simplicity, sensitivity, and free of interferences to common reagents, reducing agents (β-mercaptoethanol) and non-protein components in biological samples except detergents, flavonoids, and protein buffers [170]. The Bradford assay is based on Coomassie Blue G250 dye binding process, which exhibits distinct color changes upon interacting with specific amino acid residues in proteins including arginine, tryptophan, tyrosine, histidine, and phenylalanine. In an acidic environment, the free dye initially appears as a cationic red form and transforms into an anionic blue form with an absorbance maximum at 590 nm after binding to amino acids. By measuring the absorbance of the solution at 595 nm wavelength, the quantity of protein can be determined [171, 172].

A protein standard curve is constructed using BSA with the linear concentration range of 0.05 – 0.5 μg/μL for the following microplate procedure. A volume of 1000 μL of BSA solution with concentrations of 0.0755, 0.151, 0.2265, 0.302, 0.3775, 0.453 μg/μL were prepared in sodium phosphate buffer pH 7.0 from the stock (1.51 mg/mL) as presented in **Table S.*1*** in **Appendix B.3**. A polystyrene 96-well flat bottom non treated microplate (Corning, NY, USA) was used in which a volume of 200 μL of diluted Bio-rad dye reagent was added into 10 μL of BSA solution at different concentrations or phosphate buffer as blank and mixed gently to avoid the foam formation. The absorbance of the mixtures at the wavelength of 595 nm was measured after 10 min, using microplate reader (Bio tek) [168, 173, 174]. Measuring time was chosen based on the color stability period of dye – samples which falls into the time range of 5 – 20 min [174]. Polystyrene microplate was selected instead of silica as the dye binds to silica material. Each protein concentration was assayed in triplicates.

To confirm the interference of chemical components present in soaking solutions (SA, SB, SC, SD) including (0.05 – 0.6 M) NaCl and (1.5 – 8 M) urea in phosphate buffer pH 7.0 to the Bradford

assay, it was suggested to create BSA standard curves both in phosphate buffer and soaking SD that prepared from the highest concentration of both NaCl (0.6 M) and urea (8 M). The comparison of their slopes would reveal if there was any interference. The construction of BSA standard curves in soaking solution SD followed the similar procedure with BSA standard curves in buffer above, with BSA solutions prepared following **Table S. 2** in **Appendix B.3**. Soaking solution SD was 10-fold diluted in BSA solutions to obtain similar concentrations as those found in the examined soy gel samples (calculation is explained in **Table S. 3** in **Appendix B.3**

An initial calculation of soluble protein content of soy gels in soaking solutions was performed, as shown in **Table S. 3** in **Appendix B.3**. The supernatant obtained from the mixture of soy gels and soaking solutions, after the ultracentrifugation, was diluted 10-fold with phosphate buffer to ensure the protein concentration falls within the linear range of BSA standard curve from 0.05 – 0.5 μg/μL. Subsequently, a volume of 200 μL of diluted Bio-rad dye reagent and 10 μL of diluted supernatant or phosphate buffer as blank are added into microplate (Corning 96-well, flat bottom, non treated, NY, USA) and mixed gently to prevent foam formation. The absorbance of the sample was measured at the wavelength of 595 nm after 10 min, using microplate reader (Bio tek). This absorbance value was transformed in a protein content using the BSA protein standard curve to determine the soluble protein content in the sample. Each sample was assayed in triplicates.

4.3. Results and Discussion

4.3.1. Effect of Sample Preparation on the Reproducibility of Rheological Properties

The storage (G') and loss (G'') modulus obtained during frequency sweep test of soymilk okara gels (M, MO) prepared in beaker and petri dish are summarized in **Figure 4. 4**.

Similar relative magnitudes of G' and G'' between MO and M were approximately fifteen times higher for gels prepared in beakers and prepared in petri dishes. This result suggested that the alternative method had a similar impact to the viscoelasticity of soymilk okara gels (M, MO), compared to the conventional one. In addition, viscoelasticity of soy gels prepared in petri dishes showed lower standard deviation, which may reflect the absence of the cutting step to create the required sample thickness. especially in MO sample, in comparison to that made in beakers.

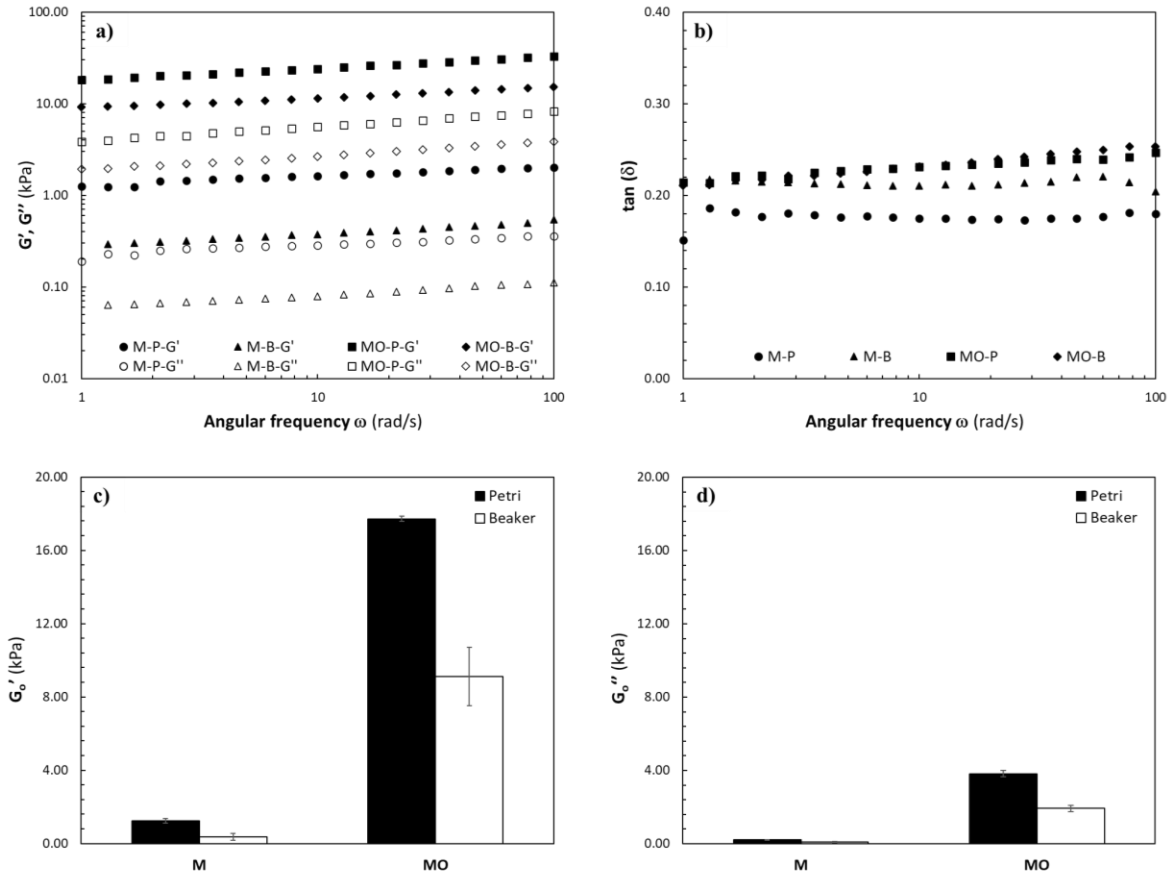


Figure 4. 4: Viscoelasticity properties of soymilk okara gels (M, MO) prepared in petri dish (P) and beaker (B): Typical curves of a) storage modulus G' (filled symbols) and loss modulus G'' (empty symbols), b) tan(δ) over angular frequency. (c) Storage (G_o') and (d) viscous (G_o'') moduli at 1 rad/s. Data of c – d expressed in mean ± standard deviation (n = 3).

4.3.2. Effect of Sample Preparations on the Reproducibility of Mechanical Properties

The mechanical properties of soy gels M and MO prepared in 100-mL beakers and 250-mL beakers are summarized in **Figure 4. *5***. Generally, the true fracture stress and Young's modulus values of gel M prepared in 100-mL beakers were similar to those prepared in 250-mL beakers, while the true fracture strain increased significantly. The mechanical properties of gel MO were similar when prepared in the 2 types of beakers.

Considering the reproducibility of the mechanical properties estimation, soy gel (M) in small beakers had a narrower standard deviation, while soymilk okara gel (MO) prepared in big beakers displayed a slightly enhanced reproducibility. These observations may reflect the difference in surface area of samples (100-mL beaker with the diameter of 40 mm, 250-mL beaker with the diameter of 60 mm) and the heat transfer taking place during the heating step in the water bath. Visual observation of the M soy gels prepared in 250-mL beakers displayed a softer texture in the center than at the rim which may have contributed to the non-uniformity of its mechanical properties. Therefore, 100-mL beaker was selected for the preparation of soymilk okara gels for mechanical properties estimation.

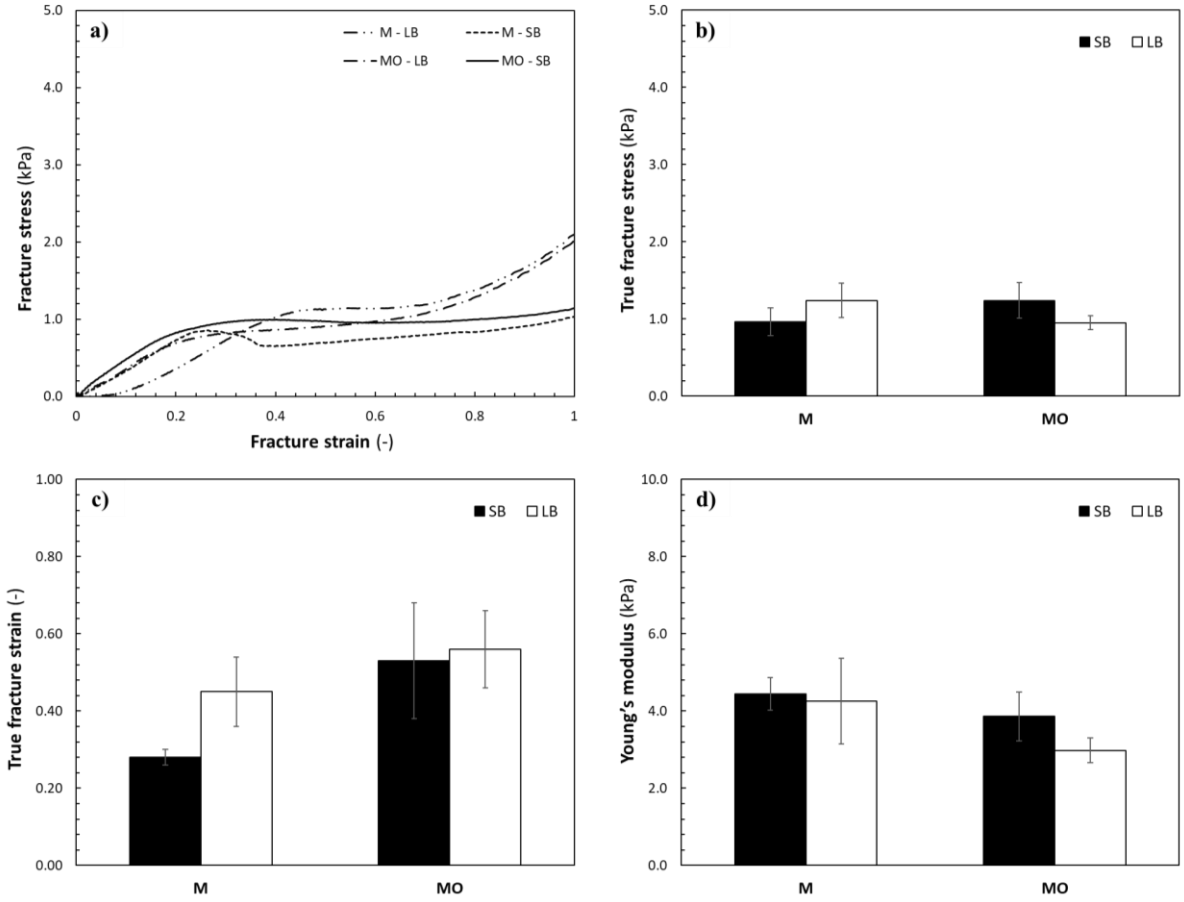


Figure 4. 5: Mechanical properties of soymilk okara gels (M, MO) prepared in 100-mL beakers (SB) and 250-mL beakers (LB): (a) Typical fracture stress – fracture strain curves, (b) True fracture stress, (c) True fracture strain, (d) Young's modulus. Data of (b – d) expressed in mean ± standard deviation (n = 4).

4.3.3. Standardization of Protein – Protein Interactions Methodology

4.3.3.1. Dissolution of Protein – Protein Interactions in Soymilk Okara Gels

After being soaked in specific solutions (SA, SB, SC, SD) over 24 h, soymilk okara gel solutions were centrifuged at the rate of 10,000 rpm, at 25 °C for 30 min to achieve the separation of liquid and solid components. To validate the effectiveness of the predetermined centrifuge operating parameters in separating the solid and liquid phases, a preliminary experiment was carried out on soymilk okara gels, which included control samples (M, MO), as well as one containing CA

modified okara (MOCA5). **Figure 4. 6** visually illustrates the observation of soymilk okara gels (M, MO, MOCA5) soaked in different solutions (SA, SB, SC, SD) both before and after 30 minutes of centrifugation. It was noted that after the centrifugation process, the mixture of all soy gels (M, MO, and MOCA5) in the soaking solution SD remained slightly turbid compared to the gels in the other soaking solutions (SA, SB, and SC). This observation indicated that the liquid and solid phases were not completely separated. Consequently, all soy gels (M, MO, MOCA5) in the soaking solutions (SA, SB, SC, SD) underwent an additional 15 min of centrifugation at a rate of 10,000 rpm to ensure complete liquid-solid separation, resulting in obtaining a clear solution.

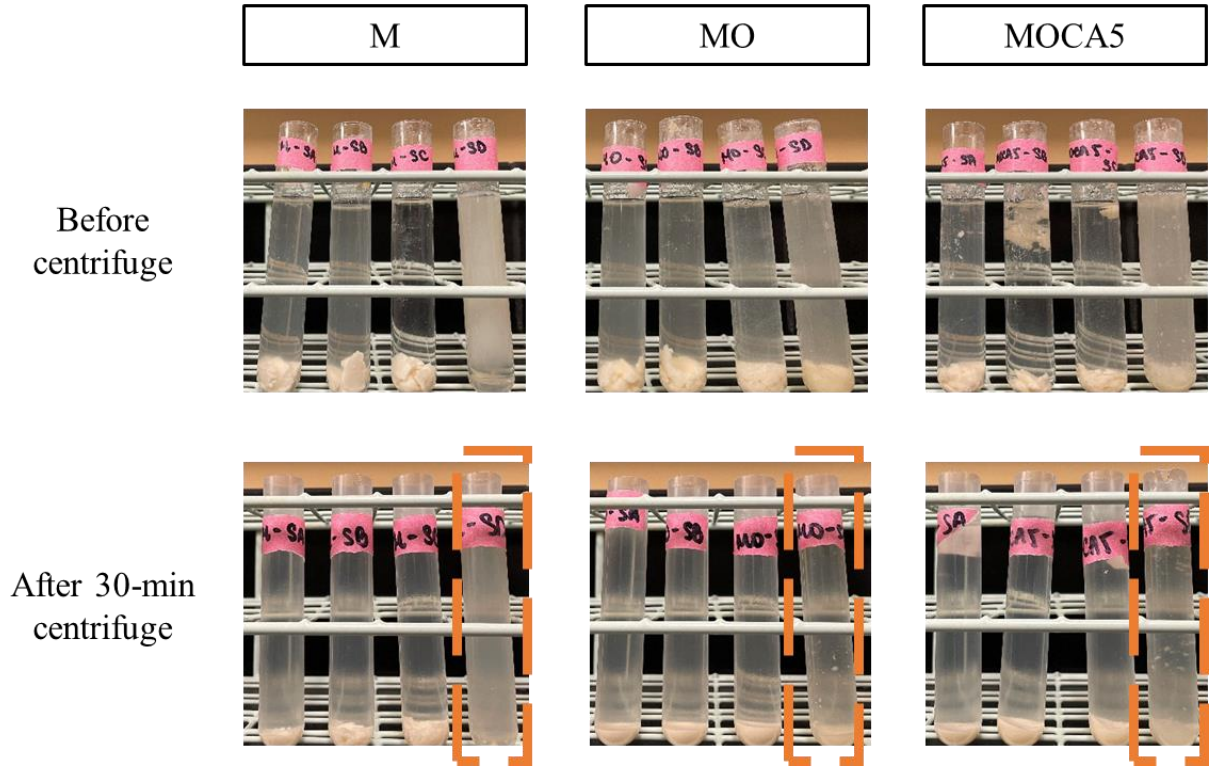


Figure 4. 6: Visual observation of soymilk okara gels (M, MO, MOCA5) soaked in solution (SA, SB, SC, SD) before and after centrifugation at 10,000 rpm, 25 °C for 30 min.

4.3.3.2. Measurement of Soluble Protein Content by Bradford Assay

Construction of BSA Standard Curve

Interference in Bradford assay may be caused by chemical – dye and (or) chemical – protein interactions, with higher sensitivity to several ionic and non-ionic detergents and glycosylated proteins [173]. To minimize the effect of chemicals to the dye, blank sample containing similar concentration of chemicals is performed alongside the assay. However, assessing the impact of chemicals on protein measurements in the Bradford assay can be more challenging.

Figure 4. 7 depicted the BSA standard curve in phosphate buffer and its comparison with the curve in soaking solution SD, proving that urea 8M and NaCl 0.6M did not interfere with the Bradford dye and protein within the concentration range of 0.05 – 0.5 mg/mL during the test. As a result, the BSA standard curve constructed in phosphate buffer was used to calculate the soluble protein content of soy gel samples in all soaking solutions (SA, SB, SC, SD). This finding also aligned with the manual from Bio-rad Laboratories [168] and study in [175] that the use of β-mercaptoethanol (5%), urea concentrations (4 – 8 M) and their combination did not interfere with native BSA protein concentration measurements by the Bradford assay.

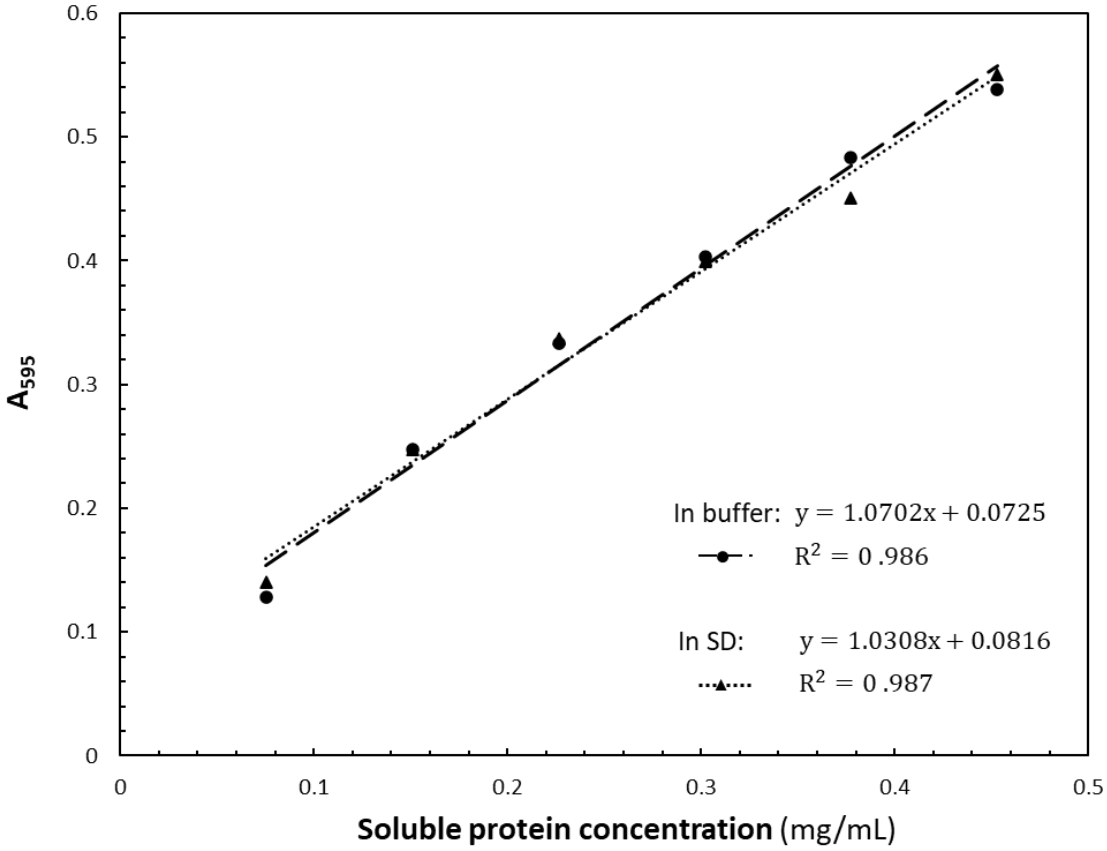


Figure 4. 7: Comparison of BSA standard curves constructed in phosphate buffer pH 7.0 solution (dashed line) and soaking solution SD (0.6M NaCl + 8M urea) (dotted line).

Soluble Protein Content in Soy Gel Samples

In Bradford assay, the concentration of protein in samples should be within the linear range of 0.05 – 0.5 mg/mL of the BSA calibration curve to ensure the accuracy of measurements. We estimated the protein content for the various soy gels by using the nutrition information of the package, 13 g of protein in 35 g of dry whole soybean. Calculations for the approximate soluble protein content in the mixture of 0.6 g of soymilk gel and 10 mL of soaking solutions are shown in **Table S. 3**, indicate that a 10-fold dilution is required, such that the absorbance of the diluted sample would fall within the linear range of the BSA standard curve.

We also looked at the sensitivity of the Bradford assay and preventing protein – dye precipitation by adding NaOH 1M solution at 5 – 10 % volume to the total volume of samples and dye mixture. as proposed in previous studies [172, 176]. To address this, a preliminary experiment was conducted to assess the formation of precipitates when the dye reagent was added to the sample, thereby indicating the necessity of adding NaOH to the Bradford assay procedure.

Bradford assay was performed in 10-fold diluted mixture of soymilk okara gels (M, MO, MOCA5) in soaking solutions (SA, SB, SC, SD) following procedure outlined in **section 4.2.5.3**. **Figure 3. 8** visually presents the observation of soymilk okara gels (M, MO, MOCA5) in soaking solutions (SA, SB, SC, SD) at 10 min and 45 min after the addition of Bradford dye. Notably, no precipitation was observed in all samples at the 10-minute mark. However, after 45 minutes, precipitation was observed for soy gel samples soaked in solution SD. Based on this observation, it can be concluded that there was no requirement to add NaOH 1M to the Bradford assay. However, to maintain accuracy and avoid precipitation, it was essential to measure the absorbance of samples around the 10-minute mark rather than after 45 minutes.

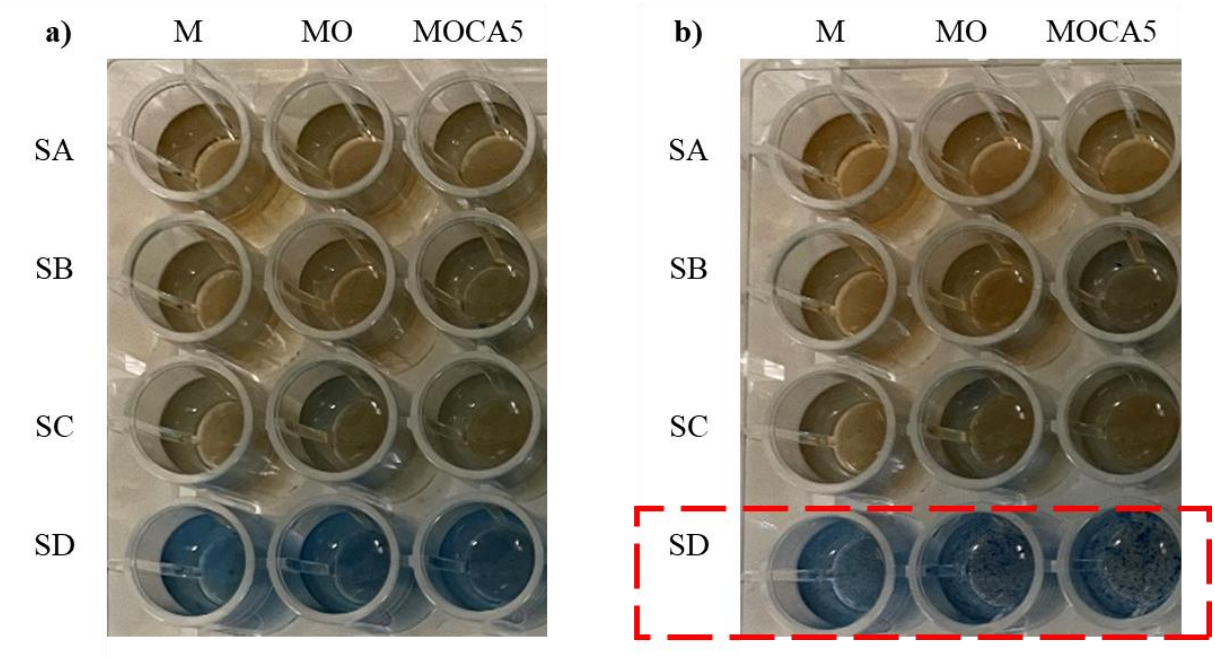


Figure 3. 8: Visual observation of soymilk okara gels (M, MO, MOCA5) in soaking solutions (SA, SB, SC, SD) at a) 10 min and b) 45 min after the addition of Bradford dye.

4.4. Conclusions

The methodology for the preparation of soymilk okara gel samples for rheological and mechanical properties tests was reviewed and adjusted to improve the reproducibility and accuracy of the measurements as follows:

- The sample preparation for rheological properties measurements was revised such that the gel is produced with the required thickness, avoiding the need to cut slices from a bulk gel. Soymilk okara gels are gelled at 2 to 3-mm thickness in glass petri dish covered with parchment paper and oiled with Pam. Gelled samples are then stored in the fridge overnight before the cutting into thin square disk with the dimension of 40x40x2 mm by a sharp blade.

- The sample preparation for mechanical properties measurements was revised such that the gel is produced with the required thickness, avoiding the need to cut slices from a bulk gel. Soymilk okara gels are gelled at 10-mm height in 100-mL beakers oiled with Pam. Gelled samples are then stored in the fridge overnight before the cutting into cylindrical shapes dimension of 10x20 mm by a metal corer.

The methodology to examine protein – protein interactions in the network of soymilk okara gels is adapted from [10], with following modifications based on preliminary experiments:

- The conditions for the separation of the gels from the soaking solution obtained by ultracentrifugation were adjusted to 10,000 rpm, 25 °C for 45 min using ultracentrifuge.
- The dilution conditions for the measurement of soluble protein content by Bradford assay were identified such that the absorbance would fall in the linear range of the BSA standard curve constructed in phosphate buffer. The addition of NaOH 1M solution to the Bradford assay procedure will not be required as no dye – protein precipitation was observed.

Chapter 5: Unveiling the Effects of Citric Acid on Texture Profiles and Chemical Interactions in Soymilk Okara Gels

5.1. Abstract

This study aimed to enhance the compatibility between okara and soymilk gels, ultimately improving the homogeneity of soymilk okara gel by evaluate the effects of citric acid (CA) on the characteristics of okara structure and the resulting gel. Initially, okara was modified with CA solutions at concentrations ranging from 2.5 to 10 %, followed by the heat-induced gelation with soymilk at 95 °C. Control soymilk unmodified okara gel exhibited a heterogenous texture, disrupted by okara particles. With the modification of okara 2.5 % CA solution, soymilk okara gels exhibited increase in level of homogeneity and protein-protein interactions of soymilk okara gels, indicating an improvement in the compatibility between okara and soymilk gel. This finding might be attributed to the extensive okara fiber degradation, release of pectin and formation of amphiphilic protein-polysaccharides conjugates via Maillard reaction, as confirmed by TGA and FTIR. When increasing the CA concentration from 2.5 to 5 and 10 %, the soymilk okara gels exhibited even higher levels of homogeneity, accompanied with the reduction in viscoelasticity by around 4 times and in hydrophobic protein-protein interactions from 62.8 to 37.2 mg protein/g sample. Concurrently, the water holding capacity (72 – 80 %) and mechanical properties including true fracture stress (1400 – 1700 Pa) and Young's modulus (7000 – 10000 Pa) remained similar. Additionally, at the micro-scale, soymilk okara gels modified by CA exhibited a particulate protein matrix, compared to fine-stranded structure observed in gels without CA, which might be attributed to the unreacted CA's effect on protein during the gelation process.

Keywords: Soy-based gels; Okara; Citric Acid; Texture Profiles; Chemical Interactions; Microstructure

5.2. Introduction

Tofu, also referred as soybean curd, is a traditional gel-like food in East Asia. The conventional tofu-making process involves the heating of raw soymilk, followed by the solidification using acid, salt or enzyme coagulant [82]. Okara, also known as soy pulp, is the residue left behind after soybeans have been ground to extract the water-extractable portion used in the production of soy milk and tofu. Typically, for every kilogram of soybeans processed to make soy milk, approximately 1.1 kilograms of fresh okara is generated [67]. With a significant volume of okara being generated as a byproduct of the soy milk and tofu manufacturing processes, despite its nutritional richness, okara has often been disposed as animal feed, incineration, or landfill disposal [67].

Okara is a valuable resource, containing high levels of fiber (53 – 58 %), protein (25 – 28 %), and lipids (9 – 11 %), along with significant amounts of isoflavones and essential minerals [1]. Hence, okara processes high nutritional values and health-promoting effects including antioxidant, hypolipidemic, and hypoglycemic properties [2]. Recent research has focused on enhancing the utilization of okara as a dietary fiber source and functional ingredients in high-fiber tofu applications [3, 4, 5, 6, 7]. However, high-fiber tofu prepared from whole soybean milk without separating okara obtained a heterogenous, disrupt network structure, a gritty mouthfeel, possibly due to high water-absorbing capacity and the large particle size of okara [7].

To enhance the textural qualities and sensory attributes of soy gels incorporating okara, there are various okara modification approaches have been employed that can be categorized into two

groups: physical and non-physical methods. Physical methods encompass various techniques, including wet media milling, ultrasound, and ultra-high-pressure homogenization with the primarily aim of diminishing the particle size of okara [3, 4, 5]. The reduction in particle size resulted in the increase surface hydrophobicity and free sulfhydryl group content of protein component of okara and subsequently led to the development of a more uniform, compact and filamentous gel network [4, 5]. However, incorporating nano-sized okara can decrease the gel strength due to the high surface charge and water absorption capacity, preventing protein aggregation of nano-sized okara [3, 8]. Non-physical methods offer alternatives to modify okara or the protein network in different ways [6, 7, 96]. For example, a study in [6] focused on enhancing the hydrophilicity and smoothness of okara by applying a layer-by-layer coating with chitosan and pectin. This method, while effective, is complex and challenging to scale up. Another approach involved the use of microbial transglutaminase, which enhanced protein aggregate formation, resulting in a more organized protein structure enveloping okara particles [7]. While physical method requires the control in size of okara particles for a strong gel, current non-physical approaches are complex and extensive. To the best of the authors' knowledge, the application of okara modified by non-physical approach using food grade chemical in high-fiber tofu remain limited.

Citric acid (CA) is a tricarboxylic acid, appears as a colorless and crystalline powder [9]. In tofu production, CA has been employed as a coagulant, yielding gels with high storage modulus, hardness and water-holding capacity due to its rapid acidification rate, in comparison to other organic acids [10]. Besides, CA also has various applications in the treatments and modifications of polysaccharides with its unique acidic and chelating properties. CA has been used as a pre-treatment method to initiate and facilitate the enzymatic hydrolysis of polysaccharides contained

in agricultural biomass by partial removing cellulose, hemicellulose, and lignin [11, 12, 13]. This process created surface grooves and structural alterations in the pretreated material for further enzymatic hydrolysis [12]. CA also finds wide application in the extraction of pectic substances from various sources, such as soy hulls and various fruit peels like citrus and apple. Citric-acid-extracted pectin has a higher molecular weight and improved viscosity, making it an excellent candidate for natural thickening and emulsifying purposes [14, 15, 16, 17].

The present study aimed to explore the effects of CA on structure of okara, and its subsequent effects on the texture profiles and protein-protein interactions within soymilk okara gels. After the modification with CA, the fiber in okara were hypothesized to be hydrolysis, along with the release of soluble polysaccharides such as pectic substances, ultimately enhancing the compatibility between CA modified okara and the soymilk protein matrix. The appropriate level of CA for okara modification was also investigated, considering its impact on fiber degradation. Moreover, since there was no washing step after CA modification of okara before its incorporation with soymilk, the excess CA might also affect the soymilk gelation process. The structural alterations in okara following CA modifications were confirmed through visual observations, TGA and FTIR. The impact of CA-modified okara on the characterization of soy gel was further assessed through visualizations using confocal laser scanning microscopy, measurements of syneresis, water holding capacity, rheological and mechanical properties, and evaluations of protein-protein interactions.

5.3. Materials and Methods

5.3.1. Materials

A mass of 4.5 kg of soybeans (lot 11741D and 20181D, Nupak) were purchased from a local supermarket (Waterloo, ON, Canada) and kept in Ziploc bags. Citric acid anhydrous (lot 221510) was obtained from Fisher Scientific (Fair Lawn, NJ). Rhodamine B (lot SLBF0620V) was purchased from Sigma Aldrich (India).

Phosphate buffer 0.05M was prepared from sodium phosphate dibasic heptahydrate (lot A0386400), sodium dihydrogen phosphate dihydrate (lot A0399326) obtained from Acros Organics (India) and adjusted with either sodium hydroxide (lot MKCH5997) or hydrochloric acid (lot 209268) obtained from Sigma Aldrich (India) and Fisher Scientific (Fair Lawn, NJ). Urea (lot BDH4602) and sodium chloride (lot 132465) were purchased from VWR (Canada) and Fisher Scientific (Fair Lawn, NJ). Bovine serum albumin (BSA) (lot 64499500) and concentrated Bradford dye reagent (lot 64509872) were purchased from Bio-rad (USA).

5.3.2. Preparation of Soymilk and Okara

Soymilk and okara were prepared following the procedure described in **section 3.2.2** and summarized in **Figure 5. 1**. The solid content of soymilk was determined by drying triplicates of 1 g of soymilk at 60 °C in forced oven (Fischer Isotemp 737F) for 3 h and calculated with **Equation 5. 1**, where $W_{soymilk}$ and W_{solid} were the mass of sample before and after drying, respectively. The changes in mass of soybeans after hydration, dehulling and extraction stage, accompanied with the percentage of solid content in extracted soymilk in three experimental sets are presented in **Table 5. 1**.

$$Solid\ content\ (\%) = \frac{W_{solid}}{W_{soymilk}} \times 100$$ **Equation 5. 1**

Table 5. 1: Mass of soybeans after hydration, dehulling, corresponding soymilk and okara for three different batches. The percentage of solid content was calculated using **Equation 5. 1**. Data was expressed in mean ± standard deviation (n = 3).

Hydrated soybeans [a]	225.9 ± 1.9
Dehulled hydrated soybeans [a]	198.1 ± 1.2
Okara (O_w) [a]	78.3 ± 1.1
Soymilk (M) [a]	332.8 ± 3.3
O:M Ratio [b]	0.234 ± 0.01
% solid in soymilk [c]	15.42 ± 1.21

a: Calculated based on 100 g dry soybeans.

b: Calculated by dividing the mass of wet okara to soymilk.

c: Calculated with **Equation 5. 1**.

5.3.3. Okara Modifications with Citric Acid

The citric acid modified okara, OCA2.5, OCA5, OCA10, were prepared by adding 10 g of wet okara into 50 g of citric acid (CA) solution 3 %, 6 %, 12 % (w:w) respectively such that the final citric acid concentration was 2.5 % (w:w) (OCA2.5), 5 % (w:w) (OCA5) and 10 % (w:w) (OCA10). The mixture was mixed by magnetic stirring on high speed at room temperature for 1 h. The pH value of the mixtures was measured after the stirring was completed using pH meter (Mettler Toledo, S47 SevenMulti Dual). The citric acid modified samples were then poured into petri dishes, dried in a forced air oven (Fischer Isotemp 737F) at 60 °C for 22 h.

In the same manner, dried unmodified okara O was obtained by drying a mixture containing 10 g of wet okara and 50 mL of DI water under identical conditions as for the CA modified okara

materials and used as control sample. Dried okara materials were ground in a grinder (Blenderpro) for 1 min to reduce particle size and stored at room temperature in capped container no longer than one month for soymilk okara gels preparation.

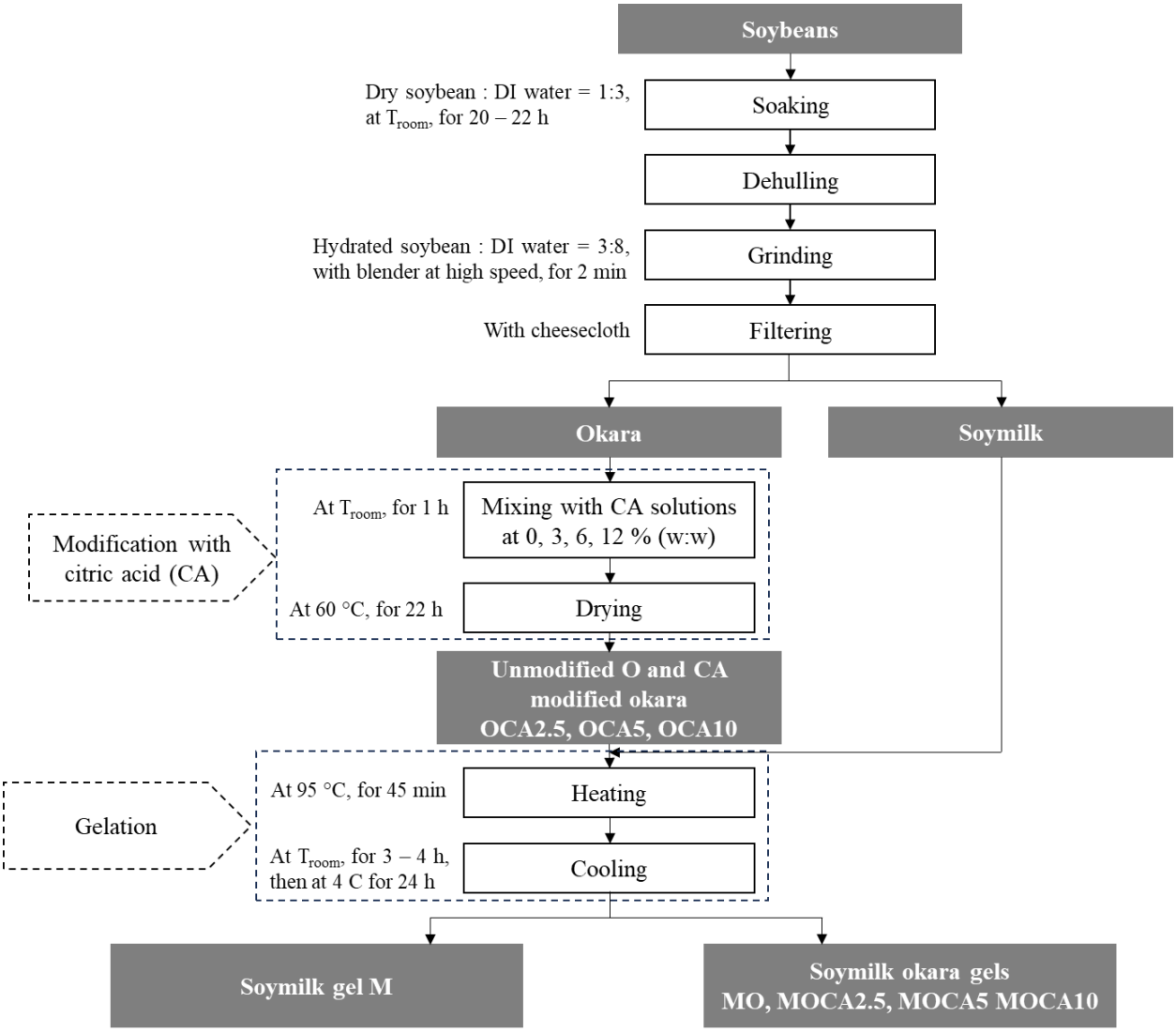


Figure 5. 1: The flowchart of making soymilk and soymilk okara gels (M, MO, MOCA2.5, MOCA5, MOCA10).

5.3.4. Characterization of Modified Okara

5.3.4.1. Thermogravimetric Analysis (TGA)

The thermal stability of dried soymilk (M), okara (O), CA modified okara materials (OCA2.5, OCA5, OCA10) and citric acid (CA) were evaluated by thermogravimetric analysis (TA Instrument, TGA Q500). A mass of 13 ± 2 mg of sample was heated from room temperature to 600 °C at the rate of 10 °C/min under nitrogen atmosphere. The weight loss with respect to temperature was recorded concurrently. Derivative thermogravimetric (DTG) data representing the rate of mass change upon heating was obtained from the Universal Analysis 2000 software (TA Instruments).

5.3.4.2. Fourier Transform Infrared Spectroscopy (FTIR)

FTIR spectra of dried soymilk (M), okara (O) and CA modified okara materials (OCA2.5, OCA5, OCA10) and citric acid (CA) were collected with the use of Nicolet 6700 FTIR spectrometer (Thermo Scientific Nicolet 6700, Waltham, MA, USA), with 32 scans between the wavenumber range of 500 to 4000 cm^{-1} and a resolution of 4 cm^{-1}. Transmittance was baseline corrected and normalized using Omnic software (Thermo Scientific) for the ease of comparison.

5.3.5. Preparation of Soymilk Okara Gels

Dried and ground okara materials (O, OCA2.5, OCA5, OCA10) were introduced back to the soymilk (M) with the O_w:M ratio of 0.23 for the preparation of soymilk okara gels (MO, MOCA2.5, MOCA5, MOCA10). The okara solids were evenly distributed into the soymilk with the aid of magnetic stirrer at 500 – 600 rpm for 15 min in 200-mL beakers. Care was taken to avoid excessive mixing, which could lead to the formation of air bubbles in the mixture and heterogeneity

in the gels thereafter. During the mixing process, pH was measured at following timeline 1, 2, 3, 6, 9, 12, 15 using pH meter (Mettler Toledo, S47 SevenMulti Dual).

Subsequently, the mixture of soymilk with unmodified or CA modified okara was then transferred to a 100-mL beaker coated with a thin layer of Pam oil cooking pray to prevent gel sticking. The beakers were then placed in the water bath and heated at 95°C for 45 min, followed by cooling to room temperature for 3 h before overnight storage in the fridge for later use. As a comparison, a soymilk gel (M), was obtained by heating around 50 mL of soymilk in the water bath at 95 °C for 45 min. Soymilk gels (M, MO, MOCA2.5, MOCA5, MOCA10) were examined for their visual appearance, water holding capacity and protein – protein interactions immediately after 24-h storage in the fridge to prevent any changes in properties caused by potential syneresis.

Three different sets of soymilk and okara were prepared. One replicate of soymilk (M) and soymilk okara gels (MO, MOCA2.5, MOCA5, MOCA10) were prepared from each set of soymilk and okara and characterized with the properties and corresponding number of replicates indicated in **Figure 5. 2**.

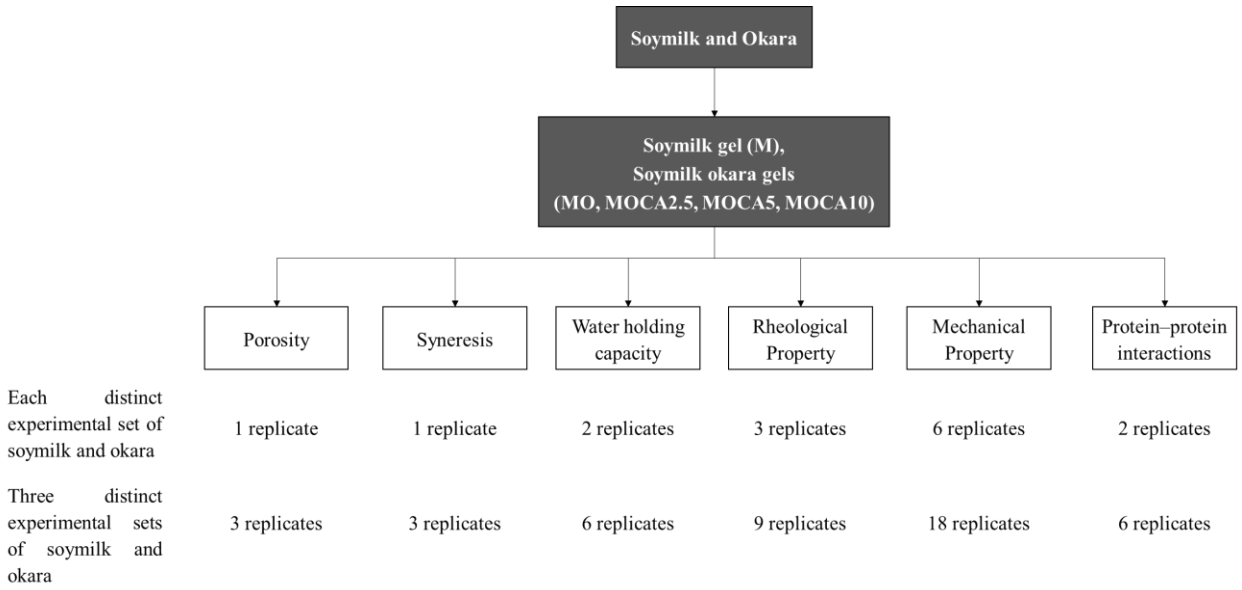


Figure 5. 2: Characterization of soymilk (M) and soymilk okara gels (MO, MOCA2.5, MOCA5, MOCA10) with the total number of replicates for each experimental test.

5.3.6. Structural Characterization of Soymilk Okara Gels

5.3.6.1. Macrostructural Characterization with Cross-sectional Images

Soymilk okara gel (M, MO, MOCA2.5, MOCA5, MOCA10) samples were prepared by cutting in half the gels with a diameter of 40 mm. An image of the two cut surfaces was obtained with a dual-lens camera (Iphone 12). A ruler was placed on the side for size reference.

The analysis of the gel morphology was conducted using the Analyze Particles tool in ImageJ (v1.53s, U.S. National Institutes of Health, available at http://rsb.info.nih.gov/ij/). To avoid the effects of the rim region of the sample, on the analysis the image was first cropped to a square size of 30 x 30 mm at the center, then converted to a binary format. Adjustments were made to the brightness and contrast using the auto function that relied on the analysis of the image's histogram, followed by the setting of threshold to 75. Analyze Particles command was then applied with specific settings, inclusion of holes and edges, a pore size ranging from 0 to infinity, and circularity

values within the range of 0 to 1. The pore size (mm^2), total porous area (mm^2) and porosity (%) were then estimated and recorded.

5.3.6.2. Microstructural Characterization with Confocal Laser Scanning Microscopy (CLSM) Images

Sample preparation for CLSM analysis was performed as described in [128] with some modifications. A mass of 4 g of the mixture of soymilk and either unmodified or modified okara (prepared in **section 5.3.4**) was combined with 20 µL of a 0.2 % (w:v) solution of rhodamine B, then stirred using a magnetic stirrer at 400 rpm for 1 h at room temperature while covered with aluminum foil to prevent the degradation caused by light. The rhodamine B labelled soy solutions were stored in vials covered with aluminum foil and placed overnight in the fridge for a complete reaction. The Rhodamine B dye binds non-covalently to the protein network [129].

Subsequently, two drops of rhodamine labelled soy solution were placed into concave microscope slides (Eisco, 1'' x 3'' – 1.0-1.2 mm) and gently pressed down with a cover slide (Fisherbrand, 22x22 – 1.5mm) to prevent bubble formation and wrapped in aluminum foil. The slides containing the soy solution were subjected to heating in a forced air oven (Fischer Isotemp 737F) at 95 °C for 45 minutes to replicate the gelling conditions. After cooling to room temperature, the slides with dyed soy gel were ready for analysis using CLSM.

The microstructure of the gel was captured using a confocal laser scanning microscope (Zeiss LSM 700, AxioObserver) equipped with objective lens including Plan Apochromat 20x/0.8, Plan Apochromat 63x/1.4 Oil and alpha Plan Apochromat 100x/1.46 Oil. The rhodamine B was excited at wavelength of 555 nm and the emission wavelength was recorded between the range of 560 – 800 nm. Similar settings were used for all samples and included a pinhole size of 1 airy unit, laser power of 2.0%, and a detector gain of 500. Images were captured with a size of 1024 x 1024 pixel

resolution, bit depth of 12 bit, at the averaging of 4 and scanning speed of 7. Image contrast was improved through post-processing using a gamma value of 0.45. For each gel sample, a representative image was chosen in a minimum of five images collected at different locations to illustrate each gel type.

5.3.7. Measurement of Syneresis and Water Holding Capacity (WHC) of Soymilk Okara Gels

5.3.7.1. Estimation of Syneresis

The syneresis of soymilk gels (M, MO, MOCA2.5, MOCA5, MOCA10) after 24 hours storage in a fridge was measured following [3] as the ratio between mass of liquid released ($W_{liquid\ released}$), and the mass of the gel (W_{gel}), calculated as in **Equation 5. 2**. The syneresis was estimated in triplicates for each distinct set and 3 distinct sets were prepared for each type of soy gel as presented in **Figure 5. 2**.

$$\%\ syneresis = \frac{W_{liquid\ released}}{W_{gel}} \times 100 \qquad \textbf{Equation 5. 2}$$

5.3.7.2. Estimation of Water Holding Capacity (WHC)

The water holding capacity was conducted following [10] with modifications. A mass of 5 ± 1 g of soy gel (M, MO, MOCA2.5, MOCA5, MOCA10) was obtained by cutting the initial gel sample with a metal corer, weighed (W_t) and placed into 13.2-mL polypropylene thin-wall centrifuge tube (Beckman Coulter). Samples were centrifuged in an ultracentrifuge (Beckman Coulter, Optima XPN100, swing bucket SW 41 Ti) at room temperature for 20 min at centrifugal force of 12,074 x g, corresponding to the rotor speed of 10,000 rpm. After centrifugation, the released water was

decanted and recorded as W_r. Water holding capacity of gels was measured in duplicates in 3 sets of each type of soy gel and calculated according to **Equation 5. 3**.

$$WHC\ (\%) = \frac{W_t - W_r}{W_t} \times 100 \qquad \textbf{Equation 5. 3}$$

5.3.8. Rheological Properties of Soymilk Okara Gels

5.3.8.1. Sample Preparation

Gel samples were obtained with approximately 20 – 25 g of mixture of soymilk with either unmodified or modified okara obtained from **section 5.3.4** subsequently gelled in glass petri dish covered with parchment paper and oiled with Pam spray to obtain the final gel thickness of 2 – 3 mm. The gelation occurred at the same conditions as the original gel **section 5.3.4** (at 95 °C, for 45 min in water bath). Subsequently, gels were stored in the fridge overnight before cutting into thin square disks with the dimension of 40x40x2 mm by a sharp blade. Samples were equilibrated at room temperature for 1 h prior to analysis.

5.3.8.2. Rheological Properties Measurement and Analysis

The rheological properties of soymilk okara gels were measured and analyzed following the procedure described in **section 3.2.8**. The linear viscoelastic region of samples determined from the strain sweep test is presented in **Figure S. 7** in **Appendix B.1**. The frequency sweep test was performed in triplicates for each distinct set with a total of 3 sets of each type of soy gel as presented in **Figure 5. 2**.

5.3.9. Mechanical Properties of Soymilk Okara Gels

5.3.9.1. Sample Preparation

Gel samples were prepared with approximately 20 – 25 g of mixture of soymilk with either unmodified or modified okara obtained from **section 5.3.4** and subsequently gelled in 100-mL beakers oiled with Pam spray to obtain a gel with the desired final height of 10 mm. The gelation occurred at the same conditions as for the original gel preparation described in **section 5.3.4** (at 95 °C, for 45 min in water bath). Subsequently, gel samples were stored in the fridge overnight before cutting into cylindrical shape with the dimension of 10x20 mm by a metal corer. Samples were equilibrated at room temperature for 1 h prior to analysis.

5.3.9.2. Mechanical Properties Measurement and Analysis

The mechanical properties of soymilk okara gels were measured and analyzed following the procedure described in **section 3.2.9**. The measurement of mechanical property was performed in six replicates for each distinct set of soymilk gel type with 3 distinct sets for each type of soy gel as presented in **Figure 5. 2**.

5.3.10. Protein – protein Interactions

The investigation of protein-protein interactions in the soymilk gels was based on the solubilization of proteins after soaking a gel sample in a variety of solutions that disrupts specific interactions, as described in [10] with some modifications. The process involves two main steps including gel dissolution in particular soaking solutions and measurement of soluble protein in samples by Bradford assay.

5.3.10.1. Dissolution of Protein – Protein Interactions in Soymilk Okara Gels

A mass of 0.6 g (W_{gel}) of soymilk okara gel (M, MO, MOCA2.5, MOCA5, MOCA10) was solubilized into 10 mL of a given soaking solution. Four different soaking solutions prepared in 0.05M phosphate buffer pH 7.0 were investigated, SA (0.05M NaCl), SB (0.6M NaCl), SC (0.6M

NaCl + 1.5M urea), SD (0.6M NaCl + 8M urea). To prepare 500 mL of 0.05M phosphate buffer pH 7.0, an amount of 3.872 g of sodium phosphate dibasic heptahydrate ($Na_2HPO_4.7H_2O$) and 1.646 g of sodium dihydrogen phosphate dihydrate ($NaH_2PO_4.2H_2O$) were dissolved into 400 mL of DI water in a 1000mL beaker. HCl 1M or NaOH 1M solution was used to adjust pH of buffer to 7.0 with a pH meter (Mettler Toledo, S47 SevenMulti Dual) while constant stirring. Subsequently, solution was transferred to a 500 mL volumetric flask and filled with DI water to the mark.

The gel and soaking solution mixture was then homogenized using vortex at room temperature for 1 min, incubated at room temperature (25 °C) for 24 h and subsequently centrifuged at10,000 rpm, 25 °C for 45 min in an ultracentrifuge (Optima XPN, Beckman Coulter) equipped with swing bucket rotor (SW 41 Ti, Beckman Coulter) [169]. The supernatant phase was carefully pipetted out using a micropipette (Eppendorf) for analysis. The protein content of the supernatant phase represented the amount of protein solubilized from the gel upon incubation in the soaking solution and was determined using Bradford assay.

5.3.10.2.Measurement of Soluble Protein Content by Bradford Assay

A Bovine serum albumin (BSA) protein standard curve was constructed in the linear concentration range of 0.05 – 0.5 μg/μL obtained by preparing a BSA stock solution containing 1.51 mg/mL of BSA protein (Bio-rad, USA) in ultra-pure water. The BSA stock solution was stored in the fridge at 4 °C for use within 60 days. The Bio-rad dye reagent was prepared by diluting 1 part of volume of concentrate Bio-rad dye reagent (Bio-rad, USA) with 4 parts volume of DI water. The diluted solution was then filtered through Whatman no.1 filter paper to remove particles and stored in amber bottle at room temperature for 2 weeks [168].

A volume of 1000 μL of BSA protein solution with concentrations of 0.0755, 0.151, 0.2265, 0.302, 0.3775, 0.453 μg/μL were prepared in sodium phosphate buffer pH 7.0 from the stock (1.51 mg/mL) to construct standard BSA curve. In a polystyrene microplate (Corning 96-well, flat bottom, non treated, NY, USA), a volume of 200 μL of diluted Bio-rad dye reagent was added into 10 μL of BSA solution at different concentrations or phosphate buffer as blank and mixed gently to avoid the foam formation. The absorbance of final mixtures at the wavelength of 595 nm was measured after 10 min, using microplate reader (Bio tek) [168, 173, 174]. Polystyrene microplate was selected to avoid potential interferences caused by the binding of the dye to silica surfaces. The BSA standard curve constructed in phosphate buffer was used to determine the soluble protein content of all soaking solutions (SA, SB, SC, SD) as per **Equation 5. 4**.

Bradford assay was performed in 10-fold diluted mixture of soymilk okara gels (M, MO, MOCA2.5, MOCA5, MOCA10) in soaking solutions (SA, SB, SC, SD) following the similar procedure to construct BSA standard curve. The distribution of protein – protein interactions was calculated based on the difference in protein content calculated by **Equation 5. 5** between SB and SA for ionic bonds, SC and SB for hydrogen bonds, SD and SC for hydrophobic interactions.

$$Soluble\ protein\ (mg/mL\ solution) = \frac{A_{595} - 0.0725}{1.0702} \qquad \textbf{Equation 5. 4}$$

$$Soluble\ protein\ (mg/mg\ gel) = \frac{A_{595} - 0.0725}{1.0702} \times \frac{100}{W_{gel}} \qquad \textbf{Equation 5. 5}$$

5.3.11. Statistical Analysis

Statistical analysis was performed using Statistica (version 14.0.0.15, TIBCO software Inc.). Analysis of variance (ANOVA) was used to determine significant differences between the results, followed by Tukey test to identify statistical differences between paired means at 0.05 level.

5.4. Results and Discussion

5.4.1. Characterization of Modified Okara

5.4.1.1. Visual Observations

The preparation of citric acid (CA) modified okara (O) is presented in **Table 5. *2***, along with the visual observation of unmodified okara (O) and citric acid modified okara materials (OCA2.5, OCA5, OCA10), as shown in **Figure 5. 3**. As expected, the CA modifications of okara induced a significant decrease in pH values of the mixture, dropping from 6.71 (O) to 2.66 (OCA2.5), 2.41 (OCA5), and 2.19 (OCA10). These alterations were accompanied by noticeable changes in both color and texture.

The dried unmodified okara (O) was crumbly, displayed a bright yellow hue and could easily be grinded into fine flour after the oven drying at 60 °C. When okara underwent citric acid modification with a 2.5% (w:w) CA, although there was no significant change in color, the material became harder and crispier and the powder obtained after grinding was not as fluffy as O. As the CA concentration increased to 5 % and 10 % (w:w), the darkness and gumminess increased. This gumminess resulted in stickiness and the formation of lumps after grinding, which was most pronounced in OCA10.

Table 5. 2: Preparation of okara mixtures (O, OCA2.5, OCA5, OCA10), mass, pH values after CA modifications and mass of dried solid. Data was expressed as mean standard deviation (n = 3).

Samples	**Components**			**pH** [a]	**Dried solid** [b] (g)
	Wet okara (g)	CA (g)	Water (g)		
O (control)	10	0	50	6.71 ± 0.18	2.39 ± 0.24
OCA2.5	10	1.5	48.5	2.66 ± 0.13	4.15 ± 0.08

OCA5	10	3	47	2.41 ± 0.12	6.02 ± 0.26
OCA10	10	6	44	2.19 ± 0.13	9.53 ± 0.31

[a] Final pH values of okara and citric acid solution mixture after 15-min mixing period.

[b] Mass of solid after 20-h drying at 60 °C in forced air oven.

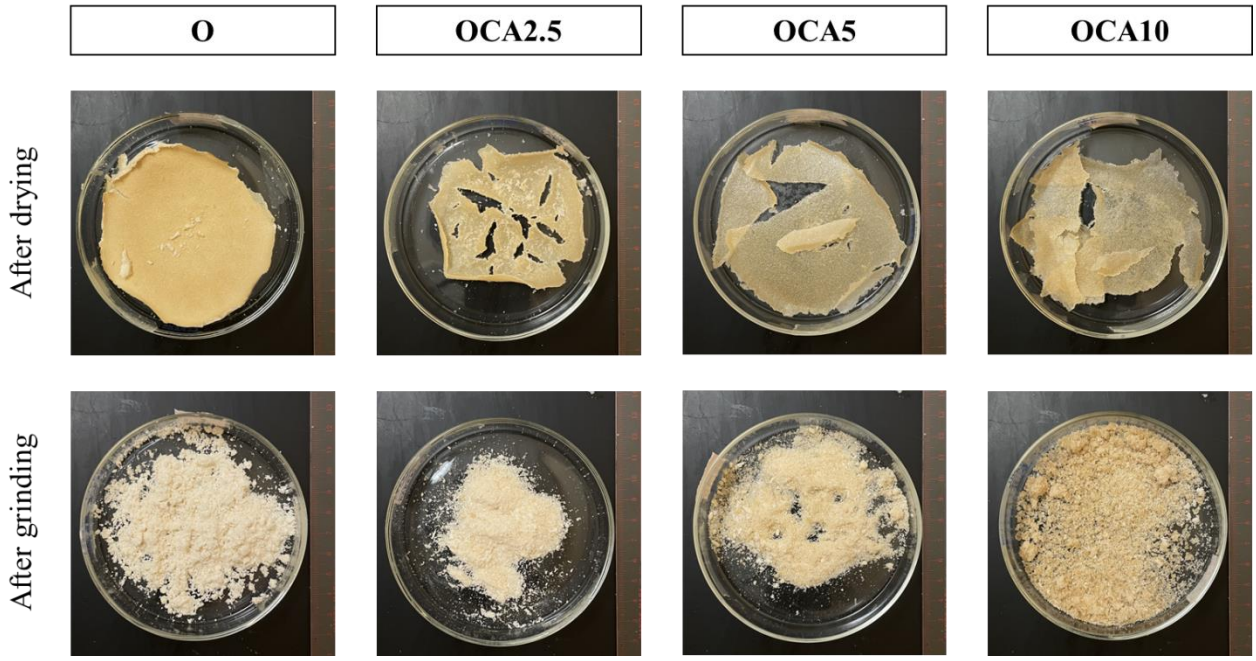


Figure 5. 3: Visual observation of okara materials (O, OCA2.5, OCA5, OCA10) after drying in oven and after grinding.

5.4.1.2. Thermogravimetric Analysis (TGA)

The effect of citric acid (CA) modification on the thermal stability of okara was obtained by thermogravimetric analysis (TGA). The weight loss (TGA) and derivative of the weight loss (DTG) curves of control (M, O, CA) and CA modified okara materials (OCA2.5, OCA5, OCA10) were recorded from 23 to 600 °C as illustrated in **Figure 5. 4**.

The mass loss profiles were analyzed based on the five main weigh-loss stage of soy protein and polysaccharide constituents and their thermal stability. Dried soymilk (M), okara (O) and citric acid (CA) were used as control samples. Dried soymilk consists of 38 % protein, 16 % total dietary

fiber and 13 % lipid [177], while dried okara contained approximately 50 % dietary fiber, 25 % protein and 10 % lipid [155]. The initial stage from 23 – 150 °C was attributed primarily to the adsorbed water and thermal breakdown of volatile components [178]. The second stage occurring around 150 – 220 °C corresponds to the decomposition of unstable hydrogen bond in protein with peak at ~ 150 °C [179] and hydrolytic cleavage of neutral sugar side chains including arabinose and galactose with peak at 220 – 240 °C [147, 180]. A major mass decrease of M and O dropped during the third stage from 220 – 320 °C which is associated with the rupture of the main peptide chain of soy protein, including C-O, C-C, and C-N bonds [179] and the main chain of the galacturonan contained in the soy soluble polysaccharides (SSPS), a major constituent of okara [147, 180, 181], with the most significant drop occurring from 290 – 310 °C. The thermal degradation of soy lipid, the breakdown of the glycoside bonds in cellulose and hemicellulose occurred in the fourth stage from 320 – 450 °C [147, 182, 178, 183, 184]. The last stage from 450 – 600 °C was associated with the decomposition of residual cellulose, lignin and with the char fraction [185, 186].

The thermal decomposition of citric acid (CA) aligns with previously reported observations in [187] with an initial slow degradation at around 160 °C and a substantial increased rate after surpassing 190 °C with the maximum rate of weight loss (~ 43 %) attained at approximately 206 °C. These phenomena relate to observations previously reported on the dehydration of CA, resulting in the formation of aconitic acid. Approximately 80 % of CA was degraded within the second stage. Subsequent heating led to the emergence of methyl maleic anhydride and its decomposition presented by the shoulder in DTG data at around 230 °C [187].

The okara materials after modifications with different CA concentrations (2.5%, 5%, 10%, w:w), okara materials (OCA2.5, OCA5, OCA10) share similarities during the initial decomposition

stage, followed by disparities for temperatures above 170 °C. The most substantial mass loss for all CA modified okara materials occurred during the second stage, at around 200°C, which corresponds to the thermal degradation peak of CA and carboxylate groups as reported in [188, 189]. After the second stage, the mass of OCA2.5, OCA5 and OCA10 decreased by about 32 %, 36 % and 55 %, respectively, which are notably higher than for O with 8% mass loss. During the third decomposition stage, the mass loss of OCA2.5, 26 %, was nearly doubled when compared to OCA5, OCA10 at ~ 13 – 18 %. The analysis of the DTG data for OCA2.5, OCA5, OCA10 revealed new peaks at ~ 330 – 337 °C and ~ 370 – 385 °C, which were not present in unmodified O. This observation suggests the occurrence of new constituents, such as products of the esterification between polysaccharides and CA and pectin release, leading to a more heterogeneous compositions in okara modified by CA. These observations align with previous findings in [147, 189]. The mass of residue at 600 °C for O, OCA2.5, OCA5 and OCA10 was 18 %, 7 %, 20 % and 13 %, respectively. The increased mass of residue might be due to the increased number of cross-linking events at different CA concentrations [190].

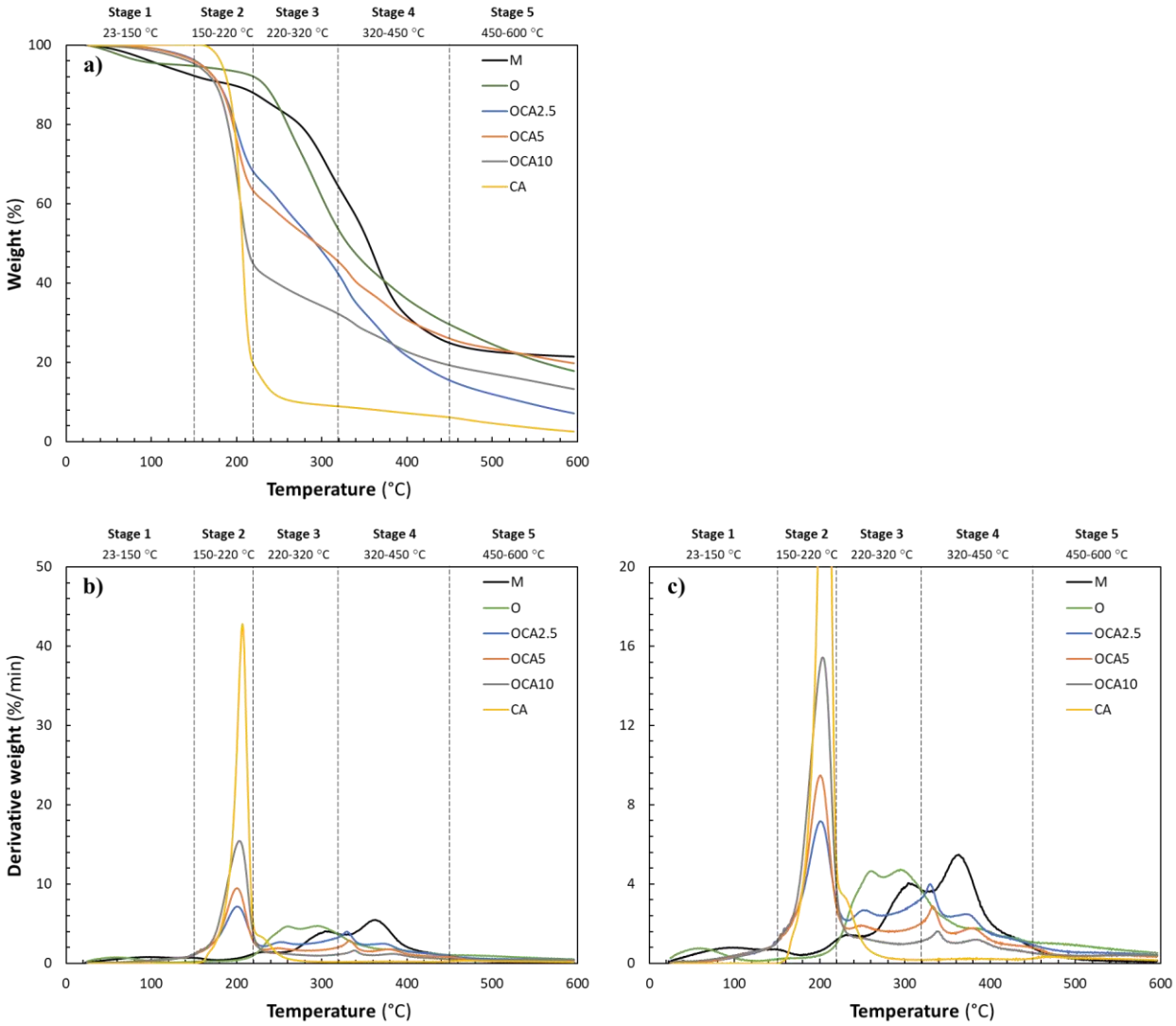


Figure 5. 4: a) Thermogravimetry (TGA), b) derivative thermogravimetry (DTG) curves of control (M, O, CA) and CA modified okara materials (OCA2.5, OCA5, OCA10), c) zoomed-in view of DTG.

5.4.1.3. Fourier Transform Infrared Spectroscopy (FTIR)

FTIR spectra were employed to investigate the effect of the citric acid (CA) concentrations on the chemical structure and functional groups present in CA modified okara (OCA2.5, OCA5, OCA10) as illustrated in **Figure 5. 5**. FTIR spectra of M, O, CA and OCA2.5, OCA5, OCA10 were divided in four regions, including region 1 (3650 – 3100 cm^{-1}); region 2 (3020 – 2750 cm^{-1}); region 3 (1800

– 1500 cm^{-1}) and region 4 (1300 – 800 cm^{-1}). The summary of detected peaks, wavenumbers and assignments are presented in **Error! Reference source not found.**.

Soymilk (M) and unmodified okara (O) exhibited similar peaks within region 1 and 2. In region 1, the strong and broad absorption peak observed at ~ 3500 – 3200 cm^{-1} was related to O-H stretching vibrations of intra- and intermolecular hydrogen bonds in polymer and moisture [144] or amine (N-H) stretching vibrations in protein [145, 146]. Region 2 (3020 – 2750 cm^{-1}) with peaks at ~ 2960 – 2850 can be associated with CH_n symmetrical and asymmetrical vibration presenting in typical structure of soy protein, lipid and polysaccharide [148, 149]. Region 3 (1800 – 1500 cm^{-1}) could provide information about the degree of esterification of polysaccharides as well as the protein structure. Two peaks in range of 1760 – 1730 cm^{-1} and 1640 – 1620 cm^{-1} were associated to the stretching vibrations of C=O in ester carbonyl groups (-COOR) and C=C in carboxylate ion (-COOH), respectively [147, 150]. Amide I and II bonds in protein had peaks at wavelength of 1690 – 1600 cm^{-1} and 1560 – 1530 cm^{-1} [151, 152]. Soymilk M with higher content of protein demonstrated more intense amide I (~ 1633 cm^{-1}) and amide II (~ 1540 cm^{-1}) peaks compared to okara (O). Region 4 from 1300 – 800 cm^{-1} is called the fingerprint region, in which the bands' location and intensity reflect different types of polysaccharides [153]. Major peaks in the range of 1200 – 1000 cm^{-1} characterized C-O-H stretching vibrations overlapping C-O-C glycosidic bond vibrations, which are distinguishing characteristics of hemicellulose, cellulose, and lignin [154]. The higher polysaccharide content in unmodified okara O, showed more notable peaks compared to soymilk M. The peak at 1163 cm^{-1} represents the tensile vibration of C-O in C-O-H, while the broad and strong band from 1130 – 930 cm^{-1} with the most intense peak at 1035 cm^{-1} represents the tensile vibration peak of C–O in C-O-C of sugar rings in cellulose and hemicellulose [144]. The soy soluble polysaccharides have a pectin-like structure with the backbone composed of

rhamnogalacturonan linked by the intervention of galacturonan chains, which is associated with peaks at 1011 cm^{-1}, 1035 cm^{-1} and 1065 cm^{-1} [152, 156]. The absorption peak at 891 cm^{-1} corresponds to the β-glycosidic linkage in hemicellulose [157].

The FTIR spectra of CA has absorption peaks (~ 3496, 3283 cm^{-1}) in region 1 which can be attributed to free hydroxyl groups or O-H bonds of carboxylic acids [147] while the sharp peaks at ~ 1743 and 1693 cm^{-1} can represent the stretching of C=O [191].

The FTIR spectra of CA modified okara (OCA2.5, OCA5, OCA10) has a notable reduction in intensity of O-H stretching vibration peak (~ 3496 – 3283 cm^{-1}) and CH_n stretching vibration peaks (~ 2960 – 2850 cm^{-1}). The extent of the reduction in these mentioned peaks was proportional to the citric acid concentration employed, with the most pronounced effect observed in OCA10. This observation suggests the destruction of hydrogen bonds from hydroxyl groups of polysaccharides [192]. Additionally, peaks corresponding to CH_2 stretching at 1417 and 1369 cm^{-1} [192], along with C-O tensile vibration in C-O-H (1163 cm^{-1}) and C-O-C (1130 – 930 cm^{-1}) of sugar rings and β-glycosidic linkage (891 cm^{-1}) exhibited a substantial decrease in intensity in all CA modified okara materials. These observations indicate that increasing CA concentration resulted in higher degree of decomposition of the fibers into oligosaccharides in okara [144, 192].

FTIR spectra of OCA2.5, OCA5, OCA10 in region 3 and 4 revealed release of pectic substances. In comparison to unmodified okara O, while the peak associated with ester carbonyl groups (~ 1743 cm^{-1}) slightly shifting to ~ 1710 cm^{-1}, along with an increase in intensity, the carboxylate ion peak overlapping with amide I at 1633 cm^{-1} experienced a decrease in intensity as well as a minor shift to ~ 1627 cm^{-1}. In FTIR spectral analysis targeting pectin, the primary characteristics peaks assigned to esterified galacturonic acids (1760 – 1710 cm^{-1}) and non-esterified poly galacturonic

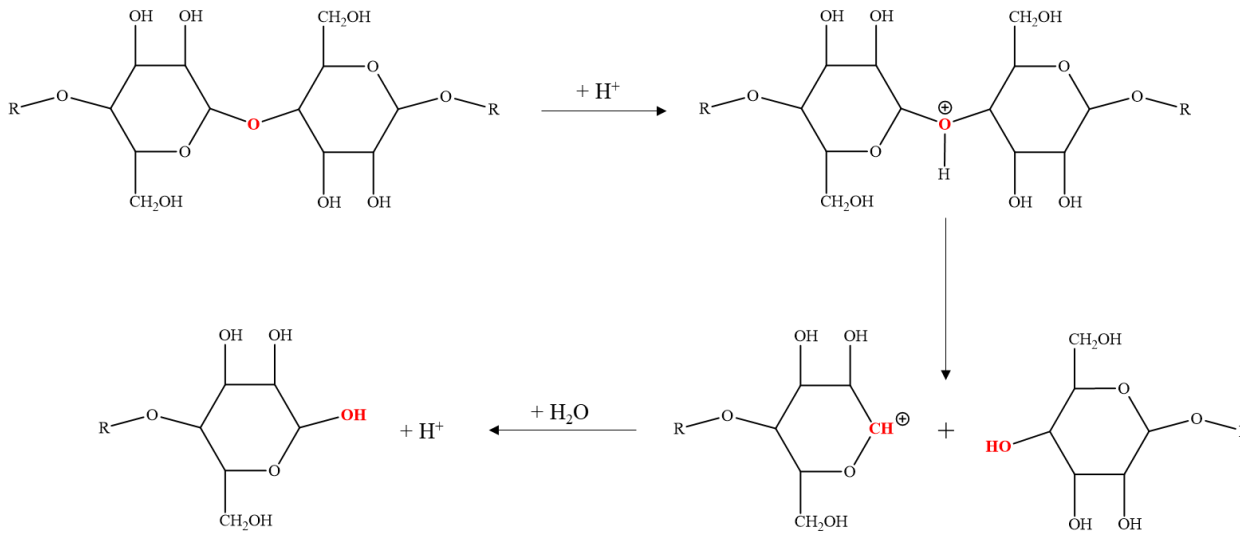
acid (1640 – 1600 cm^{-1}) exhibited consistent pattern across several studies [159, 160, 161]. The presence of peaks within range of 1150 – 1000 cm^{-1} represent homogalacturonans, the principal constituent of pectin, were also stable regardless of their state [147, 162]. Peaks situated in range of 1200 – 850 are associated with the monosaccharides of pectic substances including uronic acid (1110, 1018 cm^{-1}), rhamnose (1150, 1110, 1020 cm^{-1}), arabinose (1060 – 1040, 975 cm^{-1}) and galactose (945 cm^{-1}) [147, 193]. This finding is consistent with existing body of literature, in which CA has been employed for pectin extraction from diverse plant-based food residues and byproducts [159, 194, 160, 161], encompassing soy hulls [195, 14]. Furthermore, additional peaks appeared within pectic substances region (1200 – 850 cm^{-1}) of OCA5, OCA10, in comparison to OCA2.5, indicating the release of more uronic acid [193]. This phenomenon can explain the higher level of gumminess observed for OCA10.

The higher darkness in CA modified okara might be due to caramelization and Maillard reactions [196]. These two phenomena, caramelization and Maillard reaction can occur simultaneously in the reducing sugars and amino acids in the system. Prominent regions in the FTIR spectrum of the protein – polysaccharide system, based on the covalent linkage between the carbonyl groups of reducing sugars and amino groups of proteins can serve as significant markers for reaction occurrences [165]. Along with the a decrease in the C-O stretching vibrations (~1163 and 1035 cm^{-1}) corresponding to sugar rings, CA modified okara materials (OCA2.5, OCA5, OCA10) also experienced reductions in the intensity of protein including amide I (80% C=O stretching at 1627 cm^{-1}), amide II (N-H bending at 1540 cm^{-1}), and amide III (C-N stretching and N-H deformation at 1234 cm^{-1}). The appearance of a peak at 1120 cm^{-1} in OCA5 and OCA10 was attributed to the C-N stretching characteristic of secondary amine in the Amadori product formed during the Maillard reaction [152]. The formation of amphiphilic soy protein – polysaccharides conjugates

by Maillard reaction, which obtains the hydrophobicity of protein, and the hydrophilic character from polysaccharides [197], is expected to assist in the improvement of compatibility between okara and soymilk gel.

Table 5. 3: Reaction scheme of A – Acid hydrolysis, B – Esterification of pectin, C – Maillard reaction and the corresponding FTIR frequencies (cm^{-1}) of their functional groups in unmodified and modified okara reported in the literature and observed in this study.

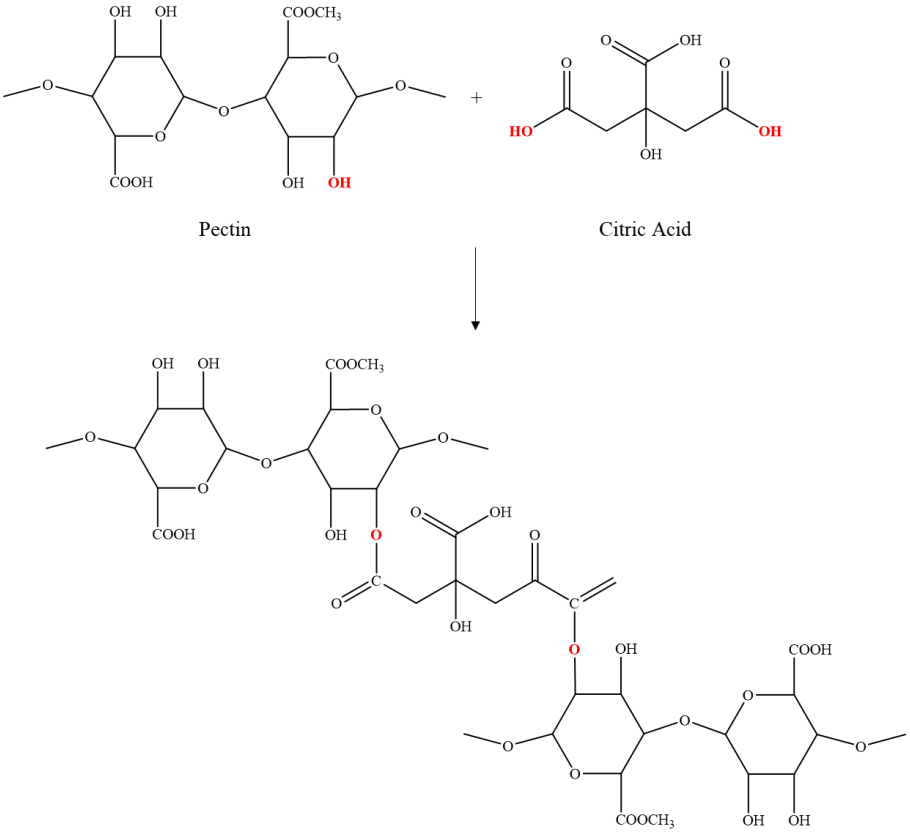
A – Acid Hydrolysis – Reaction Scheme [198]



Literature frequency range (cm^{-1})	**Observed frequency** (cm^{-1})	**Corresponding functional groups**	**Changes in intensity** (compared to unmodified okara)
3650 – 3000 **[144, 145, 146]**	3650 – 3100	O-H stretching vibrations. N-H stretching vibrations.	Decrease
2960 – 2850 **[148, 149]**	2955, 2921, 2855	CH_n stretching	Decrease

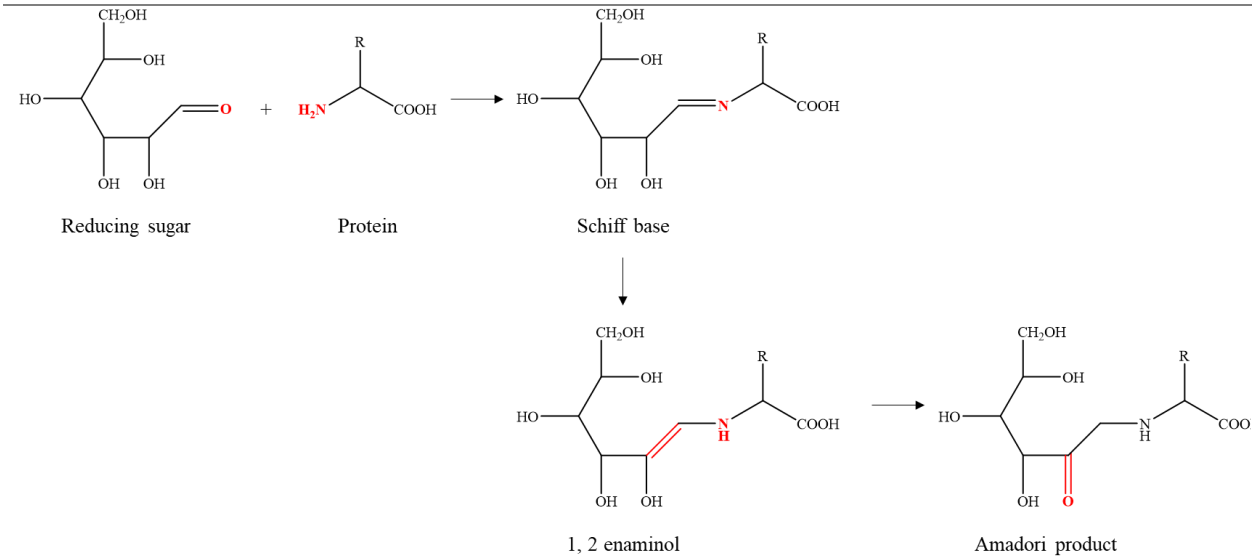
1417, 1369 **[192]**	1417, 1369	CH_2 stretching in cellulose	Decrease
1200 – 1000 **[144, 154]**	1163, 1035	C-O tensile vibration in C-O-H and C-O-C of sugar rings	Decrease
900 – 890 **[157]**	891	β-glycosidic linkage in hemicellulose	Decrease

B – Esterification of Pectin – Reaction Scheme [199]



Literature frequency range (cm^{-1})	**Observed frequency** (cm^{-1})	**Corresponding functional groups**	**Changes in intensity**

			(compared to unmodified okara)
1760 – 1730 **[147, 150]**	1743 – 1710	C=O stretching of ester carbonyl group (COOR)	Increase
1640 – 1620 **[147, 150]**	1633 – 1627	C=C of carboxylate ion stretching (COOH)	Decrease
1200 – 850 **[147, 193]**	1110, 1018	Uronic acid	Increase
	1150, 1110 and 1020	Rhamnose	Increase
	1060 – 1040 and 975	Arabinose	Increase
	945	Galactose Are monosaccharides of pectic substances	Increase
C – Maillard Reaction – Reaction Scheme [200]			



Literature frequency range (cm^{-1})	**Observed frequency** (cm^{-1})	**Corresponding functional groups**	**Changes in intensity** (compared to unmodified okara)
1690 – 1600 **[151, 152]**	1633 – 1627	C=O stretching (80%) and C-N (20%) of amide I bond	Decrease
1560 – 1530 **[151, 152]**	1540	N-H bending (60%) and C-N (40%) of amide II bond	Decrease
1480 – 1200 **[151, 152]**	1234	C-N stretching and N-H deformation of amide III bond	Decrease
1160 – 1120 **[152]**	1120	C-N stretching characteristic of secondary amine in the Amadori product	Increase

1200 – 1000 **[144, 154]**	1163, 1035	C-O tensile vibration in C-O-H and C-O-C of sugar rings	Decrease

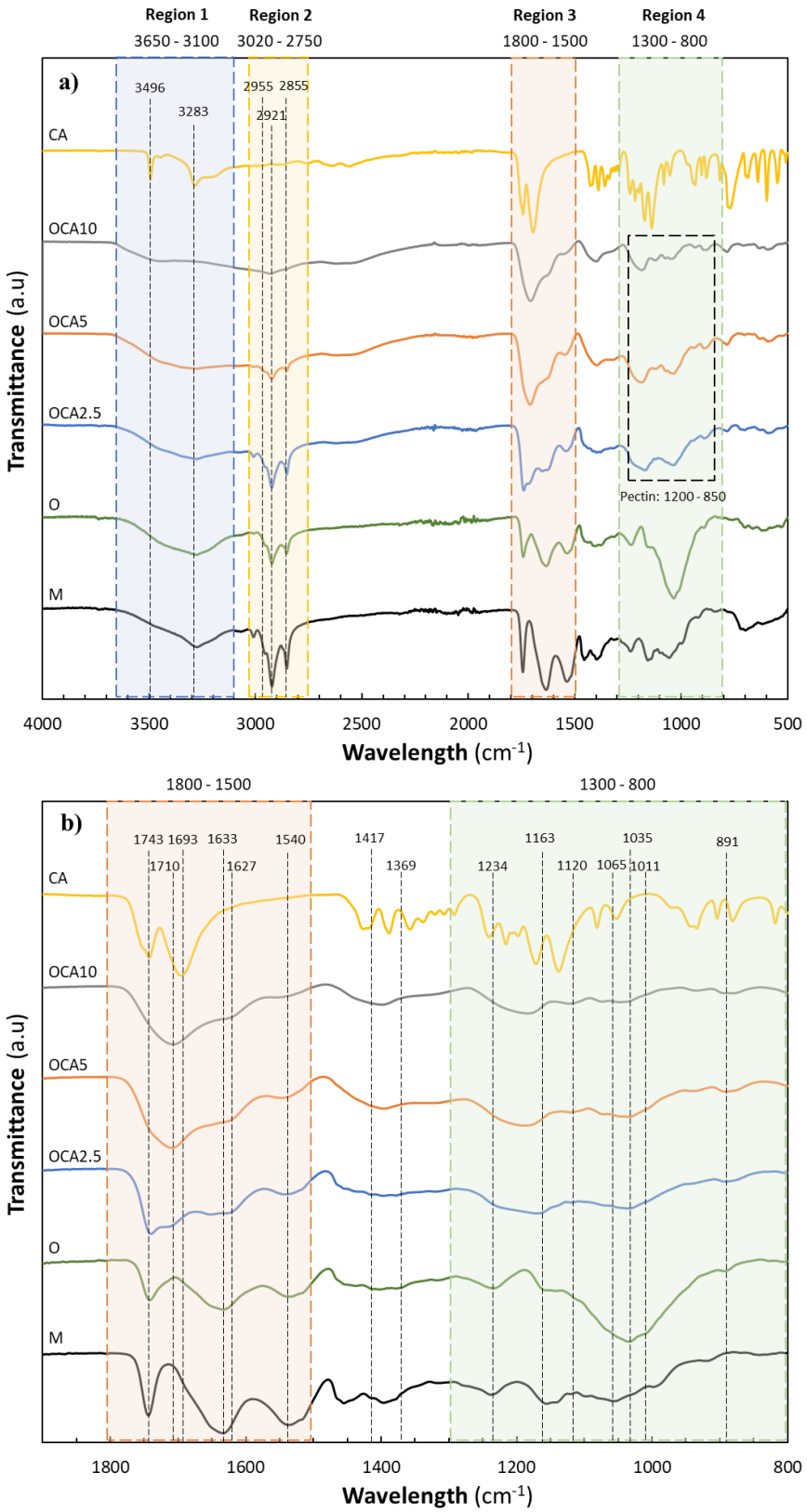


Figure 5. 5: a) Full FTIR spectra of M, O, citric acid (CA), and CA modified okara (OCA2.5, OCA5, OCA10) and b) FTIR spectra within the range from 2000 – 800 cm^{-1}.

5.4.2. Structural Characterization of Soymilk Okara Gels

5.4.2.1. Macrostructural Characterization of Gel Cross-sections

Figure 5. 6 presents the effects of CA okara modification on the macroscopic structure of soymilk okara gels (MOCA2.5, MOCA5, MOCA10) in comparison to M and MO gels. The surface characteristics of soymilk okara gels are presented in **Table 5. 4**. The soymilk gel M was light yellow in color and displayed a smooth, homogenous surface with minimal porosity, 0.09 ± 0.08 %. When unmodified okara was incorporated in the soymilk gel (MO), the gel surface was heterogenous with a noticeably higher porosity of 5.0 %.

Soymilk gels containing CA modified okara (MOCA2.5, MOCA5, MOCA10) exhibited distinctive cross-sectional surface characteristics compared to MO with a more shinning surface indicating a higher level of free water captured inside the gels structure. Soymilk okara gels MOCA2.5 and MOCA5 obtained porosity from 5.2 – 5.3 %, which was not statistically significant different from MO ($p < 0.05$). When increasing the CA concentration of CA to 10 %, the porosity of MOCA10 gel was much lower, 3.14 % and its color was browner when compared to MOCA5 gel, possibly attributable to the formation of Maillard and caramelization products.

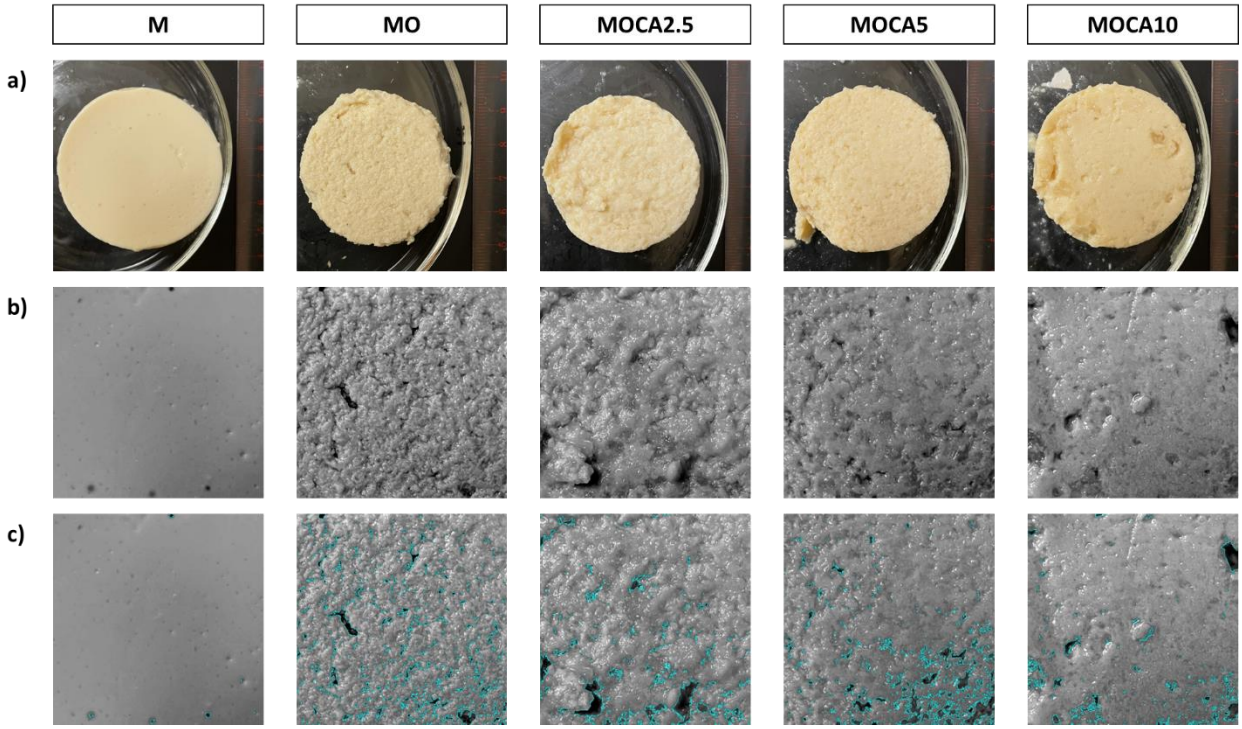


Figure 5. 6: a) Visual observations of the cross-section surface of soymilk okara gels (M, MO, MOCA2.5, MOCA5, MOCA10); b) Binary images generated by ImageJ with the gel size of 30 x 30 mm; c) Porous regions (blue lines) detected by ImageJ.

Table 5. 4: Porosity estimates of soymilk okara gels (M, MO, MOCA2.5, MOCA5, MOCA10) based on binary images with the aid of ImageJ. Data expressed as mean standard deviation (n = 3). Means within one column that do not share a common letter are statistically different (ANOVA followed by Tukey's post-hoc: $p < 0.05$).

Type of gel	Mean pore size (mm^2)	Total porous area (mm^2)	Porosity (%)
M	0.05 ± 0.03^a	0.85 ± 0.70^a	0.09 ± 0.08^a
MO	0.05 ± 0.01^a	45.4 ± 3.7^b	5.0 ± 0.40^b
MOCA2.5	0.06 ± 0.01^a	46.6 ± 1.0^b	5.2 ± 0.14^b
MOCA5	0.07 ± 0.01^a	52.4 ± 8.2^b	5.8 ± 0.90^b
MOCA10	0.08 ± 0.04^a	28.3 ± 4.9^c	3.1 ± 0.54^c

5.4.2.2. Microstructural Characterization of Gels by Confocal Laser Scanning Microscopy (CLSM)

The microstructure of soymilk okara gels (M, MO, MOCA2.5, MOCA5, MOCA10) determined by CLSM at different magnifications is illustrated in **Figure 5. 7**. In the CLSM images, the red region represents the protein matrix labelled non-covalently by rhodamine B [128], while arrows indicate fiber strain from okara [69]. The protein matrix of soymilk gel (M) at all three magnifications exhibited a compact and uniform structure with high density. This observation was in good agreement with previous studies in [201, 202, 83, 203], which describe heat-denatured globular protein aggregations. However, with the incorporation of unmodified okara, the protein matrix of MO displayed a fine-stranded gel structure disrupted by the presence of fiber strains

In the case of soymilk gels containing CA modified okara (MOCA2.5, MOCA5, MOCA10), differences were observed in protein aggregation, forming particulate structures (as shown in **Figure 5. 7 b**)**,** in comparison to the fine-stranded structure observed in M and MO gels. The

modified okara might contain an excess of CA, resulting in reduced pH values within the gels (as shown in

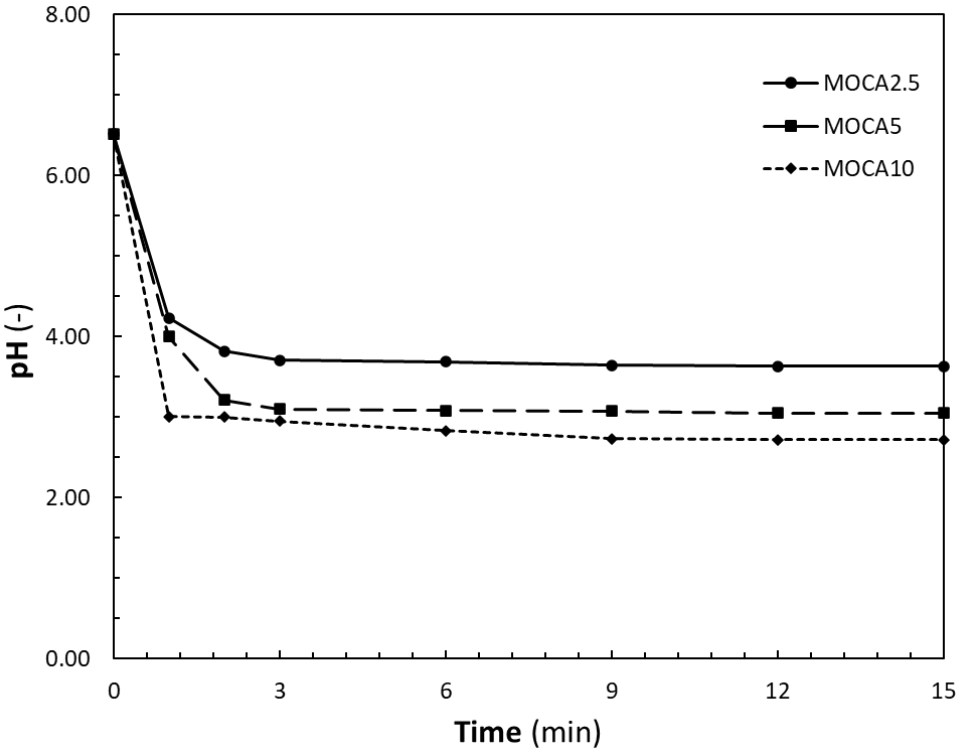


Figure S. *6*: Changes in pH of soymilk and modified okara mixture during the 15-min mixing.

Table S. *4* in **Appendix C**.), which may have contributed to higher protein gelation rate and the formation of spherical denatured protein particles with a larger hydrodynamic radius [204]. The MOCA10 gel exhibited a more compact protein structure compared to the MOCA2.5 and MOCA5 gels, consistent with the visual observations of their cross-sectional area. Additionally, MOCA2.5, MOCA5 and MOCA10 gels contained shorter-length fiber compared to those in MO.

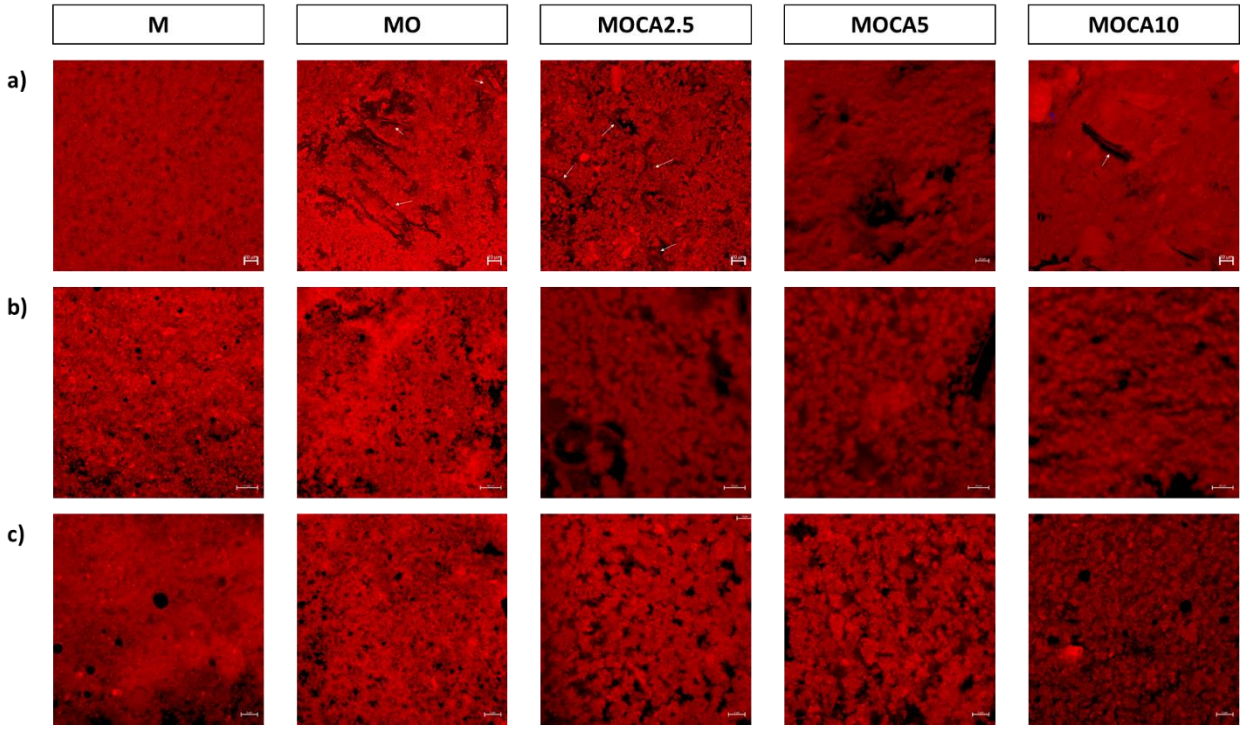


Figure 5. 7: CLSM images at three different magnifications a) 20 x, b) 63 x and c) 100 x of soymilk okara gels (M, MO, MOCA2.5, MOCA5, MOCA10). The red region represents the Rhodamine B labelled protein, and the scale bars represent 20 μm (for 20 x), 10 μm (for 63 x), 5 μm (for 100 x).

5.4.3. Syneresis and Water Holding Capacity (WHC) of Soymilk Okara Gels

The syneresis and water holding capacity of soymilk okara gels (M, MO, MOCA2.5, MOCA5, MOCA10) is depicted in **Figure 5. 8**. Syneresis represents the amount of liquid expelled or that passively diffused out of the gel during storage [3, 5], while water holding capacity indicates the ability of the gel to retain water through capillary effects of the gel matrices after centrifugation [10, 3]. In a gel system, water molecule can be attached to polysaccharides and proteins via their hydroxyl groups, loosely held within large pores and, or tightly entrapped in micro voids of gel network. The texture and stability characteristics of gels are influenced directly by the water distribution within gel system [8, 205].

Syneresis was different according to gel type. The soymilk gel M, characterized by its compact structure, exhibited minimal liquid release, approximately 0.22 %, after a 24-hour storage period. On the other hand, soymilk gel incorporating unmodified okara (MO) displayed no measurable syneresis, likely attributable to the substantial dietary fiber content in okara effectively retaining water [7]. Upon the introduction of CA modified okara into the soymilk gels (MOCA2.5, MOCA5, MOCA10), there was a notable and statistically significant ($p < 0.05$) increase of syneresis. Among these, MOCA5 gel exhibited the highest rate of syneresis at 3.6 %, while the MOCA10 gel had the lowest syneresis, 0.83 %. This observed syneresis can be explained by previous research findings [206, 207, 208], which suggest that protein crosslinking occurring during storage can expel the water entrapped within the protein network, leading to syneresis of protein gels. One ca assume that the gelation of the soymilk and CA-modified okara was still ongoing during the storage period, contributing to the increased syneresis compared to the M, MO gels.

The water holding capacity (WHC) revealed that the M and MO gels retained between 65.9 % and 69.9 % of liquid post-centrifugation. Notably, there was no statistically significant difference ($p > 0.05$) between the WHC values of the M and MO gels. With the incorporation of modified okara by CA at concentrations of 2.5 % (w:w) and 5 % (w:w), the WHC of the gels remained comparable ($p > 0.05$) to the M and MO gels. However, a noteworthy increase in WHC of approximately 10 % (w:w) was observed, reaching 80.9 %, for the MOCA10 gel. The above results suggest that 10% (w/w) CA concentration could modify okara and protein matrix to increase the water binding properties of gels and be more resistant to the external centrifugation forces.

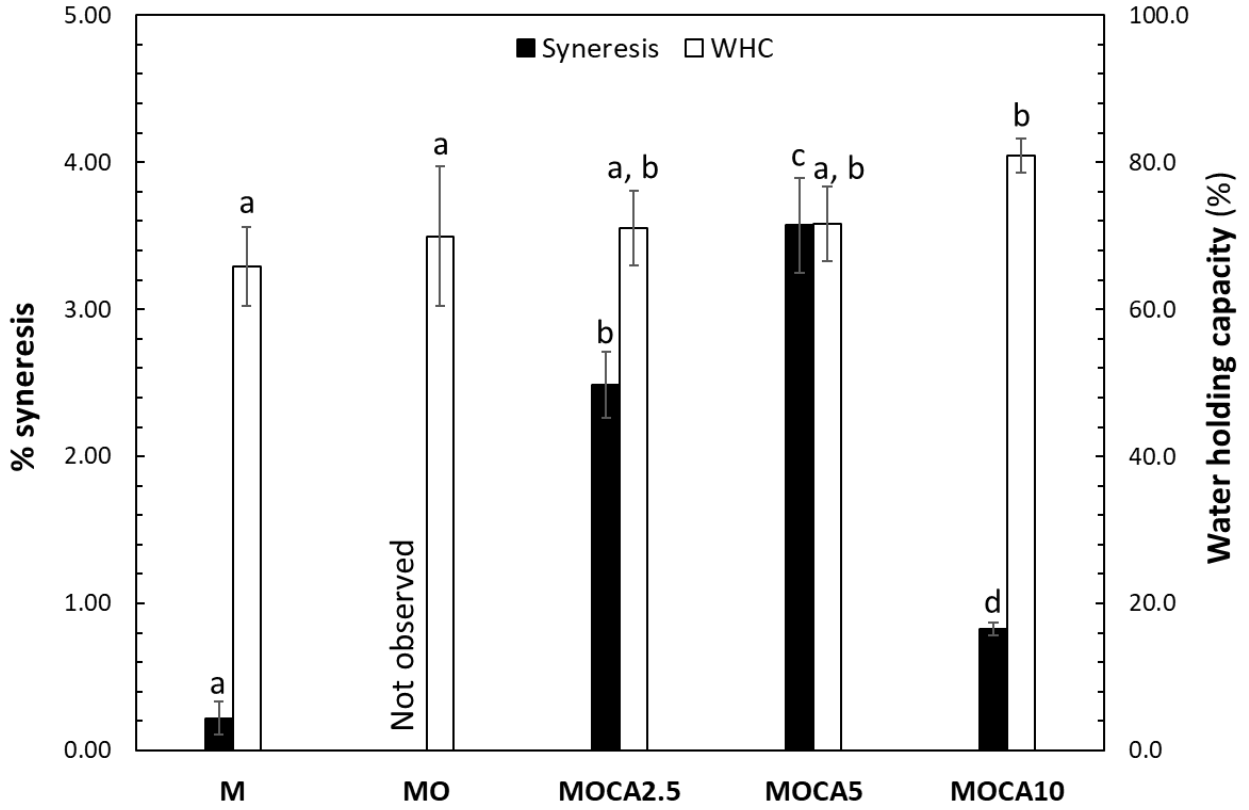


Figure 5. 8: Syneresis and water holding capacity (WHC) of soymilk okara gels after 24-h storage at 4 ^{o}C. Data of syneresis expressed as mean standard deviation (n = 3). Data of WHC expressed as mean standard deviation (n = 6). Means within one column that do not share a common letter are statistically different (ANOVA followed by Tukey's post-hoc: $p < 0.05$).

5.4.4. Texture Properties of Soymilk Okara Gels

5.4.4.1. Rheological Properties

The viscoelastic properties of soymilk okara gels (M, MO, MOCA2.5, MOCA5, MOCA10) were assessed using the methodology outlined in section **5.3.8.1** with results summarized in **Figure 5. 9** and **Table 5. 5**. The estimated G' and G'' recorded over the change of angular frequency represent the degree of elasticity and viscosity of gel, correspondingly [141]. Power law parameters n', n'' calculated from ***Error! Reference source not found.*** and ***Error! Reference source not found.*** are associated with weak- or strong-gel behaviour, and type of interactive forces within sample. As indicated in [132, 133] strong gels which are characterized by n' and n'' values smaller

than 0.05, are formed by breakable or deformable non-covalent cross-links and exhibit typical viscoelastic solids characteristic when subjected to small deformations. When increasing beyond critical deformation threshold, they experience rupture than flow. Conversely, weak gels, which are indicated by n' and n'' values larger than 0.05, display more frequency-independent behavior, falling between the rheological characteristics of solutions and strong gels. Although under small deformation, weak gels resemble strong gels in mechanical behavior, their networks break into smaller cluster with the increase in deformation level. The network structure within weak gels is formed by strong permanent covalent crosslinks, but more vulnerable to disruption than strong gel system.

All soymilk okara gels exhibited weak gel characteristic with G' consistently higher than G'' at all angular frequencies in range from 1 – 100 rad/s and n', n'' are 0.11 – 0.17 with no statistically significant difference between types of soymilk okara gels ($p > 0.05$). The increase of G' and G'' with increasing angular frequency from 1 to 100 rad/s and no crossover of G' and G'' indicate the formation of a continuous network [209, 210]. Complex viscosity describes the total resistance to flow of a material that it is considered as a viscous liquid [211]. All soy gel materials showed a decrease in complex viscosity when increasing the angular frequency indicating solid-like behavior [212].

Soymilk gel M had the lowest rigidity (G_o') and viscosity (G_o'') in comparison to soymilk gels containing unmodified MO or CA modified okara. The viscoelasticity of soy gel improved significantly when adding unmodified okara (MO: G_o' = 21.01 kPa, G_o'' = 5.01 kPa). The improvement in rheological properties of MO may relate to higher fiber content compared to M. The addition of fibers has been reported to contribute to the reinforcement (G') of gels by enabling a more extensive transfer of stress at the interface from the matrix to the fibers [213, 214].

Additionally, the presence of fibers in okara may absorb a portion of the free water within the gel and promote the immobility of solid particles. This phenomenon can lead to the obstruction of gel flow under shear stress, thus resulting in a rise in viscosity [213, 215].

Within examined soymilk (M) and soymilk okara gels (MO, MOCA2.5, MOCA5, MOCA10), The soymilk gel containing modified CA okara (MOCA2.5) displayed the highest elastic (G_o' = 31.39 kPa) and viscous (G_o'' = 7.30 kPa) properties of all soymilk gels. However, as the concentration of CA increased to 5 and 10 % (w:w), the viscoelastic properties of the MOCA5, and MOCA10 gels decreased drastically, with G_o' decreasing to 21.65 and 7.10 kPa and G_o" decreasing from 5.34 and 1.79 kPa. These results may be attributed to the more extensive degradation of the okara structure at higher CA concentrations as supported by TGA and FTIR data. This degradation may ultimately diminish the rigidity of okara and contribute to the observed decrease of the viscoelastic properties of the soymilk okara gel system.

Table 5. 5: Viscoelastic properties of soymilk okara gels (M, MO, MOCA2.5, MOCA5, MOCA10) based on power law parameters of **Error! Reference source not found.** and **Error! Reference source not found.** from frequency sweep tests. Data expressed as mean ± standard deviation (n = 9). Means within one column that do not share a common letter are statistically different (ANOVA followed by Tukey's post-hoc: $p < 0.05$).

Sample	G_o' (kPa)	n'	R^2	G_o'' (kPa)	n''	R^2
M	0.51 ± 0.16^{a}	0.11 ± 0.02^{a}	0.97	0.09 ± 0.03^{a}	0.11 ± 0.03^{a}	0.79
MO	21.01 ± 2.79^{b}	0.14 ± 0.01^{b}	1.00	5.01 ± 0.08^{b}	0.12 ± 0.02^{a}	0.99
MOCA2.5	31.39 ± 2.99^{c}	0.13 ± 0.01^{b}	0.99	7.30 ± 0.64^{c}	0.17 ± 0.02^{b}	0.99
MOCA5	21.65 ± 1.31^{b}	0.15 ± 0.01^{b}	0.99	5.34 ± 0.29^{b}	0.16 ± 0.02^{b}	0.99
MOCA10	7.10 ± 2.70^{d}	0.15 ± 0.02^{b}	0.99	1.79 ± 0.71^{c}	0.16 ± 0.02^{b}	0.99

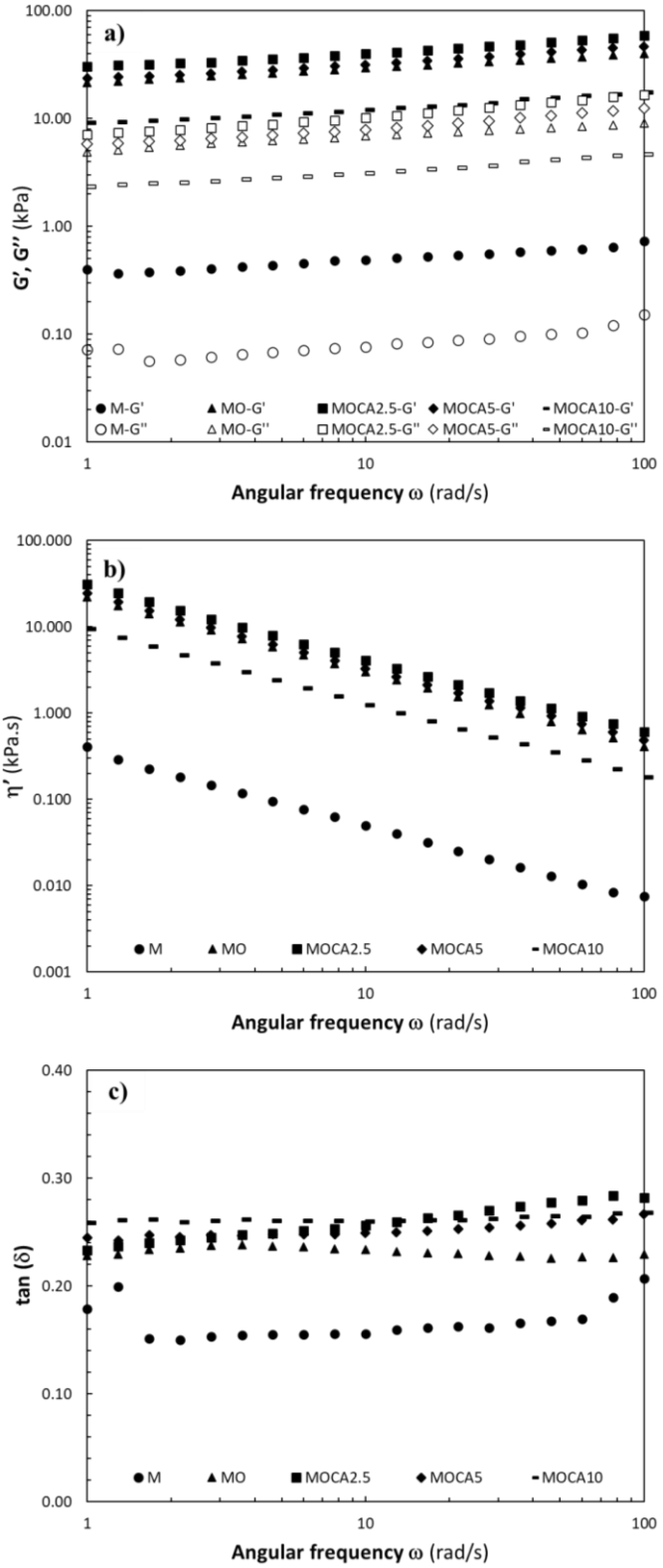


Figure 5. 9: Viscoelasticity properties of soymilk okara gels (M, MO, MOCA2.5, MOCA5, MOCA10): Typical curves of a) storage modulus G' (filled symbols) and loss modulus G'' (open symbols), b) complex viscosity and c) tan(δ) over angular frequency.

5.4.4.2. Mechanical Properties

Mechanical properties of soymilk okara gels (M, MO, MOCAS5, MOCA5) were obtained by uniaxial compression, following methodology in **section 5.3.9** with results summarized in **Figure 5. 10**. The Young's modulus (or elastic modulus) is associated with texture characteristics such as firmness or hardness, while the true fracture stress relates to toughness or chewiness, which also accounts for springiness and cohesiveness in addition to firmness properties of material. It is important to note that foods with higher true fracture stress may not necessarily be perceived as firm or hard [136]. The degree of deformation prior to gel fracture was represented by true fracture strain value [142].

Gel prepared from soymilk only (M) had lower true fracture stress and Young's modulus, along with higher true fracture strain, when compared to soymilk gel with unmodified okara (MO). These findings suggest that M possess characteristics of a weak but deformable gel, while MO gels have strong and brittle material characteristics [143]. The improvement in the gel strength of MO may be attributed to the rigidity characteristics of unmodified okara, which also enhanced the viscoelasticity of soymilk okara gel as above.

The modification of okara with 2.5 % (w:w) CA did not affect, the true fracture stress (MOCA2.5) when compared to MO ($p > 0.05$), while there was a notable increase in the Young's modulus, approximately doubling in value. Furthermore, there were no significant differences ($p < 0.05$) in the mechanical properties of all three soymilk CA-modified okara gels (MOCA2.5, MOCA5, MOCA10). This observation may be attributed to the comparable homogeneity observed in MOCA2.5, MOCA5, and MOCA10. The gel fracture is suggested to occur by the generation of cracks at structural defects, establishing a relationship between large deformation properties (true fracture stress and strain) and the homogeneity of the matrix [216, 217]. In contrast, small

deformation properties are more influenced by the continuous phase and active filler particles within gel system [217], which can be explained by the Young's modulus and viscoelasticity characteristics of soymilk modified okara gels.

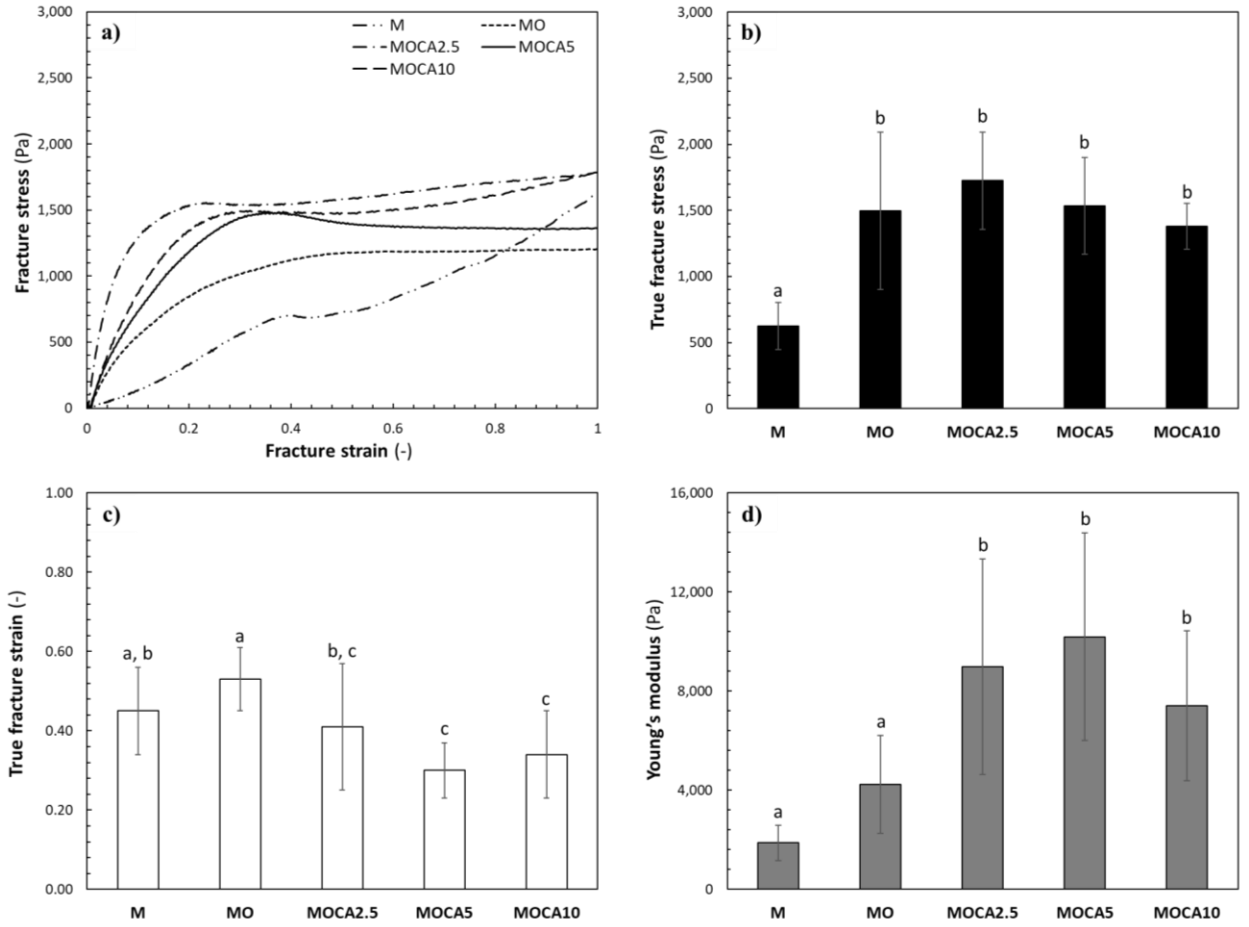


Figure 5. 10: Mechanical properties of soymilk okara gels (M, MO, MOCA2.5, MOCA5, MOca10): (a) Typical fracture stress – fracture strain curves, (b) True fracture stress, (c) True fracture strain, (d) Young's modulus. Data of (b – d) expressed as mean ± standard deviation (n = 18). Means within one column that do not share a common letter are statistically different (ANOVA followed by Tukey's post-hoc: $p < 0.05$).

5.4.5. Protein – Protein Interactions

The analysis of non-covalent protein – protein interactions including ionic bonds, hydrogen bonds and hydrophobic interactions of soymilk (M) and soymilk okara gels (MO, MOCA2.5, MOCA5,

MOCA10) is illustrated in **Figure 5. 11**. Hydrophobic interactions constituted the largest proportion of non-covalent intermolecular forces in all types of soymilk okara gels, which is similar to previous studies on heat-induced and acid induced plant protein gels [7, 218, 219, 220] Within the gel system, protein – water interactions are mainly driven by ionic and hydrogen bonds [220], whereas the formation of gel networks is primarily influenced by hydrophobic interactions [218, 219].

In comparison to soymilk gel M, the MO gel containing unmodified okara displayed a substantial reduction in hydrophobic interactions by approximately 30 %, while the distribution of ionic and hydrogen bonds was similar ($p > 0.05$). This observation indicate that the abundance of insoluble fiber in okara may have hindered the self-aggregation of the proteins, leading to the decrease in surface hydrophobicity and hydrophobic interactions of the protein in the gels [220, 221, 99].

In contrast, soymilk gels containing CA modified okara materials (MOCA2.5, MOCA5, MOCA10), contained very little ionic bonds, while the level of hydrogen bonds remained similar when compared to M and MO. The similar level of hydrogen bonds for all soymilk gel types except MOCA10 can be attributed and correlated to their WHC (as shown in **Figure 5. 8**), indicated the interactions between protein and water [99, 221]. Additionally, the hydrophobic interactions between protein molecules in all MOCA2.5, MOCA5, MOCA10 gels improved significantly, in comparison to MO, indicating that CA modification on okara reduced the hindrance to protein aggregation caused by unmodified okara.

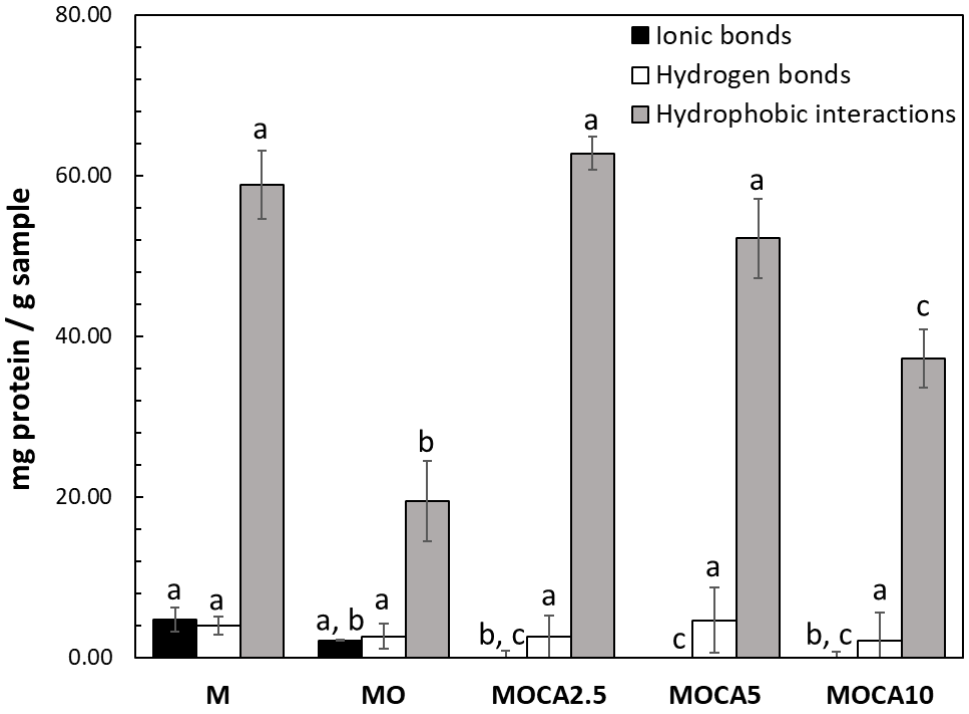


Figure 5. 11: Protein – protein interactions including ionic bonds, hydrogen bonds and hydrophobic interactions of soymilk okara gels (M, MO, MOCA2.5, MOCA5, MOCA10). Data expressed as mean ± standard deviation (n = 3). Means within one column that do not share a common letter are statistically different (ANOVA followed by Tukey's post-hoc: $p < 0.05$).

5.4.6. Proposed Mechanism of CA Okara Modification

The effect of citric acid (CA) on the modification of okara and the gelation of soymilk okara gels is discussed in this section with a schematic illustration of the proposed mechanism presented in **Figure 5. 12**.

5.4.6.1. Modification of Okara using Citric Acid (CA)

The proposed mechanism for the effects of citric acid (CA) on structure of okara is illustrated in **Figure 5. 12 (stage 1)**.

The structure of okara consists of intact cotyledon cells, cell walls of disrupted cells and agglomerated material in okara [69]. Plant cell wall is a complex matrix of polysaccharides, with

around 30 % cellulose, 30% hemicellulose and 35 % pectic substances, along with a minor 1 – 5 % content of structural protein. Within plant cell wall, cellulose and hemicellulose polymers contribute to the wall's rigidity, while pectin imparts fluidity to the gel-like polysaccharide matrix. Cellulose, an insoluble unbranched polymer of β-(1,4)-D-glucose, forms a crystalline microfibril with a diameter of roughly 3 nm by associating with other cellulose chains through hydrogen bonding and Van der Waals forces. Hemicelluloses, are a heterogeneous group of polysaccharides with β-(1,4)-linked backbones featuring an equatorial configuration at C1 and C4, share a structural similarity among their backbones and are recognized for their tight binding to cellulose microfibrils via hydrogen bonds [70, 71]. Pectin contains “egg-box” regions where pectin molecules crosslink with others through calcium ion bridges. [71, 72]

The effects of the CA concentration on the thermal stability (TGA) and functional group mapping (FTIR) of okara indicate that there was disruption in the hydrogen interactions within the polysaccharides, leading to the decomposition of okara fibers into oligosaccharides and the release of pectic substances. Notably, a higher concentration of CA resulted in more extensive fiber degradation and increased pectin release. These results were consistent with visual observations where the gumminess of CA-modified okara increased as the CA concentration increased from 2.5 to 10% (w/w). From both experimental data presented in this study and literature, it is suggested that along with the ability in promoting the hydrolysis of the okara polysaccharide [222, 223], CA, with its unique tri-carboxylic acid structure, could function as a chelator as well. This chelating effect enabled CA to capture and remove Ca^{2+} ions, thereby loosening the structure of okara and facilitating the release of more soluble polysaccharides, particularly pectic substances [159, 194, 160, 14, 72]. Literature also refers to the chelating properties of CA that could enhance the hydrolysis of cellulose and hemicellulose materials, exposing more active hydroxyl sites for

subsequent crosslinking reactions [224, 12, 11, 225]. Additionally, the formation of amphiphilic soy protein – polysaccharides conjugates by Maillard reaction was also detected by FTIR, that is expected to assist in the improvement of compatibility between okara and soymilk gel.

5.4.6.2. Gelation of Soymilk and CA Modified Okara

The proposed mechanism for the effects of citric acid (CA) on the gelation of soymilk and CA modified okara is depicted in **Figure 5. 12 (stage 2)**.

According to the study in [77], the heat-induced gelation of soy protein comprises 4 main steps including the initial dissociation of native globulins; the subsequent reassociation of proteins into compact spherical particles; the self-similar aggregation of the dense protein domains; and the eventual gelation or formation of a system spanning network. Under neutral pH conditions, the primary driving force behind protein-protein interactions in the formation of soy protein gel systems is hydrophobic interactions [220]. Experimental CLSM, protein-protein interactions analysis, mechanical and rheological characteristics presented in this study, accompanied with insights from existing literature [4, 7, 220], indicate that the addition of okara somewhat hindered the self-aggregation of proteins, resulting in a reduction in both hydrophobic interactions and the overall homogeneity of the soy gel. However, okara, with its rigid structure, contributed positively to the improvement of viscoelasticity and mechanical properties of gel system.

In all three soymilk gel systems containing CA-modified okara at different concentrations (2.5, 5 and 10 %, w:w), noteworthy enhancements were observed in terms of homogeneity, rheological and mechanical properties, as well as hydrophobic interactions, compared to soymilk gel containing unmodified okara. These observations can likely be attributed to the structural degradation of okara, along with the amphiphilicity of soy protein – polysaccharides conjugates

formed during the okara modification process, resulting in better distribution in the protein matrix and reduced disruption to protein – protein interactions. Additionally, the excess CA in the modified okara may also have contributed to enhancing the gel quality by its protein crosslinking capability. As the concentration of CA for okara modification increased (ranging from 2.5% to 5% and 10%, w:w), the soymilk containing CA modified okara gel exhibited improved homogeneity and higher water-holding capacity (WHC), while there was reduction in viscoelasticity and hydrophobic interactions, accompanied with no measurable change in mechanical properties between gels.

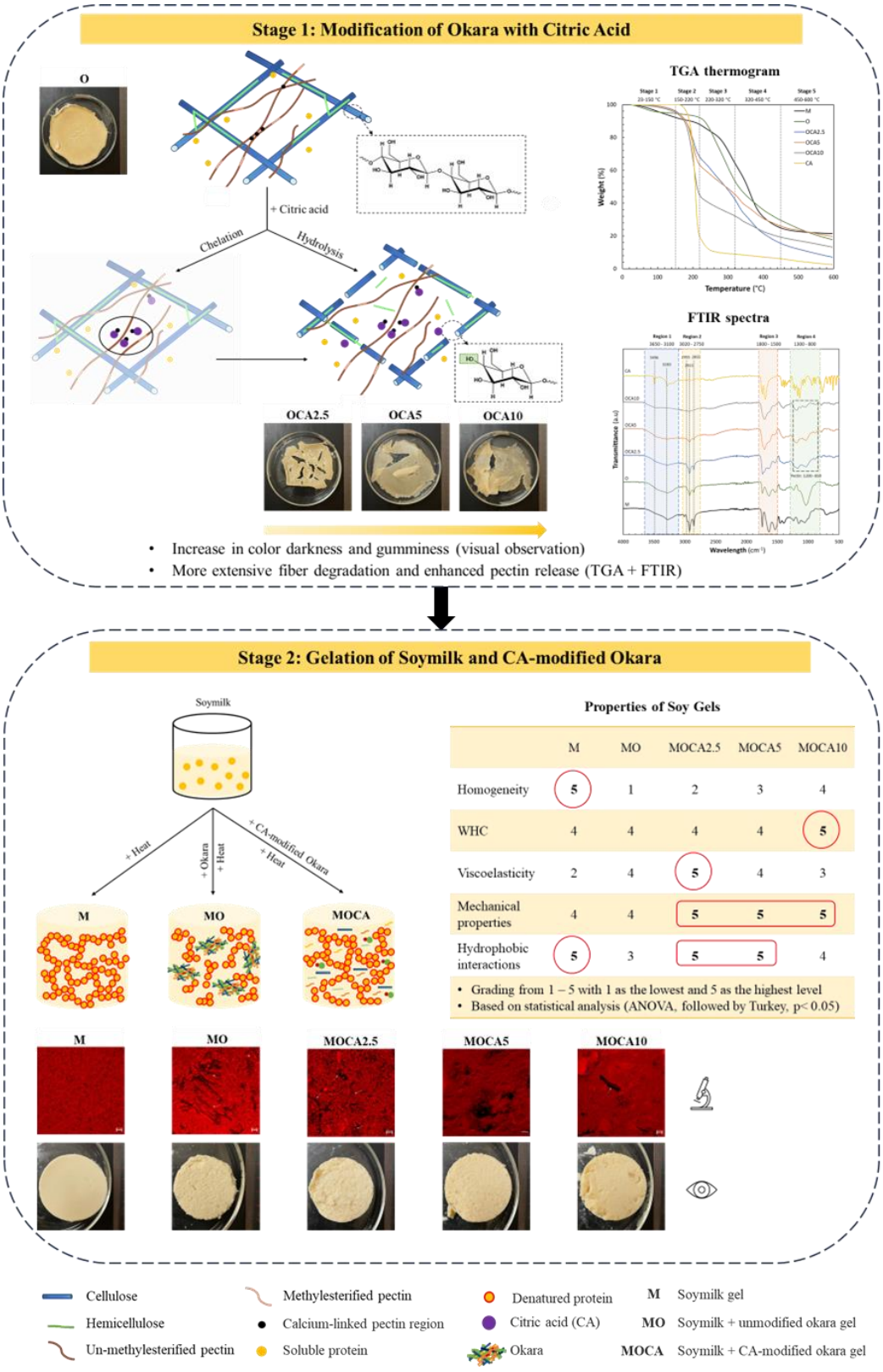


Figure 5. 12: Proposed mechanism for the effect of citric acid modification on okara's structure (Stage 1) and on soymilk okara gels (Stage 2).

5.5. Conclusion

In this study, the effects of citric acid (CA) modification to okara on the structure of okara, and its subsequent effects on soymilk gels containing CA-modified okara, with the aim of enhancing the compatibility between okara and the soymilk gel matrix. The investigation revealed distinct alterations in okara's structure via TGA and FTIR. With the acid hydrolysis and chelating properties, CA can induce the breakdown of cellulose and hemicellulose leading to the exposure of more active hydroxyl sites, accompanied with the extraction of soluble polysaccharides. The formation of amphiphilic protein-polysaccharide conjugates was also observed in FTIR spectra of CA modified okara materials. At the higher concentration of CA used, the more extensive fiber degradation and release of pectin was observed.

The effects of CA on the soymilk okara gels were analyzed through several properties, including the homogeneity, microstructure, water holding capacity (WHC), viscoelasticity, mechanical properties and protein – protein interactions. Within soymilk okara gel system, unmodified okara disrupted the formation of soy gel's protein network, resulting in a textural heterogeneity, and a significant low protein-protein interactions, particularly the hydrophobic ones. At the micro scale, the protein matrix of unmodified soymilk and okara gel displayed a fine-stranded structure. Following the modification of okara with 2.5 % CA solution (w:w), the resulting soymilk okara gels displayed improved homogeneity and increased in the hydrophobic interactions between protein molecules. The viscoelasticity and mechanical properties of soymilk gel containing okara modified with CA at 2.5 % also showed enhancement in its properties in comparison to the unmodified gel. These findings indicated that CA had potential in the improvement the compatibility between okara and soymilk gels, while forming a strong protein matrix.

As the concentration of CA increased from 2.5 to 5 and 10 %, the soymilk okara gel exhibited higher levels of homogeneity, observed in both optical and CLSM images, as well as increased WHC. Simultaneously, there was a slight reduction in viscoelasticity and hydrophobic interactions, accompanied with similar mechanical properties observed across all CA modified samples. This finding might be related to higher level of fiber degradation and the excess CA on modified okara materials. The examined alternations in the textural profiles and protein – protein interactions when varying the concentration of CA solution may offer valuable insights for achieving desired textural profiles aligned with commercial products in further studies.

Further research could involve the comparative studies between the characterization of dehulled soybean gel containing CA modified okara materials and commercial products. Additionally, the sensory evaluation could also be conducted for the development of high-fiber plant-based products.

Chapter 6: Conclusions and Recommendations

The research presented in this thesis focused on (1) the standardization of soymilk and soymilk okara gels preparation, (2) the revision of methodology of sample preparation for texture characterization and protein – protein interactions characterization of soymilk okara gels and (3) the characterization of okara modified by citric acid (CA) and its resulting gels.

The first objective in this study was to standardize the preparation of soymilk and soymilk okara gels. The consistency in the quality of soymilk was obtained through the solid content, while the standardization of soymilk okara gel preparation was assessed based on the effect of physical states (liquid or solid) of CA and drying time for okara, rheological and mechanical properties of resulting gels. To maintain uniform soymilk quality across experiments, the solid content of soymilk was measured by drying at 60 °C for 3 h in the oven and kept constant at the level of 15 – 16 % (w:w). The use of solid and liquid state of CA at the final concentrations of 5 % (w:w) in okara modification showed similar effects in improving homogeneity and mechanical properties, along with the decrease in viscoelasticity of the gels, in comparison to unmodified gel. However, the CA solution was selected for further studies due to its improved distribution in the mixture, leading to a higher reproducibility in texture properties. the duration of the drying of okara materials, 20 h was selected as the appropriate time to obtain constant weight without major alternations in colour and composition, in comparison to longer durations (26, 44 and 50 h).

The second objective of this study was to finalize the methodology of sample preparation for texture characterization and protein – protein interactions characterization of soymilk okara gels. To overcome the challenges of cutting soy gel into precise shapes and dimensions from bulk gels for subsequent measurements of rheological and mechanical properties without causing damage,

alternative methods were investigated. For rheological properties measurements, soymilk okara gels were gelled at 2 to 3-mm thickness in glass petri dish, while soymilk okara gels were gelled at 10-mm height in 100-mL beakers for the subsequent measurement of mechanical properties. These alternative methods reduced the number of cutting steps, while producing a more uniform shapes of soy gels. The Bradford assay methodology for the measurement of protein – protein interactions in soy gels was adapted for the measurement of soluble protein content due to the compatibility between chemicals used and the assay. The recovery of the supernatant containing soluble protein from the gel, the centrifugation settings were adjusted to 10,000 rpm, 25 ℃ for 45 min.

The third objective in this study was the characterization of okara modified by CA and its resulting gels. Based on the preliminary results, the final procedure for preparing soymilk okara gels was established as follows: okara was modified with CA solutions at concentrations ranging from 2.5 to 10 %, dried at 60 ℃ for 20 h, followed by the gelation with soymilk induced by heat treatment at 95 °C for 45 min. In comparison to the heterogenous texture of soy gel containing unmodified okara, the modification of okara with CA showed significant increase in the visual homogeneity of the gel and the protein-protein interactions across all three concentrations, reflecting the improvement in the compatibility between okara and soymilk gel. This finding might be attributed to fiber degradation leading to the exposure of more active hydroxyl sites, facilitating the occurrence of cross-linking reactions. As the concentration of CA increased from 2.5 to 5 and 10 % (w/w), the soymilk okara gel increased gel homogeneity, was observed in both optical and CLSM images, as well as increased water holding capacity (WHC). Simultaneously, there was a slight reduction in viscoelasticity and hydrophobic interactions, accompanied with similar mechanical properties observed across all CA modified soymilk gels. This finding might be related

to higher degree of fiber degradation and the excess CA on modified okara materials. The examined alterations in the textural profiles and protein – protein interactions when varying the concentration of CA solution may offer valuable insights for achieving desired textural profiles aligned with commercial cheese analogue products in further studies.

The results presented in this work led to the formulation of the following recommendations for future work on okara-added soymilk gel:

Exploration of protein - polysaccharides interactions:

Investigating the interactions between proteins and polysaccharides, such as okara, can provide valuable insights into understanding the compatibility mechanism between okara and the soy protein matrix. Therefore, okara modification technique can be improved, based on the compatibility mechanism. It is proposed to employ the CLSM technique with double staining system to visualize both protein and polysaccharides in microscale. Scanning electron microscopy (SEM) can also be used to visualize the gel system in nanoscale.

Characterization of soymilk okara gels using textural profile analysis (TPA):

While the rheological and uniaxial compression tests have provided information about viscoelasticity, gel strength, and elastic modulus of soymilk okara gels, it is recommended to incorporate Textural Profile Analysis (TPA) for a comprehensive evaluation. TPA can provide insights into sensory attributes such as hardness, springiness, chewiness, and resilience of the gel, offering a better understanding of the gel's textural properties.

Comparison with the characterization of commercial products:

Comparative studies between the characterization of soymilk gels containing CA-modified okara materials and commercial cheese analogue products can yield valuable insights for the

development of high-fiber plant-based products. This approach can help improve the textural properties of soy gel to mimic those of commercial products, enhancing their market appeal.

Sensory evaluation

Conducting sensory evaluations enables the objective analysis of foods, focusing on properties like taste, flavor, and texture. By incorporating sensory testing, it becomes possible to fine-tune these properties to align with customer expectations, thereby enhancing the overall appeal of high-fiber plant-based products.

Letters of Copyright Permission

This Agreement between Ms. Minh Xuan Nguyen ("You") and John Wiley and Sons ("John Wiley and Sons") consists of your license details and the terms and conditions provided by John Wiley and Sons and Copyright Clearance Center.

License Number	5646621494697
License date	Oct 12, 2023
Licensed Content Publisher	John Wiley and Sons
Licensed Content Publication	International Journal of Dairy Technology
Licensed Content Title	Cheese technology
Licensed Content Author	Nana Y Farkye
Licensed Content Date	Apr 26, 2004
Licensed Content Volume	57
Licensed Content Issue	2-3
Licensed Content Pages	8
Type of use	Dissertation/Thesis
Requestor type	Author of this Wiley article
Format	Print and electronic
Portion	Figure/table
Number of figures/tables	1
Will you be translating?	No
Title	MASc student
Institution name	University of Waterloo
Expected presentation date	Nov 2023
Portions	Figure 1 on page 92

This Agreement between Ms. Minh Xuan Nguyen ("You") and Elsevier ("Elsevier") consists of your license details and the terms and conditions provided by Elsevier and Copyright Clearance Center.

License Number	5646630348156
License date	Oct 12, 2023
Licensed Content Publisher	Elsevier
Licensed Content Publication	International Dairy Journal
Licensed Content Title	Casein Interactions: Casting Light on the Black Boxes, the Structure in Dairy Products
Licensed Content Author	David S. Horne
Licensed Content Date	Mar 1, 1998
Licensed Content Volume	8
Licensed Content Issue	3
Licensed Content Pages	7
Start Page	171
End Page	177
Type of Use	reuse in a thesis/dissertation
Portion	figures/tables/illustrations
Number of figures/tables/illustrations	1
Format	both print and electronic
Are you the author of this Elsevier article?	No
Will you be translating?	No
Title	MASc student
Institution name	University of Waterloo
Expected presentation date	Nov 2023
Portions	Figure 3 on page 174

This Agreement between Ms. Minh Xuan Nguyen ("You") and Elsevier ("Elsevier") consists of your license details and the terms and conditions provided by Elsevier and Copyright Clearance Center.

License Number	5646631069162
License date	Oct 12, 2023
Licensed Content Publisher	Elsevier
Licensed Content Publication	International Dairy Journal
Licensed Content Title	Casein sub-micelles: do they exist?
Licensed Content Author	Pieter Walstra
Licensed Content Date	Mar 1, 1999
Licensed Content Volume	9
Licensed Content Issue	3-6
Licensed Content Pages	4
Start Page	189
End Page	192
Type of Use	reuse in a thesis/dissertation
Portion	figures/tables/illustrations
Number of figures/tables/illustrations	1
Format	both print and electronic
Are you the author of this Elsevier article?	No
Will you be translating?	No
Title	MASc student
Institution name	University of Waterloo
Expected presentation date	Nov 2023
Portions	Figure 1 on page 190

This Agreement between Ms. Minh Xuan Nguyen ("You") and Springer Nature ("Springer Nature") consists of your license details and the terms and conditions provided by Springer Nature and Copyright Clearance Center.

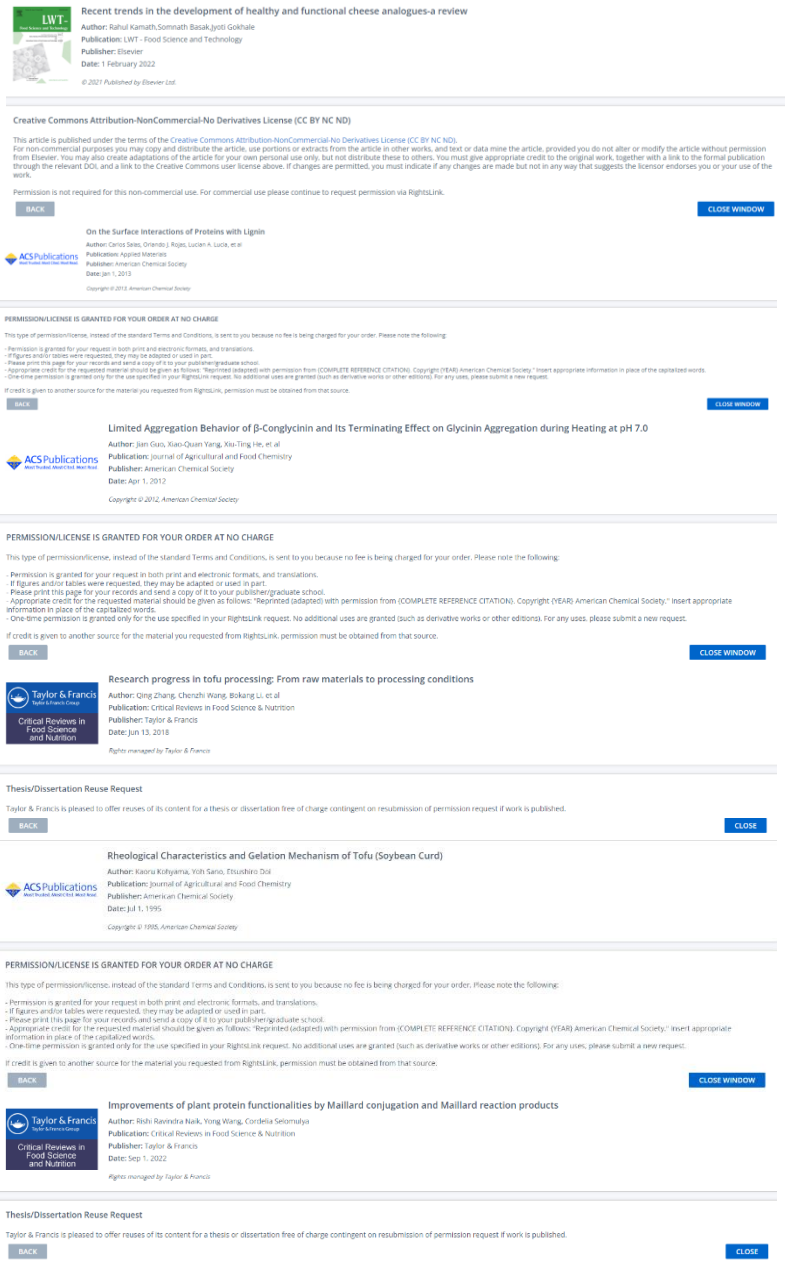
License Number	5646631411561
License date	Oct 12, 2023
Licensed Content Publisher	Springer Nature
Licensed Content Publication	Springer eBook
Licensed Content Title	Enzymatic Coagulation of Milk
Licensed Content Author	Patrick F. Fox, Timothy P. Guinee, Timothy M. Cogan et al
Licensed Content Date	Jan 1, 2017
Type of Use	Thesis/Dissertation
Requestor type	academic/university or research institute
Format	print and electronic
Portion	figures/tables/illustrations
Number of figures/tables/illustrations	1
Will you be translating?	no
Circulation/distribution	1 - 29
Author of this Springer Nature content	no
Title	MASc student
Institution name	University of Waterloo
Expected presentation date	Nov 2023
Portions	Figure 7.8

This Agreement between Ms. Minh Xuan Nguyen ("You") and John Wiley and Sons ("John Wiley and Sons") consists of your license details and the terms and conditions provided by John Wiley and Sons and Copyright Clearance Center.

License Number	5646640232912
License date	Oct 12, 2023
Licensed Content Publisher	John Wiley and Sons
Licensed Content Publication	International Journal of Dairy Technology
Licensed Content Title	Subject: Novel cheeses and cheese-making processes
Licensed Content Author	MICHAEL SHAW
Licensed Content Date	Aug 9, 2007
Licensed Content Volume	37
Licensed Content Issue	1
Licensed Content Pages	5
Type of use	Dissertation/Thesis
Requestor type	Author of this Wiley article
Format	Print and electronic
Portion	Figure/table
Number of figures/tables	1
Will you be translating?	No
Title	MASc student
Institution name	University of Waterloo
Expected presentation date	Nov 2023
Portions	Figure 1 on page 28

This Agreement between Ms. Minh Xuan Nguyen ("You") and Elsevier ("Elsevier") consists of your license details and the terms and conditions provided by Elsevier and Copyright Clearance Center.

License Number	5646640918861
License date	Oct 12, 2023
Licensed Content Publisher	Elsevier
Licensed Content Publication	Trends in Food Science & Technology
Licensed Content Title	The science of plant-based foods: Approaches to create nutritious and sustainable plant-based cheese analogs
Licensed Content Author	Lutz Grossmann,David Julian McClements
Licensed Content Date	Dec 1, 2021
Licensed Content Volume	118
Licensed Content Issue	n/a
Licensed Content Pages	23
Start Page	207
End Page	229
Type of Use	reuse in a thesis/dissertation
Portion	figures/tables/illustrations
Number of figures/tables/illustrations	2
Format	both print and electronic
Are you the author of this Elsevier article?	No
Will you be translating?	No
Title	MASc student
Institution name	University of Waterloo
Expected presentation date	Nov 2023
Portions	Figure 2 on page 214, figure 3 on page 216



Recent trends in the development of healthy and functional cheese analogues-a review
Author: Rahul Kamath,Somnath Basak,Jyoti Gokhale
Publication: LWT - Food Science and Technology
Publisher: Elsevier
Date: 1 February 2022
© 2021 Published by Elsevier Ltd.

Creative Commons Attribution-NonCommercial-No Derivatives License (CC BY NC ND)

This article is published under the terms of the Creative Commons Attribution-NonCommercial-No Derivatives License (CC BY NC ND).
For non-commercial purposes you may copy and distribute the article, use portions or extracts from the article in other works, and text or data mine the article, provided you do not alter or modify the article without permission from Elsevier. You may also create adaptations of the article for your own personal use only, but not distribute these to others. You must give appropriate credit to the original work, together with a link to the formal publication through the relevant DOI, and a link to the Creative Commons user license above. If changes are permitted, you must indicate if any changes are made but not in any way that suggests the licensor endorses you or your use of the work.

Permission is not required for this non-commercial use. For commercial use please continue to request permission via RightsLink.

BACK CLOSE WINDOW

On the Surface Interactions of Proteins with Lignin
Author: Carlos Salas, Orlando J. Rojas, Lucian A. Lucia, et al
Publication: Applied Materials
Publisher: American Chemical Society
Date: Jan 1, 2013
Copyright © 2013, American Chemical Society

PERMISSION/LICENSE IS GRANTED FOR YOUR ORDER AT NO CHARGE

This type of permission/license, instead of the standard Terms and Conditions, is sent to you because no fee is being charged for your order. Please note the following:

- Permission is granted for your request in both print and electronic formats, and translations.
- If figures and/or tables were requested, they may be adapted or used in part.
- Please print this page for your records and send a copy of it to your publisher/graduate school.
- Appropriate credit for the requested material should be given as follows: "Reprinted (adapted) with permission from (COMPLETE REFERENCE CITATION). Copyright (YEAR) American Chemical Society." Insert appropriate information in place of the capitalized words.
- One-time permission is granted only for the use specified in your RightsLink request. No additional uses are granted (such as derivative works or other editions). For any uses, please submit a new request.

If credit is given to another source for the material you requested from RightsLink, permission must be obtained from that source.

BACK CLOSE WINDOW

Limited Aggregation Behavior of β-Conglycinin and Its Terminating Effect on Glycinin Aggregation during Heating at pH 7.0
Author: Jian Guo, Xiao-Quan Yang, Xiu-Ting He, et al
Publication: Journal of Agricultural and Food Chemistry
Publisher: American Chemical Society
Date: Apr 1, 2012
Copyright © 2012, American Chemical Society

PERMISSION/LICENSE IS GRANTED FOR YOUR ORDER AT NO CHARGE

This type of permission/license, instead of the standard Terms and Conditions, is sent to you because no fee is being charged for your order. Please note the following:

- Permission is granted for your request in both print and electronic formats, and translations.
- If figures and/or tables were requested, they may be adapted or used in part.
- Please print this page for your records and send a copy of it to your publisher/graduate school.
- Appropriate credit for the requested material should be given as follows: "Reprinted (adapted) with permission from (COMPLETE REFERENCE CITATION). Copyright (YEAR) American Chemical Society." Insert appropriate information in place of the capitalized words.
- One-time permission is granted only for the use specified in your RightsLink request. No additional uses are granted (such as derivative works or other editions). For any uses, please submit a new request.

If credit is given to another source for the material you requested from RightsLink, permission must be obtained from that source.

BACK CLOSE WINDOW

Research progress in tofu processing: From raw materials to processing conditions
Author: Qing Zhang, Chenzhi Wang, Bokang Li, et al
Publication: Critical Reviews in Food Science & Nutrition
Publisher: Taylor & Francis
Date: Jun 13, 2018
Rights managed by Taylor & Francis

Thesis/Dissertation Reuse Request

Taylor & Francis is pleased to offer reuses of its content for a thesis or dissertation free of charge contingent on resubmission of permission request if work is published.

BACK CLOSE

Rheological Characteristics and Gelation Mechanism of Tofu (Soybean Curd)
Author: Kaoru Kohyama, Yoh Sano, Etsushiro Doi
Publication: Journal of Agricultural and Food Chemistry
Publisher: American Chemical Society
Date: Jul 1, 1995
Copyright © 1995, American Chemical Society

PERMISSION/LICENSE IS GRANTED FOR YOUR ORDER AT NO CHARGE

This type of permission/license, instead of the standard Terms and Conditions, is sent to you because no fee is being charged for your order. Please note the following:

- Permission is granted for your request in both print and electronic formats, and translations.
- If figures and/or tables were requested, they may be adapted or used in part.
- Please print this page for your records and send a copy of it to your publisher/graduate school.
- Appropriate credit for the requested material should be given as follows: "Reprinted (adapted) with permission from (COMPLETE REFERENCE CITATION). Copyright (YEAR) American Chemical Society." Insert appropriate information in place of the capitalized words.
- One-time permission is granted only for the use specified in your RightsLink request. No additional uses are granted (such as derivative works or other editions). For any uses, please submit a new request.

If credit is given to another source for the material you requested from RightsLink, permission must be obtained from that source.

BACK CLOSE WINDOW

Improvements of plant protein functionalities by Maillard conjugation and Maillard reaction products
Author: Rishi Ravindra Naik, Yong Wang, Cordelia Selomulya
Publication: Critical Reviews in Food Science & Nutrition
Publisher: Taylor & Francis
Date: Sep 1, 2022
Rights managed by Taylor & Francis

Thesis/Dissertation Reuse Request

Taylor & Francis is pleased to offer reuses of its content for a thesis or dissertation free of charge contingent on resubmission of permission request if work is published.

BACK CLOSE

This Agreement between Ms. Minh Xuan Nguyen ("You") and Elsevier ("Elsevier") consists of your license details and the terms and conditions provided by Elsevier and Copyright Clearance Center.

License Number	5646641176330
License date	Oct 12, 2023
Licensed Content Publisher	Elsevier
Licensed Content Publication	Innovative Food Science & Emerging Technologies
Licensed Content Title	Whole soybean protein extraction processes: A review
Licensed Content Author	K.E. Preece,N. Hooshyar,N.J. Zuidam
Licensed Content Date	Oct 1, 2017
Licensed Content Volume	43
Licensed Content Issue	n/a
Licensed Content Pages	10
Start Page	163
End Page	172
Type of Use	reuse in a thesis/dissertation
Portion	figures/tables/illustrations
Number of figures/tables/illustrations	1
Format	both print and electronic
Are you the author of this Elsevier article?	No
Will you be translating?	No
Title	MASc student
Institution name	University of Waterloo
Expected presentation date	Nov 2023
Portions	Figure 3 on page 166

This Agreement between Ms. Minh Xuan Nguyen ("You") and Elsevier ("Elsevier") consists of your license details and the terms and conditions provided by Elsevier and Copyright Clearance Center.

License Number	5652571305532
License date	Oct 19, 2023
Licensed Content Publisher	Elsevier
Licensed Content Publication	Current Opinion in Food Science
Licensed Content Title	Heat-induced gelation of plant globulins
Licensed Content Author	Taco Nicolai,Christophe Chassenieux
Licensed Content Date	Jun 1, 2019
Licensed Content Volume	27
Licensed Content Issue	n/a
Licensed Content Pages	5
Start Page	18
End Page	22
Type of Use	reuse in a thesis/dissertation
Portion	figures/tables/illustrations
Number of figures/tables/illustrations	1
Format	both print and electronic
Are you the author of this Elsevier article?	No
Will you be translating?	No
Title of new work	MASc student
Institution name	University of Waterloo
Expected presentation date	Nov 2023
Portions	Figure 1 on page 20

This Agreement between Ms. Minh Xuan Nguyen ("You") and Oxford University Press ("Oxford University Press") consists of your license details and the terms and conditions provided by Oxford University Press and Copyright Clearance Center.

License Number	5656720071017
License date	Oct 26, 2023
Licensed content publisher	Oxford University Press
Licensed content publication	Bioscience Biotechnology and Biochemistry
Licensed content title	Hydrolysis Kinetics of Okara and Characterization of Its Water-soluble Polysaccharides
Licensed content author	Yoshii, Hidefumi; Furuta, Takeshi
Licensed content date	Jan 1, 1996
Type of Use	Thesis/Dissertation
Institution name	
Title of your work	MASc student
Publisher of your work	University of Waterloo
Expected publication date	Nov 2023
Permissions cost	0.00 USD
Value added tax	0.00 USD
Total	0.00 USD
Title of new work	MASc student
Institution name	University of Waterloo
Expected presentation date	Nov 2023
Portions	Figure 6 on page 1408

References

[1] W. d. Riet, A.W.Wight, J.J.L.Cilliers and J.M.Datel, "Food chemical investigation of tofu and its byproduct okara," *Food Chemistry,* vol. 34, no. 3, pp. 193-202, 1989.

[2] A. Jiménez-Escrig, M. D. Tenorio, I. Espinosa-Martos and P. Rupérez, "Health-Promoting Effects of a Dietary Fiber Concentrate from the Soybean Byproduct Okara in Rats," *Journal of Agricultural and Food Chemistry,* vol. 56, no. 16, p. 7495 – 7501, 2008.

[3] I. Ullah, Y. Hu, J. You, T. Yin, S. Xiong, Z.-u. Din, Q. Huang and R. Liu, "Influence of okara dietary fiber with varying particle sizes on gelling properties, water state and microstructure of tofu gel," *Food Hydrocolloids,* no. 89, pp. 512-522, 2019.

[4] X. Fan, S. Li, A. Zhang, H. Chang, X. Zhao, Y. Lin and Z. Feng, "Mechanism of change of the physicochemical characteristics, gelation process, water state, and microstructure of okara tofu analogues induced by high-intensity ultrasound treatment," *Food Hydrocolloids,* vol. 111, 2021.

[5] H.-H. Liu, J.-T. Chien and M.-I. Kuo, "Ultra high pressure homogenized soy flour for tofu making," *Food Hydrocolloids,* vol. 32, no. 2, pp. 278 - 285, 2013.

[6] F. Wei, F. Ye, S. Li, L. Wang, J. Li and G. Zhao, "Layer-by-layer coating of chitosan/pectin effectively improves the hydration capacity, water suspendability and tofu gel compatibility of okara powder," *Food Hydrocolloids,* vol. 77, pp. 465 - 473, 2018.

[7] M. Zhang, P. Wang, M. Zou, R. Yang, M. Tian and Z. Gu, "Microbial transglutaminase-modified protein network and its importance in enhancing the quality of high-fiber tofu with okara," *Food Chemistry,* vol. 289, pp. 169 - 176, 2019.

[8] I. Ullah, R. M. Khoder, T. Yin, J. You, Q. Huang, R. Liu and S. Xiong, "Gelation properties of tofu induced by different coagulants: Effects of molecular interactions between nano-sized okara dietary fiber and soybean proteins," *Food Chemistry,* vol. 403, p. 134056, 2023.

[9] B. C. Behera, R. Mishra and S. Mohapatra, "Microbial citric acid: Production, properties, application, and future perspectives," *Food Frontiers,* vol. 2, no. 1, pp. 62 - 76, 2021.

[10] F.-H. Cao, X.-J. Li, S.-Z. Luo, D.-D. Mu, X.-Y. Zhong, S.-T. Jiang, Z. Zheng and Y.-Y. Zhao, "Effects of organic acid coagulants on the physical properties of and chemical interactions in tofu," *LWT - Food Science and Technology ,* vol. 85, pp. 58-65, 2017.

[11] G. A. Bittencourt, L. P. d. S. Vandenberghe, K. K. Valladares-Diestra and C. R. Soccol, "Soybean hull valorization for sugar production through the optimization of citric acid pretreatment and enzymatic hydrolysis," *Industrial Crops and Products,* vol. 186, p. 115178, 2022.

[12] M. G. Gomes, L. V. A. Gurgel, M. A. Baffi and D. Pasquini, "Pretreatment of sugarcane bagasse using citric acid and its use in enzymatic hydrolysis," *Renewable Energy,* vol. 157, pp. 332 - 341, 2020.

[13] P. Amnuaycheewa, R. Hengaroonprasan, K. Rattanaporn, S. Kirdponpattara, K. Cheenkachorn and M. Sriariyanun, "Enhancing enzymatic hydrolysis and biogas production from rice straw by pretreatment with organic acids," *Industrial Crops and Products,* vol. 87, pp. 247 - 254, 2016.

[14] W. Cai, H. Zhang, X. Chen, S. Yan, L. Yang, H. Song, J. Li, J. Liu, H. Yu, H. Liu and D. Zhu, "Effect of microwave-assisted acid extraction on the physicochemical properties and structure of soy hull polysaccharides," *International Journal of Food Science and Techonology,* vol. 57, no. 10, pp. 6744 - 6754, 2022.

[15] J. Zhou, D. Liu, W. Xia, Y. Guo, Y. Luo and J. Xue, "Physicochemical and functional properties of RG-I enriched pectin extracted from thinned-young apples," *International Journal of Biological Macromolecules,* vol. 236, p. 123953, 2023.

[16] E.-H. Cho, H.-T. Jung, B.-H. Lee, H.-S. Kim, J.-K. Rhee and S.-H. Yoo, "Green process development for apple-peel pectin production by organic acid extraction," *Carbohydrte Polymers,* vol. 204, pp. 97 - 103, 2019.

[17] O. Kurita, T. Fujiwara and E. Yamazaki, "Characterization of the pectin extracted from citrus peel in the presence of citric acid," *Carbohydrate Polymers,* vol. 74, no. 3, pp. 725 - 730, 2008.

[18] C. d. i. centre, "National dairy code - part II and III," 2005. [Online]. Available: https://agriculture.canada.ca/en/sector/animal-industry/canadian-dairy-information-centre/acts-regulations-codes-and-standards/national-dairy-code-part-ii-and-iii. [Accessed October 2023].

[19] N. Y. Farkye, "Cheese technology," *International Journal of Dairy Technology,* vol. 57, no. 2 - 3, pp. 91 - 98, 2004.

[20] P. F. Fox, P. L. McSweeney, T. M. Cogan and T. P. Guinee, "Fundamentals of Cheese Science," 2 ed., Springer, 2017.

[21] H. F. Jr., R. Jimenez-Flores, G. Bleck, E. Brown, J. Butler, L. Creamer, C. Hicks, C. Hollar, K. Ng-Kwai-Hang and H. Swaisgood, "Nomenclature of the Proteins of Cows' Milk—Sixth Revision," *Journal of Dairy Science,* vol. 87, no. 6, pp. 1641 - 1674, 2004.

[22] H. F. Jr., E. Malin, E. Brown and P. Q, "Casein micelle structure: What can be learned from milk synthesis and structural biology?," *Current Opinion in Colloid & Interface Science,* vol. 11, no. 2 - 3, pp. 135 - 147, 2006.

[23] D. S. Horne, "Casein Interactions: Casting Light on the Black Boxes, the Structure in Dairy Products," *International Dairy Journal,* vol. 8, no. 3, pp. 171 - 177, 1998.

[24] C. G. D. Kruif and C. Holt, "Casein Micelle Structure, Functions and Interactions," in *Advanced Dairy Chemistry - 1 Proteins*, P. Fox and P. McSweeney, Eds., Boston, Springer, 2003.

[25] P. Walstra, "Casein sub-micelles: do they exist?," *International Dairy Journal,* vol. 9, no. 3 - 6, pp. 189 - 192, 1999.

[26] L. Grossmann and D. J. McClements, "The science of plant-based foods: Approaches to create nutritious and sustainable plant-based cheese analogs," *Trends in Food Science & Technology,* vol. 118, pp. 207 - 229, 2021.

[27] R. Chandan, "CHEESE | Cheese in the Marketplace," in *Encyclopedia of Food Microbiology (Second Edition)*, C. A. Batt and M. L. Tortorello, Eds., Academic Press, 2014, pp. 384 - 394.

[28] M. Shaw, "Cheese substitues: threat or opportunity?," *Journal of the Society of Dairy Technology,* vol. 37, pp. 27 - 31, 1984.

[29] R. Kamath, S. Basak and J. Gokhale, "Recent trends in the development of healthy and functional cheese analogues-a review," *LWT - Food Science and Techonology,* vol. 155, p. 112991, 2022.

[30] C. N. Dharaiya, A. H. Jana and K. D. Aparnathi, "Functionality of Mozzarella cheese analogues prepared using varying protein sources as influenced by refrigerated storage," *Journal of Food Science and Technology,* vol. 56, p. 5243 – 5252, 2019.

[31] H.-P. Bachmann, "Cheese analogues: a review," *International Dairy Journal,* vol. 11, no. 4 - 7, pp. 505 - 515, 2001.

[32] P. Bart, B. Yves, S. J. MG, G. A. P, K. Harm and v. L. L. JC, "Whey protein stimulates postprandial muscle protein accretion more effectively than do casein and casein hydrolysate in older men," *The American Journal of Clinical Nutrition,* vol. 93, no. 5, pp. 997 - 1005, 2011.

[33] B. Sołowiej, P. Glibowski, S. Muszyński, J. Wydrych, A. Gawron and T. Jeliński, "The effect of fat replacement by inulin on the physicochemical properties and microstructure of acid casein processed cheese analogues with added whey protein polymers," *Food Hydrocolloids,* vol. 44, pp. 1 - 11, 2015.

[34] M. Nastaj, K. Terpiłowski and B. G. Sołowiej, "The effect of native and polymerised whey protein isolate addition on surface and microstructural properties of processed cheeses and

their meltability determined by Turbiscan," *International Journal of Food Science and Technology,* vol. 55, no. 5, pp. 2179 - 2187, 2019.

[35] B. Sołowiej, I. W. Cheung and E. C. Li-Chan, "Texture, rheology and meltability of processed cheese analogues prepared using rennet or acid casein with or without added whey proteins," *International Dairy Journal,* vol. 37, no. 2, pp. 87 - 94, 2014.

[36] P. Dhanraj, A. Jana, H. Modha and K. D. Aparnathi, "Influence of using a blend of rennet casein and whey protein concentrate as protein source on the quality of Mozzarella cheese analogue," *Journal of Food Science and Technology,* vol. 54, pp. 822 - 831, 2017.

[37] R. S. Chavan and A. Jana, "Cheese substitutes: An alternative to natural cheese - A review," *International Journal of Food Science, Technology & Nutrition,* vol. 2, no. 2, pp. 25 - 39, 2007.

[38] C. Lobato-Calleros, E. Vernon-Carter, I. Guerrero-Legarreta, J. Soriano-Santos and H. Escalona-Beundia, "Use of fat blends in cheese analogs: Influence on sensory and instrumental textural characteristics," *Journal of Texture Studies,* vol. 28, pp. 619 - 632, 1997.

[39] C. R. Cunha, R. Grimaldi, M. R. Alcântara and W. H. Viotto, "Effect of the type of fat on rheology, functional properties and sensory acceptance of spreadable cheese analogue," *International Journal of Dairy Technology,* vol. 66, no. 1, pp. 54 - 62, 2013.

[40] C. Lobato-Calleros, E. J. Vernon-Carter and Y. Hornelas-Uribe, "Microstructure and texture of cheese analogs containing different types of fat," *Journal of Texture Studies,* vol. 29, no. 5, pp. 569 - 586, 1998.

[41] V. Giha, M. J. Ordoñez and R. A. Villamil, "How does milk fat replacement influence cheese analogue microstructure, rheology, and texture profile?," *Journal of Food Science,* vol. 86, no. 7, pp. 2802 - 2815, 2021.

[42] C. Montesinos-Herrero, D. C. Cottell, E. D. O'Riordan and M. O'Sullivan, "Partial replacement of fat by functional fibre in imitation cheese: Effects on rheology and microstructure," *International Dairy Journal,* vol. 16, no. 8, pp. 910 - 919, 2006.

[43] M. M. Kasprzak, W. Macnaughtan, S. Harding, P. Wilde and B. Wolf, "Stabilisation of oil-in-water emulsions with non-chemical modified gelatinised starch," *Food Hydrocolloids,* vol. 81, pp. 409 - 418, 2018.

[44] N. Noronha, E. Duggan, G. Ziegler, E. O'Riordan and M. O'Sullivan, "Inclusion of starch in imitation cheese: Its influence on water mobility and cheese functionality," *Food Hydrocolloids,* vol. 22, no. 8, pp. 1612 - 1621, 2008.

[45] M. Chen, J. Lu, F. Liu, J. Nsor-Atindana, F. Xu, H. D. Goff, J. Ma and F. Zhong, "Study on the emulsifying stability and interfacial adsorption of pea proteins," *Food Hydrocolloids*, vol. 88, pp. 247 - 255, 2019.

[46] M. P. S. Ben-Harb a, D. Huc-Mathis, G. Moulin, A. Saint-Eve, F. Irlinger, P. Bonnarme, C. Michon and I. Souchon, "The rheological and microstructural properties of pea, milk, mixed pea/milk gels and gelled emulsions designed by thermal, acid, and enzyme treatments," *Food Hydrocolloids*, vol. 77, pp. 75 - 84, 2018.

[47] J. Medic, C. Atkinson and C. R. H. Jr., "Current Knowledge in Soybean Composition," *Journal of the American Oil Chemists' Society*, vol. 91, pp. 363 - 384, 2014.

[48] K.E.Preece, N.Hooshyar and N.J.Zuidamc, "Whole soybean protein extraction processes: A review," *Innovative Food Science & Emerging Technologies*, vol. 43, pp. 163-172, 2017.

[49] K. A. Campbell, C. E. Glatz, L. A. Johnson, S. Jung, J. M. N. d. Moura, V. Kapchie and P. Murphy, "Advances in Aqueous Extraction Processing of Soybeans," *Journal of the American Oil Chemists' Society*, vol. 88, p. 449–465, 2011.

[50] "Chemistry and Nutritional Value of Soybean Components," in *Soybeans*, Springer, 1997.

[51] D. Fukushima, "Recent progress of soybean protein foods: Chemistry, technology, and nutrition," *Food Reviews International*, vol. 7, no. 3, pp. 323 - 351, 1991.

[52] K. Nishinari, Y. Fang, S. Guo and G. Phillips, "Soy proteins: A review on composition, aggregation and emulsification," *Food Hydrocolloids*, vol. 39, pp. 301 - 318, 2014.

[53] P. A. Murphy, "Soybean Proteins," in *Soybeans - Chemistry, Production Processing, and Utilization, Volume 2*, AOCS Press, 2008.

[54] C. Salas, O. J. Rojas, L. A. Lucia, M. A. Hubbe and J. Genzer, "On the Surface Interactions of Proteins with Lignin," *ACS Applies Materials and Interfaces*, vol. 5, no. 1, pp. 199 - 206, 2013.

[55] L. Karr-Lilienthal, C. Kadzere, C. Grieshop and G. F. Jr., "Chemical and nutritional properties of soybean carbohydrates as related to nonruminants: A review," *Livestock Production Science*, vol. 97, no. 1, pp. 1 - 12, 2005.

[56] C. M. Grieshop, C. T. Kadzere, G. M. Clapper, E. A. Flickinger, L. L. Bauer, R. L. Frazier and G. C. Fahey, "Chemical and Nutritional Characteristics of United States Soybeans and Soybean Meals," *Journal of Agricultural and Food Chemistry*, vol. 51, no. 26, p. 7684 – 7691, 2003.

[57] I. Ouhida, J. F. Pérez and J. Gasa, "Soybean (Glycine max) Cell Wall Composition and Availability to Feed Enzymes," *Journal of Agricultural and Food Chemistry,* vol. 50, no. 7, pp. 1933 - 1938, 2002.

[58] A. A. Loman and L.-K. Ju, "Enzyme-based processing of soybean carbohydrate: Recent developments and future prospects," *Enzyme and Microbial Technology,* vol. 106, pp. 35 - 47, 2017.

[59] A. Nakamura, H. Furuta, H. Maeda, T. Takao and Y. Nagamatsu, "Structural Studies by Stepwise Enzymatic Degradation of the Main Backbone of Soybean Soluble Polysaccharides Consisting of Galacturonan and Rhamnogalacturonan," *Bioscience, Biotechnology, and Biochemistry,* vol. 66, no. 6, pp. 1301 - 1313, 2002.

[60] J. A. Gerde and P. J. White, "Lipids," in *Soybeans chemistry, production, processing, and utilization*, AOCS Press, 2008.

[61] S. Giri and S. Mangaraj, "Processing influences on composition and quality attributes of soymilk and its powder," *Food Engineering Reviews,* vol. 4, pp. 149 - 164, 2012.

[62] H. Ang, W. Kwik and C. Theng, "Development of soymilk - A review," *Food Chemistry,* vol. 17, no. 4, pp. 235 - 250, 1985.

[63] I. E. Liener, "Implications of antinutritional components in soybean foods," *Critical Reviews in Food Science and Nutrition,* vol. 34, no. 1, pp. 31 - 67, 1994.

[64] D. J. Schroder and H. Jackson, "Preparation and evaluation of soybean curd with reduced beany flavor," *Journal of Food Science,* vol. 37, no. 3, pp. 450 - 451, 1972.

[65] K. Vishwanathan, V. Singh and R. Subramanian, "Wet grinding characteristics of soybean for soymilk extraction," *Journal of Food Engineering,* vol. 106, no. 1, pp. 28 - 34, 2011.

[66] K.-C. Kwok and K. Niranjan, "Review: Effect of thermal processing on soymilk," *International Journal of Food Science and Technology,* vol. 30, no. 3, pp. 263 - 295, 1995.

[67] D. K. O'Toole, "Characteristics and Use of Okara, the Soybean Residue from Soy Milk Productions A Review," *Journal of agricultural and food chemistry,* vol. 47, no. 2, p. 363–371, 1999.

[68] P. Davy and Q. Vuong, "Soy Milk By-product: Its Composition and Utilisation," *FOOD REVIEWS INTERNATIONAL,* pp. 1-23, 2020.

[69] K. E.Preece, E. Drost, N. Hooshyar, A. Krijgsman, P. W.Cox and N. J.Zuidam, "Confocal imaging to reveal the microstructure of soybean processing materials," *Journal of Food Engineering,* vol. 47, pp. 8 - 13, 2015.

[70] K. Keegstra, "Plant Cell Walls," *Plant Physiology,* vol. 154, no. 2, pp. 483 - 486, 2010.

[71] M. Ochoa-Villarreal, E. Aispuro-Hernández, I. Vargas-Arispuro and M. Á. Martínez-Téllez, "Plant Cell Wall Polymers: Function, Structure and Biological Activity of Their Derivatives," *Polymerization,* 2012.

[72] H. Yoshii, T. Furuta, H. Maeda and H. Mori, "Hydrolysis Kinetics of Okara and Characterization of Its Water-soluble Polysaccharides," *Bioscience, Biotechnology, and Biochemistry,* vol. 60, no. 9, p. 1406–1409, 1996.

[73] F. Lu, Y. Liu and B. Li, "Okara dietary fiber and hypoglycemic effect of okara foods," *Bioactive Carbohydrates and Dietary Fibre,* vol. 2, no. 2, pp. 126-132, 2013.

[74] S. Khare, K. Jha and A. Gandhi, "Citric acid production from Okara (soy-residue) by solid-state fermentation," *Bioresource Technology,* vol. 54, no. 3, pp. 323 - 325, 1995.

[75] L. Zheng, J. M. Regenstein, F. Teng and Y. Li, "Tofu products: A review of their raw materials, processing conditions and packaging," *Comprehensive Reviews in Food Science and Food Safety,* vol. 19, no. 6, pp. 3683-3714, 2020.

[76] Q. Zhang, C. Wang, B. Li, L. Li, D. Lin, H. Chen, Y. Liu, S. Li, W. Qin, J. Liu, W. Liu and W. Yang, "Research progress in tofu processing: From raw materials to processing conditions," *Critical Reviews in Food Science and Nutrition,* vol. 58, no. 9, pp. 1448 - 1467, 2017.

[77] T. Nicolai and C. Chassenieux, "Heat-induced gelation of plant globulins," *Current Opinion in Food Science,* vol. 27, pp. 18 - 22, 2019.

[78] J. Guo, X.-Q. Yang, X.-T. He, N.-N. Wu, J.-M. Wang, W. Gu and Y.-Y. Zhang, "Limited aggregation behavior of β-conglycinin and its terminating effect on glycinin aggregation during heating at pH 7.0," *Journal of Agricultural and Food Chemistry,* vol. 60, no. 14, pp. 3782 - 3791, 2012.

[79] B. German, S. Damodaran and J. E. Kinsella, "Thermal dissociation and association behavior of soy proteins," *Journal of Agricultural and Food Chemistry,* vol. 30, no. 5, pp. 801 - 1004, 1982.

[80] S. Utsumi, S. Damodaran and J. E. Kinsella, "Heat-induced interactions between soybean proteins: preferential association of 11S basic subunits and beta subunits of 7S," *Journal of Agricultural and Food Chemistry,* vol. 32, pp. 1406 - 1412, 1984.

[81] Z.-S. Liu, S. K. Chang, L.-T. Li and E. Tatsumi, "Effect of selective thermal denaturation of soybean proteins on soymilk viscosity and tofu's physical properties," *Food Research International,* vol. 37, no. 8, pp. 815 - 822, 2004.

[82] Q. Zhang, C. Wang, B. Li, L. Li, D. Lin, H. Chen, Y. Liu, S. Li, W. Qin, J. Liu, W. Liu and W. Yang, "Research progress in tofu processing: From raw materials to processing

conditions," *Crtitical Reviews in Food Science and Nitrition,* vol. 58, no. 9, pp. 1448 - 1467, 2017.

[83] K. Kohyama, Y. Sano and E. Doi, "Rheological characteristics and gelation mechanism of tofu (soybean curd)," *Journal of Agricultural and Food Chemistry,* vol. 43, pp. 1808 - 1812, 1995.

[84] X. Yang, Y. Ren, H. Liu, C. Huo and L. Li, "Differences in the physicochemical, digestion and microstructural characteristics of soy protein gel acidified with lactic acid bacteria, glucono-δ-lactone and organic acid," *International Journal of Biological Macromolecules,* vol. 185, pp. 462 - 470, 2021.

[85] F.-J. Kao, N.-W. Su and M.-H. Lee, "Effect of calcium sulfate concentration in soymilk on the microstructure of firm tofu and the protein constitutions in tofu whey," *Journal of Agricultural and Food Chemistry,* vol. 51, no. 21, pp. 6211 - 6216, 2003.

[86] R. Wang, L. Xie and S. Guo, "Effects of small molecular compounds in soymilk on the protein coagulation process: Ca2 + as coagulant," *Food Research International,* vol. 77, pp. 34 - 42, 2015.

[87] J. Li, Y. Cheng, E. Tatsumi, M. Saito and L. Yin, "The use of W/O/W controlled-release coagulants to improve the quality of bittern-solidified tofu," *Food Hydrocolloids,* vol. 35, pp. 627 - 635, 2014.

[88] J. Zhu, H. Deng, A. Yang, Z. Wu, X. Li, P. Tong and H. Chen, "Effect of microbial transglutaminase cross-linking on the quality characteristics and potential allergenicity of tofu," *Food and Function,* vol. 10, pp. 5485 - 5497, 2019.

[89] C.-H. Tang, L. Chen and E. A. Foegeding, "Mechanical and Water-Holding Properties and Microstructures of Soy Protein Isolate Emulsion Gels Induced by CaCl2, Glucono-δ-lactone (GDL), and Transglutaminase: Influence of Thermal Treatments before and/or after Emulsification," *Journal of Agricultural and Food Chemistry,* vol. 59, no. 8, p. 4071 – 4077, 2011.

[90] C.-H. Tang, "Effect of thermal pretreatment of raw soymilk on the gel strength and microstructure of tofu induced by microbial transglutaminase," *LWT - Food Science and Technology,* vol. 40, no. 8, pp. 1403 - 1409, 2007.

[91] W. C. Vong and S.-Q. Liu, "Biovalorisation of okara (soybean residue) for food and nutrition," *Trends in Food Science & Technology,* vol. 52, pp. 139 - 147, 2016.

[92] R. M. Guimarães, T. E. Silva, A. C. Lemes, M. C. F. Boldrin, M. A. P. d. Silva, F. G. Silva and M. B. Egea, "Okara: A soybean by-product as an alternative to enrich vegetable paste," *LWT - Food Science and Technology,* vol. 92, pp. 593 - 599, 2018.

[93] M. J. Kang, I. Y. Bae and H. G. Lee, "Rice noodle enriched with okara: Cooking property, texture, and in vitro starch digestibility," *Food Science,* vol. 22, pp. 178 - 183, 2018.

[94] T. Chang, C. Wang, S. Wang, L. Shi, H. Yang and M. Cui, "Effect of Okara on Textural, Color and Rheological Properties of Pork Meat Gels," *Journal of Food Quality,* vol. 37, no. 5, pp. 339 - 348, 2014.

[95] B. Li, W. Yang, Y. Nie, F. Kang, H. D. Goff and S. W. Cui, "Effect of steam explosion on dietary fiber, polysaccharide, protein and physicochemical properties of okara," *Food Hydrocolloids,* vol. 94, pp. 48 - 56, 2019.

[96] Q. Zhang, S. Zhou, J. Chen, W. Qin, J. Liu, W. Yang and L. Zhang, "Fabrication of whole soybean curd using three soymilk preparation techniques," *LWT - Food Science and Technology,* vol. 104, pp. 91 - 99, 2019.

[97] B. Y. Yoshida and S. H. Prudencio, "Alkaline hydrogen peroxide improves physical, chemical, and techno-functional properties of okara," *Food Chemistry,* vol. 323, p. 126776, 2020.

[98] D. Lin, X. Long, Y. Huang, Y. Yang, Z. Wu, H. Chen, Q. Zhang, D. Wu, W. Qin and Z. Tu, "Effects of microbial fermentation and microwave treatment on the composition, structural characteristics, and functional properties of modified okara dietary fiber," *LWT - Food Science and Technology,* vol. 123, p. 109059, 2020.

[99] N. Zhao, J. Wu, X. Geng, C. Wang, T. Wu, R. Liu, W. Sui and M. Zhang, "Gelation mechanism of high soluble dietary fiber okara-egg tofu induced by combined treatment of steam explosion and enzymatic hydrolysis," *Food Hydrocolloids,* vol. 140, no. 108602, 2023.

[100] R. Ciriminna, F. Meneguzzo, R. Delisi and M. Pagliaro, "Citric acid: emerging applications of key biotechnology industrial product," *Chemsitry Central Journal,* vol. 22, 2017.

[101] R. Salihu, S. I. A. Razak, N. A. Zawawi, M. R. A. Kadir, N. I. Ismail, N. Jusoh, M. R. Mohamad and N. H. M. Nayan, "Citric acid: A green cross-linker of biomaterials for biomedical applications," *European Polymer Journal,* vol. 146, p. 110271, 2021.

[102] W. Zhang, S. Roy, E. Assadpour, X. Cong and S. M. Jafari, "Cross-linked biopolymeric films by citric acid for food packaging and preservation," *Advances in Colloid and Interface Science,* vol. 314, p. 102886, 2023.

[103] Y. Yang and N. Reddy, "Properties and potential medical applications of regenerated casein fibers crosslinked with citric acid," *International Journal of Biological Macromolecules,* vol. 51, no. 1 - 2, pp. 37 - 44, 2012.

[104] H. Xu, L. Shen, L. Xu and Y. Yang, "Low-temperature crosslinking of proteins using non-toxic citric acid in neutral aqueous medium: Mechanism and kinetic study," *Industrial Crops and Products,* vol. 74, pp. 234 - 240, 2015.

[105] F. C. d. Oliveira, J. S. d. R. Coimbra, E. B. d. Oliveira, A. D. G. Zuñiga and E. E. G. Rojas, "Food Protein-polysaccharide Conjugates Obtained via the Maillard Reaction: A Review," *Critical Reviews in Food Science and Nutrition,* vol. 56, no. 7, pp. 1108-1125, 2016.

[106] R. R. Naik, Y. Wang and C. Selomulya, "Improvements of plant protein functionalities by Maillard conjugation and Maillard reaction products," *Critical Reviews in Food Science and Nutrition,* vol. 62, no. 25, pp. 7036 - 7061, 2022.

[107] I. Kutzli, J. Weiss and M. Gibis, "Glycation of Plant Proteins Via Maillard Reaction: Reaction Chemistry, Technofunctional Properties, and Potential Food Application," *Foods,* vol. 10, no. 2, 2021.

[108] X.-Y. Zhuo, J.-R. Qi, S.-W. Yin, X.-Q. Yang, J.-H. Zhu and L.-X. Huang, "Formation of soy protein isolate–dextran conjugates by moderate Maillard reaction in macromolecular crowding conditions," *Journal of the Science of Food and Agriculture,* vol. 93, no. 2, pp. 316 - 323, 2012.

[109] F.-L. Gu, J. M. Kim, S. Abbas, X.-M. Zhang, S.-Q. Xia and Z.-X. Chen, "Structure and antioxidant activity of high molecular weight Maillard reaction products from casein–glucose," *Food Chemistry,* vol. 120, no. 2, pp. 50 - 511, 2010.

[110] C. Ke and L. Li, "Influence mechanism of polysaccharides induced Maillard reaction on plant proteins structure and functional properties: A review," *Carbohydrate Polymers,* vol. 302, p. 120430, 2023.

[111] F. Zha, S. Dong, J. Rao and B. Chen, "The structural modification of pea protein concentrate with gum Arabic by controlled Maillard reaction enhances its functional properties and flavor attributes," *Food Hydrocolloids,* vol. 92, pp. 30 - 40, 2019.

[112] Z.-Z. Xu, G.-Q. Huang, T.-C. Xu, L.-N. Liu and J.-X. Xiao, "Comparative study on the Maillard reaction of chitosan oligosaccharide and glucose with soybean protein isolate," *International Journal of Biological Macromolecules,* vol. 131, pp. 601 - 607, 2019.

[113] Y. Yang, S. W. Cui, J. Gong, Q. Guo, Q. Wang and Y. Hua, "A soy protein-polysaccharides Maillard reaction product enhanced the physical stability of oil-in-water emulsions containing citral," *Food Hydrocolloids,* vol. 48, pp. 155-164, 2015.

[114] C. Zhao, Z. Chu, Y. Mao, Y. Xu, P. Fei, H. Zhang, X. Xu, Y. Wu, M. Zheng and J. Liu, "Structural characteristics and acid-induced emulsion gel properties of heated soy protein isolate–soy oligosaccharide glycation conjugates," *Food Hydrocolloids,* vol. 137, p. 108408, 2023.

[115] L. Wang, M. Wu and H.-M. Liu, "Emulsifying and physicochemical properties of soy hull hemicelluloses-soy protein isolate conjugates," *Carbohydrate Polymers,* vol. 163, pp. 181 - 190, 2017.

[116] S. Tian, J. Chen and D. M. Small, "Enhancement of solubility and emulsifying properties of soy protein isolates by glucose conjugation," *Journal of Food Processing and Preservation,* vol. 35, no. 1, pp. 80 - 95, 2011.

[117] T. J. Ashaolu and G. Zhao, "Fabricating a Pickering Stabilizer from Okara Dietary Fibre Particulates by Conjugating with Soy Protein Isolate via Maillard Reaction," *Foods,* vol. 9, no. 2, 2020.

[118] X. Ma, W. Chen, T. Yan, D. Wang, F. Hou, S. Miao and D. Liu, "Comparison of citrus pectin and apple pectin in conjugation with soy protein isolate (SPI) under controlled dry-heating conditions," *Food Chemistry,* vol. 309, p. 125501, 2020.

[119] Q. Cui, A. Zhang, R. Li, X. Wang, L. Sun and L. Jiang, "Ultrasonic treatment affects emulsifying properties and molecular flexibility of soybean protein isolate-glucose conjugates," *Food Bioscience,* vol. 38, p. 100747, 2020.

[120] R. Li, Q. Cui, G. Wang, J. Liu, S. Chen, X. Wang, X. Wang and L. Jiang, "Relationship between surface functional properties and flexibility of soy protein isolate-glucose conjugates," *Food Hydrocolloids,* vol. 95, pp. 349 - 357, 2019.

[121] X. Ma, F. Hou, H. Zhao, D. Wang, W. Chen, S. Miao and D. Liu, "Conjugation of soy protein isolate (SPI) with pectin by ultrasound treatment," *Food Hydrocolloids,* vol. 108, p. 106056, 2020.

[122] D. Liu, L. Zhang, Y. Wang, Z. Li, Z. Wang and J. Han, "Effect of high hydrostatic pressure on solubility and conformation changes of soybean protein isolate glycated with flaxseed gum," *Food Chemistry,* vol. 333, p. 127530, 2020.

[123] M. J. Spotti, P. A. Loyeau, A. Marangón, H. Noir and C. R. C. Amelia Catalina Rubiolo, "Influence of Maillard reaction extent on acid induced gels of whey proteins and dextrans," *Food Hydrocolloids,* vol. 91, pp. 224 - 231, 2019.

[124] M. J. Spotti, M. J. Martinez, A. M. Pilosof, M. Candioti, A. C. Rubiolo and a. R. Carrara, "Influence of Maillard conjugation on structural characteristics and rheological properties of whey protein/dextran systems," *Food Hydrocolloids,* vol. 39, pp. 223 - 230, 2014.

[125] J. Sy, "Plant-Based Cheese Analogues and Value-Added, High-Fiber Soymilk Gels Containing Okara," 2022.

[126] L. D. Johnson and L. A. Wilson, "Influence of soybean variety and the method of processing in tofu manufacturing: Comparison of methods for measuring soluble solids in soymilk," *Journal of Food Science,* vol. 49, no. 1, pp. 202 - 204, 1984.

[127] M. J. Schaefer and J. Love, "Relationships between Soybean Components and Tofu Texture," *Journal of Food Quality,* vol. 15, no. 1, pp. 53 - 66, 1992.

[128] W. N. Ainis, C. Ersch, C. Farinet, Q. Yang, Z. J.Glover and R. Ipsen, "Rheological and water holding alterations in mixed gels prepared from whey proteins and rapeseed proteins," *Food Hydrocolloids,* vol. 87, pp. 723 - 733, 2019.

[129] L. v. d. Berg, T. v. Vliet, E. v. d. Linden, M. v. Boekel and F. v. d. Velde, "Serum release: The hidden quality in fracturing composites," *Food Hydrocolloids,* vol. 21, no. 3, pp. 420 - 432, 2007.

[130] M. Nicole, Z. Caimeng, H. Joseph, K. Eric and H. Yufei, "Soybean Oil Volume Fraction Effects on the Rheology Characteristics and Gelation Behavior of Glucono-δ-Lactone and Calcium Sulfate-Induced Tofu Gels," *Journal of Texture Studies,* vol. 47, no. 2, pp. 112 - 130, 2016.

[131] J. A. Lucey, "The relationship between rheological parameters and whey separation in milk gels," *Food Hydrocolloids,* vol. 15, no. 4 - 6, pp. 603 - 608, 2001.

[132] N. Murekatete, Y. Hua, M. V. M. Chamba, O. Djakpo and C. Zhang, "Gelation behavior and rheological properties of salt-or acid-induced soy proteins soft tofu-type gels," *Journal of Texture Studies,* vol. 45, no. 1, pp. 62-73, 2014.

[133] X. Wang, K. Luo, S. Liu, M. Zeng, B. Adhikari, Z. He and J. Chen, "Textural and Rheological Properties of Soy Protein Isolate Tofu-Type Emulsion Gels: Influence of Soybean Variety and Coagulant Type," *Food Biophysics,* vol. 13, pp. 324 - 332, 2018.

[134] V. D. Truong and C. R. Daubert, "Comparative tudy of large strain methods for assessing failure characteristics of selected food gels," *Journal of Textile Studies,* vol. 31, no. 3, pp. 335 - 353, 2000.

[135] G. Sala, T. v. Vliet, M. A. C. Stuart, G. A. v. Aken and F. v. d. Velde, "Deformation and fracture of emulsion-filled gels: Effect of oil content and deformation speed," *Food Hydrocolloids,* vol. 23, no. 5, pp. 1381 - 1393, 2009.

[136] T. Funami, "Next target for food hydrocolloid studies: Texture design of foods using hydrocolloid technology," *Food Hydrocolloids,* vol. 25, no. 8, pp. 1904 - 1914, 2011.

[137] J. Guo, Y.-C. Liu, X.-Q. Yang, Y.-C. Jin, S.-J. Yu, J.-M. Wang, J.-J. Hou and S.-W. Yin, "Fabrication of edible gellan gum/soy protein ionic-covalent entanglement gels with

diverse mechanical and oral processing properties," *Food Research International,* vol. 62, pp. 917 - 925, 2014.

[138] C. R. Rekha and G. Vijayalakshmi, "Influence of processing parameters on the quality of soycurd (tofu)," *Journal of Food Science and Technology,* vol. 50, pp. 176 - 180, 2013.

[139] T. Cai and K. Chang, "Dry tofu characteristics affected by soymilk solid content and coagulation time," *Journal of Food Quality,* vol. 20, no. 5, pp. 391 - 402, 1997.

[140] B. Lim, J. DeMan, L. DeMan and R. Buzzell, "Yield and Quality of Tofu as Affected by Soybean and Soymilk Characteristics. Calcium Sulfate Coagulant," *Journal of Food Science,* vol. 55, no. 4, pp. 1088 - 1092, 1990.

[141] Y. Chen, M.-L. Liao and D. E. Dunstan, "The rheology of K+-κ-carrageenan as a weak gel," *Carbohydrate Polymers,* vol. 50, no. 2, pp. 109-116, 2002.

[142] E. Gwartney, D. Larick and E. Foegeding, "Sensory Texture and Mechanical Properties of Stranded and Particulate Whey Protein Emulsion Gels," *Journal of Food Science,* vol. 69, no. 9, pp. S333 -S339, 2004.

[143] A. D. Errington and E. A. Foegeding, "Factors Determining Fracture Stress and Strain of Fine-Stranded Whey Protein Gels," *Journal of Agricultural and Food Chemistry,* vol. 46, pp. 2963 - 2967, 1998.

[144] D. Lin, X. Long, Y. Huang, Y. Yang, Z. Wu, H. Chen, Q. Zhang, D. Wu, W. Qin and Z. Tu, "Effects of microbial fermentation and microwave treatment on the composition, structural characteristics, and functional properties of modified okara dietary fiber," *LWT - Food Science and Technoloy,* vol. 123, 2020.

[145] P. Qu, H. Huang, G. Wu, E. Sun and Z. Chang, "Effects of hydrolysis degree of soy protein isolate on the structure and performance of hydrolyzed soy protein isolate/urea/formaldehyde copolymer resin," *Journal of Applied Polymer Science,* vol. 132, no. 7, 2015.

[146] P. K. Nanda, K. K. Rao, R. K. Kar and P. L. Nayak, "Biodegradable plastics of soy protein isolate modified with thiourea," *Journal of Thermal Analysis and Calorimetry,* vol. 89, pp. 935-940, 2007.

[147] E. E. Santos, R. C. Amaro, C. C. C. Bustamante, M. H. A. Guerra, L. C. Soares and R. E. S. Froes, "Extraction of pectin from agroindustrial residue with an ecofriendly solvent: use of FTIR and chemometrics to differentiate pectins according to degree of methyl esterification," *Food Hydrocolloids,* vol. 107, p. 105921, 2020.

[148] J. M. M. Canaan, G. S. P. Brasil, N. R. d. Barros, C. U. Mussagy, N. B. Guerra and R. D. Herculano, "Soybean processing wastes and their potential in the generation of high value added products," *Food Chemistry,* vol. 373, p. 131476, 2022.

[149] K. NAKASATO, T. ONO, T. ISHIGURO, M. TAKAMATSU, C. TSUKAMOTO and M. MIKAMI, "Rapid Quantitative Analysis of the Major Components in Soymilk Using Fourier-Transform Infrared Spectroscopy (FT-IR)," *Food Science and Technology Reseach,* vol. 10, no. 2, pp. 137 - 142, 2004.

[150] Q. Wang, Y. Xie, Z. Xiong, X. Gu, X. Nie, Y. Lan and B. Chen, "Structural and physical properties of spray-dried fish oil microcapsules via pea protein isolate based emulsification or complex coacervation with sugar beet pectin," *Journal of Food Engineering,* vol. 335, p. 111173, 2022.

[151] P. Jaiswal, S. N. Jha, A. Borah, A. Gautam, M. K. Grewal and G. Jindal, "Detection and quantification of soymilk in cow–buffalo milk using Attenuated Total Reflectance Fourier Transform Infrared spectroscopy (ATR–FTIR)," *Food Chemistry,* vol. 168, pp. 41 - 47, 2015.

[152] Y. Yang, J. G. Steve W. Cui, Q. Guo, Q. Wang and Y. Hua, "A soy protein-polysaccharides Maillard reaction product enhanced the physical stability of oil-in-water emulsions containing citral," *Food Hydrocolloids,* vol. 48, pp. 155 - 164, 2015.

[153] R. Gnanasambandam and A. Proctor, "Determination of pectin degree of esterification by diffuse reflectance Fourier transform infrared spectroscopy," *Food Chemistry,* vol. 68, no. 3, pp. 327 - 332, 2000.

[154] J. Liu, C. Liu, X. Zheng, M. Chen and K. Tang, "Soluble soybean polysaccharide/nano zinc oxide antimicrobial nanocomposite films reinforced with microfibrillated cellulose," *International Journal of Biological Macromolecules,* vol. 159, pp. 793 - 803, 2020.

[155] B. Li, M. Qiao and F. Lu, "Composition, Nutrition, and Utilization of Okara (Soybean Residue)," *Food Reviews International,* vol. 28, no. 3, 2012.

[156] A. NAKAMURA, H. FURUTA, H. MAEDA, Y. NAGAMATSU and A. YOSHIMOTO, "Analysis of Structural Components and Molecular Construction of Soybean Soluble Polysaccharides by Stepwise Enzymatic Degradation," *Bioscience, Biotechnology, and Biochemistry,* vol. 65, no. 10, 2001.

[157] I. Mateos-Aparicio, C. Mateos-Peinado and P. R. A. Jiménez-Escrig, "Multifunctional antioxidant activity of polysaccharide fractions from the soybean byproduct okara," *Carbohydrate Polymers,* vol. 82, no. 2, pp. 245 - 250, 2010.

[158] Z. V. Bobyleva, O. A. Drozhzhin, A. M. Alekseeva, K. A. Dosaev, G. S. Peters, G. P. Lakienko, T. I. Perfilyeva, N. A. Sobolev, K. I. Maslakov, S. V. Savilov, A. M. Abakumov

and E. V. Antipov, "Caramelization as a Key Stage for the Preparation of Monolithic Hard Carbon with Advanced Performance in Sodium-Ion Batteries," *Applied Energy Materials,* vol. 6, no. 1, pp. 181 - 190, 2023.

[159] M. Marić, A. N. Grassino, Z. Zhu, F. J. Barba, M. Brnčić and S. R. Brnčić, "An overview of the traditional and innovative approaches for pectin extraction from plant food wastes and by-products: Ultrasound-, microwaves-, and enzyme-assisted extraction," *Trends in Food Science & Technology,* vol. 76, pp. 28 - 37, 2018.

[160] P. H. F. Pereira, T. Í. S. Oliveira, M. F. Rosa, F. L. Cavalcante, G. K. Moates, N. Wellner, K. W. Waldron and H. M. Azeredo, "Pectin extraction from pomegranate peels with citric acid," *International Journal of Biological Macromolecules,* vol. 88, pp. 373 - 379, 2016.

[161] J.-S. Yang, T.-H. Mu and M.-M. Ma, "Extraction, structure, and emulsifying properties of pectin from potato pulp," *Food Chemistry,* vol. 244, pp. 197 - 205, 2018.

[162] X. Liu, C. M. Renard, S. Bureau and C. L. Bourvellec, "Revisiting the contribution of ATR-FTIR spectroscopy to characterize plant cell wall polysaccharides," *Carbohydrate Polymers,* vol. 262, p. 117935, 2021.

[163] W. Chen, X. Ma, W. Wang, R. Lv, M. Guo, T. Ding, X. Ye, S. Miao and D. Liu, "Preparation of modified whey protein isolate with gum acacia by ultrasound maillard reaction," *Food Hydrocolloids,* vol. 95, pp. 298 - 307, 2019.

[164]]. Naresh Kumar, M. Raghavendra, J. Tokas and H. R. Singal, "Chapter 10 - Flavor Addition in Dairy Products: Health Benefits and Risks," in *Nutrients in Dairy and their Implications on Health and Disease,* Academic Press, 2017, pp. 123 - 135.

[165] W. Wen-qiong, B. Yi-hong and C. Ying, "Characteristics and antioxidant activity of water-soluble Maillard reaction products from interactions in a whey protein isolate and sugars system," *Food Chemistry,* vol. 139, no. 1 - 4, pp. 355 - 361, 2013.

[166] F. Yan, X. Yu and Y. Jing, "Optimized preparation, characterization, and antioxidant activity of chitooligosaccharide–glycine Maillard reaction products," *Journal of Food Science and Technology,* vol. 55, pp. 712 - 720, 2018.

[167] M.C.Gómez-Guillén, A.J.Borderías and P.Montero, "Chemical Interactions of Nonmuscle Proteins in the Network of Sardine (Sardina pilchardus) Muscle Gels," *LWT - Food Science and Technology,* vol. 30, no. 6, pp. 6602-608, 1997.

[168] Bio-rad, "Bio-rad Protein assay - Manual".

[169] H. Zhao, J. Chen, Y. Hemar and B. Cui, "Improvement of the rheological and textural properties of calcium sulfate-induced soy protein isolate gels by the incorporation of different polysaccharides," *Food Chemistry,* vol. 310, 2020.

[170] S. J.Compton and C. G.Jones, "Mechanism of dye response and interference in the Bradford protein assay," *Analytical Biochemistry,* vol. 151, no. 2, pp. 369-374, 1985.

[171] C. H.J., T. H.B. and S. A.G., "A Spectral Study of the Charge Forms of Coomassie Blue G," *Analytical Biochemistry,* vol. 209, no. 2, pp. 258-266, 1993.

[172] B. J. Olson and J. Markwell, "Assays for Determination of Protein Concentration," *Current Protocols in Pharmacology,* 2007.

[173] N. J. Kruger, "The Bradford Method For Protein Quantitation," in *The Protein Protocols Handbook*, 2002, pp. 17-24.

[174] M. M.Bradford, "A rapid and sensitive method for the quantitation of microgram quantities of protein utilizing the principle of protein-dye binding," *Analytical Biochemistry,* vol. 72, no. 1-2, pp. 248-254, 1976.

[175] S. M. Gotham, P. J. Fryer and W. R. Paterson, "The Measurement of Insoluble Proteins Using a Modified Bradford Assay," *Analytical Biochemistry,* vol. 173, no. 2, pp. 353-358, 1988.

[176] C. M.Stoscheck, "Increased Uniformity in the Response of the Coomassie Blue G Protein Assay to Different Proteins," *Analytical Biochemistry ,* vol. 184, no. 1, pp. 111-116, 1990.

[177] D. Nilufer, D. Boyacioglu and Y. Vodovotz, "Functionality of Soymilk Powder and Its Components in Fresh Soy Bread," *Journal of Food Science,* vol. 73, no. 4, pp. C275-C281, 2008.

[178] C. Wu, D. J. McClements, M. He, L. Zheng, T. Tian, F. Teng and Y. Li, "Preparation and characterization of okara nanocellulose fabricated using sonication or high-pressure homogenization treatments," *Carbohydrate Polymers,* vol. 255, p. 117364, 2021.

[179] Y. Xu, Y. Han, M. Chen, J. Li, J. Li, J. Luo and Q. Gao, "A soy protein-based film by mixed covalent cross-linking and flexibilizing networks," *Industrial Crops and Products,* vol. 183, p. 114952, 2022.

[180] Y. Zhang, M. Zhang, M. Chen, J. Luo, X. Li, Q. Gao and J. Li, "Preparation and characterization of a soy protein-based high-performance adhesive with a hyperbranched cross-linked structure," *Chemical Engineering Journal,* vol. 354, pp. 1032 - 1041, 2018.

[181] J. Liu, Z. Ma, Y. Liu, X. Zheng, Y. Pei and K. Tang, "Soluble soybean polysaccharide films containing in-situ generated silver nanoparticles for antibacterial food packaging applications," *Food Packaging and Shelf Life,* vol. 31, p. 100800, 2022.

[182] P. Camiscia, E. D. Giordano, M. E. Brassesco, P. Fuciños, L. Pastrana, M. C. b, G. A. Picó and N. W. Valetti, "Comparison of soybean hull pre-treatments to obtain cellulose and

chemical derivatives: Physical chemistry characterization," *Carbohydrate Polymers,* vol. 198, pp. 601 - 610, 2018.

[183] L. Zhang, X. Wang, Y. Hu, O. A. Fakayode, H. Ma, C. Zhou, Z. Hu, A. Xia and Q. Li, "Dual-frequency multi-angle ultrasonic processing technology and its real-time monitoring on physicochemical properties of raw soymilk and soybean protein," *Ultrasonics Sonochemistry,* vol. 80, p. 105803, 2021.

[184] J.-S. Lin, K. T. Chuang, M.-S. Huang and K.-M. Wei, "Emission of ethylene oxide during frying of foods in soybean oil," *Food and Chemical Toxicology,* vol. 45, no. 4, pp. 568 - 574, 2007.

[185] X. Huang, J.-P. Cao, X.-Y. Zhao, J.-X. Wang, X. Fan, Y.-P. Zhao and X.-Y. Wei, "Pyrolysis kinetics of soybean straw using thermogravimetric analysis," *Fuel,* vol. 169, pp. 93 - 98, 2016.

[186] O. P. Bamboriya, A. K. Varma, R. Shankar, V. Aniya, P. Mondal and L. S. Thakur, "Thermal analysis and determination of kinetics and thermodynamics for pyrolysis of soybean de-oiled cake using thermogravimetric analysis," *Journal of Thermal Analysis and Calorimetry,* vol. 147, p. 14381–14392, 2022.

[187] M. M. Barbooti and D. A. Al-Sammerrai, "Thermal decomposition of citric acid," *Thermochimica Acta,* vol. 98, pp. 119 - 126, 1986.

[188] M.-A. Berube, D. Schorr, R. J. Ball, V. Landry and P. Blanchet, "Determination of In Situ Esterification Parameters of Citric Acid-Glycerol Based Polymers for Wood Impregnation," *Journal of Polymers and the Environment,* vol. 26, p. 970 – 979, 2018.

[189] B.-S. Chiou, H. Jafri, T. Cao, G. H. Robertson, K. S. Gregorski, S. H. Imam, G. M. Glenn and W. J. Orts, "Modification of wheat gluten with citric acid to produce superabsorbent materials," *Journal of Applied Polymer Science,* vol. 129, no. 6, pp. 3192 - 3197, 2013.

[190] S. Spinella, A. Maiorana, Q. Qian, N. J. Dawson, V. Hepworth, S. A. McCallum, M. Ganesh, K. D. Singer and R. A. Gross, "Concurrent Cellulose Hydrolysis and Esterification to Prepare a Surface-Modified Cellulose Nanocrystal Decorated with Carboxylic Acid Moieties," *ACS Sustainable Chemistry and Engineering,* vol. 4, no. 3, p. 1538 – 1550, 2016.

[191] V. S. Ghorpade, A. V. Yadav, R. J. Dias, K. K. Mali, S. S. Pargaonkar, P. V. Shinde and N. S. Dhane, "Citric acid crosslinked carboxymethylcellulose-poly(ethylene glycol) hydrogel films for delivery of poorly soluble drugs," *International Journal of Biological Macromolecules,* vol. 118, pp. 783 - 791, 2018.

[192] X. Fan, H. Chang, Y. Lin, X. Zhao, A. Zhang, S. Lia and Z. Fenga, "Effects of ultrasound-assisted enzyme hydrolysis on the microstructure and physicochemical properties of okara fibers," *Ultrasonics - Sonochemistry,* vol. 69, p. 105247, 2020.

[193] M. A. Coimbra, A. Barros, M. Barros, D. N. Rutledge and I. Delgadillo, "Multivariate analysis of uronic acid and neutral sugars in whole pectic samples by FT-IR spectroscopy," *Carbohydrate Polymers,* vol. 37, no. 3, pp. 241 - 248, 1998.

[194] S. Liew, N. Chin, Y. Yusof and K. Sowndhararajan, "Comparison of Acidic and Enzymatic Pectin Extraction from Passion Fruit Peels and Its Gel Properties," *Journal of Food Process Engineering,* vol. 39, no. 5, pp. 501 - 5011, 2016.

[195] J. Li, H. Cui, X. Xu, J. Li, M. Lu, X. Guan, D. Zhu and H. Liu, "Emulsifying properties of different soy hull pectin polysaccharides and application in mayonnaise," *Food Science and Biotechnology,* vol. 31, pp. 699 - 710, 2022.

[196] C. Wu, F. Teng, D. J. McClements, S. Zhang, Y. Li and Z. Wang, "Effect of cavitation jet processing on the physicochemical properties and structural characteristics of okara dietary fiber," *Food Research International,* vol. 134, 2020.

[197] N. Diftis and V. Kiosseoglou, "Competitive adsorption between a dry-heated soy protein–dextran mixture and surface-active materials in oil-in-water emulsions," *Food Hydrocolloids,* vol. 18, no. 4, pp. 639 - 646, 2004.

[198] S. Sasmal and K. Mohanty, "Pretreatment of Lignocellulosic Biomass Toward Biofuel Production," in *Biorefining of Biomass to Biofuels. Biofuel and Biorefinery Technologies*, Springer, 2018, p. 203 – 221.

[199] P. Singh, P. Baisthakurb and O. S.Yemul, "Synthesis,characterization and application of crosslinked alginate as green packaging material," *Heliyon,* vol. 6, no. 1, 2020.

[200] M. N. Lund and O. C. A. Ray, "Control of Maillard Reactions in Foods: Strategies and Chemical Mechanisms," *Journal of Agricultural and Food Chemistry,* vol. 65, no. 23, p. 4537 – 4552, 2017.

[201] X. Peng, C. Ren and S. Guo, "Particle formation and gelation of soymilk: Effect of heat," *Trends in Food Science & Technology,* vol. 54, pp. 138-147, 2016.

[202] E. A. Foegeding, E. L. Bowland and C. C. Hardin, "Factors that determine the fracture properties and microstructure of globular protein gels," *Food Hydrocolloids,* vol. 9, no. 4, pp. 237 - 249, 1995.

[203] E. Doi, "Gels and gelling of globular proteins," *Trends in Food Science & Technology,* vol. 4, no. 1, pp. 1 - 5, 1993.

[204] N. Chen, M. Zhao, F. Niepceron, T. Nicolai and C. Chassenieux, "The effect of the pH on thermal aggregation and gelation of soy proteins," *Food Hydrocolloids,* vol. 66, pp. 27 - 36, 2017.

[205] T. Li, X. Rui, W. Li, X. Chen, M. Jiang and M. Dong, "Water distribution in tofu and application of T2 relaxation measurements in determination of tofu's water holding capacity," *Journal of Agricultural and Food Chemistry,* vol. 62, pp. 8594 - 8691, 2014.

[206] Y.-R. Shen and M.-I. Kuo, "Effects of differnt carrageenan types on the rheological and water-holding properties of tofu," *LWT - Food Science and Technology,* vol. 78, pp. 122 - 128, 2017.

[207] N. Sun and W. M. Breene, "Calcium Sulfate Concentration Influence on Yield and Quality of Tofu From Five Soybean Varieties," *Journal of Food Science,* vol. 56, no. 6, pp. 1604 - 1607, 1991.

[208] C.-Y. Lee and M.-I. Kuo, "Effect of γ-polyglutamate on the rheological properties and microstructure of tofu," *Food Hydrocolloids,* vol. 25, no. 5, pp. 1034 - 1040, 2011.

[209] A. H. Clark and S. B. Ross-Murphy, "Structural and mechanical properties of biopolymer gels," *Biopolymers,* pp. 57 - 192, 1987.

[210] W. Xia, L. Zhu, R. J. Delahaije, Z. Cheng, X. Zhou and L. M. Sagis, "Acid-induced gels from soy and whey protein thermally-induced mixed aggregates: Rheology and microstructure," *Food Hydrocolloids,* vol. 125, p. 107376, 2022.

[211] G. Dimitreli and A. S. Thomareis, "Instrumental Textural and Viscoelastic Properties of Processed Cheese as Affected by Emulsifying Salts and in Relation to its Apparent Viscosity," *International Journal of Food Properties,* vol. 12, no. 1, pp. 261 - 275, 2009.

[212] G. Dimitreli and A. S. Thomareis, "Effect of chemical composition on the linear viscoelastic properties of spreadable-type processed cheese," *Journal of Food Engineering,* vol. 84, no. 3, pp. 368 - 374, 2008.

[213] S. K. Giri, M. K. Tripathi and N. Kotwaliwale, "Effect of composition and storage time on some physico-chemical and rheological properties of probiotic soy-cheese spread," *Journal of Food Science Technology,* vol. 55, no. 5, p. 1667–1674, 2018.

[214] S. Mohanty, S. K. Verma and S. K. Nayak, "Dynamic mechanical and thermal properties of MAPE treated jute/HDPE composites," *Composites Science and Technology,* vol. 66, no. 3 - 4, pp. 538 - 547, 2006.

[215] A. O. Ogah, J. N. Afiukwa and A. A. Nduji, "Characterization and Comparison of Rheological Properties of Agro Fiber Filled High-Density Polyethylene Bio-Composites," *Open Journal of Polymer Chemistry,* vol. 4, no. 1, pp. 12 - 19, 2014.

[216] M. Dille, K. Draget and M. Hattrem, "The effect of filler particles on the texture of food gels," in *Modifying Food Texture,* Woodhead Publishing, 2015, pp. 183 - 200.

[217] M. Johansson, D. Johansson, A. Ström, J. Rydén, K. Nilsson, J. Karlsson, R. Moriana and M. Langton, "Effect of starch and fibre on faba bean protein gel characteristics," *Food Hydrocolloids,* vol. 131, p. 107741, 2022.

[218] O. Abdelhedi, I. Jemil, R. Nasri, L. Mora, M. Jridi, A. Mbarek, F. Toldrá, M.-A. Ayedi and M. Nasri, "Molecular forces study and microstructure and gelling properties of smooth hound protein gels prepared by heat-induced gelation process: Effect of pH variation on textural and functional properties," *Process Biochemistry,* vol. 51, no. 10, pp. 1511 - 1520, 2016.

[219] K.-Q. Wang, S.-Z. Luo, X.-Y. Zhong, J. Cai, S.-T. Jiang and Z. Zheng, "Changes in chemical interactions and protein conformation during heat-induced wheat gluten gel formation," *Food Chemistry,* vol. 214, pp. 393 - 399, 2017.

[220] Y. Lv, J. Wang, L. Xu, T. Tang, Y. Su, L. Gu, C. Chang, M. Zhang, Y. Yang and J. Li, "Gel properties of okara dietary fiber-fortified soy protein isolate gel with/without NaCl," *Journal of the Science of Food and Agriculture,* vol. 103, no. 1, pp. 411 - 419, 2023.

[221] Y. Lv, T. Tang, L. Xu, J. Wang, Y. Su, J. Li, L. Gu, M. Zhang, Y. Yang and C. Chang, "Influence of soybean dietary fiber with varying particle sizes and transglutaminase on soy protein isolate gel," *Food Research International,* vol. 161, p. 111876, 2022.

[222] J. Umeda and K. Kondoh, "High-purification of amorphous silica originated from rice husks by combination of polysaccharide hydrolysis and metallic impurities removal," *Industrial Crops and Products,* vol. 32, no. 3, pp. 539 - 544, 2010.

[223] C. S. V. Ramirez, F. Temelli and M. D. Saldaña, "Production of pea hull soluble fiber-derived oligosaccharides using subcritical water with carboxylic acids," *The Journal of Supercritical Fluids,* vol. 178, p. 105349, 2021.

[224] S. MahfuzulIslam, A. A.Loman and Lu-KwangJu, "High monomeric sugar yields from enzymatic hydrolysis of soybean meal and effects of mild heat pretreatments with chelators," *Bioresource Technology,* vol. 256, pp. 438-445, 2018.

[225] P. Amnuaycheewa, R. Hengaroonprasan, K. Rattanaporn, S. Kirdponpattara, K. Cheenkachorn and M. Sriariyanun, "Enhancing enzymatic hydrolysis and biogas production from rice straw by pretreatment with organic acids".

[226] B. Coulter, "SW 41 Ti Rotor - Manual," 2002.

[227] User Guide - Optima XPN Series, Beckman Coulter, 2021.

[228] L. Sun, W. Chen, Y. Liu, J. Li and H. Yu, "Soy protein isolate/cellulose nanofiber complex gels as fat substitutes: rheological and textural properties and extent of cream imitation," *Cellulose,* vol. 22, pp. 2618 - 2627, 2015.

[229] M. Tunick, "Rheology of Dairy Foods that Gel, Stretch, and Fracture," *Journal of Dairy Science*, vol. 83, no. 8, pp. 1892 - 1898, 2000.

Appendices

Appendix A: Standardization of Soymilk Okara Gels Preparation

Appendix A.1: Standardization of Soymilk Preparation and Measurement of Its Solid Content

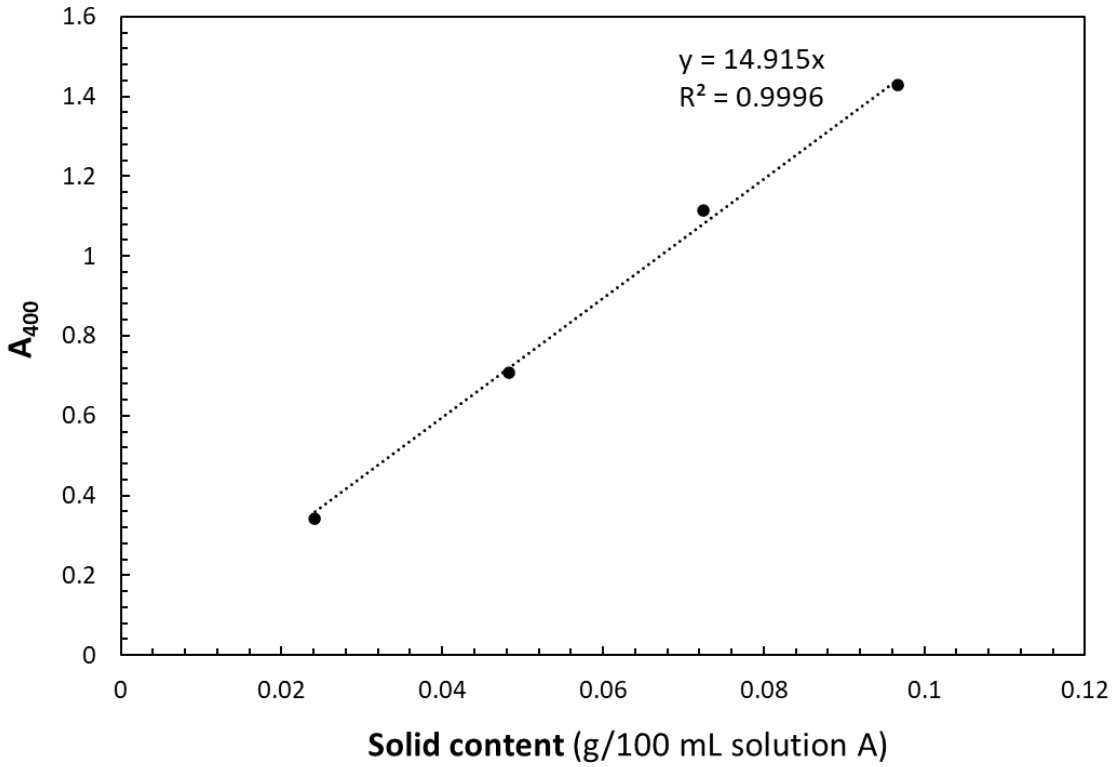


Figure S. 1: Standard curve of solid content in soymilk (g/100 mL solution A), measured at the wavelength of 400 nm.

Appendix A.2: Effect of States of Citric Acid in Okara Modification on the Structural and Textural Characteristics of Soymilk Okara Gels

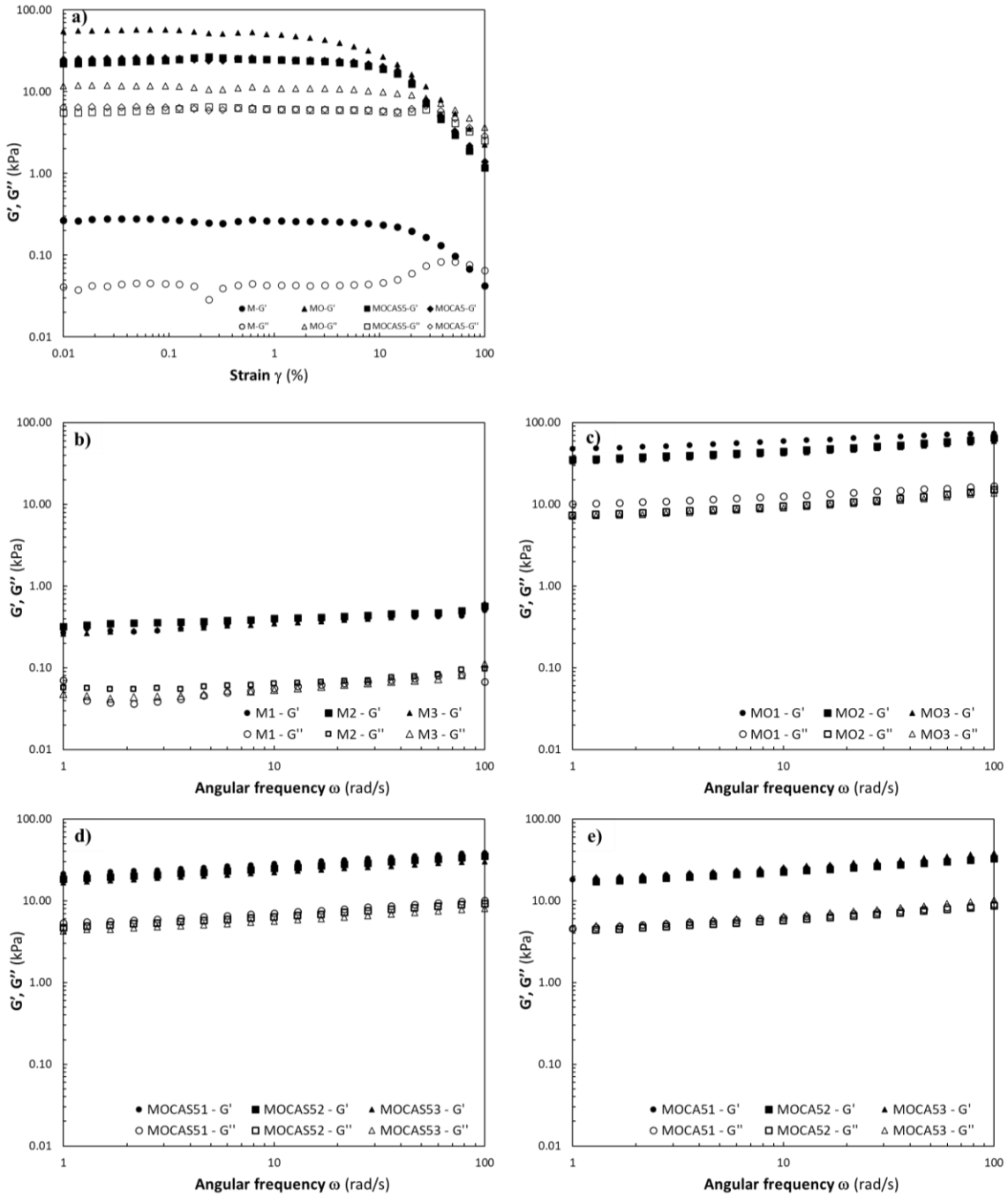


Figure S. 2: a) Curves of storage modulus (G') and loss modulus (G'') over strain (γ) of different type of soymilk okara gels. Curves of G' and G'' over angular frequency (ω) of b) M, c) MO, d) MOCAS5, e) MOCA5.

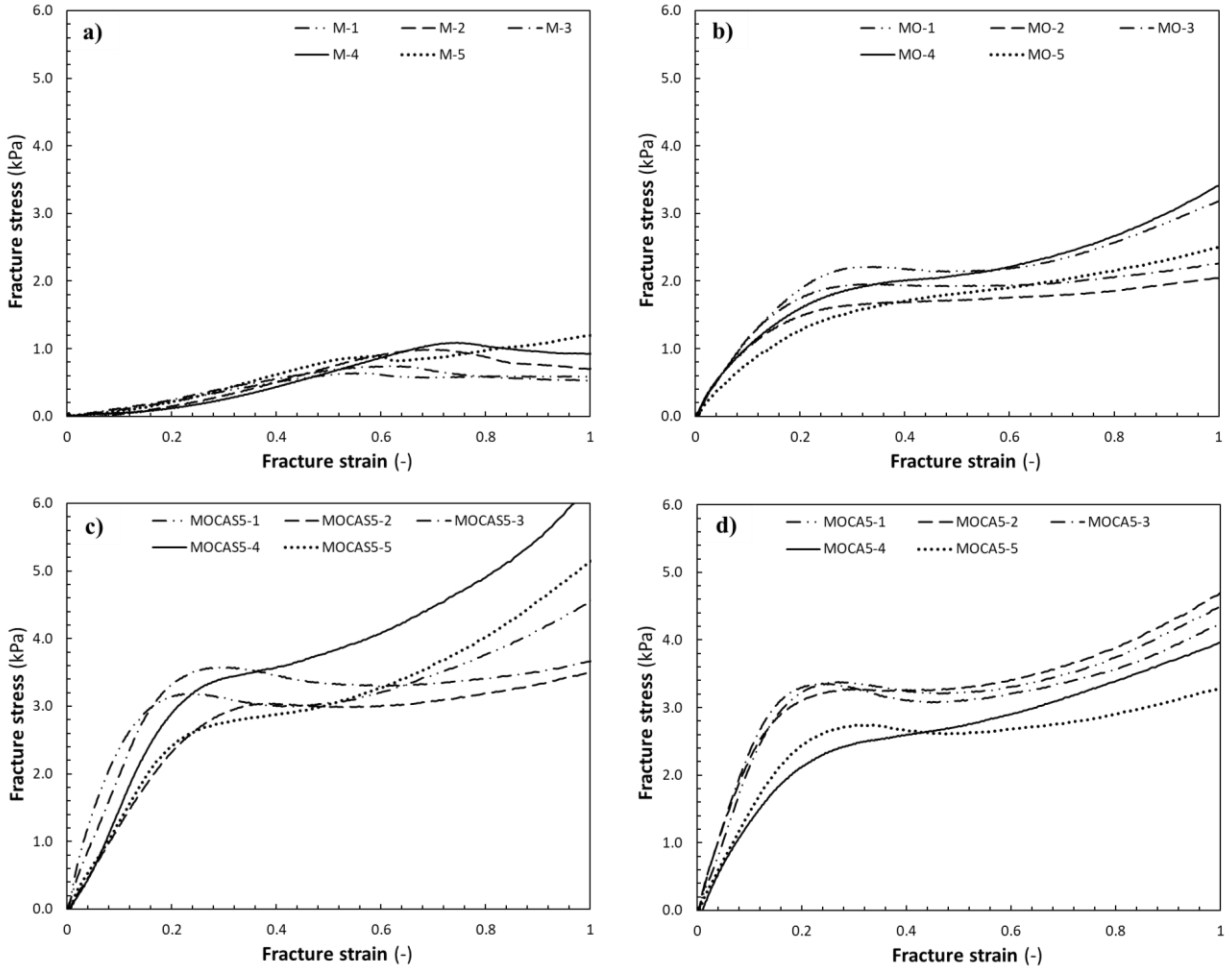


Figure S. 3*:* Fracture stress – fracture stain curves of different type of soymilk okara gels: a) M, b) MO, c) MOCAS5, d) MOCA5).

Appendix B: Methodology of Sample Preparation for Texture Characterization and Protein – Protein Interactions Characterization of Soymilk Okara Gels

Appendix B.1: Effect of Sample Preparation on the Reproducibility of Rheological Properties

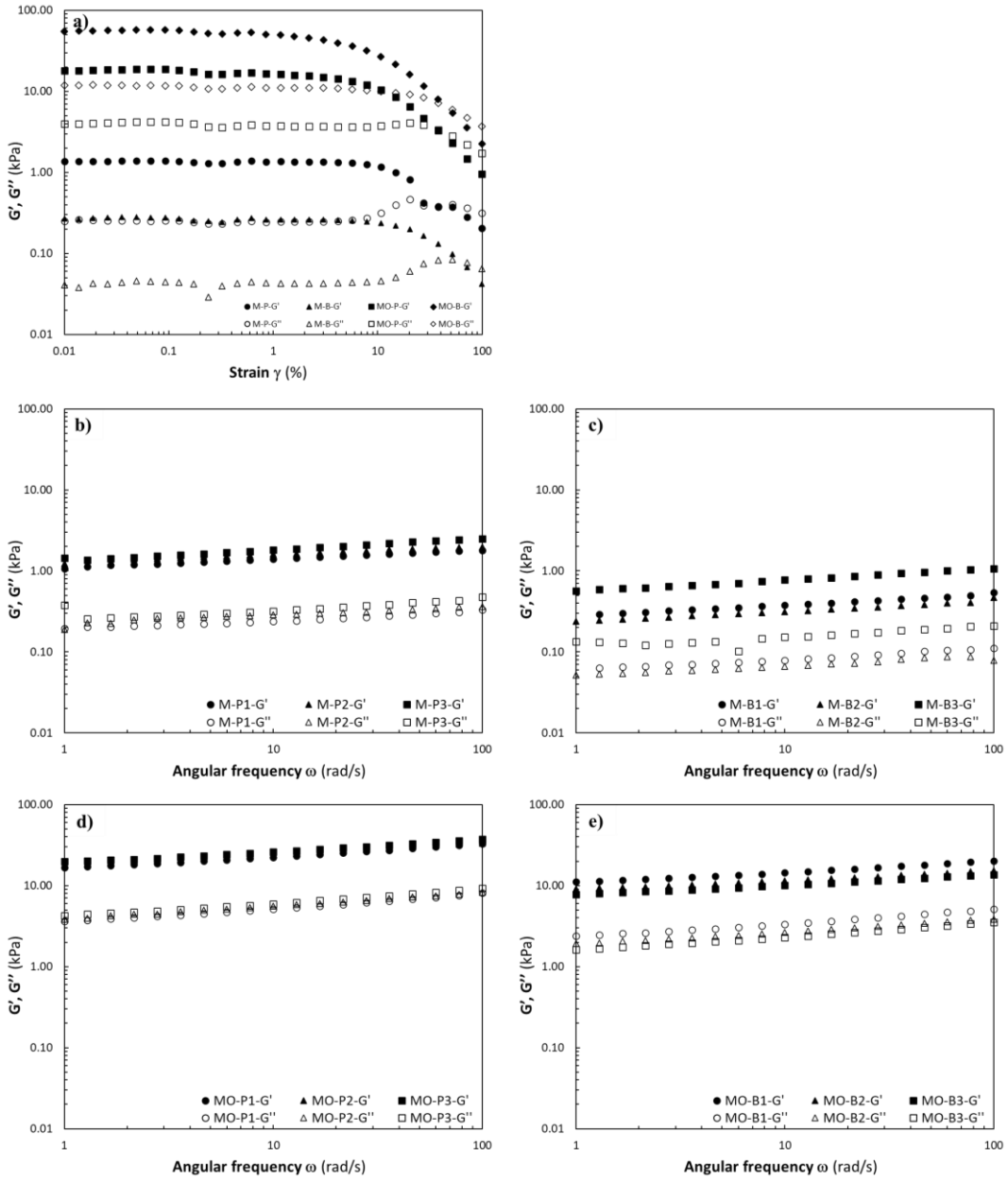


Figure S. 4: a) Curves of storage modulus (G') and loss modulus (G'') over strain (γ) of M and MO prepared in beakers (B) and petri dish (P). Curves of G' and G'' over angular frequency (ω) of b) M – P, c) M – B, d) MO – P, e) MO – B.

Appendix B.2: Effect of Sample Preparation on the Reproducibility of Mechanical Properties

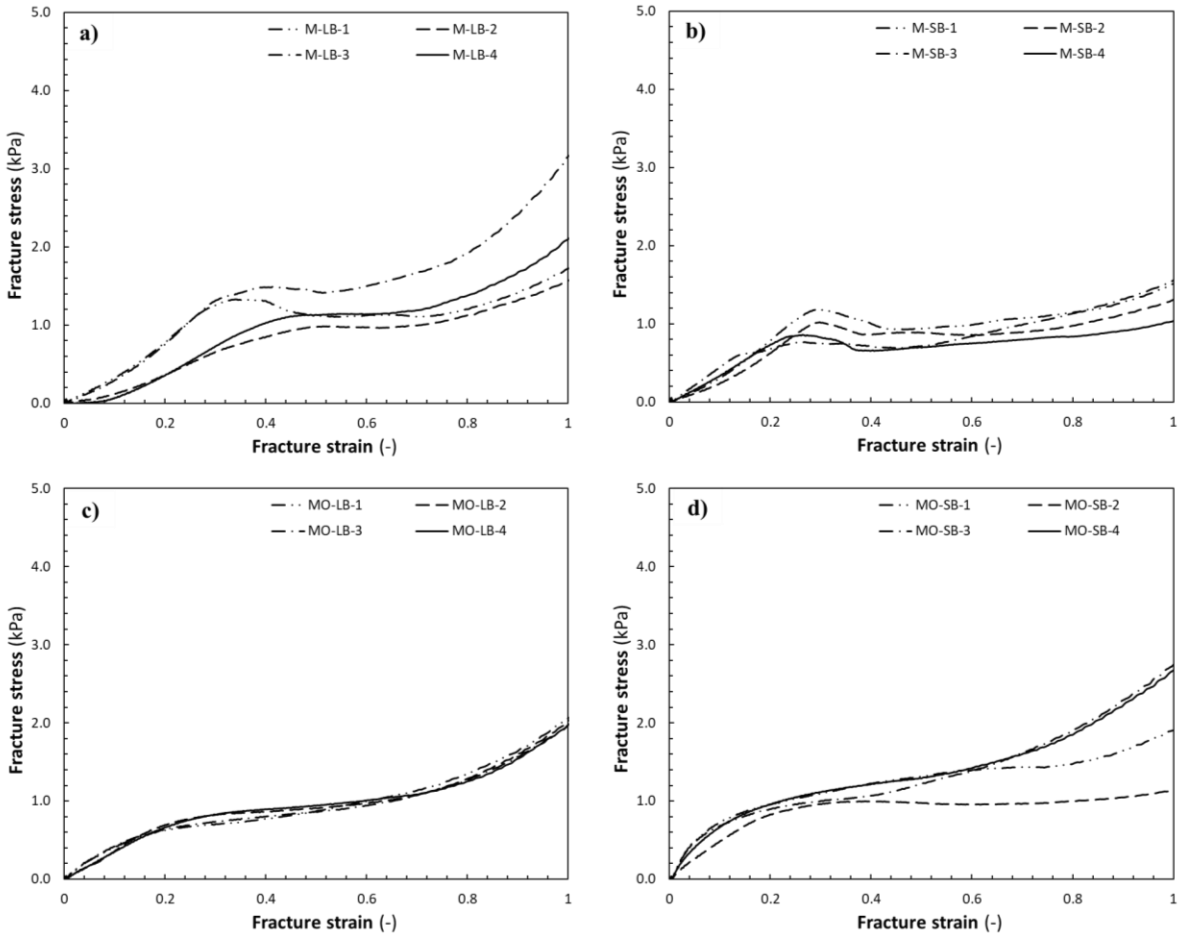


Figure S. 5: Fracture stress – fracture stain curves of soymilk gel (M) prepared in a) 250-mL beaker (LB), b) 100-mL beaker (SB); soymilk unmodified okara gel (MO) prepared in c) 250-mL beaker (LB), d) 100-mL beaker (SB).

Appendix B.3: Methodology of Protein – Protein Interactions Characterization of Soymilk Okara Gels

The conversion of rotor speed from g-force

The conversion of rotor speed from g-force was performed using **Equation S. 1**, where RPM and RCF represents for relative centrifugal field (x g) and rotor speed (rpm), respectively. The radius of rotor is denoted as r (mm) with the value of 110 mm for the swing bucket rotor (SW 41 Ti, Beckman Coulter) [226, 227].

$$RPM = \sqrt{\frac{RCF \times 10^6}{1.12 \times r}} \qquad \textbf{Equation S. 1}$$

Formulation of BSA standard solutions in 0.05M phosphate buffer pH 7.0, in soaking solution SD at different concentrations in range of 0.05 – 0.50 μg/μL

Table S. 1: BSA standard solutions in 0.05M phosphate buffer pH 7.0 at different concentrations in range of 0.05 – 0.50 μg/μL.

BSA standard concentrations (μg/μL)	**BSA stock solution 1.51 mg/mL** (μL)	**0.05M phosphate buffer pH 7.0** (μL)
0.0 (Blank)	0	1000
0.0755	50	950
0.1510	100	900
0.2265	150	850

0.3020	200	800
0.3375	250	750
0.4530	300	700

Table S. 2: BSA standard solutions in soaking solution SD at different concentrations in range of 0.05 – 0.50 mg/mL.

BSA standard concentrations (μg/μL)	**BSA stock solution 1.51 mg/mL** (μL)	**Soaking solution SD** (μL)	**0.05 M phosphate buffer pH 7.0** (μL)
0.0 (Blank)	0	100	900
0.0755	50	100	850
0.1510	100	100	800
0.2265	150	100	750
0.3020	200	100	700
0.3375	250	100	650
0.4530	300	100	600

Calculations for the approximate soluble protein content in the mixture of 0.6 g of soymilk gel and 10 mL

Assuming 100% dissolution of the gel, the maximum soluble protein content in the mixture of 0.6 g of soymilk gel in 10 mL of soaking solution should be around 5.28 mg/mL. Solution requires a 10-fold dilution with 0.05 M phosphate buffer (pH 7.0) to reach the protein concentration of 0.528 mg/mL and fit within the linear range of the Bradford assay.

Table S. 3: Calculations of protein concentration in different types of soy samples.

Calculations	Protein concentration
Dry whole soybean (SB):	
13 g protein / 35 g dry BS [a]	≈ 37 % (in dry weight basis)
Overnight hydrated soybean:	
After overnight hydration, 100 g dry SB produces approximately 227 g hydrated SB (i.e., 100 g dry SB absorbs 127 g water) [b]	
Soybean slurry made from dry SB : DI water with ratio of 3:8 (w:v): $\frac{W_{dry\,SB} \times \%protein_{dry\,SB}}{W_{dry\,SB} + W_{water} + W_{water\,absorbed\,during\,hydration}} \times 100$ $= \frac{3 \times 0.37}{3 + 8 + \frac{3 \times 127}{100}} \times 100$	≈ 7.5 g protein / 100 g soybean slurry [c]

Soymilk gel made from dry okara and soymilk [d, e]:

$$\frac{\%protein_{SB\ slurry} \times 100}{W_{dried\ okara} + W_{soymilk}} \times 100 = \frac{7.5}{4 + 81.7} \times 100$$

≈ 8.8 g protein / 100 g soymilk gel

Solution containing 0.6 g soy gel and 10 mL soaking solution:

$$= \frac{0.6 \times 8.8}{100} \times 1000$$

≈ 52.8 mg protein / 10 mL solution

≈ 5.28 mg protein / mL solution

[a] Nutrition values printed on soybean package (Nupak, lot 20181D)

[b] Based on experimental data

[c] 100 g soybean slurry contains 18.3 g wet okara and 81.7 g of soymilk, based on experimental data

[d] Soymilk gel is made from dry okara and soymilk, with the ratio of 0.22 (wet okara : soymilk, w:w).

[e] After the drying at 60 °C, in 20 – 24 h, a mass of 2.2 g dried okara is collected from 10 g of wet okara (i.e., 4.0 g dry okara is collected from 18.3 g wet okara), based on experimental data.

Appendix C: Unveiling the Effects of Citric Acid on Textural Profiles and Chemical Interactions in Soymilk Okara Gels

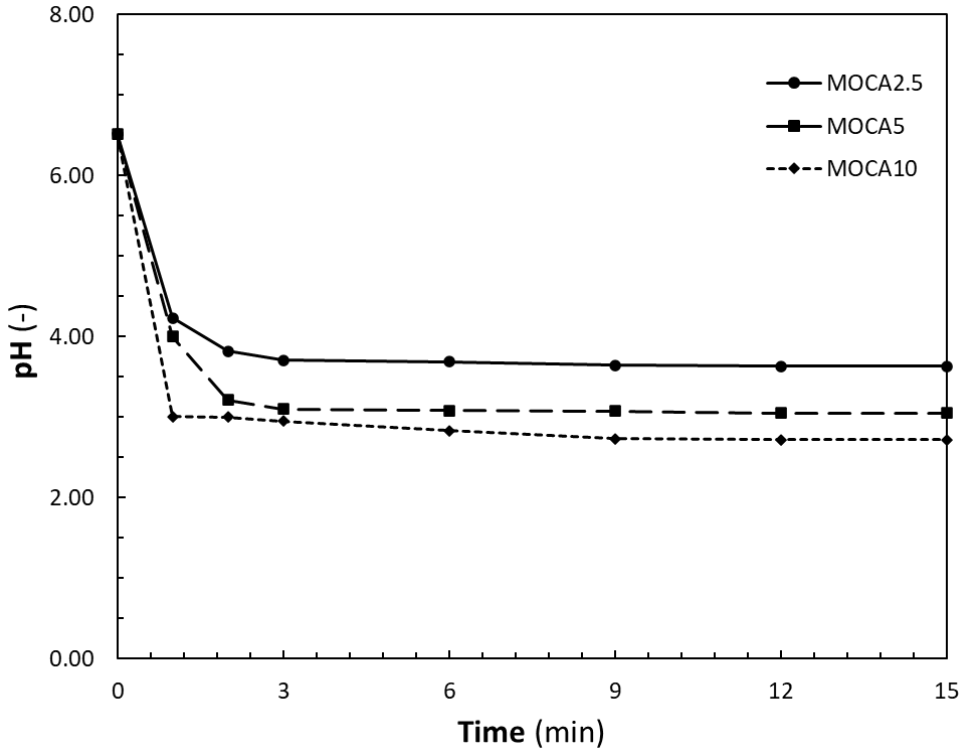


Figure S. 6: Changes in pH of soymilk and modified okara mixture during the 15-min mixing.

Table S. 4: Final pH values of soymilk okara gels (M, MO, MOCA2.5, MOCA5, MOCA10) at the end of 15-min mixing. Data expressed as mean standard deviation (n = 3). Means within one column that do not share a common letter are statistically different (ANOVA followed by Tukey's post-hoc: $p < 0.05$).

Final pH values of soy gels at the end of mixing				
M	**MO**	**MOCA2.5**	**MOCA5**	**MOCA10**
6.63 ± 0.15^{a}	6.64 ± 0.12^{a}	3.67 ± 0.07^{b}	3.11 ± 0.06^{c}	2.79 ± 0.13^{d}

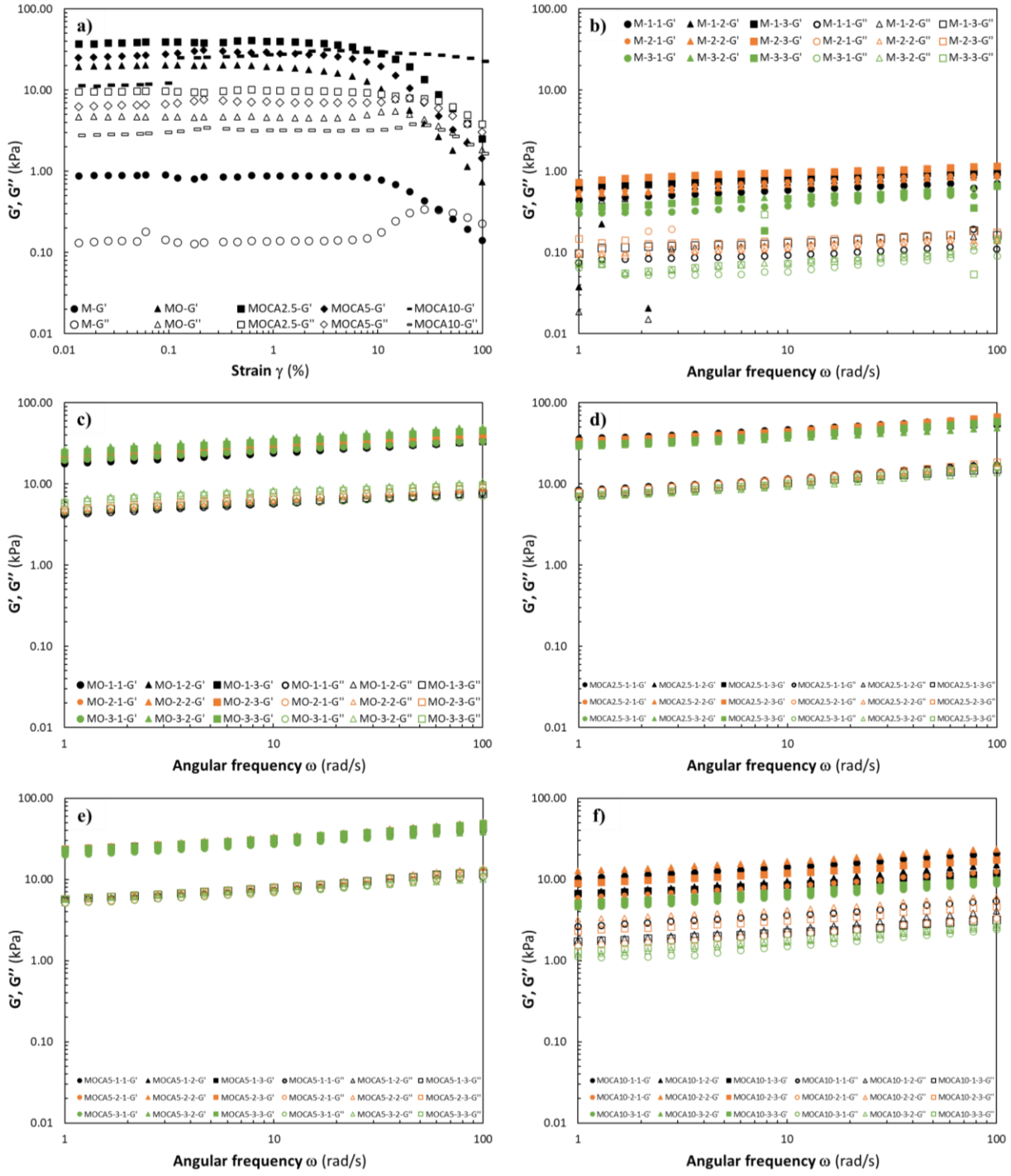


Figure S. 7: a) Curves of storage modulus (G') and loss modulus (G'') over strain (γ) of soymilk okara gels (M, MO, MOCA2.5, MOCA5, MOCA10). Curves of G' and G'' over angular frequency (ω) of b) M, c) MO, d) MOCA2.5, e) MOCA5, f) MOCA10.

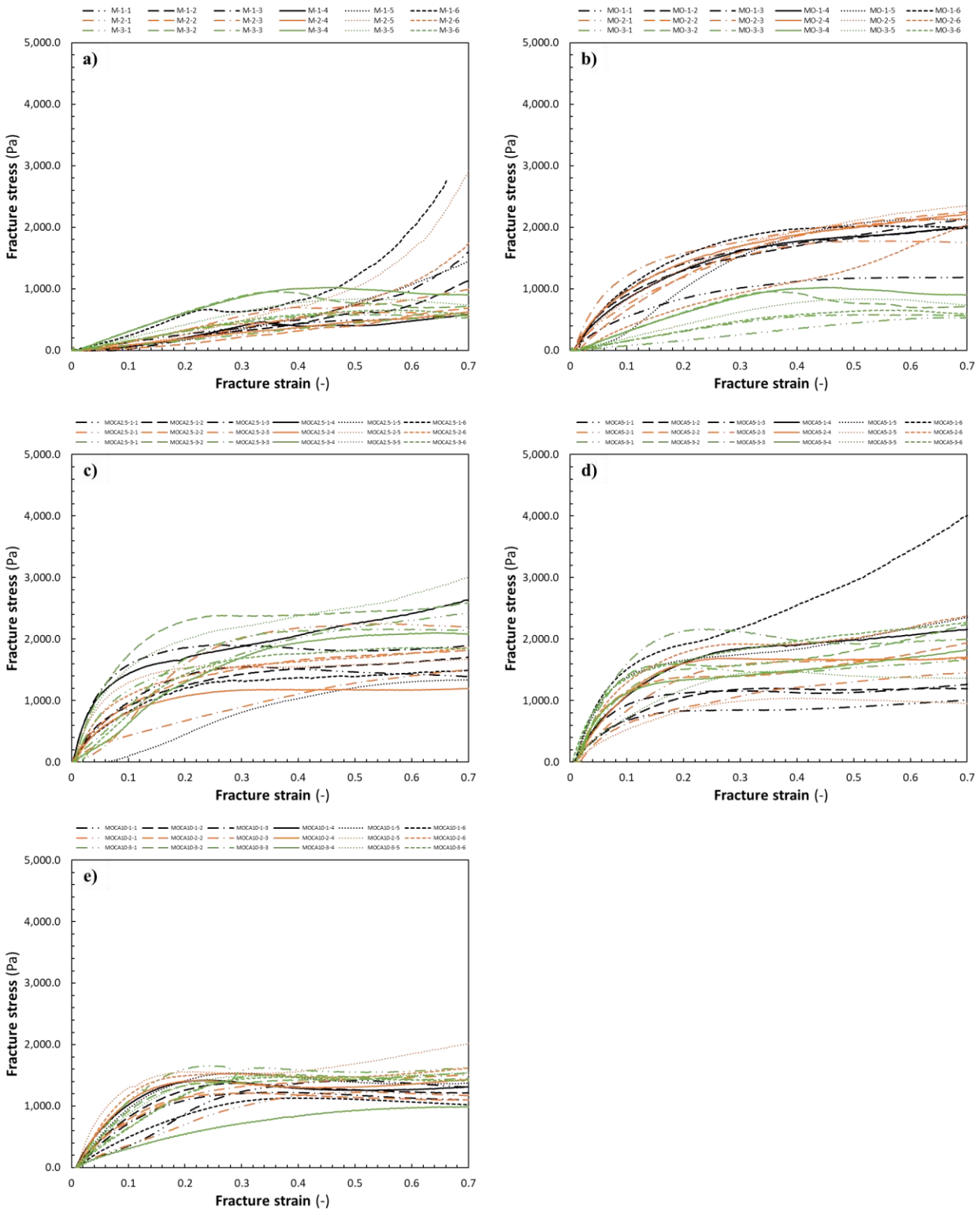


Figure S. 8: Fracture stress – fracture stain curves of soymilk gel of soymilk okara gels a) M, b) MO, c) MOCA2.5, d) MOCA5, e) MOCA10.